Characterization of Major Components of SUF Pathway (Iron-Sulphur Cluster Biogenesis) Functional in the Apicoplast of *Plasmodium vivax*

THESIS

Submitted in partial fulfilment
of the requirements for the degree of
DOCTOR OF PHILOSOPHY

by

ZARNA RAJESHKUMAR PALA

Under the Supervision of

Prof. Vishal Saxena

BITS Pilani
Pilani I Dubai I Goa I Hyderabad

BIRLA INSTITUTE OF TECHNOLOGY AND SCIENCE

PILANI (RAJASTHAN)

2017

BIRLA INSTITUTE OF TECHNOLOGY AND SCIENCE PILANI, RAJASTHAN, INDIA

CERTIFICATE

This is to certify that the thesis entitled **"Characterization of Major Components of SUF Pathway (Iron-Sulphur Cluster Biogenesis) Functional in the Apicoplast of *Plasmodium vivax*"** and submitted by Zarna Rajeshkumar Pala, ID. No. 2011PHXF010P for award of Ph.D. Degree of the institute embodies original work done by her under my supervision.

Signature (Supervisor) :
Name (Supervisor) : Vishal Saxena, PhD
Designation : Associate Professor
Department of Biological Sciences
BITS, Pilani, Pilani Campus

Date :

ACKNOWLEDGEMENTS

तस्मादसक्तः सततं कार्यं कर्म समाचर।

Therefore do thy duty perfectly, without care for the results,

असक्तो ह्याचरन्कर्म परमाप्नोति पूरुषः।।3.19।।

For he who works without attachment attains to the Supreme.

कर्मणैव हि संसिद्धिमास्थिता जनकादयः।

King Janaka and others attained perfection through action alone,

लोकसंग्रहमेवापि संपश्यन्कर्तुमर्हसि।।3.20।।

Even for the sake of enlightening the world, it is thy duty to act.

-The Bhagavad Gita

First and foremost I would like to thank almighty God, as he is the sole reason why even in pain, I smile; in confusion, I understand; in betrayal, I trust and in fear, I continue to fight.

As it is well said by Lao Tzu "The journey of a thousand miles begins with one step", Ph.D. is a tough journey and to get through this hardest journey we need to take only step at a time, but we must keep stepping. This is the thought that has helped me achieve the best things in life. This journey at BITS Pilani, has been a blend of happiness and sorrows, it's often been difficult and incredibly cruel, but the thought that it's going to give me life changing experiences, made me well equipped to tackle it and allowed me to blossom. This thesis is the end of my journey in obtaining my Ph.D. and I have not travelled in a vacuum in this journey. This thesis has been kept on track and been seen through to completion with the support and encouragement of numerous people including my family, teachers, friends, colleagues and well wishers. At the end of my thesis, I would like to thank all those people who contributed in many ways to the success of this study in the form of this thesis and an unforgettable experience for me.

I would like to express my deepest appreciation to my supervisor, ***Prof. Vishal Saxena*** *for his inspiring guidance, his endless support and his sincere encouragement throughout this work. I am deeply indebted to him for his efforts in moulding me in the field of malaria research and successful execution of activities related to my Ph. D. training. He was always patient to me, to my upset and to my research. His constant drive for finding the truth in any problem has served as a model for my scientific upbringing. His mentorship and support throughout the past six years have been tremendously valuable. I would also like to thank him for giving me the opportunity to attend several national and international conferences during which I was able to interact with other experts in the field and broaden my scientific knowledge. Although words are not sufficient, I preserve an everlasting gratitude to him.*

I would like to give a heartfelt thanks to ***Dr. Shilpi Garg****, who despite not being officially assigned my co-supervisor, played this crucial role in my thesis. She has taught me, both consciously and unconsciously, how good research is done. I appreciate all her contributions of time, ideas, and funding to make my Ph.D. experience productive and stimulating. The joy*

and enthusiasm she has for her research was contagious and motivational for me, even during tough times in the Ph. D. pursuit.

I gratefully acknowledge ***Prof. Ashis K. Das*** *and* ***Prof. Sanjay K. Verma****, members of my Doctoral Advisory Committee (DAC) for their valuable advice, constructive criticism and helpful suggestions and comments during my thesis progress.*

With profound reverence, I express my gratitude to the Vice Chancellor, Prof. Souvik Bhattacharyya and the former, Prof. Bijendra Nath Jain, Director Prof. Ashoke K. Sarkar and the former, Prof. G. Raghurama, Dean Academic Research Division (ARD) Prof. Sanjay K. Verma and the former, Prof. Ashis K. Das, Associate Dean, Academic Research Division Prof. Hemant R Jadav, for academic and administrative supports. I also express my gratitude to the office staff (Mr. Mahipal and Mr. Raghuveer) of ARD, whose secretarial assistance helped me in submitting the various evaluation documents in time.

It's my pleasure to gratefully thank the present and the past Head of the Department, Prof. Prabhat Nath Jha, Prof. Rajesh Mehrotra, Prof. Jitendra Panwar, Prof. Shibasish Chowdhury and other faculty members of the Department for their care, understanding, suggestions and specially providing an environment which makes feel every research scholar of the Department like being in home. I am also grateful to them for providing me with all the basic facilities and bringing some high end facilities also in the department despite the budget constraints and the geographical location of Pilani. I feel privileged in expressing high regards to ***Prof. Shibasish Chowdhury*** *for constructive discussions on various fundamental aspects of Bioinformatics. My thanks are due to all the research scholars of the Department for their cooperation and help. My high regards goes to the non-teaching staff of the Department Mr. Kamlesh Soni, Mr. Mukesh Saini, Mr. Naresh Saini, Mr. Parmeswar, Mr. Subhash and Mr. Ajay for their timely help.*

This thesis would not have been completed without the close collaboration with Sardar Patel Medical College, Bikaner. I am extremely indebted to Prof. Dhanpat K Kochar, and Prof. Sanjay Kumar Kochar, for providing invaluable malaria infected blood samples. We (our group) have always enjoyed their warm hospitality and the delicacies they offered during our visit to Bikaner for blood sample collection. I am also thankful to Dr. R. P. Pareek, Medical Superintendent, BITS Pilani, for his collaboration and helping us collect samples from Pilani for the study.

Heartfelt thanks to my senior and colleague ***Dr. Gagandeep****, for his untiring and continued support during my work. I would always be grateful to him for sharing all the bitter sweet experiences during Ph. D. I would like to sincerely thank* ***Dr. Sushil Yadav****, for helping me in the animal studies, sharing some lessons of life and for all the small get togethers. I always had a hearty inspiration from my seniors and lab mates Dr. Deepak, Dr. Amit, Dr. Narayan, Mr. Boopathi. I extend my gratitude to* ***Dr. Arpit*** *and* ***Dr. Kuldeep*** *for being my true seniors, supporting and helping me in my work and always being by my side during tough times. I extend deep gratitude to my friends who are my family at BITS,* ***Gurpreet****,* ***Panchsheela****,* ***Isha Di****, and* ***Purva Di*** *for always helping me make correct decisions both personally and professionally and for being on toes in case of any medical emergency. Their precious contribution towards this work and my journey will always be unforgettable.*

Interdependence is certainly more valuable than independence and learning is an interdependent phenomenon. I am indebted to many student colleagues for providing me a stimulating and fun filled environment in the lab. I thank ***Ritika*** *and* ***Yamini*** *for teaching me some basics of lab during the initial phase of my journey. I would further like to thank* ***Satish*** *for helping me perform experiments, your time and efforts resulted into some fruitful results that form an integral part of this thesis. The contribution of* ***Renuka***, ***Kanka***, ***Ramya*** *and* ***Anish*** *in the daily chores of lab is sincerely appreciated. My special appreciation goes to* ***Sukalpa*** *for his never ending scientific queries which forced me to think beyond existent scientific theories and add new perspective to them. I am grateful to* ***Atif***, ***Deepankar***, ***Shishir***, ***Brijesh***, ***Azeem***, ***Lohitesh***, ***Udit***, ***Shrayans*** *for their ever smiling faces in the department and always appreciating me and my work. I would like to especially thank* ***Naveen*** *for helping me with the EPR studies despite all odds. I am indebted for the support obtained from* ***Anshu*** *and* ***Jitesh*** *for the confocal microscopy. I extend my thanks to* ***Dr. Parvez***, ***Dr. Mukund***, ***Devesh***, ***Vishal***, ***Subodh*** *for their assistance in creating the anaerobic conditions for the biochemical assays. I am grateful to* ***Yashwant***, ***Saurabh***, ***Santosh***, ***Anuradha***, ***Almesh***, ***Vajir*** *for teaching me the basics of animal handling. I appreciate the assistance obtained from* ***Dr. Mithilesh***, ***Parik***, ***Tania***, ***Rini***, ***Vikas*** *and* ***Tripti*** *for the studies in mice malaria.*

I would like to extend my gratitude towards my juniors and friends ***Ramandeep***, ***Dilip***, ***Vikram***, ***Sandeep***, ***Shraddha***, ***Poonam*** *for their scholastic company during the short revitalizing breaks. The discussions from science to spirituality and beyond during these breaks always helped break the everyday monotonous routine and stimulated my neurons to discuss any topic under the sun. The cheerful faces of* ***Subhra***, ***Leena*** *and* ***Heena*** *brought a smile to my face even when I had a bad day. I thank* ***Vidushi***, ***Vandana***, ***Shobha***, ***Monika***, ***Akanksha***, ***Nidhi***, ***Avinash*** *and* ***Ranita*** *for their support during this journey.*

I would like to extend a huge and warm thanks to ***Jyothi*** *for being a pillar of support through all the inevitable ups and downs of my life and Ph.D. She always reminded me life's true priorities and her approach towards science was truly motivational throughout my work. I would also like to extend my gratitude to* ***Dr. Emil*** *not only for all his support during my work but also for being there to listen when I needed an ear. I am thankful to* ***Dr. Prashant*** *for his never ending support throughout my study. I am grateful to* ***Vishnu*** *for being the 4:00 A.M. friend with whom I could discuss weird and the "not so" interesting topics of scientific research. I wish to thank* ***Kruti*** *for being the younger sister I always wanted and listening to all my happy and sad stories. I appreciate the support of* ***Hardik***, *who has managed to cheer me up always although, we are miles apart. I am thankful to* ***Aditi***, ***Nikita*** *and* ***Anubhuti*** *for always being there in my life, to share all my joys and sorrows. I am grateful to* ***Dr. Krunal*** *for his expert medical advice and treatment during my injury, and for always appreciating my work. I owe my gratitude to* ***Aditya***, ***John*** *and* ***Suraj*** *for their moral support always. I would also like to thank* ***Siddharth***, ***Deeptanshu***, ***Tanmay, Akshat*** *and* ***Siddhant*** *for making my stay in Pilani joyous and fun. I owe special thanks to* ***Binay*** *for instigating in me the fire to always be the best at whatever I pursue, for encouraging and motivating me to pursue my dreams, for appreciating my culinary skills, for entertaining me with this poetry and for giving me some unforgettable memories. A special thanks to* ***Imran*** *for keeping me in your prayers as that is what sustained me thus far and incented me to strive towards my goal, for giving me few of the best moments of my life.*

Ph. D. students often talk about loneliness during the course of their study but this is something which I rarely experienced at BITS Pilani. Heartfelt thanks to the really active ***Students Union*** *for organizing cultural, technical and sports fest every year and making my stay in Pilani a memorable one.*

The very existence of me in this universe in any given form is because of my beloved Parents: ***Mr. Rajeshkumar Pala*** *and* ***Mrs. Jayshree Pala****. Words and my deeds would always be insufficient to express my gratitude and love towards them. Despite coming from a conservative background where education for girls is not given prime importance and where girls are treated as a liability rather than asset, they fought the world for me, made thousands of sacrifices unknown to me, educated me and made me what I am today. I dedicate this thesis to my parents, whose role in shaping me will always remain colossal as it is because of their love, prayers, encouragement, constant support and strong belief that motivated me to keep going on in this journey. I thank them for infecting me with their wisdom, intelligence, energy for life, thirst for knowledge and constant strive for learning something new each day. Both of them have instilled many admirable qualities in me and given me the best foundation with which I can face life and the world. Dad has taught me about hard work and self-respect, about persistence and about how to be independent. Mom, especially, was a great role model of resilience, strength and character. I am grateful for both of them and for the 'smart genes' they passed on to me.*

This list is incomplete without paying high regards to ***Prof. Neetin Desai****, who has been my scientific guru since my undergraduate days. His guidance and never ending support has always energized me to pursue research. I sincerely hope I continue to have opportunities to interact with him for the rest of my research career.*

*I take this opportunity to sincerely acknowledge Department of Science and Technology (****DST****), University Grants Commission (****UGC****) and Council of Scientific and Industrial Research (****CSIR****), Government of India, New Delhi, for providing financial assistance in the form of Project Assistantship (PA), Basic Scientific Research (BSR) Fellowship and Senior Research Fellowship (SRF) respectively, which buttressed me to perform my work comfortably.*

Last but not the least; I owe my deepest gratitude to all the ***Patients*** *who donated their blood and the* ***mice*** *which were sacrificed during the course of this study.*

Zarna Rajeshkumar Jayshree Pala.

CONTENTS

ABSTRACT

Fe-S clusters are critical metallo-cofactors required for cell function. To avoid the toxicity associated with the ferrous iron and sulfide to the cell, *in vivo* Fe-S cluster assembly occurs in a highly coordinated fashion via a multifaceted protein network. *Plasmodium* contains two Fe-S cluster assembly systems; the ISC pathway functional in the mitochondria and the SUF pathway residing in the apicoplast. Except SufB, all the proteins reported for the SUF pathway are nuclear encoded in *Plasmodium* and then targeted to its functional site: mitochondria or apicoplast. The prokaryotic nature of the pathway suggesting absence of similar proteins in the host and its essentiality for the parasite erythrocytic stages makes it a potential and putative drug target.

The pathway begins with a cysteine desulfurase SufS, which along with partner protein SufE mobilize persulfide from L-cysteine, followed by assembly of the Fe-S cluster onto a scaffold protein where the source of iron is yet unknown. This assembled cluster is than transferred to the apo-proteins via several carrier proteins. Since the proteins involved in these Fe-S cluster biogenesis pathways are still of putative or hypothetical nature in *Plasmodium vivax*, it substantiates the need for characterization of these proteins. Thus, the overall aim of this study was to characterize the SUF pathway for Fe-S cluster biogenesis from *P. vivax*.

The study initiated with the shortlisting of proteins predicted to be involved in the SUF pathway based on various sequence alignments and conserved domain analysis. *In silico* analysis revealed a Fe-S cluster assembly protein putative to harbour a SufA domain, a hypothetical protein with a SufE domain and two cysteine desulfurases; cysteine desulfurase putative and cysteine desulfurase (mitochondrial precursor). The genes for these proteins were amplified from samples collected from clinical isolates and cloned in prokaryotic-based system for expression studies. The amplicons depicted the presence of conserved domains with a major deletion near the active site in *Pv*SufE and an addition in *Pv*SufS. To check for the effect of these sequence variations on the function of protein we purified these proteins and performed biochemical assays to check for their

functionality. The desulfurase activity of these proteins was preserved even after these variations, which suggest the proteins to retain their activity through evolution.

The mystery of scaffold protein required for the assembly of Fe-S clusters needs to be resolved. Thus, we examined various proteins and found a putative Fe-S cluster assembly protein showing the presence of conserved cysteine residues ($X_{87}CX_{155}CGCX_{159}$) present in A type carrier proteins required for binding of Fe-S clusters. The purified protein was evaluated for its efficacy in formation of these clusters under anaerobic environment by performing biochemical assays, which suggested the formation of 4Fe-4S clusters on the protein by EPR spectroscopy.

To elucidate the whole SUF pathway from *Plasmodium vivax* we further tried to examine whether the clusters formed on the scaffold protein be transferred to the apo protein. For the same, we performed the biochemical mobilization of sulphur via SufSE complex to form the Fe-S clusters on *Pv*SufA (iron provided via external source) and then incubated this reconstituted protein with an apo-protein *Pv*IspG (functional in isoprenoid pathway), where we could observe the transfer of Fe-S clusters from *Pv*SufA to *Pv*IspG. SufBCD complex has been previously reported to act as an accessory protein in *Plasmodium*, and in bacteria is reported to enhance the desulfurase activity of SufSE manifolds. Our studies exhibiting the interaction of *Pv*SufBD with *Pv*SufA *in silico* suggests its role in conjunction with *Pv*SufA for Fe-S cluster biogenesis. We also localized all the proteins in the study to the apicoplast, the functional site of the SUF pathway further confirming these proteins to be involved in SUF pathway.

LIST OF TABLES

LIST OF FIGURES

Abbreviations

RBC	Red Blood Corpuscles
RNA	Ribo Nucleic Acid
DNA	Deoxyribo Nucleic Acid
Mb	Megabases
LSU	Large subunit
SSU	Small subunit
IR	Inverted repeat
EF	Elongation Factor
TOM	Transporter Outer Membrane
TIM	Transporter Inner Membrane
NEAT	Nuclear Encoded Apicoplast Targeted
plDNA	Plastid DNA
ER	Endoplasmic Reticulum
SP	Signal Peptide
TP	Transit Peptide
mt	Mitochondrial
ETC	Electron Transport Chain
NAD	Nicotinamide adenine dinucleotide
NADP	Nicotinamide adenine dinucleotide phosphate
PDH	Pyruvate Dehydrogenase
FA	Fatty Acid
DHOD	Duhydroorotate Dehydrogenase
TCA	Tricarboxylic acid
FAS	Fatty Acid Synthesis
IPP	Isopentenyl-5-pyrophosphate
DMPP	Dimethylallyl Diphosphate

DOXP	1-deoxy-D-xylose-5-phosphate
ATP	Adenosine triphosphate
ISC	Iron Sulfur Cluster
NIF	Nitrogen Fixation
SUF	Sulfur mobilization
CIA	Cytosolic Iron-sulphur cluster Assembly
Fe-S	Iron-Sulphur
PLP	Pyridoxal Phosphate
ABC	ATP Binding Cassette
ACD	Acid Citrate Dextrose
BSA	Bovine Serum Albumin
DAPI	4',6-diamidino-2-phenylindole
DEPC	Diethyl Pyrocarbonate
DNA	Deoxy ribonucleic acid
dNTP's	Deoxy ribonucleoside triphosphates
DTT	Dithiothreitol
EDTA	Ethylene Diamine tetra acetic acid
FITC	Fluorescein isothiocyanate
IPTG	Isopropyl-β-D-thiogalactopyranoside
LB	Luria Bertani
M	Molar
Min	Minute
mM	milimolar
MOPS	3-[N-Morpholino]propanesulfonic acid
nm	Nanometer
P.	*Plasmodium*
PAGE	Poly Acrylamide Gel Electrophoresis
PBS	Phosphate Buffered Saline

Pf	*Plasmodium falciparum*
Pv	*Plasmodium vivax*
q. s.	Quantity sufficient
nt	Nucleotides
O. D.	Optical Density
RDTs	Rapid diagnostic tests
RNA	Ribonucleic acid
rRNA	Ribosomal RNA
SDS	Sodium Dodecyl Sulphate
TEMED	N, N, N', N'-tetramethylethylenediamine
Tris	2-Hydroxy methylamine

Amino Acid

Alanine	ala	A
Arginine	arg	R
Asparagine	asn	N
Aspartic acid	asp	D
Cysteine	cys	C
Glutamine	gln	Q
Glutamic acid	glu	E
Glycine	gly	G
Histidine	his	H
Isoleucine	ile	I
Leucine	leu	L
Lysine	lys	K
Methionine	met	M
Phenylalanine	phe	F
Proline	pro	P
Serine	ser	S
Threonine	thr	T
Tryptophane	trp	W
Tyrosine	tyr	Y
Valine	val	V

Nucleotide bases

Adenine	A
Guanine	G
Cytosine	C
Thymine	T
Uracil	U

Chapter I

Introduction

INTRODUCTION

1. MALARIA

1.1 The Disease

Malaria is an infectious disease that plagues mankind and is responsible for over half a million deaths annually. In 2015 alone, approximately 212 million cases of malaria infections and 438,000 deaths were reported worldwide, with maximum number of infections from Africa (90%) followed by South East Asia (7%). This high incidence rate can be attributed to still inaccessible prevention and treatment strategies to millions of individuals in these places (WHO,World Malaria Report, 2015).

Malaria is a vector-borne disease caused by a protozoan parasite *Plasmodium*. Over 156 different species of *Plasmodium* are known to cause infection in various vertebrates, of which the members known to cause human malaria are *P. falciparum*, *P. vivax*, *P. malariae*, *P. ovale*, and recently reported *P. knowlesi* (Singh et al., 2004), *and P. cynomolgi* (Ta et al., 2014). Although, *P. falciparum* is recognized to be the most notorious and is responsible for causing most mortality due to severe malaria in sub-Saharan Africa, *P. vivax* malaria predominates in some of the densely populated and impoverished regions across the globe sometimes resulting in severe and fatal outcomes. Fever, chills, sweats, headaches, nausea and vomiting comprise regular symptoms experienced in uncomplicated malaria. Severe malaria is characterized by more acute symptoms than those seen in uncomplicated malaria which include acute respiratory distress, cerebral malaria, severe anemia, kidney failure, haemoglobinuria, jaundice, hepatic failure. (CDC, 2015).

1.2 Life cycle of *Plasmodium spp.*

The apicomplexan parasite *Plasmodium* has multistaged complex life cycle traversing across two hosts; a female *Anopheline* mosquito and a vertebrate. The parasite divides in multiple cell types while circumventing host immune system

clearance due to varying surface protein expression profile (Greenwood et al., 2008). The *Plasmodium* life cycle begins with a bite from an infected female *Anopheles* mosquito to the human host during a blood meal (**Figure 1.1**). About 10-100 sporozoites are injected with this bite into the blood vessels which finally migrates to the liver within few hours of infection (Doolan et al., 2009; Nkhoma et al., 2012). This initiates the pre-erythrocytic phase (schizogony), an asymptomatic phase.

Each sporozoite invades a single hepatic cell, develops and multiplies to form 10,000- 30,000 merozoites (Jones & Good 2006). In *P. vivax* and *P. ovale*, some of the parasites can remain in the liver for years as hypnozoites and may cause recurrent episodes of the disease. The schizogony stage in the liver takes approximately 6 days in *P. falciparum*, 8 days in *P. vivax*, 13 days in *P. malariae* and 9 days in both *P. ovale* and *P. knowlesi* (www.malariasite.com/malaria-parasites)

The merozoites get discharged into the blood stream by rupture of hepatocytes and immediately invade red blood cells (RBCs), initiating the blood stage infection. In RBCs these merozoites develop to a 'ring' stage followed by a trophozoite stage which replicates to form a multinucleated schizont containing an average of 10 merozoites (Greenwood et al., 2008). Upon maturation of the schizont, the erythrocyte ruptures releasing hundreds of merozoites along with various malarial antigens and toxic metabolites, resulting in periodic fevers with shivering which are characteristics of malaria infection.

Some of the ring stages/early trophozoites however, rather than maturing into schizonts, develop to male and female sexual gametocytes. These haploid gametocytes are ingested by female mosquito as part of its blood meal initiating sporogony (sexual reproduction) in the mosquito's gut. The male gametocyte nucleus undergoes three rounds of DNA replication producing eight nuclei with each forming a flagellum in a process known as exflagellation. Thus, 8 motile male microgametes are produced. The male and female gametes fuse to form a diploid

zygote. At this stage, if a mosquito ingests two genetically distinct parasite clones, recombination takes place leading to emergence of novel genotypes.

The motile zygote (ookinete) migrates through, and encysts on, the outer surface of the gut wall (as an oocyst). Asexual division within this oocyst produces numerous haploid sporozoites which migrate to the mosquito's salivary gland ready to be transmitted to the human host in a blood meal. The sporogonic phase lasts between 8-15 days in the mosquito (Carter & Graves, 1988; Eichner et al., 2001).

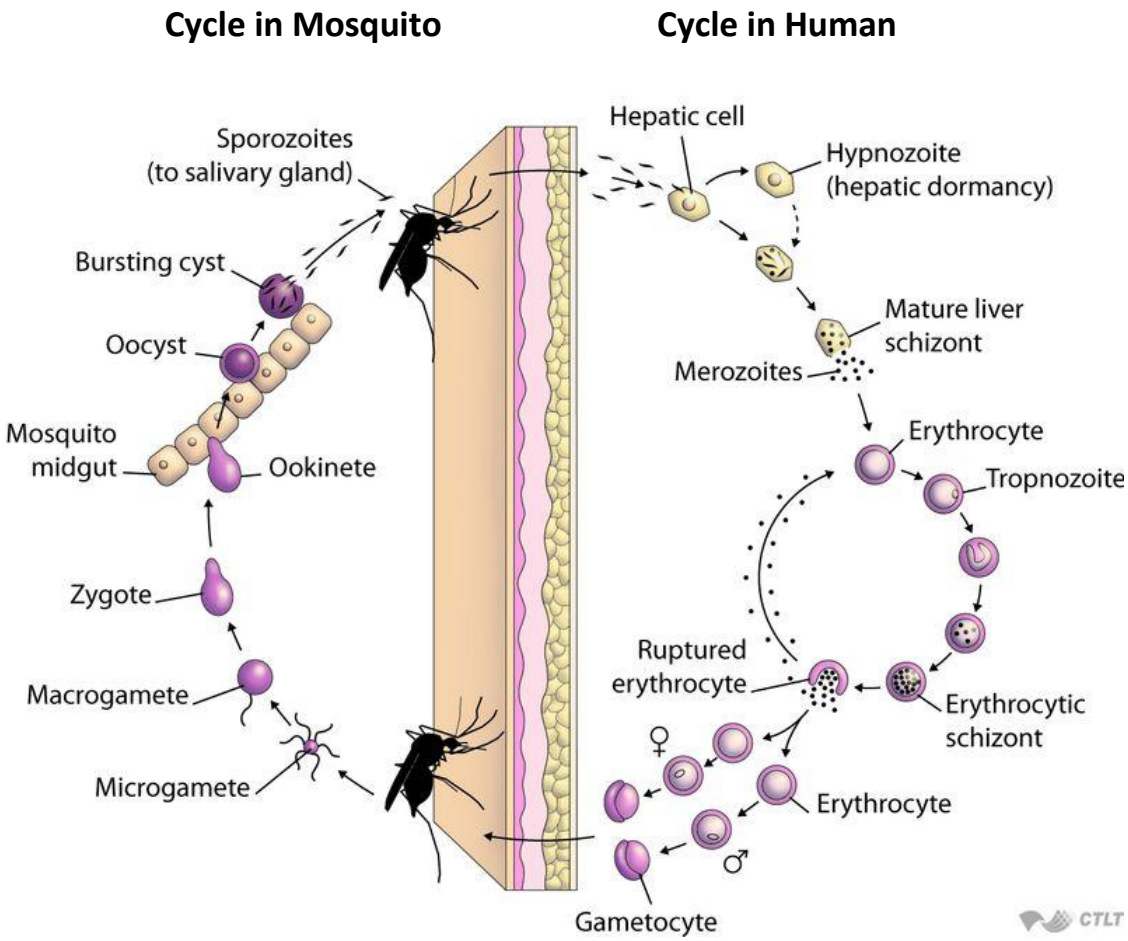

Figure 1.1: **Lifecycle of *Plasmodium* showing the asexual phase in the human host and the sexual stage in the female *Anopheles* mosquito**. (Copyright © Johns Hopkins Bloomberg School of Public Health)

1.3 Burden of *Plasmodium vivax* malaria

P. vivax malaria is an important public health issue especially in tropical regions of the world. It is the most widespread human malaria, with majority of the cases

reported from South-East Asia Region (58%), followed by the Eastern Mediterranean Region (16%) and the African Region (12%) amongst which Ethiopia, **India**, Indonesia and Pakistan accounted for 78% of the cases (WHO World Malaria Report, 2016). Globally in 2015, the total mortality due to *P. vivax* infections was estimated in between 1400 - 14,900 (WHO World Malaria Report, 2015). In addition, reports of severe manifestations due to *P. vivax* infections (Kochar et al., 2005) from all malaria endemic regions have raised huge concern.

The unique biological and epidemiological features of the parasite make it distinct from *P. falciparum*, posing challenges to develop control strategies. Biologically, *P. vivax* infections have typically low blood-stage parasitemia, compared to *P. falciparum*, with gametocytes emerging before illness manifests, and dormant liver stages (hypnozoites) causing relapses. The distinct traits of these two parasites, thus affect both its geographic distribution and transmission patterns (Howes et al., 2016). The spreading incidences of chloroquine resistance, the acute attack and low efficacy of primaquine against the relapses, aggravates the levels of illness and severity among the millions of people suffering from *P. vivax* infection. The vaccine trials are still underway and only RTS, S/ AS01 vaccine against *P. falciparum* has been able to complete phase 3 clinical trial, showing reduction in clinical incidence by only 39%. In the absence of strategic control to *P. vivax* malaria due to these specific characteristics, progress towards the eradication of endemic malaria transmission will be significantly hampered. For this reason, it becomes necessary to study the biology of the parasite and investigate new drug targets for the upcoming resistant strains, thus validating the importance of reversing the historic neglect of this infection. In light of this, the non-photosynthetic plastid of *Plasmodium*, the apicoplast is being looked upon as a putative drug target.

1.4 Apicoplast as a putative drug target

In the race to identify new array of anti-malarials, a plastid like organelle called Apicoplast in *Plasmodium spp*. have come into focus due to its essentiality for development of the parasites and indispensability for the parasite survival. However,

to understand the significance of this organelle as a potential drug target, its evolution and metabolic functioning needs to be exploited in detail.

1.4.1 Origin and evolution of Apicoplast

Plasmodium belongs to the phylum Apicomplexa, which is characterized by the possession of specialized apical organelle complex that aids in host cell invasion (Corliss, 1994; Levine, 1973). In addition to *Plasmodium*, the phylum Apicomplexans include parasites like *Babesia*, *Cryptosporidium*, *Eimeria*, *Theileria* and *Toxoplasma* that are well-studied and others which are relatively under investigated like *Gregarina*, *Hepatozoon*, *Lankesterella*, *Monocystis* and *Sarcocystis* (Lee et al., 2000). All apicomplexans except *Cryptosporidium* possess a non-photosynthetic plastid organelle called the apicoplast. The apicoplast is present in all the stages of parasite development and cannot be formed *de novo* (McFadden et al., 1996). It is a semi-autonomous organelle that carries its own genome (Wilson et al., 1996; Wilson and Williamson, 1997). It stays in close proximity with the mitochondrion as a small tubular structure which increases in length at the trophozoite stage and branches extensively prior to separation at schizogony leaving one apicoplast per daughter cell (Stanway et al., 2009; van Dooren et al., 2005; van Dooren et al., 2006).

The apicoplast is believed to have originated through secondary endosymbiosis where a eukaryotic red alga was engulfed by a plasmodial ancestor that might itself have originated *via* primary endosymbiosis of a cyanobacterium (Kalanon and McFadden, 2010). The apicoplast thus is hypothesized to possess more than two enclosing membranes viz. two membranes of the primary cyanobacterial plastid, the plasma membrane of the primary endosymbiont alga and the phagosomal membrane of the engulfing eukaryote. Earlier reports (Bannister et al., 2000; Hopkins et al., 1999) suggested that the plastid may have lost one of its four outer membranes but cryo-electron tomography of *P. falciparum* apicoplast revealed that it in fact possesses a four membrane organization (Lemgruber et al., 2013).

1.4.2 Genome organization and Protein targeting of the Apicoplast

During evolution, most of the genes from apicoplast DNA (plDNA) were transferred to the nuclear genome and only a small fraction of the apicoplast proteome is now encoded by the apicoplast genome (Kohler et al., 1997). The plDNA of almost all the *Plasmodium spp*. has been completely sequenced, showing high A+T content (84.9 to 86.9%) and varying size ranging from ~27 kb to ~35 kb in different species (Wilson et al., 1996; Sato et al., 2000; Saxena et al., 2012; Arisue et al., 2012). It is completely packed with open reading frames, each separated by only a few nucleotides. The plDNA consists of inverted repeat regions (IR-A and IR-B) which spans one-third of the genome circle and encodes for duplicated LSU and SSU rRNA and tRNA genes (Gardner et al., 1991, Saxena et al., 2012). It also encodes for genes of a translation elongation factor EF-Tu (*tufA*), RNA polymerase subunits (*rpoB, rpoC1*, and *rpoC2*), Fe-S cluster protein SufB (*orf470*) and a member of caseinolytic protease family (*clpC*). A nuclear-encoded histone-like protein HU has been shown to play a major role in DNA organization in the apicoplast (Ram et al., 2008; Sasaki et al., 2009).

The apicoplast has to import proteins encoded by the nuclear genome to carry out all the resident functions. Nuclear-encoded apicoplast-targeted (NEAT) proteins contain a bi-partite N-terminal leader for organellar sorting (Waller et al., 1998). Besides the signal peptide (SP) which mediates transport of the nascent polypeptide into the ER, NEAT proteins require a transit peptide (TP) to cross the four apicoplast membranes. The SP consists of a short hydrophobic domain of 20-30 amino acids followed by a von Heijne-type cleavage motif, predicted to be present in *P. falciparum* apicoplast-targeted proteins (Waller et al., 2000). In contrast, the TP is complex, lacks consensus in length, sequence or motif and is rich in hydrophilic and basic residues (Foth et al., 2003). It is cleaved by specialized peptidases in the apicoplast to form the mature protein (Ponpuak et al., 2007; van Dooren et al., 2002). Passage of the protein across the peri-plastid membrane is thought to occur via specialized endosymbiont derived ER-associated degradation complex (Kalanon and McFadden, 2010; Sommer et al., 2007; Spork et al., 2009).

Proteomic studies of *P. vivax* have revealed approximately 320 proteins to be encoded by nuclear genome and then targeted to the apicoplast. Of these 320 proteins, 157 proteins are putatively characterized as enzymes participating in different metabolic pathways taking place in the apicoplast, while functions for remaining 159 proteins are still hypothetical (Carlton et al., 2008). Recent reports suggest that some of the proteins being targeted to apicoplast are also targeted to the mitochondria unfolding another probability of dual targeting of these proteins (Gunther et al., 2010; Read et al., 2010; Chaudhari et al., 2012).

1.4.3 Metabolic functions of the apicoplast

The apicoplast, despite having a reduced coding capacity, is a site for many important metabolic pathways (**Figure 1.2**), the products of which are essential for parasite at different stages of development (Jomaa et al., 1999; Ralph et al., 2004; Sato et al., 2004; Tarun et al., 2009; Waller et al., 2000). It carries out several metabolic reactions like type- II fatty acid biosynthesis essential for late liver stage development (Vaughan et al., 2009); isoprenoid synthesis that supplies isoprene units as prosthetic groups (Jomaa et al., 1999) which are essential in the blood-stages of the parasite life-cycle (Yeh and DeRisi, 2011); heme synthesis, important for the de novo heme biosynthesis (Wilson et al., 2005; Botte et al., 2012); and the iron-sulphur cluster biogenesis that provide metal cofactors for several enzymatic reactions.

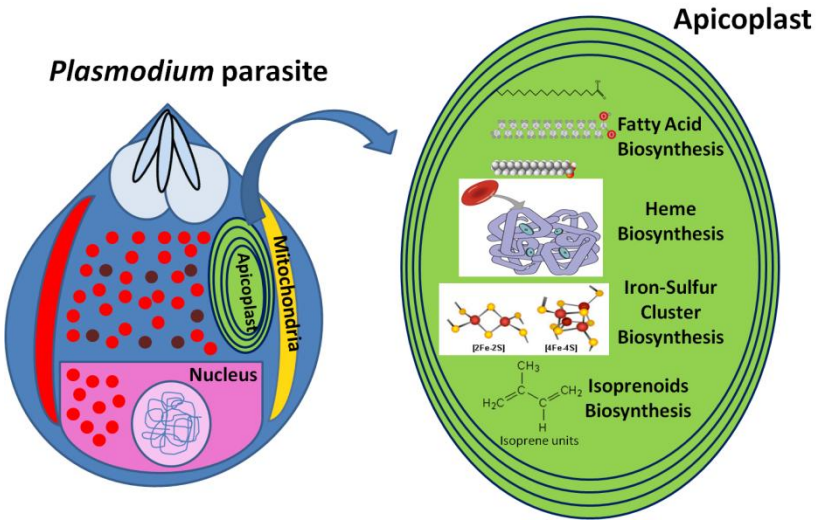

Figure 1.2: Apicoplast houses four important metabolic pathways: Fatty acid biosynthesis, Heme biosynthesis, Iron-sulphur cluster biogenesis and Isoprenoids biosynthesis.

All the enzymes involved in these metabolic pathways show evident disparity from the human host because of its prokaryotic origin. Given below are details of each of the above mentioned metabolic functions sustained by the Apicoplast.

1.4.3a Type-II Fatty acid biosynthesis pathway (FAS-II)

The FAS-II pathway helps parasite carry out de novo synthesis of fatty acids; this is in addition to scavenging fatty acids from the vertebrate host or mosquito vector. Unlike eukaryotic cytosolic fatty acid synthase, which is large multifunctional polypeptide, the apicoplast fatty acid synthase is composed of different enzymes (Ralph et al., 2004; Waller et al., 2003). Genes encoding the entire complement of enzymes for fatty acid synthesis are present in the *Plasmodium* nuclear genome (Seeber and Soldati-Favre, 2010) and these proteins are targeted to the apicoplast. Inhibition of blood stage parasite with triclosan, that targets bacterial enoyl-ACP reductase (FabI), suggested the FAS-II pathway is essential for the asexual blood stages (Surolia and Surolia, 2001); the pathway was later shown to be essential in asexual liver stages and sporozoites development in midgut of mosquito (van Schaijk et al., 2014; Vaughan et al., 2009; Yu et al., 2008).

1.4.3b Isoprenoid Biosynthesis

A crucial pathway that operates in the apicoplast is the biosynthesis of Isoprenoids isopentenyl pyrophosphate (IPP) or its isomer dimethylallyl diphosphate (DMPP) units. The synthesis of IPP in the apicoplast occurs via 1-deoxy-D-xylulose-5-phosphate (DOXP) or non-mevalonate pathway that is characteristic of eubacteria and plastids (Ralph et al., 2004). Fosmidomycin targets the *Plasmodium* DOXP pathway (Jomaa et al., 1999; Zhang et al., 2011) and its effect on blood stage parasites was reversed by the external supplementation with IPP demonstrating that it is the metabolic product that makes the plastid indispensible for parasite sustenance in blood stages (Yeh and DeRisi, 2011). Also, parasites devoid of apicoplast were able to survive and multiply for indefinite cycles in culture with externally supplied IPP suggesting the most important role of the apicoplast in the blood stages is the DOXP pathway (Yeh and DeRisi, 2011). Likely uses of IPP in the apicoplast might be for the production of membrane anchor for dolichols in ER

glycosylation complex and ubiquinone in mtETC and as a precursor of prenyl tails in some prenylated proteins like Rab (Howe et al., 2013; Sheiner et al., 2013).

1.4.3c Haem Biosynthesis

Another crucial prosthetic group of proteins such as cytochrome is haem and for this, a de novo haem biosynthesis pathway is present in the parasite. Although abundant haem is phagocytosed by the parasite from RBCs, it is toxic, and hence, it is polymerized to hemozoin (less toxic) in parasites food vacuole (specialized lysosome). Thus, to supplement the haem requirement, the parasite performs denovo haem biosynthesis, carried out jointly in the cytosol, mitochondrion and apicoplast (Nagaraj et al., 2009; Nagaraj et al., 2010a; Nagaraj et al., 2010b; Ralph et al., 2004; Surolia and Padmanaban, 1992; van Dooren et al., 2006). The pathway is initiated in the mitochondrion when glycine is converted to δ-aminolaevulinic acid (Surolia and Padmanaban, 1992; Varadharajan et al., 2002) while the subsequent four steps take place in the apicoplast and are mediated by HemB/C/D/E, respectively (Nagraj et al., 2009; Sato 2002; Sato et al., 2004). The next step is accomplished in the Cytosol by HemF following which mitochondrial HemY and HemH come into action (van Dooren et al., 2006). The pathway thus meanders through three compartments, employing enzymes of various ancestral pathways and culminates, where it began, in the mitochondrion (Koreny et al., 2013). A recent study used *P. berghei* gene knockouts and showed that the haem biosynthetic pathway is essential in mosquito and liver stages of the parasite (Nagaraj et al., 2013).

1.4.3d Iron-sulfur cluster biosynthesis

Iron-sulfur cluster proteins have crucial biological roles, one of them being in the electron transport system. In *Plasmodium*, two pathways have been reported for Fe-S cluster biogenesis: the ISC pathway in the mitochondrion (Sato et al., 2003; van Dooren et al., 2006; Gisselberg et al., 2013) and the SUF pathway in the apicoplast (Ellis et al., 2001, Kumar et al., 2011; Gisselberg et al., 2013; Charan et al., 2014; Haussig et al., 2014; Pala et al., 2016). Since this biosynthetic pathway is the prime focus of this thesis, it will be discussed in detail in the further sections.

1.5 Iron-Sulfur (Fe-S) Clusters

1.5.1 Iron

In biology, iron is abundant and is a necessary transition metal found in nearly all living organisms, ranging from the evolutionarily primitive archea to humans. There is a wide range of oxidation states in which iron exists, starting from (-2 to +6), although +2 and +3 are the most common. Iron has wide range of functions in the biological system: it can bind proteins in mono- and di-iron reaction centers; it can be incorporated into porphyrin rings to form haem which participates in many biological oxidations and in oxygen transport; and it can be combined with elemental sulfur to form iron-sulfur (Fe-S) clusters. Iron in the various forms is also required for certain key biochemical pathways, which are essential for life on Earth, most notably respiration, nitrogen fixation and photosynthesis. In humans, iron-withholding is a major non-specific immune defence system to protect against pathogen invasions (Ratledge and Dover, 2000).

1.5.2 Sulfur

Sulfur belongs to one of the non-metallic elements which are essential for life. It is the eighth most abundant element in the human body by weight. Sulfur is involved in the biosynthesis of several vital compounds like vitamins (biotin and thiamin), amino acids (cysteine and methionine), and prosthetic groups (Fe-S clusters) in all organisms. Methionine is an essential amino acid in humans that must be ingested because other sulfur-containing amino acids like cysteine can be synthesized from methionine. The principal mechanism for sulfur incorporation in plants and microorganisms is through cysteine biosynthesis via sulfate assimilation. Sulfur in cysteine can be utilized for other sulfur containing cofactor (mainly Fe-S clusters) synthesis through a group of enzymes called desulfurases.

1.5.3 What are Iron-Sulfur Clusters?

About 3 billion years ago, when the first life emerged on Earth, oxygen was not present (predicted to be less than 0.01% of the atmosphere) (Berkner & Marshall, 1965). The anaerobic primitive earth provided a reduced environment in which iron

and sulphur species were readily available. These chemically active iron and sulfur were useful for early organisms to conduct biological processes. During the first billion years in which the earth was still anaerobic, plenty of iron and sulphur were available, possibly allowing the spontaneous generation of Fe-S clusters. Furthermore in ancient proteins, iron and sulphur together formed a complex, termed as iron-sulphur cluster to catalyze cellular reactions. In particular, Fe-S clusters are considered to be one of the most primitive iron cofactors used in biology (Wachtershauser, 1992). Despite being the earliest cofactors in the history, Fe-S clusters were discovered by Helmunt Beinert and others only in the early 1960s (Beinert et al., 1997; Rees and Howard, 2003). Around 1960, when photosynthetic organisms and nitrogen-fixing bacteria were first intensively studied, researchers recognized the significance of Fe-S clusters (Silberg et al., 1998; Ollagnier-de-Choudens et al., 2003; Balk et al., 2004). The increased catalytic efficiency of the ancient proteins that obtained Fe-S clusters by chance, led early organisms to use more Fe-S cluster enzymes. As evolution went on, the usage of Fe-S clusters expanded into important cellular processes. Thus, it was concluded that, Fe and S are highly reactive and toxic *in vivo,* and need to be combined into non-toxic forms, one of them being the Fe-S clusters. Therefore, it is not surprising that cells developed machinery devoted to the assembly of Fe-S clusters (Imlay, 2006). During the last five decades, many studies have enlightened us about the Fe-S clusters, however, still we have not been able to completely unveil the 3 billion year old secret of this ancient cofactor.

1.5.4 Structure of Fe-S clusters

The basic structure of Fe-S clusters is iron atom(s) bound to sulfur atoms of cysteine and inorganic sulphides. Based on the number of iron atoms in a cluster, it can be as simple as an $Fe(Cys)_4$ centre, which is one iron atom with four cysteine residues, or can be more complicated structures such as an [8Fe-7S] cluster. Other metals such as Mo and Ni are incorporated into Fe-S clusters in some cases (Chan et al., 1993; Volbeda et al., 1995). There are multiple types or forms of Fe-S clusters assembled *in vivo,* ranging from relatively simple [2Fe-2S] clusters, found in some classes of ferredoxin, to complex, mixed-metal clusters, such as the [Mo-7Fe-9S] cluster (or

FeMo cofactor) of nitrogenase (Peters & Broderick, 2012, Hu & Ribbe, 2014). The most common forms of Fe-S clusters, [2Fe-2S] and [4Fe-4S] (**Figure 1.3**), are usually attached to the proteins by Cys residues, but there are a few exceptions where Asp, His, Ser, or backbone amides can also coordinate clusters at single sites (Moulis et al., 1996). Fe-S clusters can form spontaneously in proteins that have the correct number and arrangement of Cys ligands *in vitro* in the presence of $Fe^{2+}/^{3+}$ and S^{2-} (Malkin and Rabinowitz 1966).

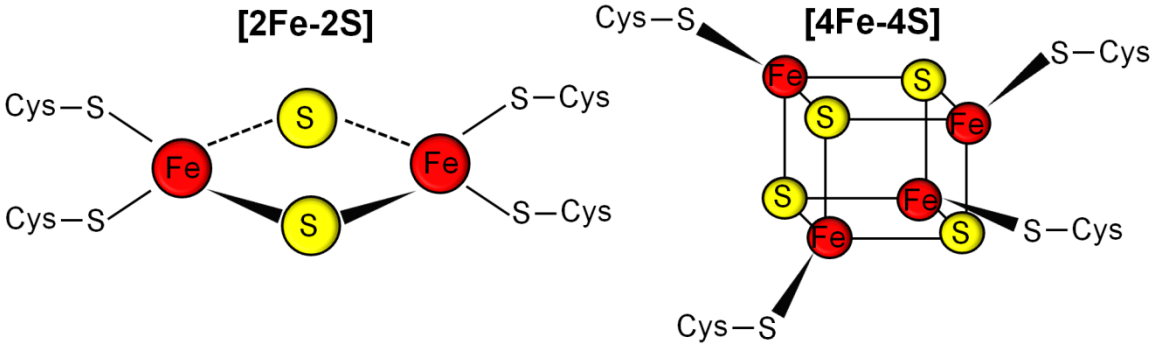

Figure 1.3: **Structure of common Fe-S clusters in nature**. (Adapted from: Rouault, 2015)

1.5.5 Functions of Fe-S clusters

Fe-S clusters, consisting of iron and elemental sulfur at diverse molar ratios have a feature of being stable at multiple oxidation states and have physiologically pertinent redox potentials (ranging from 500 to 150 mV) (Beinert and Kiley, 1999). Thus, electron transfer is a primary role for Fe-S clusters. Fe-S cluster metallo-proteins have myriad functions in a cell, ranging from amino acid biosynthesis to transcriptional regulation. Fe-S clusters also participate in substrate binding and activation of dehydratases and radical–S-adenosylmethionine enzymes (Ruzicka and Beinert 1978). Due to their sensitivity to cellular redox conditions, Fe-S clusters are also used as molecular switches for gene regulation at both the transcriptional and translational levels (Kiley and Beinert 2003). However, as mentioned above both Fe and S are highly reactive and toxic *in vivo* in their native forms and thus Fe-S cluster assembly requires highly coordinated biosynthetic pathways in living organisms.

1.5.6 Mechanism of Fe-S cluster assembly

The function of the Fe-S cluster assembly system is not only building these clusters but also delivering them to the recipient proteins. These tasks are too complicated to

be performed by just one protein. Therefore, a complex of functionally different proteins is responsible for the assembly and transfer of Fe-S clusters in living organisms. The complex consists of an iron carrier, a cysteine desulphurase for mobilization of sulphur, a scaffold protein, proteins involved in the delivery of the clusters (carrier proteins), and accessory proteins. The general mechanism is, first, a pyridoxal-phosphate (PLP)-dependent desulphurase retrieves sulfur from cysteine. Then, the iron atoms which come from an unknown source (hypothesized to be CyaY/IscA in prokaryote; frataxin in eukaryotes) and sulfur atoms from the desulphurase are transferred to a scaffold protein. These iron and sulphur atoms come together to form a Fe-S cluster, probably with the help of electron donors. Second, a part of the assembly complex facilitates the delivery of the completed Fe-S clusters to a recipient apo-protein (Barras et al., 2005) (**Figure 1.4**).

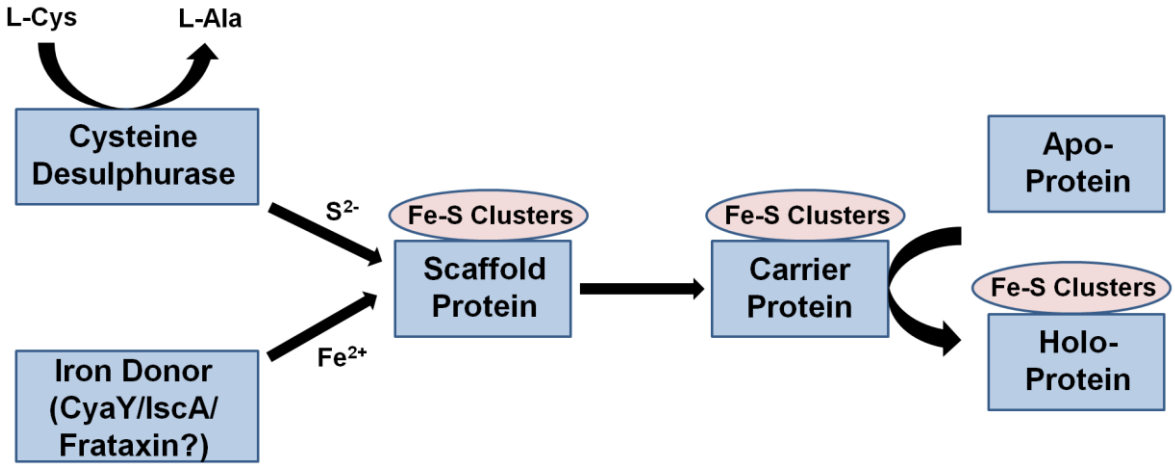

Figure 1.4: Schematic representation of the key steps and proteins involved in Fe-S cluster biogenesis.

1.6 Types of Assembly Pathways and their Distribution in Organisms

In the late 1980's Dean and colleagues reported the NIF (nitrogen fixation) system that activates nitrogenase in *Azotobacter vinelandii* (Jacobson et al., 1989; Frazzon and Dean, 2003). The NIF system was the first indication of the existence of Fe-S cluster assembly systems. Soon people realized that the mutation of the NIF system does not completely eliminate the nitrogenase activity, which implies that there is another way to activate nitrogenase. The ISC (iron sulphur cluster) system was subsequently discovered (Zheng et al., 1998). A phylogenetic study revealed that the

ISC system is distributed in most proteobacteria and in the mitochondria of eukaryotes (Tokumoto et al., 2004). A third assembly system, the so-called SUF (sulfur mobilization) system, was also found (Takahashi and Tokumoto, 2002). Surprisingly, phylogenetic analysis showed that the SUF system is present in a diverse set of organisms including most eubacteria, archaea, plants, and parasites (Tokumoto et al., 2004). Apart from the above mentioned systems, a fourth system, the CIA (cytosolic iron-sulphur cluster assembly) system is also present (**Figure 1.5**). However, the function of this system requires components from the mitochondrial ISC sytem (Roy et al., 2003; Balk et al., 2004; Balk et al., 2005; Hausmann et al., 2005). The reports of Fe-S cluster biogenesis from bacteria promoted the study of their eukaryotic counterparts. Fe-S cluster enzymes in eukaryotes are found mainly in three compartments: the cytosol, mitochondria, and the nucleus, with the fourth compartment being a plastid for only those eukaryotes bearing one (Lill and Mühlenhoff, 2008). Therefore, it has been a question whether each compartment has its own dedicated Fe-S cluster assembly system. So far, the accepted model in eukaryotes is that the mitochondrial ISC system is responsible for Fe-S cluster biogenesis in all the compartments (Barras et al., 2005; Johnson et al., 2005; Mansy and Cowan, 2004; Molik et al., 2007; Stehling et al., 2007). All these systems mentioned will be discussed in depth in the following sections.

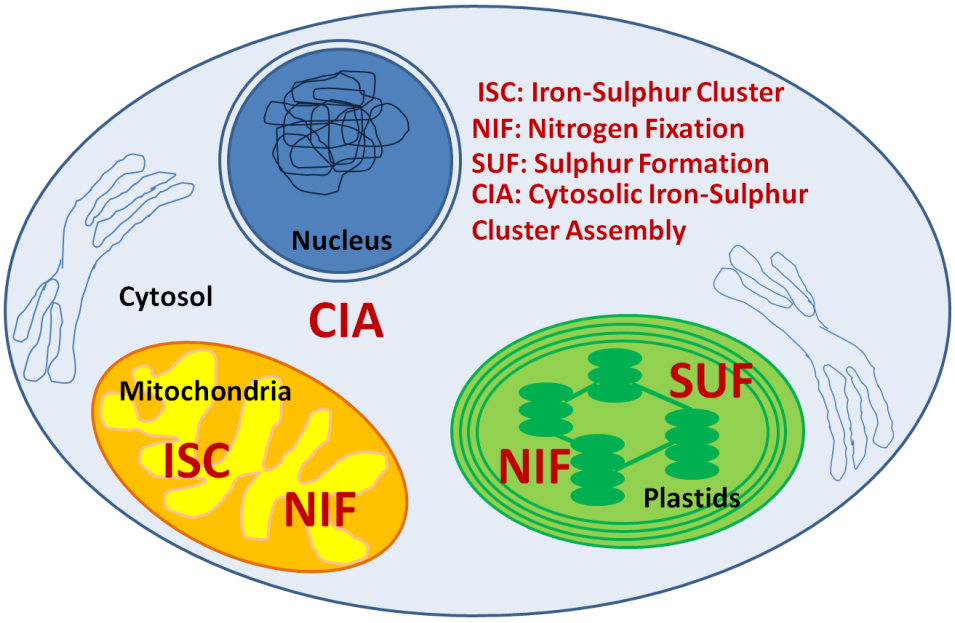

Figure 1.5: Iron sulphur cluster pathways in nature.

1.6.1 NIF Pathway for Fe-S cluster assembly

Nitrogen fixation is the process by which atmospheric nitrogen is reduced to ammonia. This chemically difficult process is catalyzed by nitrogenase, a large (~300kDa) oligomeric protein complex composed of dinitrogen reductase (the Fe protein) and dinitrogenase (the MoFe protein) (Burgess and Lowe, 1996). The dinitrogen reductase is a [4Fe-4S] containing homodimer, while the dinitrogenase is an α2-β2 tetramer coordinating eight Fe ions and two FeMo cofactors (Smith and Eady, 1992). Much of the physiological data pertaining to nitrogen fixation has been obtained from studies on *A. vinelandii*. *A. vinelandii* is a non-symbiotic, aerobic, nitrogen fixing bacterium that expresses large quantities of nitrogenase observable by the red cell pellets of diazotrophically grown cells. Bacteriological studies by Dean and colleagues found that unlike other *A. vinelandii nif* (genes encoding components required for *in vivo* nitrogenase activity) mutant phenotypes, inactivation of either *nifS* or *nifU* resulted in light brown cells lacking nitrogenase activity, i.e. nitrogenase deficient in both Fe and MoFe cofactors were produced (Dean et al., 1993). The result clearly suggested that *nifS* and *nifU* are needed for *in vivo* Fe-S cluster coordination to nitrogenase (Zheng et al., 1993; Fu et al., 1994). Subsequent work revealed that NifS is a pyridoxal 5-phosphate (PLP) containing enzyme that converts L-cysteine to L-alanine and sulfur via an enzyme-bound cysteine persulfide intermediate (Zheng et al., 1994).

Since NifS appeared to provide the sulfur necessary for Fe-S cluster formation within nitrogenase, it was hypothesized that NifU may be the iron or iron-sulfur cluster donor (Dean et al., 1993). NifU is a modular protein with amino-terminal, central, and carboxy-terminal domains (Fu et al., 1994; Hwang et al., 1996; Agar et al., 2000) where, the central domain coordinates one stable [2Fe-2S] cluster per subunit of dimeric NifU. Initially not much was known regarding the remaining domains, except that the amino-terminus contained three additional conserved cysteines, and that the carboxy-terminal region possessed two conserved cysteines. Although the role of this Fe-S cluster is not known, it is required for *in vivo* and *in vitro* formation of holo-nitrogenase (Frazzon et al., 2002).

1.6.2 ISC Pathway for Fe-S cluster assembly

The ISC system in *E. coli* is the housekeeping assembly system during normal growth of the cells. It is encoded by a seven-gene operon: *iscRSUA-hscBA-fdx*. IscR is an autoregulator for the transcription of *iscRSUA*. Holo IscR contains a [2Fe-2S] cluster and decreases the expression of IscRSUA by acting as a repressor (Schwartz et al., 2001). On the other hand, the depletion of Fe-S clusters renders IscR in the apo-form, causing the derepression of IscRSUA expression (Outten et al., 2004). The second gene in this operon encodes a desulphurase IscS. Mutation of *iscS* causes growth defects and reduced activity of Fe-S cluster enzymes, including aconitase, 6-phosphogluconate dehydratase, glutamate synthase, fumarase and NADH dehydrogenase (Schwartz et al., 2000; Lauhon and Kambampati, 2000; Djaman et al., 2004). These studies indicate that IscS is the major source of sulphur for Fe-S cluster assembly under normal conditions. Genetic analysis also revealed that IscS is a sulfur donor for thiolation process, such as tRNA modification (Kambampati and Lauhon, 2003; Lauhon et al., 2004).

Crystal structure, electron paramagnetic resonance (EPR), Mossbauer spectra analyses indicated that homodimer IscU contains [2Fe-2S] and/or [4Fe-4S] clusters (Agar et al., 2000; Chandramouli et al., 2007; Shimomura et al., 2008). In addition, *in vitro* biochemical studies showed that Fe-S clusters can be transferred from holo IscU to apo-ferredoxin, which suggests that IscU serves as a scaffold and transfer protein (Mühlenhoff et al., 2003; Ollagnier-de-Choudens et al., 2004; Wu et al., 2002). The function of IscA is quite debatable because, *in vitro* data have suggested that IscA could harbour [2Fe-2S]/[4Fe-4S] clusters or an iron atom (Huangen and Clark, 2004; Djaman et al., 2004; Morimoto et al., 2006; Ollagnier-de-Choudens et al., 2004; Zeng et al., 2007). Therefore, it could be either a secondary scaffold protein or an iron carrier. Further *in vivo* experimental validation is required to answer this question.

Long before their function in Fe-S cluster biogenesis was recognized, HscA and HscB were identified as members of the Hsp70 and Hsp40 chaperone families (Vickery et al., 1997; Silberg et al., 1998). An *hscA* mutation decreases the activity

of Fe-S cluster enzymes as low as an *iscS* mutation does, indicating the essential role of HscA in Fe-S cluster assembly (Djaman et al., 2004). Currently, HscA/HscB are thought to facilitate the transfer of a Fe-S cluster from IscU to a recipient protein by hydrolyzing ATP (Hoff et al., 2000; Silberg et al., 2001; Cupp-Vickery et al., 2004). The last member of the ISC system is ferredoxin (fdx), containing a [2Fe-2S] cluster. Like other *isc* mutants, an *fdx* mutant has growth defects and the reduced activity of Fe-S cluster enzymes (Djaman et al., 2004). The nature of the ferredoxin family leads to an idea that Fdx donates an electron at some point during Fe-S cluster biogenesis. However, the specific *in vivo* role of Fdx still remains to be unveiled.

1.6.3 SUF Pathway for Fe-S cluster assembly

Since the discovery of the ISC system in *E. coli*, Tokumoto and his colleagues sought mutations that suppress deletion of the ISC system. Most of the suppressors had mutation that could potentially induce the *suf* operon (*sufABCDSE*) (Takahashi and Tokumoto, 2002). In subsequent experiments, they found that the over-expression of SufABCDSE complements most defects in the *isc* deletion mutants (Takahashi and Tokumoto, 2002).

SufA, the first member of the *suf* operon, shares 40% amino acid sequence identity with IscA (Ollagnier-de-Choudens et al., 2004). SufA is able to assemble Fe-S clusters and transfer them to the apo-protein recipients *in vitro* (Ollagnier-de-Choudens et al., 2003; Ollagnier-de-Choudens et al., 2004). The role of SufA, however, is unclear due to lack of *in vivo* data. The proteins encoded by the following three genes, *sufBCD*, are thought to make a complex ($SufBC_2D$) (Rangachari et al., 2002; Nachin et al., 2003; Outten et al., 2003) where, SufC is an atypical member of the ABC-ATPase superfamily (Kitaoka et al., 2006). Unlike other ABC transporters, the SufBCD complex localizes in the Cytosol of *E. coli*, which raises an intriguing question about the function of its ATPase activity (Nachin et al., 2003; Outten et al., 2003). Since SufBCD is postulated as a scaffold, it may work as the ATP dependent IscU/HscAB complex. The SUF system also contains a desulphurase SufS. The poor desulphurase activity of SufS in early studies puzzled

researchers (Mihara et al., 1997; Mihara et al., 2000). Subsequent studies revealed that another member of the SUF system, SufE, binds to SufS and increases the SufS desulphurase activity to a level comparable to IscS (Loiseau et al., 2003; Ollagnier-de-Choudens et al., 2003; Outten et al., 2003; Tirupati et al., 2004) thus, making SufSE complex a true desulphurase rather than SufS alone. Moreover, the addition of the SufBCD complex increases SufSE activity even higher (Layer et al., 2007).

1.6.4 Regulation of the ISC and SUF system

The general function of the ISC and the SUF systems seem redundant. A query would be why *E. coli* has the SUF system, since, unlike *isc* mutations, *suf* mutations did not significantly change the activity of Fe-S cluster enzymes (Djaman et al., 2004). Differences in regulation suggest that ISC and SUF may be expressed under different conditions. As described earlier, the ISC system is regulated by the pool of Fe-S clusters, which IscR senses (Schwartz et al., 2001; Giel et al., 2006). The cluster synthesis is co-ordinated by IscR where, the transcription of the *isc* operon is repressed by [2Fe-2S]-IscR and the expression of the *suf* operon is activated. In the absence of ISC, IscR-dependent SUF activation is vital as, the organisms lacking both the ISC pathway and IscR did not survive unless the SUF system is expressed ectopically. The removal of IscR binding site in the *sufA* promoter also necessitates the requirement for ISC. It is hypothesized that due to increased IscR levels the SUF expression is increased in a Δ*isc* mutant. Additionally, Fur derepression is insufficient for viability in the absence of IscR and the ISC pathway, highlighting the importance of direct IscR activation. Also, the SUF expression is increased to the highest level in a mutant lacking Fur and the ISC pathway and it almost restored [2Fe-2S]-IscR activity, thus, suggesting a mechanism for regulating IscR activity under stress conditions. Thus, IscR, seems to be the key molecule involved in the regulation of different Fe-S cluster biogenesis pathways.

1.6.5 CIA Pathway for Fe-S cluster assembly

The CIA system is considered as a cytosolic Fe-S cluster assembly system. Present in eukaryotic organisms, most components of CIA system also have counterparts in *Arabidopsis thaliana* based on the amino acid sequence similarity. Because of the

absence of a cytosolic cysteine desulfurase, this function of procuring sulphur depends on the mitochondrial ISC machinery. The requirement of mitochondrial Nfs1 for the assembly of extra-mitochondrial Fe-S proteins in yeast and human has been shown (Mühlenhoff et al., 2004; Kispal et al., 2005; Biederbick et al., 2006). Its significant role has been highlighted in recent years by the identification of several Fe-S proteins involved in DNA/RNA metabolism (White and Dillingham, 2012; Wu and Brosh, 2012). The electrons required for the Fe-S cluster assembly are provided by the complex of the reductase Tah18 and Dre2 which are a part of an electron transfer chain that functions in the CIA machinery (Netz et al., 2010). P-loop NTPases; Cfd1 and Nbp35 function as scaffolds for this Fe-S cluster assembly (Hausmann et al., 2005) while, the final step involving the transfer of the assembled clusters is carried out by Nar1 and Cia1 (Balk et al., 2004, 2005). This hypothesis suggest that the interplay between the mitochondrial ISC system, the ISC export machinery and the cytosolic machinery give rise to cytosolic, mitochondrial and nuclear Fe-S proteins in eukaryotes (Xu and Møller, 2008).

1.6.6 Other proteins involved in Fe-S cluster assembly

Another desulphurase, CsdA (cysteine sulfinate desulphurase), was discovered by a search of the *E. coli* genome (Mihara et al., 1997). Although the highest *in vitro* desulphurase activity of CsdA compares to those of IscS and SufS, no obvious phenotype was observed in a *csdA* mutant (Lambeth et al., 2007). Recently, a possible role of CsdA in Fe-S cluster assembly, which is mediated by SufBCD complex was also postulated (Trotter et al., 2009). However, since the experiment was done with over-expressed CsdA from a plasmid, its involvement in Fe-S cluster biogenesis is still unclear.

Frataxin is a protein that is conserved from prokaryotes to eukaryotes (Huynen et al., 2001). In humans, a deficiency of frataxin causes Friedreich's ataxia, a neurodegenerative disorder (Puccio and Kœnig, 2000). Research on Yfh1, a yeast homologue, revealed that the deletion of Yfh1 causes decreased activity of Fe-S cluster enzymes as well as accumulation of iron in mitochondria, which suggests that Yfh1 has a role in Fe-S cluster biogenesis (Babock et al., 1997; Foury and

Cazzalini, 1997; Wilson et al., 1997; Chen et al., 2002; Duby et al., 2002; Mühlenhoff et al., 2002). The current functional hypothesis is that Yfh1 is an iron carrier. *E. coli* also has a frataxin homologue, CyaY. Although it shows iron-binding capacity *in vitro* and interaction with IscS *in vivo*, no phenotypes have been observed for cyaY mutant (Layer et al., 2006; Adinolfi et al., 2009).

ErpA and NfuA are other so-called scaffold, as are IscA and SufA (Loiseau et al., 2007; Angelini et al., 2008). The functions of these two are believed to be similar to those of IscA and SufA. The hypothesis is that each A-type scaffold delivers Fe-S clusters to a specific subset of recipient apo-proteins. And this hypothesis needs more experimental validation.

1.7 Components of SUF System for Fe-S cluster assembly

Since the major aim of this work is focussed on the SUF pathway for Fe-S cluster assembly, the further sections would elaborate on individual components of this pathway.

1.7.1 Cysteine Desulphurases

The cysteine desulfurases involved in the Fe-S cluster assembly can be classified into group I and group II on the basis of overall sequence homology. Based on the above classification, NifS and IscS belong to group I whereas SufS and CsdA belong to group II cysteine desulphurases (Mihara et al., 1997). Two different consensus sequences present around the active-site Cys residue in the C-terminal domain of the enzyme distinguish these two groups from each other. Group I enzymes contain the conserved SSGSACTS sequence, while the group II enzymes contain the sequence RXGHHCA. These different groups of cysteine desulphurases have vital structural and enzymatic differences but the biochemical reason for these differences in the conserved regions is lacking.

Cysteine desulphurase, SufS, catalyzes the sulfur donation, *via* donation of a persulfide to the scaffold protein. The reaction mechanism of cysteine desulfurases with slight but not essential differences have been proposed (**Figure 1.6**). The

reaction starts with binding of L-cysteine to the active site of the enzyme followed by the nucleophilic attack of the deprotonated amino group of the substrate on the C4′ of PLP to produce the external aldimine and release the neutral side chain of the Lys residue. Next, the α-proton of the substrate is eliminated to yield a quinonoid intermediate. Following this, it is proposed that the active site Cys or Lys adds a proton to the C4′ of the quinonoid intermediate, producing the substrate-ketamine intermediate. A nucleophilic attack by the deprotonated Cys residue on the substrate-ketamine intermediate then forms an enzyme-bound cysteine persulfide (Cys–S–SH) and the enamine. The protonation at Cβ of the aminoacrylate moiety in the final few steps leads to the formation of the alanine-ketamine intermediate, which is followed by transaldimination with the catalytic Lys residue to release the product L-alanine (Zheng et al., 1994; Mihara et al., 2000, Behshad et al., 2004; Behshad and Bollinger, 2009, Hidese et al., 2011).

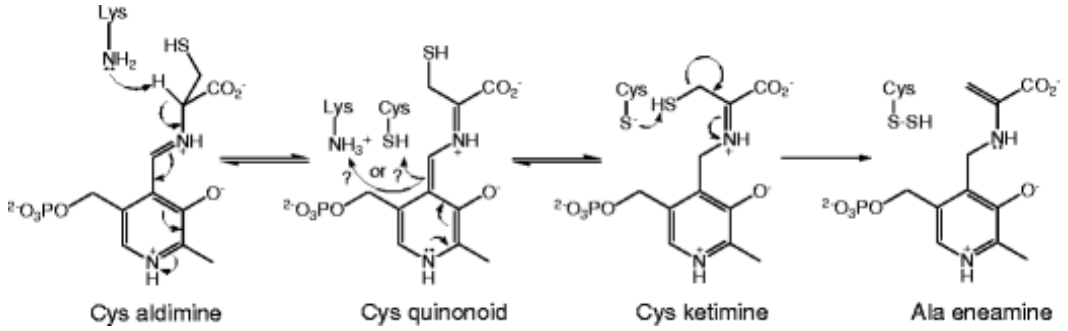

Figure 1.6: Proposed mechanism for mechanism of cysteine desulphurase. (Hidese et al., 2011).

The partner protein, SufE accepts sulfane sulphur from SufS and enhances the cysteine desulphurase activity of SufS upto 8 folds. Finally, this sulphur is transferred to SufBCD complex for Fe-S cluster assembly.

1.7.2 SufBCD Complex

The simplest *suf* operon which consists of minimal functional core is composed solely of *sufBC* (Takahashi and Tokumoto, 2002; Boyd et al, 2015). Despite the presence of SufB and SufC in many archaea and bacteria, they have been most comprehensively explored at the biochemical and genetic levels only in bacteria (specifically *E. coli* and *Erwinia chrysanthemi*). When iron and sulfide salts are provided as starting materials, the *E. coli* SufB protein triggers Fe–S cluster assembly and insertion of a $[2Fe\text{-}2S]^{2+}$ cluster into the adrenodoxin-like ferredoxin

protein Fdx (Chahal and Outten, 2012). During *in vitro* reconstitution, SufB also assembles a stable $[4Fe\text{-}4S]^{2+}$ cluster and it can accept sulfane sulphur from SufE (Layer et al., 2007; Wollers et al., 2010). This indicates the possibility of SufB being a novel scaffold protein for the SUF pathway.

The *E. coli* SufD is said to be the duplicated form of SufB gene and hence both these proteins are homologous to each other throughout their C-terminal domain, while showing divergence at the N-terminal region. There are 13 Cys residues in the SufB amino acid sequence, with 4 highly conserved Cys residues. In contrast, the *E. coli* SufD consist only three Cys, of which only one is highly conserved, thus raising questions about the formation of a Fe-S cluster on SufD. A putative Fe-S binding motif, $C\text{-}X_2\text{-}C\text{-}X_3\text{-}C$, is present in the N terminus of *E. coli* SufB, although this motif is not strictly conserved in more divergent SufB homologues. The SufD amino acid sequence contains 23 His residues compared to SufB sequence, which has only 12 His residues. Eight out these 23 His residues in SufD are arranged in two repeating patterns of H-X11 or 13-H-X2-HX13-H. These motifs may be used for iron binding, as the imidazole moiety of His residues is an excellent ligand for ferrous iron coordination (Badger et al., 2005). Thus, there is a possibility that SufD could provide a Fe-S ligand (such as Cys or His) once it is bound in a complex with SufB and SufC.

SufB and SufD interact directly with the SufC protein, to form the SufBCD complex (Nachin et al., 2003; Outten et al., 2003; Rangachari et al., 2002). These interactions possibly occur between the C-terminal regions of SufB and SufD with the SufC protein. SufC is known as a canonical ABC transporter ATPase subunit with conserved Walker A and Walker B motifs as well as the Q loop and D loop motifs. The crystal structure of *E. coli* SufC suggests that it is an atypical member of the ABC-ATPase superfamily. This is because of the irregular structural position of Glu171, a highly conserved residue playing a crucial role of catalytic base in the conversion of ATP to ADP and Pi. The Glu171 is flipped out of its usual orientation in the *E. coli* SufC structure, ensuing in low basal ATPase activity for SufC (Kitaoka et al., 2006). The rate of ATP hydrolysis by SufC is stimulated up to 100-fold by

addition of SufB, perhaps by supplying a catalytic residue or by causing reorientation of SufC Glu171 (Eccleston et al., 2006). The role of the SufC ATPase activity *in vivo* is yet unknown. It is hypothesized that SufC ATPase activity may be involved in some other step of cluster assembly, such as iron acquisition or cluster transfer to apoprotein (Eccleston et al., 2006; Outten et al., 2003). Fascinatingly, SufB must be in a complex with SufC for SufB to interact with SufE for sulfur transfer (Layer et al., 2006). Hence, both the stimulation of SufC ATPase activity and SufE sulfur transfer to SufB occurs simultaneously, providing a harmonized regulation of these two important processes during Fe-S cluster assembly (Ayala-Castro et al., 2008).

1.7.3 Scaffold Proteins

The final step of the pathway involves the assembly and the transfer of the Fe-S clusters, which is facilitated by scaffold proteins. The broad classification of the scaffold proteins includes two categories A-type and U-type. The A-type scaffold proteins contain three highly conserved Cys residues in the C-X_{42-44}-D-X_{20}-C-G-C conserved motif present in their C-terminal regions. The exact function of the A-type scaffold proteins in Fe-S cluster assembly is unclear, however, two hypotheses for its biochemical function have been postulated. The first one suggests that the A-type proteins are alternative Fe-S scaffolds and may act as a scaffold for the assembly of the Fe-S clusters. In this model, the A type scaffolds may act as carriers for cluster donation to a subset of Fe-S apo-proteins or may act as intermediates in cluster transfer from U-type scaffolds to apo-proteins. The probability of them acting as intermediates has some evidence in the ISC system where *in vitro* studies have revealed that IscA can accept a cluster from IscU but it cannot transfer a cluster to IscU (Ollagnier-de-Choudens et al., 2004). The second hypothesis suggests that the A-type scaffolds are iron chaperones and they donate iron for Fe-S cluster assembly on U-type scaffolds. But, there is no noteworthy experimental evidence in support of this hypothesis (Ayala-Castro et al., 2008).

Functional, structural, and genomic analyses of U-type proteins revealed at least four noteworthy differences between IscU/NifU- and SufU-type proteins where SufU

shows the following features: (1) the presence of an adjacent gene coding for class II cysteine desulfurase SufS, (2) the insertion of 18−21 amino acid sequence between the second and the third cysteine residues in SufU, (3) a conserved lysine residue occupying the position of the essential histidine preceding the third conserved cysteine, and (4) its ability to increase the rate of alanine formation of SufS by nearly 200 fold (Selbach et al., 2013). The involvement of a thiol group of SufU during sulfur transfer from SufS persulfide sulfur to a cysteine residue of SufU was proven by alkylation experiments (Selbach et al., 2010). Mutagenesis studies showed that all three cysteine residues were obligatory for the SufU sulfur transferase activity, while only the Cys41 to Ala substitution retained its capability to interact with SufS (Albrecht et al., 2010). Subsequent structural analysis of SufU from *B. subtilis* and *Streptococcus pyogenes* indicated the presence of a zinc atom coordinated by these three essential cysteine residues along with a conserved aspartate residue (Kornhaber, et al., 2006; Liu et al., 2005). Whether this zinc atom examined in these protein structures is strongly bound or is just an element required for the reactivity of SufU has not been experimentally validated.

1.8 SUF Pathway in *Plasmodium*

The distribution of the SUF genes is limited to major groups of archaea and bacteria, as well as plastid-containing organisms (Ellis et al., 2001). Very few organisms contain all the SUF genes. Only *sufB* and *sufC* occur invariably together in the bacterial genomes. Although a few pathogenic bacteria appear to lack the entire *suf* operon, *sufB* is still maintained in the plastid genome of the apicomplexan parasite *P. falciparum* (Wilson et al, 1996). The pioneering work of Ellis and colleagues in the early 2000's gave the first evidence of the presence of SUF pathway genes in *Plasmodium* (Ellis et al., 2001). Following this report, nearly after a decade the first experimental evidence of the SUF pathway was given by Dr. Habib's lab (Kumar et al., 2011).

To start with the SUF pathway, the initial components of the pathway i.e the cysteine desulphurases were recently characterized in *P. falciparum*. In two distinct studies it was shown that *Pf*SufS complements the loss of *E. coli* SufS and functions

as a PLP-dependent cysteine desulphurase enzyme. Like the bacterial SufE, the *Plasmodium* SufE is also crucial for enhancing the activity of SufS. The reverse genetics findings in *P. berghei* also indicate that *Pb*SufS and *Pb*SufE perform critical functions during blood infection of the malarial parasite. Also, apicoplast was shown to be the functional site of the two enzymes suggesting a functional SUF pathway in the apicoplast of the parasite (Gisselberg et al., 2013; Charan et al., 2014; Haussig et al., 2014).

The next step in the pathway involves the SufBCD complex. As mentioned earlier, in *Plasmodium* spp., the gene encoding for SufB is retained by the apicoplast genome but the gene encoding for SufC have been translocated to the nucleus. The *P. falciparum* SufB orthologue is predicted to possess transmembrane regions and in addition exhibits ATPase activity, as observed for the *Arabidopsis* plastid SufB (Moller et al., 2001; Xu et al., 2005), signifying acquisition of supplementary specialised roles by SufB in plastids compared to the bacterial counterparts. *P. falciparum* SufC on the other hand, like the *E. coli* SufC, is a member of the ABC superfamily with a conserved nucleotide-binding domain but it lacks a transmembrane domain (Koenderink et al., 2010). However, a fraction of SufC has been shown to be carbonate-insoluble which is indicative of the fact that SufC has a peripheral membrane association (Kumar et al., 2011). Another report indicated that the disruption of *P. falciparum sufC* gene, resulted in inactivation of apicoplast Fe-S proteins, confirming the vitality of the SUF pathway for apicoplast maintenance and parasite survival in erythrocytic stages of the parasite life cycle (Gisselberg et al., 2013). Further, systematic experimental genetics study in *P. berghei* also revealed that, *sufC* and *sufD* are refractory to gene deletion and, hence, may be considered essential for blood stage proliferation (Haussig et al., 2014).

The final step involves the assembly and transfer of the Fe-S clusters. The only available data for the proteins involved in this step is from *P. berghei*. Targeted deletion of genes encoding for potential Fe-S transfer proteins namely *Pbsuf*A and *Pbnfu*api was achieved, indicative of a dispensable role during asexual blood stage growth *in vivo* (Haussig et al., 2013; Haussig et al, 2014). Thus, from the above

review of literature, it is clear that there is a huge lacuna still remaining in the assembly and transfer of Fe-S clusters in *Plasmodium* with no reports from the less studied and neglected parasite *P. vivax*.

1.9 Gaps in Existing Research

As mentioned earlier, there are several shortcomings in the development of a vaccine against malaria and with the currently available chemotherapeutics losing their efficacy, there is an urgent need for the discovery of novel drug targets. For this, the prokaryotic non-photosynthetic plastid called apicoplast is looked upon as a putative drug target due to the presence of indispensable metabolic pathways functional in it. Most of the enzymes involved in these metabolic pathways are nuclear encoded and apicoplast targeted. They are conserved throughout the *Plasmodium* species and apicomplexans and cannot be replaced by any other components thus, making these pathways indispensible for parasite survival.

The most extensively studied metabolic pathways functional in apicoplast are the fatty acid biosynthesis and heme biosynthesis pathway, whereas a gap in our understanding remains for the less studied isoprenoids biosynthesis and Fe-S cluster biosynthesis pathway. The first report of characterization of *P. vivax* IspG, an enzyme involved in the pen-ultimate step of the Isoprenoids biosynthesis pathway was recently given by our lab (Saggu et al., 2017). This directs the focus of this thesis to the final pathway which is yet unexplored in *P. vivax*: the SUF pathway for Fe-S cluster biogenesis. All the reports available till date for this pathway are available only in *P. falciparum* and *P. berghei* creating a lacuna in our knowledge of this pathway in the less studied but equally virulent parasite *P. vivax*. Apart from this, the components studied in the above two parasites, are also not functionally characterized. Therefore, a complete detailed study of the components of this pathway becomes the need of the hour for the development of an effective treatment strategy in future.

1.9.1 Aims and Objectives

- To identify/investigate the components of the SUF pathway from *Plasmodium vivax.*
- Expression profiling and immune-localization of major components of the SUF pathway.
- *In silico* and *in vitro* biochemical characterization of these components for elucidation of complete SUF pathway in *P. vivax.*

1.9.2 Organization of Thesis

This work aims to characterize the proteins involved in the SUF pathway for Fe-S cluster biogenesis from *P. vivax*. The thesis is organized according to the aims set as above. Chapter 1 is an introduction of the problem based on literature available till date. Chapter 2 gives general information related with various materials and methods used to achieve the proposed objectives. Chapter 3 and 4 details the characterization of the cysteine desulphurases *Pv*SufS and *Pv*SufE respectively. Chapter 5 details the structural and functional characterization of scaffold protein *Pv*SufA, Chapter 6 details interaction of different components of the SUF pathway to elucidate the complete pathway from *P. vivax* and Chapter 7 lists the various conclusions drawn out of the complete work and the future prospects of the work.

Chapter II

Materials and Methods

MATERIALS AND METHODS

2.1 Short listing of genes involved in Fe-S cluster biosynthesis SUF pathway

In *Plasmodium*, SUF pathway for the Fe-S cluster biosynthesis is believed to be functional inside the organelle known as apicoplast. Despite the fact, that apicoplast possess its own DNA, most of the proteins involved in this pathway are synthesized by the parasite nucleus and targeted to the apicoplast by the help of a bi-partite N-terminal leader sequence containing a signal and transit peptide. Thus, the proteins involved in this pathway belong to the category known as NEAT proteins (Parsons et al., 2007). However, in the SUF pathway, one of the components SufB is encoded by the apicoplast genome. There are over 300 proteins in *Plasmodium vivax* (Carlton et al., 2008) and over 500 proteins in *Plasmodium falciparum* (Gardner et al., 2002) which are believed to be targeted to the apicoplast to participate in various housekeeping and metabolic functions.

In the present study, the proteins hypothesized to be functional in the SUF pathway were identified from the **PlasmoDB (**Aurrecoechea et al., 2009) database based on the presence of conserved domains and signature motifs as predicted by **Conserved Domain Search** (Marchler-Bauer et al., 2015) tool from **NCBI** and **PROSITE** (Sigrist et al., 2002) from **ExPASy**, respectively. Like the plants possess translocons of the Inner and Outer Chloroplast (Tic-Toc) membrane complexes, *P. falciparum* also have Tic-Toc membrane complexes which aid in transport of a NEAT protein through the last pair of apicoplast membranes (van Dooren et al., 2002). Based on analyses of Transit peptide (TP) in the amino acid sequences of apicoplast-targeted proteins in *P. falciparum*, software algorithms **PlasmoAP** (Foth et al., 2003) and **PATS** (Zuegge et al., 2001) were developed to allow prediction of *Plasmodium* proteins for apicoplast import. PlasmoAP is based on an algorithm that uses amino-acid frequency and distribution to identify putative apicoplast-targeting peptides, while PATS utilizes neural network, which has been trained with known apicoplast targeting and non-targeting proteins in *P. falciparum* to determine the apicoplast transit peptide. To analyze for the presence of apicoplast transit peptide in our

sequences, PlasmoAP and PATS were used. We also checked for mitochondrial targeting using servers like **MitoProtII** (Claros and Vincens, 1996) and **PlasMit** (Bender et al., 2003), which calculates the N-terminal protein region that can support a mitochondrial targeting sequence and the cleavage site. This was essential as the other pathway for Fe-S cluster biogenesis i.e. ISC pathway is said to be functional in the mitochondria. While the PlasMit server specifically predicts mitochondrial targeting in proteins of *Plasmodium,* MitoProtII can be employed to the proteins from any organism. Some sequences showing targeting to both apicoplast and mitochondria, suggests their dual targeting demanding further experimental verification.

2.2 Study site and Malaria infected blood sample collection

P. vivax infected patient's blood samples (3-6mL) were collected by trained clinicians at P. B. M. and associated group of Hospitals, Bikaner, Rajasthan, India. They were preserved either in acid citrate dextrose (ACD) anticoagulant for DNA isolation or in Tri-Reagent after separating RBCs from Peripheral Blood Mononuclear Cells (PBMCs) using density gradient separation for RNA isolation. The infections in these samples were clinically detected by standard Microscopy and Rapid Diagnostic Tests (OptiMAL® and Falcivax). A formal approval of participating Institute's Human Ethics Committees (Approval No. IHEC-35/13-14) and consent of patients was obtained for further studies. These samples were then shipped to our lab at BITS Pilani in cold chain where they were stored at -70°C.

2.3 Parasite DNA isolation

Parasite DNA was extracted from blood samples collected from study site using standard protocols with slight modification (Sambrook and Russell, 2001; Saxena et al., 2007) as described below:

Reagents

1. Lysis buffer (1X): 10mM NaCl; 50mM Tris (pH=8.0); 10mM EDTA (pH=8.0); 1% SDS
2. Lysozyme (50mg/mL) (Ameresco)
3. Proteinase K (20mg/mL) (Merck Bioscience)

4. RNase A (20mg/mL) (Merck Bioscience)
5. 3M Sodium Acetate (pH 5.2)
6. Tris-saturated Phenol (pH 8.0)
7. Chloroform : Isoamyl alcohol (24:1)
8. Absolute alcohol (99.5%) and 70% Ethanol

The *Plasmodium* parasite infected frozen blood samples were thawed at room temperature, and transferred to a micro-centrifuge tube. The extraction procedure was based upon the lysis of cells with equal volume of 1X lysis buffer. Contents were mixed properly by repeated inversion followed by centrifugation at 10,000 rpm for 10 min at 4°C (Eppendorf, Germany). Supernatant was decanted and the pellet was re-suspended in 2X lysis buffer. RNase A was added to a final concentration of 20µg/mL and the sample was incubated at 37°C for 15 min. Following this, lysozyme was added (final concentration of 100µg/mL) and the sample was incubated at 37°C for 45 min in a water bath. To digest the proteins, Proteinase K was added to a final concentration of 100µg/mL and mixture was incubated at 50°C with frequent mixing (water bath) for 2-2.5 hrs. A conventional phenol: chloroform: iso-amyl alcohol (25:24:1) extraction was performed to remove proteins and DNA was precipitated from the aqueous phase using chilled absolute ethanol in the presence of 0.3M sodium acetate at -20°C overnight. The precipitated DNA was pelleted by centrifuging the tubes at 8,000 rpm for 30 min at 4°C. The pellet was washed with 70% ethanol to remove excess of salts, air dried and re-dissolved in 1X TE buffer (pH 8.0). Integrity of DNA was checked using agarose gel electrophoresis and DNA fragments were viewed in UV gel documentation (Syngene USA) (**Figure 2.1**). Purity of DNA was checked by UV-vis Spectrophotometer (Simpli Nano GE, UK).

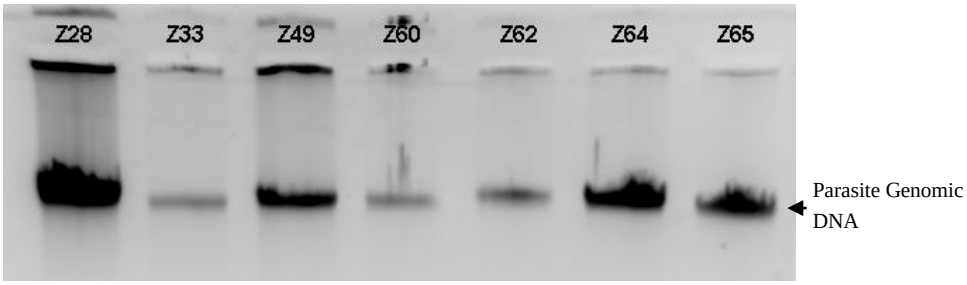

Figure 2.1: DNA isolation from the patient's blood infected with *Plasmodium* (Z28, Z33, Z49, Z60, Z62, Z64, Z65 are the field isolates).

2.4 Confirmation of parasite infection

The samples collected from hospitals were thoroughly checked by trained technicians using Microscopy for detecting type of infection and further confirmed using Rapid-Diagnostic Kits (RDTs) such as Optimal (for *P. falciparum* and non- *P. falciparum* antigens) or FalciVax (for both *P. falciparum* and *P. vivax* antigens). However in areas like Bikaner both *P. falciparum* and *P. vivax* infection coexists, and hence there are chances of misdiagnosis of parasite infections. To ensure, the type of infection as *P. falciparum* or *P. vivax* or a combination of both, a diagnostic PCR based on 18S rRNA gene (Das et al., 1995; Kochar et al., 2005) and 28S rRNA gene (Pakalapati et al., 2013) amplification was performed.

2.4.1 Diagnostic PCR based on 18S rRNA gene

It is a multiplex PCR, which involves a single forward universal primer for the genus *Plasmodium* and two reverse species specific primers for *P. vivax* and *P. falciparum* (**Table 2.1**). The reaction conditions utilized are shown in **Figure 2.2**. The presence of *P. falciparum* is indicated by a ~1400bp amplicon whereas, *P. vivax* shows a ~500bp amplicon (**Figure 2.3**) (Das et al., 1995; Kochar et al., 2005).

Table 2.1 Diagnostic Primers for 18S rRNA gene amplification by Multiplex PCR

Primer sequence	Detection	Orientation
5’ ATC AGC TTT TGA TGT TAG G GT ATT G 3’	Genus Specific	Forward
5’ TAA CAA GGA CTT CCA AGC C 3’	*P. vivax*	Reverse
5’ GCT CAA AGA TAC AAA TAT AAG C 3’	*P. falciparum*	Reverse

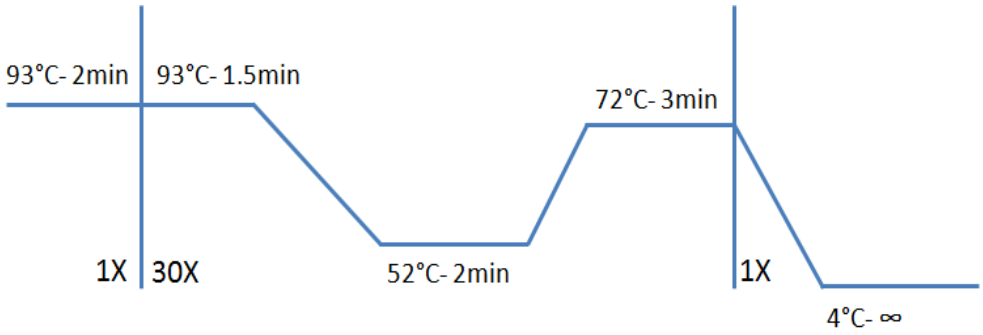

Figure 2.2: Reaction conditions used in multiplex PCR

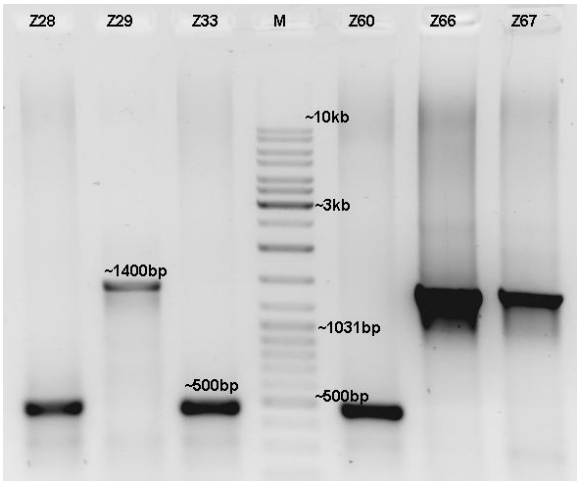

Figure 2.3: Parasite infection confirmed by multiplex PCR based on 18S rRNA gene amplification (M= Gene ruler DNA Ladder mix (SM0331 Fermentas). Z28 to Z67 are the field isolates; Z28, Z33, Z60 = *P. vivax* infected samples; Z29, Z66, Z67 = *P. falciparum* infected sample).

2.4.2 Nested PCR based on 28S rRNA

This PCR involves a primary reaction (**Figure 2.4 a**) that serves as a positive control while the second nested PCR (**Figure 2.4 b, c**) finally diagnoses the type of infection (Pakalapati et al., 2013). Primers used in the primary reaction are designed from a region common to 28S rRNA gene of human, *P. falciparum* and *P. vivax* and gives an amplification of ~790bp. For the nested amplification, 0.5µL of the amplicon from the above primary reaction is used as a template DNA. The nested PCR 1 using primers NPV2 and NPVR amplifies ~294bp region specific for *P. vivax* 28S rRNA gene, while the nested PCR 2 amplifies ~286bp region specific for *P. falciparum* 28S rRNA gene. The primers used for these primary and nested PCR are given in **Table 2.2** while the reaction conditions utilized are shown in **Figure 2.4**. The samples showing the band at desired position were utilized for further studies (**Figure 2.5**).

Table 2.2 Diagnostic Primers for 28S rRNA gene amplification by Nested PCR

Lab Id	Primer sequence	Detection	Orientation
NUF	5’ GAT TTC TGC CCA GTG CTT TGA ATG T 3’	Human, Pf & Pv	Forward
NUR	5’AAT GAT AGG AAG AGC CGA CAT CGA A 3’	Human, Pf & Pv	Reverse
NPV2	5’ TCG GTT CGC CGG GTA TTC ATA TT 3’	*P. vivax*	Forward
NPVR	5’ CAC AGT AGG AAG ATA AAT TCC T 3’	*P. vivax*	Reverse
NPF1	5’ TAT CCT TCG GGA AGG CAT TCT G 3’	*P. falciparum*	Forward
NPF2	5’ CTA TAT GCA CAG TAG TAA GTA ATT TA 3’	*P. falciparum*	Reverse

a) Primary Reaction condition:-

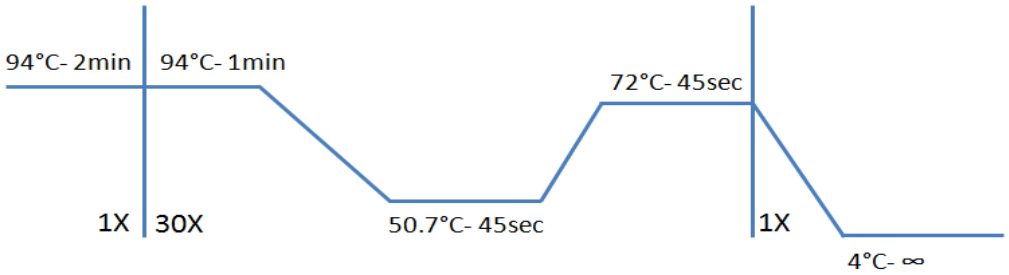

b) Nested PCR 1 (*P. vivax* specific) Reaction conditions:-

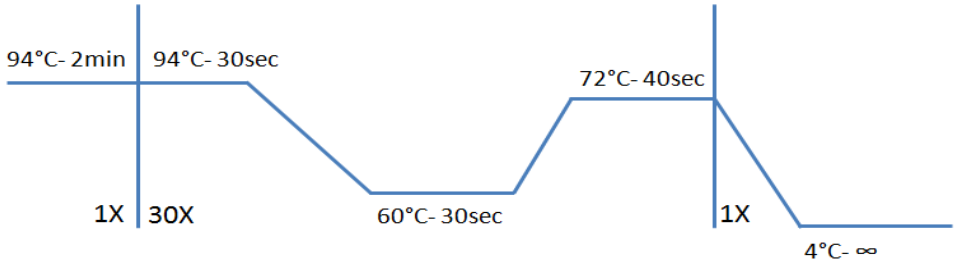

c) Nested PCR 2 (*P. falciparum*) Reaction conditions: -

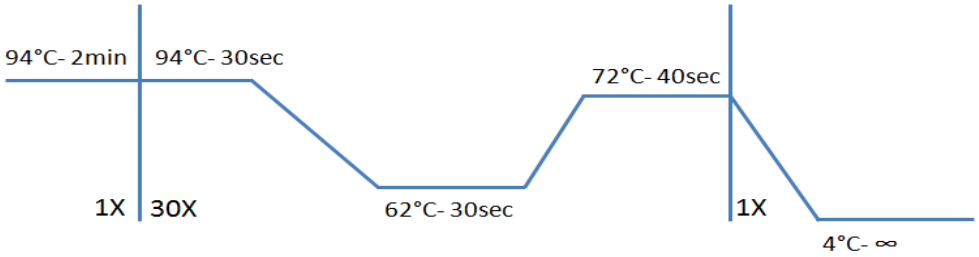

Figure 2.4: Reaction conditions used for primary and nested PCR

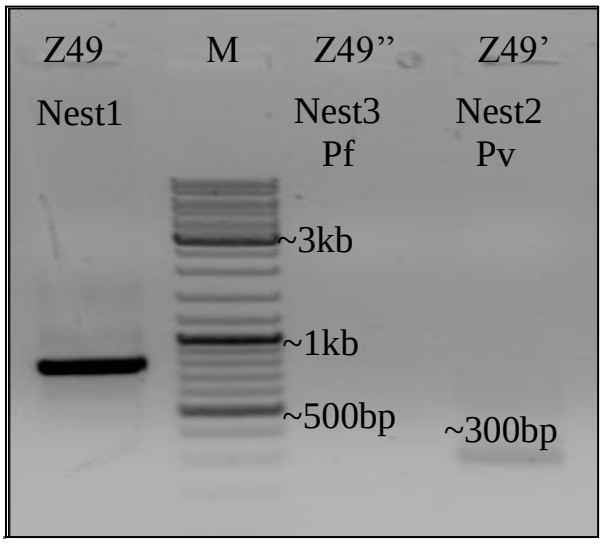

Figure 2.5: Parasite infection confirmed by Nested PCR based on 28S rRNA gene amplification

[M= Gene ruler DNA Ladder mix (SM0331 Fermentas); Z49 is a parasite field isolate]

2.5 RNA/DNA Extraction from samples preserved in Tri-Reagent

Total RNA was extracted from the RBC fraction of parasite infected blood samples preserved in Tri Reagent (Sigma Aldrich, USA). For this the parasite infected erythrocytes were separated from peripheral blood mononuclear cells (PBMCs) immediately after collection using density gradient centrifugation (Histopaque 1077, Sigma Aldrich, USA) according to manufacturer's instructions. Erythrocytes were washed with phosphate buffered saline (1X PBS), lysed using Tri-Reagent (Sigma Aldrich, USA) and preserved immediately at −80°C. All the samples were then transported in dry ice to BITS, Pilani for further processing.

2.5.1 RNA extraction

Reagents used:

1. Di-ethyl Pyrocarbonate (DEPC) (SIGMA)
2. Back Extraction Buffer: 4M Guanidine thiocyanate, 50mM Sodium citrate, 1M Tris (pH= 8.0).
3. Bromo-chloro propane (BCP) (SIGMA)
4. Isopropanol
5. 70% ethanol
6. 10X MOPS electrophoresis buffer: 0.2M MOPS; 20mM Sodium acetate; 10mM EDTA (pH=8.0).
7. 10X Formaldehyde gel loading buffer: 10mM EDTA (pH=8.0); 50% glycerol; 0.25% Bromophenol blue; 0.25% Xylene cyanol.
8. 3% Hydrogen Peroxide solution

Before proceeding for RNA isolation, all the plastic-wares and glass-wares were treated with DEPC and autoclaved. Reagents were prepared in DEPC treated and autoclaved milliQ water. Samples were processed for isolation of RNA, DNA and Protein following manufacturer's (Sigma Aldrich, USA) protocol. Briefly the samples were thawed and BCP was added to the sample ($1/10^{th}$ volume of Tri reagent) with vigorous shaking for 15 sec, followed by incubation at room temperature (RT) for 15 min. To separate the phases, the sample was centrifuged at 12,000 rpm for 15 min at 4°C. Two phases were obtained; a pink phase containing

DNA and protein while transparent phase containing RNA. The transparent phase was separated, precipitated with isopropanol and incubated for 20 mins at RT. RNA pellet was obtained by centrifugation at 12,000 rpm for 10 min at 4°C. Supernatant was discarded and the pellet was washed with 70% ethanol twice. The pellet was air dried and then resuspended in 80-90µL DEPC treated water and stored at -80°C. RNA integrity was assessed using denaturing agarose gel and RNA purity and concentration was checked by the Nano UV-Vis Spectrophotometer (Simpli Nano GE, UK). For DNA isolation, pink phase obtained initially was mixed with back extraction buffer and shaken vigorously for 15 sec followed by incubation at RT for 15 min. After centrifugation, DNA was obtained in aqueous phase that was precipitated with isopropanol. DNA pellet was washed with 70% ethanol and resuspended in 100µL of 1X TE buffer. The DNA was used to confirm the infection using 18S rRNA based multiplex PCR and 28S rRNA based nested PCR as discussed above.

2.5.2 cDNA synthesis

First Strand cDNA synthesis was carried out from total RNA obtained from each sample using a Quantitect Reverse Transcription kit (QIAGEN, Germany) according to the manufacturer's recommendations.

Genomic DNA elimination reaction

Template RNA	1µg
gDNA Wipeout buffer (7X)	2µL
RNA free water q. s.	14µL

Incubate at 42˚C for 2 minutes and immediately transfer it to ice.

Reverse Transcription master mix:

Above mix	14µL
Reverse Transcription Buffer (5X)	4µL
Reverse Transcription Primer mix	1µL
Reverse transcriptase	1µL
Total	20µL

Reaction mixture was incubated at 42°C for 30 mins and enzyme was inactivated at 95°C for 3 mins. After the completion of reaction, cDNA sample was diluted to 50µL by adding 30µL of TE buffer and stored at -80°C till further use.

2.6 Amplification of genes involved in SUF pathway

2.6.1 Primer Designing

Primers were designed for genes participating in SUF biosynthesis pathway of *P. vivax* using the sequences retrieved from online available database PlasmoDB (Aurrecoechea et al., 2009) and NCBI. For designing the primers, freely available online software's like Gene Runner (Hasting Software's Inc., USA), Primer3 (Untergrasser et al., 2012) and Primer-BLAST (Ye et al., 2012) were used. The presence of any dimers and hairpin loop Tm were also taken into consideration. The primers were synthesized commercially and the Log Tm was calculated using the standard formula-

$$\text{Log Tm} = 81.5+16.6\ [\log_{10}(Na^{+})] + [41(G+C)/n] - 675/n$$

(n = number of bases)

2.6.2 Amplification and sequence analysis

Standard PCR reaction was performed with minor modifications to amplify the genes encoding SUF pathway components: SufA, SufS and SufE. The primers and the PCR conditions used are given in the respective chapters in the thesis. The PCR amplicons obtained were commercially sequenced for both strands following Sanger's dideoxy method using ABI 3100 DNA Sequencer version 5.1.1 (Applied Biosystems, USA). The obtained raw sequences were analyzed for contig alignments using DNAMAN (Lynnon Corp). To check the similarity between different orthologues and homologs, the sequences were aligned using CLUSTAL W (Larkin et al., 2007) and BioEdit (Hall, 1999).

2.7 Cloning of *sufA, sufS* and *sufE* genes in Prokaryotic expression system

To characterize the desired proteins in *P. vivax* SUF pathway, the amplicon obtained from *P. vivax* field isolates was cloned in different cloning and expression vectors.

The amplified gene fragments for all the genes in the study had restriction sites at their ends for directional cloning. These restriction sites were incorporated during primer designing based upon desired vector and respective multiple cloning site region. The complete cloning process is a multi-step process including competent cell preparation, plasmid isolation, processing of vector (plasmid) and insert (amplified gene) using restriction enzymes, ligation, transformation and screening of recombinant clone. The protocols for each of these procedures would be discussed in detail in the following sections. For the *PvsufS* and *PvsufE* genes, the genes were first cloned in TA cloning vector (Genetix Biotech, Asia) and then sub-cloned in a suitable expression host using the above mentioned process.

2.7.1 TA Cloning

The TA cloning kit procured from Genetix Asia Pvt. Ltd. was used for this protocol. As the PCR product was purified, to ensure the poly-A residues at the 3' end, a treatment of insert with dATP was performed as follows:

Poly-A Tailing:

Contents	Quantity
Gene of interest	9.5µL
Taq DNA Polymerase Buffer (10X)	1.2µL
Taq DNA Polymerase (1U/µL)	0.5µL
dATPs	0.8µL

Reaction mix was incubated for 1 hr at 72°C.

After the adenylation, the insert was ligated to the TA vector as follows:

Ligation with TA Vector:

Contents	Quantity
Poly-A Tailed Gene of Interest	6µL
Ligation Buffer A (10X)	1.1µL
Ligation Buffer B (10X)	1.1µL
TA Vector	2µL
T4 DNA Ligase	1µL

Reaction mix was incubated for 12 hrs at 4°C.

The ligation mixture was then transformed in *E. coli* DH5α as mentioned above and the colonies were further screened for recombinant clones by performing colony PCR.

2.7.2 Competent cell preparation

Desired strains of *E. coli* host cells were streaked on a Luria Bertani (LB) Agar plate (with/without antibiotics) and grown overnight at 37°C. Thereafter, a single colony was picked and used to inoculate 5mL LB broth. The culture was allowed to grow overnight at 37°C with shaking at 150 rpm. The following day, 1 part of the overnight grown culture was used to inoculate 40 parts of 150mL fresh LB broth and again kept at 37°C, till an OD_{650} value of 0.5 was attained. After this, the culture was chilled on ice for 10 min and subsequently centrifuged at 6000 rpm, 4°C for 8 min. Supernatant was discarded, the pellet was re-suspended slowly in 80mL of ice-cold 0.1M Calcium Chloride ($CaCl_2$) and incubated on ice for 15 min after which it was again centrifuged at 6000 rpm, 4°C for 8 min. The supernatant was discarded and the pellet was re-suspended in 10mL of ice-cold $CaCl_2$, after which 1.4mL of 100% Glycerol solution was added to the re-suspended cells while stirring gently. Cells were chilled on ice for 10 min and then distributed as 300µL aliquots in each micro-centrifuge tubes. Immediately the tubes were closed and stored at -80°C for further use.

2.7.3 Plasmid DNA Isolation

Reagents

1. Solution I: 50mM Glucose; 25mM Tris-Cl (pH=8.0); 10mM EDTA (pH=8.0)
2. Solution II: 0.2N NaOH; 1% SDS (should be prepared fresh each time).
3. Solution III: 3M Sodium acetate (pH=5.2; chilled)

Individual colonies from the bacterial culture agar plate were inoculated in 5mL LB broth containing appropriate antibiotic and allowed to grow for 16 hrs at 37°C, with shaking at 200 rpm. Plasmid DNA was prepared from these cultures following the Alkaline Lysis method given by Birnboim and Doly, 1979. Briefly, the overnight grown culture was centrifuged at 5000 rpm for 5 min. Supernatant was discarded and

bacterial pellet was re-suspended in ice cold Solution I. To this, freshly prepared Solution II was added and incubated at RT for a couple of minutes with intermittent mixing. To the above mix, chilled Solution III was added, mixed gently and incubated on ice for 5 min. The lysed material was then spun at 10,000 rpm for 10 min at 4°C and the supernatant was transferred to a fresh tube. A phenol: chloroform: isoamyl alcohol treatment was then given to remove all the proteins and the DNA was precipitated overnight by adding twice the volume of 100% ethanol in presence of Na–acetate. The precipitated DNA was pelleted by centrifuging the tubes at 10,000 rpm for 15 min at 4°C. The supernatant was discarded and the pellet was washed with chilled 70% ethanol. The pellet was air dried and suspended in adequate amount of 1X TE. The integrity of the plasmid DNA was checked by running on 1% agarose gel.

2.7.4 Preparation of vector and insert (gene) for cloning

The isolated plasmid vector was double digested with appropriate restriction enzymes and purified using QIAquick Gel Extraction kit (QIAGEN, Germany) following the manufacturer's protocol. The insert being a PCR product was purified using QIAquick PCR purification kit (QIAGEN, Germany) and double digested with same restriction enzymes. After this, digested insert was gel eluted and quantified using the Nano UV-Vis Spectrophotometer (Simpli Nano, GE, UK) for setting up a ligation.

Restriction digestion of vector and gene insert

Template DNA	=	500ng – 1µg
Restriction Enzyme	=	3 – 5U
Buffer (10X)	=	5µL
Sterile Millipore Water	=	Volume to make 50µL

The reaction was incubated at the desired temperature (mostly 37°C) for 1 – 2 hours.

Gel elution of vector and insert:

Purification of DNA fragments (PCR product and digested plasmid) was performed using QIAquick Gel extraction Kit (QIAGEN, Germany) following the

manufacturer's protocol with minor modifications. DNA fragment was excised from gel using a clean scalpel and gel slices were melted in three volumes of QG buffer (w/v) by incubation at 50°C. One volume of isopropanol was added and incubated at RT for 3 min. To bind the DNA, the above mix was applied to QIAquick spin column and centrifuged at 13,000 rpm for 1 min. Spin column was washed with 500µL QG buffer and 720µL PE buffer by centrifuging it at 13,000 rpm for 1 min. After an empty spin, the spin column was transferred to fresh 1.5mL micro-centrifuge tube and DNA was eluted by using 1X TE buffer by centrifuging at 13,200 rpm for 1.5 min.

2.7.5 Ligation of insert with vector

Purified plasmid and insert after double digestion were ligated with the help of T4 DNA ligase enzyme. Equal quantity of the vector and insert were checked on gel prior to the ligation, to compare the concentration (**Figure 2.6**).

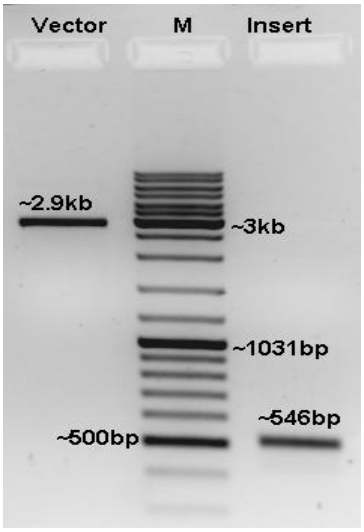

Figure 2.6: Vector and insert concentration check prior to ligation
M= Gene ruler DNA Ladder mix (SM0331 Fermentas).

Ligation mix:

Contents	Quantity
Vector (plasmid DNA)	100ng
Gene of interest	300ng
T4 DNA ligase buffer (10X)	2µL
T4 DNA ligase (5U/µL) (Thermo Scientific)	1µL
Sterile Deionized water q.s.	20µL

Reaction mix was incubated for 16 hrs at 22°C in a circulating water bath.

Following above reaction, the ligated product was transformed into *E. coli* DH5α competent cells. Briefly, competent cells (stored at -80°C) were thawed on ice and 10µL of ligated mix was added to 100µL of competent cells and mixed properly. Cells were incubated on ice for 25 min. The samples were thereafter given a heat shock in a water bath at 42°C for 90 seconds, and then immediately placed on ice, after which 800µL of LB broth medium, pre-warmed at 37°C, was added. This mixture was incubated at 37°C for 45 min followed by centrifugation at 3000 rpm for 5 min. 800µL of supernatant was removed and cells were resuspended in remaining 100µL of supernatant and plated on LB Agar plates containing the desired concentration of antibiotics. Simultaneously, a digested vector without insert was also transformed in the same bacterial host to act as a control.

2.7.6 Identification of recombinant clones

After the transformation of digested vector and ligated product, the numbers of colonies obtained in above two sets were compared and to check for the recombinant clones, following assays were performed:

2.7.6.1 Gel shift assay

The colonies obtained after transformation of ligated product were initially analyzed using the gel shift assay (Sekar, 1987). Individual colonies were streaked on LB Agar-antibiotic plates and incubated overnight at 37°C. A small part of each colony was picked and mixed with lysis buffer (0.5mM EDTA; 10% Sucrose; 0.25% SDS; 100mM NaOH; 60mM KCl) in a micro-centrifuge tube. The tubes were further incubated stepwise, at 65°C (water bath) for 5 min, on ice for 5 min, at RT for 5 min and centrifuged at 8,000 rpm for 5 min. The obtained supernatant was loaded on the gel. The presence of clone is identified by a shift in the plasmid bands due to the varied size of recombinant plasmid as compared to others or the standards (**Figure 2.7**).

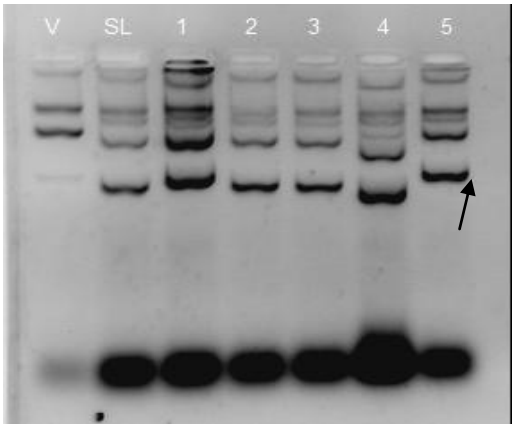

Figure 2.7: Gel shift pattern obtained after assay for clone identification [SL: Pattern from colony having self-ligated vector as a control; V= pattern of vector alone as negative control; lanes 1 to 5= patterns from different colonies obtained after the transformation of ligated product]. Lane 5 arrow indicating a positive shift.

2.7.6.2 Colony PCR

Colonies shortlisted after Gel shift assay were screened by PCR using gene specific primers to select positive clones. Colonies were picked from the plate under sterile conditions, suspended in 50µL nuclease free water, vortexed to obtain a proper suspension, followed by heating at 100°C for 4 min. After centrifugation 10µL of supernatant was used as a template for each reaction mixture. Colonies obtained from self-ligation reaction were used as a negative control. PCR reaction products were analyzed on a 1% agarose gel.

2.7.6.3 Restriction Digestion Analysis

The recombinant colonies showing positive results for colony PCR were subjected to plasmid isolation using alkaline lysis method (as discussed previously). The obtained plasmid was digested using one or more restriction enzymes to confirm the desired size of the clone and presence of single insert. Following this, confirmation of clone and chances of frame-shift were detected by sequencing of the recombinant plasmid using T7 promoter primers. These confirmed recombinant molecules were taken further for protein expression trials.

2.8 Protein Expression

Reagents

1. 1.5M Tris (SIGMA) (pH=8.8) and 0.5M Tris (pH=6.8)
2. 30% Acrylamide solution (29.2g Acrylamide and 0.8g N,N'-Methylene Bis-Acrylamide) (SIGMA)
3. 10% Ammonium Persulfate (SRL)

4. Sodium Dodecyl Sulfate (1% SDS)
5. Tetra methyl ethylene diamine (TEMED; SIGMA)
6. 2X Sample lysis buffer (Merck Bioscience, Germany)
7. Electrophoresis Running Buffer: 25mM Tris; 192mM Glycine; 0.1% SDS
8. Protein Molecular Weight Marker (Merck Bioscience, Germany)
9. Staining solution: 0.2% Coomassie Brilliant Blue (CBB) R-250 (HiMedia); 5% Methanol; 10% Acetic acid
10. Destaining solution: 40% Methanol; 7% Acetic acid in deionized water

Competent cells prepared for *E. coli* expression host system like *E. coli* BL21(DE3)pLysS were freshly transformed with recombinant plasmid containing the desired gene using heat shock method. A single colony was picked from this transformed plate, inoculated in LB broth and culture was grown overnight at 37°C with shaking. After 14 hrs, 1 part of this primary culture was inoculated to 20 parts of fresh LB broth and incubated at 37°C with shaking. When this culture reaches to an OD of 0.5-0.6 at 600nm (~3hrs), 1mL aliquot was withdrawn as a control (uninduced) sample from the culture (marked as 0 hr) and remaining culture was induced with IPTG (final concentration 0.5mM) and again incubated at 37°C. Samples were collected from this induced culture at regular intervals (2hrs, 4hrs and 6hrs) and pelleted by centrifugation at 3,000 rpm for 5 min at 4°C. The obtained pellet was resuspended in 2X sample lysis buffer, heated at 100°C for 10 min and stored at -20°C till further use. Preheated samples were loaded on a denaturing polyacrylamide gel. The obtained gel was stained with CBB solution and protein bands were viewed after destaining the gel. Analysis of the gel was done where vector and clone (uninduced and induced) samples were compared before and after induction.

2.9 Western Blotting

To confirm the expression of desired proteins, the samples were transferred to nitrocellulose membrane and the membrane was subjected to antibodies specific to the His-tag fused to the protein. If the protein is present, the antibodies will bind to it

and this can be checked by the addition of an enzyme conjugated secondary antibody (Horse-radish Peroxidase) specific against the primary antibody.

Reagents & Material for Protein transfer and detection:

1. Tris buffered saline (TBS) (50mM Tris; 150mM Sodium chloride; 100mM KCl; pH=7.5)
2. Transfer buffer: 48mM Tris; 39mM Glycine; 10-20% Methanol
3. Wash buffer: (1X TBS with 0.05% Tween20)
4. Blocking buffer: (5% Fat free milk powder (HiMedia) in 1X TBST)
5. Anti-His antibodies (QIAGEN)
6. Goat anti-mouse IgG HRP labeled antibodies (Merck Bioscience, Germany)
7. Substrate solution: TMB/H_2O_2 (SIGMA)
8. Nitrocellulose membrane (Schleicher & Schuell, Germany)
9. Mini Trans-Blot® Cell apparatus/Semi-dry Trans-Blot apparatus (Bio-Rad, USA)

A pre-run and unstained SDS polyacrylamide gel was used for the transfer of protein on the nitrocellulose membrane. The nitrocellulose membrane and filter pads were soaked in the pre-cooled transfer buffer. Assembly was set with the gel at the negative electrode and the membrane at the positive end and proteins were transferred to the membrane by electro transfer. After the transfer process, the membrane was stained with Ponceau-S (Merck Bioscience, Germany) to check the transfer efficiency and after confirmation of transfer of desired band; the Ponceau-S stain was removed by excessive washing with deionized water. To prevent the non-specific binding, the membrane was kept overnight in blocking buffer (5% fat free milk powder in 1X TBST) followed by washing thrice with wash buffer (1X TBST). After washing, the membrane was left soaked in primary antibody (dilution of antibodies varies according to the protein targeted) for 1½ hours at 37°C. The membrane was again washed thrice (as mentioned above) and incubated with secondary HRP conjugated antibody for 1½ hours at 37°C. Finally membrane was washed thrice with wash buffer and incubated for 15-20 min with TMB/H_2O_2 substrate solution in dark. The reaction was stopped by adding distilled water and bands obtained at membrane were analyzed.

2.10 Protein Purification

Once the protein was confirmed by western blotting, to perform further experiments like enzymatic assays, localization studies, etc., the protein was purified from other proteins using affinity chromatography. As the fusion tag used for our protein was His-tag, we used manually packed Ni-NTA (QIAGEN) columns for these purifications.

2.10.1 His-tagged protein purification

Reagents

1. Equilibration buffer: (25mM Tris Cl; 0.3M NaCl; 8M Urea; 20mM β-mercaptoethanol (pH 8.0)
2. Phenyl methyl sulphonyl fluoride: (PMSF; 100mM stock in Isopropanol) (SIGMA)
3. Lysozyme (50mg/mL) (Ameresco)
4. Wash buffer: [Equilibration buffer (pH 6.3)]
5. Elution buffer: [Equilibration buffer (pH 4.5)]

After 6 hrs of IPTG induction, bacterial culture was harvested by centrifugation (VS-550, Vision Scientific, Korea) at 3800g for 15 min at 4°C. To prevent the digestion of the target protein during protein solubilization, PMSF (final concentration 1mM) was added to the wet pellet to inhibit any protease activity. After this, the pellet was resuspended and maintained in equilibration buffer. Lysozyme (final concentration of 1mg/mL) was added and sonication (MISONIX, USA) was performed on the cell lysate to release the proteins from the bacterial cells, where sonication parameter includes output of 10 watts with 10 sec pulse thrice on ice. 1mL aliquot of prepared lysate was stored for total protein analysis and the rest of the sample was centrifuged at 9300g for 15 min at 4°C. Supernatant (soluble fraction) and pellet (insoluble fraction) were separated and the presence of desired protein was confirmed by running them on SDS PAGE.

Protein molecules present in soluble fraction were purified using Ni-NTA agarose resin (QIAGEN, Germany). Purification is based on electrostatic interaction between

the 6X-His peptide tag attached to the solubilized protein and Ni^{2+} cation attached to the agarose resin. 2-3mg/mL soluble fraction of protein was mixed with agarose resin, applied to the equilibrated polypropylene column and this was left undisturbed for some time to allow it to settle. Flow through of the sample was collected and the column was washed with wash buffer to remove any unbound or non-specifically bound protein. Specific 6X-His tagged protein was eluted with the help of elution buffer in separate fractions and the fractions were run on a SDS PAGE to confirm the presence of desired protein.

2.10.2 Protein purification by Gel elution

Reagents:

Protein isolation buffer: 50mM Tris-Cl (pH 7.5); 150mM NaCl; 1mM EDTA

To elute the protein from the gel, the protocol given by Kurien and Scofield, 2012 was followed. For this, the SDS-PAGE of required porosity was casted. To load the sample with protein in excess, the wells of this gel (depending upon sample volume) were clubbed, leaving three wells intact for control sample and marker. Electrophoresis was performed, after which wells with controls were cut and kept for normal staining and de-staining procedure while the remaining gel portion having protein for elution was preserved in running buffer at 4°C. Taking an estimate from the stained gel, the desired protein band was cut from the unstained gel and was directly placed in 1mL protein isolation buffer. Tubes were incubated at 30°C for 14-16 hrs with shaking at 800 rpm in thermo-shaker. After overnight incubation, tubes were spun at 12,000 rpm for 20 min at 4°C and the supernatant was collected. Samples were further concentrated using vacuum concentrator to achieve the desired concentration and protein concentration was estimated by Bradford assay as described below.

2.10.3 Protein concentration determination

Several methods are available for determining protein concentration however, the most accurate and popular Bradford method (Bradford, 1976) was selected because of its simplicity. This method relies on the electrostatic and hydrophobic interaction of sulfonic acid groups in CBB G250 dye to positively charged, aromatic, basic

amino acids that occur in low pH value. After the binding of protein, the absorbance maxima of CBB dye shifts from 465 to 495nm, which was assessed using UV-visible spectrophotometer (Jasco 630, Japan). BSA at different concentrations ranging from 6.5µg to 200µg was used for plotting the standard curve for protein estimation. By extrapolating the absorbance obtained for the unknown protein sample on this standard curve, the concentration of the protein was determined.

2.11 Biochemical Activity Assay

Activity of purified proteins was checked by performing their respective assays based on colorimetry. For this, required substrate and cofactors were provided externally in oxidized or reduced conditions as required for the functionality of the enzymes. The UV-visible spectrophotometer (Jasco 630, Japan) was used for detecting the absorbance of products formed as a result of enzyme substrate reaction. Electron paramagnetic resonance (EPR) JES-FA200 spectrophotometer was used for detecting the electron state (oxidation/ reduction) of Fe indicating its probability of binding with the enzymes to act as a co-factor. Specific assays used for the characterization of the enzymes are detailed in the respective chapters.

2.12 Protein sub-cellular localization and Antibody binding studies

The purified proteins were used to raise antibodies in mice to co-localize the protein in *P. vivax* parasite infected thin blood smears prepared from clinical patients. These antibodies were also used to detect their specificity and binding efficiency with the parasite infected blood.

2.12.1 Antibody raising and ELISA

Reagents:

1. Freund's Complete/Incomplete Adjuvant (Merck Bioscience, Germany).
2. Coating Buffer (sodium carbonate bicarbonate buffer, pH 9.4).
3. Blocking Buffer (5% fat free milk powder prepared in 1X PBS)
4. Wash Buffer (1X PBS containing 0.2% Tween 20)
5. Goat anti-mouse IgG HRP conjugate (Merck Bioscience, Germany).
6. TMB/H_2O_2 for ELISA (Merck Bioscience, Germany).

7. Stop Solution: 2N H_2SO_4

To raise antibodies against proteins involved in the SUF pathway, the purified recombinant proteins were injected intra-peritoneally in mice along with Freund's adjuvant. For each protein, 10 female Swiss albino (Out bred) mice of 4 to 5 weeks, bred under specific- pathogen free conditions and supplied by Animal House Facility, BITS Pilani, Rajasthan, were used, where 5 mice constituted the experimental group and 5 mice were considered as controls. Before injecting the mice with the desired recombinant protein, all the mice from both the groups were pre-bled to check the presence of any inherent cross reactive antibodies. Following this, for the primary injection in the experimental group, an emulsion of purified protein (25-30µg) was prepared by mixing it with equal quantity of Freund's complete adjuvant (FCA) and this emulsion was injected per mice. For control set, 1X PBS was emulsified with FCA (primary injection) and injected in mice. For booster doses, the protein/PBS was emulsified with Freund's incomplete adjuvant (FIA) in similar concentrations as above and injected after regular intervals of 21 days. All the protocols were approved by the Institute's Animal Ethics Committee (Approval No. IAEC/RES/18/30). After 9 days of each booster dose, blood samples were withdrawn from mice by retro-orbital method. Sera was separated from these samples by incubating the sample at 37°C for 1 hour, followed by overnight incubation at 4°C and centrifugation at 10,000 rpm at 4°C for 10 min. The supernatant (serum) was collected separately in a fresh micro-centrifuge tube and stored at -20°C till further use (Harlow and Lane, 1988).

Further, to check the IgG antibody titer specific against our desired recombinant proteins, ELISA was performed using different protein and serum dilutions. For this, 100µL of the recombinant protein samples (diluted to 1ng/µL in sodium carbonate bicarbonate buffer, pH=9.4) was coated in each well of 96-well flat bottom plate. The plates were kept overnight at 4°C followed by blocking with 5% fat free milk powder prepared in 1X PBS (pH=7.4) at 37°C. After incubation of 2 hrs, the plates were washed thrice with 1X PBS containing 0.2% Tween 20. Serum samples with varying dilutions (1:100 to 1:1000) were used as primary antibodies against specific

proteins and the plates were incubated for 2 hrs at 37°C. Antibodies specific to recombinant protein were detected using HRP conjugate goat anti-mouse IgG (Fc fragment specific). TMB/H_2O_2 was used as a substrate and the reaction was stopped using diluted sulphuric acid solution. The absorbance was recorded at 450nm on an ELISA plate reader (STAT FAX 2100). All tests were performed in duplicates and antibody levels were expressed as average concentration units. Serum samples collected from mice injected with 1X PBS were used as controls. The specificity of these antibodies was further confirmed by western blot analysis.

2.12.2 Immuno-localization studies

Reagents:

1. 0.05% Saponin in 1X PBS
2. 0.1% Triton X-100
3. Blocking Buffer (3% Bovine Serum Albumin (BSA) in 1X PBS)
4. DAPI (100ng/mL) (Life Technologies, USA)
5. Goat anti-mouse IgG FITC Conjugate (Merck, Germany)
6. Qdot® 585 Streptavidin conjugate (Life Technologies, USA)
7. VECTASHIELD (Vector Laboratories, USA)

To co-localize the proteins in the parasite, immuno-fluorescence microscopy was performed on thin smears prepared from blood collected from *P. vivax* infected patients. The slides were fixed with 100% cold methanol. Fixed cells were washed with 1X PBS, permeabilised with 0.05% Saponin (30 mins) followed by 0.1% Triton X-100 (5 mins), and blocked overnight using 3% BSA. After blocking, the cells were incubated with primary polyclonal antibodies raised in mice against the specific protein for 4 hrs at 37°C. For this, antibody dilutions varying from 1:100 to 1:30000 were tried. After washing the cells with 1X PBS, Goat anti-mouse IgG FITC conjugated antibodies with a dilution of 1:2000 was used as secondary antibodies and cells were incubated for one and a half hour at 37°C. Counterstaining of the parasite nucleus was done using DAPI for 10 min and apicoplast membrane using Qdot® 585 Streptavidin conjugate for 1 hr at room temperature (Jelenska et al., 2001). Intermittent washing with PBS was performed in between each step. The cells

were finally mounted with VECTASHIELD and viewed in a confocal laser scanning microscope (Leica TCS SP5) under a 63X oil immersion lens. RBCs infected with parasite were identified in bright field and protein of interest with green fluorescence emitted by FITC. DAPI was viewed as a blue dot while Qdot® 585 Streptavidin conjugate appeared as a red fluorescence under the microscope (**Table 2.3**). Exact location of the proteins was defined by the overlapping of the images of the same field.

Table 2.3: Fluorescent dyes and their excitation and emission wavelength peaks

Filter Set Description	Excitation (nm)	Emission (nm)	Barrier filter (nm)	Remarks
DAPI	359	461	450-465	Violet EX / Blue EM
FITC antibody conjugate	495	519	505-535	Blue EX / Green EM
Qdot® 585 Streptavidin conjugate	565	585	580-620	Green EX / Orange-Red EM

2.13 Parasite Lysate Preparation

Reagents:

1. 1X PBS (pH – 7.5).
2. 0.03% Saponin Lysis Buffer prepared 1X PBS.
3. Parasite Lysis Buffer: 10% SDS, 10% TritonX-100 in 1X PBS.

The parasite infected blood sample (1mL) was thawed at RT and transferred to a 15mL tube. Cells were washed with equal volume of 1X PBS by centrifugation at 5000rpm for 5 min at 4˚C. The wash was repeated two more times until the red colour disappears and to the final pellet, protease inhibitor cocktail (1µL) was added. The obtained pellet was dissolved in saponin lysis buffer, incubated on ice for 15 min after which it was centrifuged at 13,200rpm for 5 min at 4˚C. The pellet was washed again with 1X PBS as mentioned above and resuspended in parasite lysis buffer. The tube was again centrifuged at 13,200 rpm for 5 min at 4˚C and the supernatant and pellet were collected in separate tubes. The pellet was resuspended in 1X PBS and equal volume of 2X sample lysis buffer was added to both the

supernatant and the pellet. The samples were checked on SDS-PAGE as per standard protocols.

2.14 Studies on Evolutionary Position

2.14.1 Multiple sequence alignment

The PCR products of desired genes under study were sequenced commercially and the obtained gene sequences were thoroughly cross checked with the chromatogram and standard sequences available in database, to avoid any errors. The nucleic acid sequences were translated to protein sequences which were aligned against all available homologues and orthologs from different *Plasmodium* species, apicomplexans and prokaryotes using Clustal W2 (Larkin et al., 2007) and Clustal Omega (Sievers et al., 2011).

2.14.2 Phylogenetic Analysis

The evolutionary history of proteins involved in the SUF pathway from field isolates of *Plasmodium* parasites was inferred by Maximum Likelihood method using MEGA 6.0 software (Jones et al., 1992; Tamura et al., 2013). The MSA obtained from Clustal Omega was used to generate the phylogenetic tree where Neighbor-Joining and BioNJ algorithms were applied to a matrix of pairwise distances estimated using a JTT model, and then the topology with superior log likelihood value was selected (Tamura et al., 2013). The bootstrap consensus tree inferred from 1000 replicates was taken to represent the evolutionary history of the taxa analysed (Felsenstein, 1985) and all positions containing gaps and missing data were eliminated. The obtained tree was analysed for the evolutionary position of the respective proteins in study to infer their evolutionary distance from different *Plasmodium* species as well as other apicomplexans and prokaryotes.

2.15 Protein Structure Prediction

2.15.1 Secondary structure prediction

Three dimensional (3D) crystal structures of most of the enzymes involved in the SUF pathway of *Plasmodium* parasite are not available. In the absence of a 3D structure, prediction of secondary structure is a useful intermediate step, which can

facilitate the process of 3D structure prediction and helps to identify conserved domains. Secondary structures of proteins in our study were generated using PSI-PRED server (McGuffin et al., 2000) to find out the total number of α-helices and β-sheets present, to depict the conformation of amino acid residues seen that are seen repeatedly in the proteins. The obtained structures were compared with secondary structure of various other microorganisms with the help of Geneious II software (http://www.geneious.com, Kearse et al., 2012).

2.15.2 Prediction of 3D structure using Homology Modeling

To predict the 3D model of the proteins, template model was selected using HHpred server (Söding et al., 2005). For this, the translated amino acid sequences of enzymes involved in the SUF pathway of *P. vivax* were submitted to HHpred online server. Based on the sequence similarity of target with the template and resolution of template structure, the best structure was selected. This selected crystal structure was used as a template for protein structure prediction using MODELLER 9v11 (Sali and Blundell, 1993; Eswar et al., 2006). Discrete optimized protein energy (DOPE) was calculated for each structure and one with minimum DOPE score was selected. Energy Minimization (EM) is the next step in generating a protein structure, where attempts are made to obtain a perfect folding of the protein. For the same, online server YASARA (Krieger et al., 2009) was used.

To evaluate the reliability of three dimensional structures of proteins, structure validation was accomplished by using different online available servers, where quality evaluation of the models for the environment profile was done with PROCHECK (Laskowski et al., 1993), VERIFY3D (Eisenberg et al., 1997) and ERRAT (Colovos and Yeates, 1993). Atomic contacts and packing of side chains in final refined models were evaluated using WHAT IF program (Vriend, 1990). Complete assessment and evaluation of the generated models were performed by Ramachandran plot analysis using RAMPAGE (Lovell et al., 2002). RMSD (root-mean-square deviation) value was calculated by superimposition of template and modelled protein structure using Chimera (Pettersen et al., 2004).

2.15.3 Substrate docking & Protein-Protein Docking

Presence of binding site for substrates is a characteristic feature of a protein participating in different enzymatic reaction. Binding pocket made up of conserved amino acid residues were identified and based on the confidence score (C-score ranging from 0 to 1) obtained for this site, docking studies were performed by using Molegro Virtual Docker (Thomsen and Christensen, 2006). In the first step, coordinates for the proteins, substrate molecules were stored as a PDB file using Discovery studio 3.5 Client (BIOVIA, US) and uploaded to the workspace of MVD. Here in MVD, the workspace acts like a central component and represents all the information available to the user in terms of molecules (proteins, ligand, cofactors, water molecules, and poses), user-defined constraints (visualized as small spheres), cavities (visualized as a grid mesh), and various graphical objects (molecular surfaces, backbone visualizations, labels, etc.). Binding cavities were located on these proteins and selected as constraints, which were further used as a site of docking. Docking process starts and eventually times out on its own after 2000 iteration (or about 100, 000 evaluation) where generally docking engine should find a good solution in 800 iterations. Once the simulation is over, docking results were imported from the output directory together with pose organizer. In pose organizer all the poses were analyzed manually to check the interaction between protein and ligand molecule. During analysis, affinity of conserved amino acid residues towards substrate ligand molecules was studied where hydrogen bond, electrostatic interaction and steric interaction was mainly observed. Interaction of conserved amino acid residues was studied and compared with the amino acids interacting with substrate molecules.

As mentioned earlier, there are multiple players involved in the SUF pathway. Therefore, to investigate the interacting partners in the pathway itself protein-protein docking was performed using online server GRAMM-X (Tovchigrechko and Vakser, 2006). The results obtained would give us a clear picture of the important residues involved in interaction of the key components of the pathway, which would further help us elucidate the yet completely unknown SUF pathway in *Plasmodium*.

Materials used for various reactions

Vector and Bacterial strains used

pRSET A	Invitrogen, USA
RIG plasmid	Kind gift from W.G.M. Hol USA.
E. coli strain DH5α	Thermo Scientific, USA
E. coli strain BL21 (DE3)	Novagen, Germany
E. coli strain BL21 (DE3) pLysS	Novagen, Germany

Various kits used in this study

Anti-His Antibody kit	QIAGEN®, Germany
Gel extraction kit	QIAGEN®, Germany
Ni-NTA agarose Resin	QIAGEN®, Germany
PCR purification kit	QIAGEN®, Germany
Plasmid miniprep kit	QIAGEN®, Germany
Quantitect Reverse Transcriptase kit	QIAGEN®, Germany

Antibodies and Fluorescence dyes

Anti-His antibody	QIAGEN, Germany
Goat anti-Mouse IgG HRP conjugate	Merck, Germany
Goat anti-Mouse IgG FITC conjugate	Merck, Germany
Qdot® 585 Streptavidin conjugate	Life Technologies, USA
DAPI	Life Technologies, USA

Composition of various buffer and solution used in the study

Acid Citrate Dextrose (1000mL)	Sodium citrate 13.2gm Citric acid: 4.8gm Dextrose: 14.7gm
Coating buffer for ELISA (10X; 100mL)	Sodium carbonate 1.59gm Sodium bicarbonate 2.93gm

DNA loading buffer, 6X	9mg Bromophenol blue 9mg Xylene cyanol FF Dissolve in 8.8mL of 60% Glycerol and add 1.2mL of 0.5M EDTA
LB broth (1000mL)	10gm Tryptone 5gm Yeast extract 5gm NaCl Autoclave
Phosphate Buffered Saline pH 7.4 (1X)	137mM NaCl 2.7mM KCl 4.3mM Na_2HPO_4 1.4mM KH_2PO_4
RNA gel running buffer, 20X	20mM MOPS 2mM Sodium acetate 0.25mM EDTA
TE buffer (1X; pH 8.0)	10mM Tris-Cl (pH 8.0) 1mM EDTA (pH=8.0)
TAE buffer (50X; 1000mL)	40mM Tris-acetate 1mM EDTA (pH 8.0) 57.1mL Glacial acetic acid

Buffers for restriction endonucleases, T4 DNA Ligase and *Taq* DNA Polymerase

The various buffer used were provided by the manufacturer for these enzymes and used as per the instruction provided.

Accession Numbers for Sequences:

Sr. No.	Gene Name	Organism	Accession No.
1.	SufS	*P. vivax*	PVX_000600
		P. falciparum	PF3D7_0716600
		P. berghei	PBANKA_0614300
		P. chabaudii	PCHAS_0616000
		P. cynomolgi	PCYB_032030
		P. knowlesi	PKNH_0311200
		P. yoelii	PY17X_0617000
		P. reichenowi	PRCDC_0713900
		Babesia bovis	NW_001820855.1
		Toxoplasma gondii	TGME49_216170
		Arabidopsis thaliana	NC_003070.9
		Bacillus subtilis	NC_000964.3
		Escherichia coli	NP_416195.1
		Pseudomonas fluorescens	PSF113_RS36015
		Thermus thermophilus	NC_006461.1
		Mycobacterium tuberculosis	NC_000962.3
		Thermotoga maritima	NC_000853.1
2.	SufE	*P. vivax*	PVX_003740
		P. falciparum	PF3D7_0206100
		P. berghei	PBANKA_0303800
		P. chabaudii	PCHAS_0306000
		P. cynomolgi	PCYB_042410
		P. knowlesi	PKNH_0414800
		P. yoelii	PY17X_0304400
		Neospora canium	NCLIV_068570
		Toxoplasma gondii	TGMAS_277010

		Arabidopsis thaliana	NC_003075.7
		Thermus thermophilus	NC_006461.1
		Escherichia coli	NC_000913.3
		Pseudomonas fluorescens	A7318_RS05530
		Klebsiella spp.	AB185_RS19135
		Mycobacterium tuberculosis	Rv3284
3.	SufA	*P. vivax*	PVX_080115
		P. falciparum	PF3D7_0322500
		P. berghei	PBANKA_1216000
		P. chabaudii	PCHAS_1237900
		P. cynomolgi	PCYB_101900
		P. knowlesi	PKNH_1010200
		P. yoelii	PY17X_1219200
		P. inui	C922_01370
		P. vinckei	YYE_01501
		Chlamydomonas spp.	NW_001843537.1
		Toxoplasma gondii	TGME49_255910
		Arabidopsis thaliana	ASD36_RS15030
		Synechococcus spp.	ACB00485.1
		Escherichia coli	NC_000913.3
		Anabaena spp	LUHI00000000
		E. tenella	ETH_00001070

Chapter III

Characterization of SufS from P. vivax

Characterization of SufS from *P. vivax*

3.1 Introduction

A variety of cofactors such as biotin, lipoic acid, molybdopterin, and thiamine, as well as Fe-S clusters in proteins and thionucleosides in tRNA require sulphur for their biosynthesis and cysteine has been shown to be the source of sulfur for these biomolecules (Begley et al. 1999; Marquet 2001). To utilize this cysteine as a source of sulphur, cysteine desulphurases have been shown to play a pivotal role. Cysteine desulfurase is a pyridoxal 5′-phosphate (PLP)-dependent homodimeric enzyme. It catalyzes the conversion of L-cysteine to L-alanine and sulfane sulfur on a conserved cysteine residue by the formation of a protein-bound cysteine persulfide intermediate (Zheng et al., 1993, 1994), as observed in the first steps of Fe-S cluster assembly pathway. This sulphur then in subsequent steps is utilized to form Fe-S clusters.

Bacterial cysteine desulphurases are the most widely studied and belong to the group of aminotransferases class V of fold-type I (Grishin et al., 1995). They are further categorized into two main groups (I and II) based on their sequence similarity (Mihara et al., 1997). Initially it was thought that as group I enzymes are closer to NifS/IscS from *A. vinelandii*, therefore only they are involved in the formation of Fe-S clusters. But later, several lines of evidence indicated that group II enzymes are also involved in Fe-S cluster assembly as well as iron homeostasis or molybdopterin biosynthesis (Mihara and Esaki, 2002). There are reports of group II enzymes showing a weak cysteine desulphurase activity in *Erwinia chrysanthemi* (Loiseau et al., 2003) but in *E. coli* this weak cysteine desulphurase activity of SufS was greatly increased by addition of SufE (Ollagnier-de-Choudens et al., 2003). The structure of the catalytic cysteine environment for the two groups of desulfurase enzymes is different. The catalytic cysteine localizes to a shorter, more rigid loop with a more hydrophobic environment in Group II cysteine desulfurases compared to Group I enzyme (Mihara et al., 2002). This structure difference may help explain the low

basal desulfurase activity of Group II enzymes compared to group I (Mihara et al., 2002).

The mechanism of action of cysteine desulphurase involves the binding of free cysteine to PLP and formation of PLP-cysteine adduct as a Schiff base between PLP and the α-amino group of cysteine in the first step. Then in the second step, a catalytic cysteine residue from the enzyme acts as a nucleophile to attack the sulfhydryl group of the substrate cysteine bound to PLP and results in formation of an enzyme-bound persulfide. In the third and final step, this active persulfide group can then be transferred to cysteine residues in the final scaffold protein directly or via a sulfur shuttle protein using a chemical route similar to protein disulfide bond exchange (**Figure 3.1**) (Hidese et al., 2011).

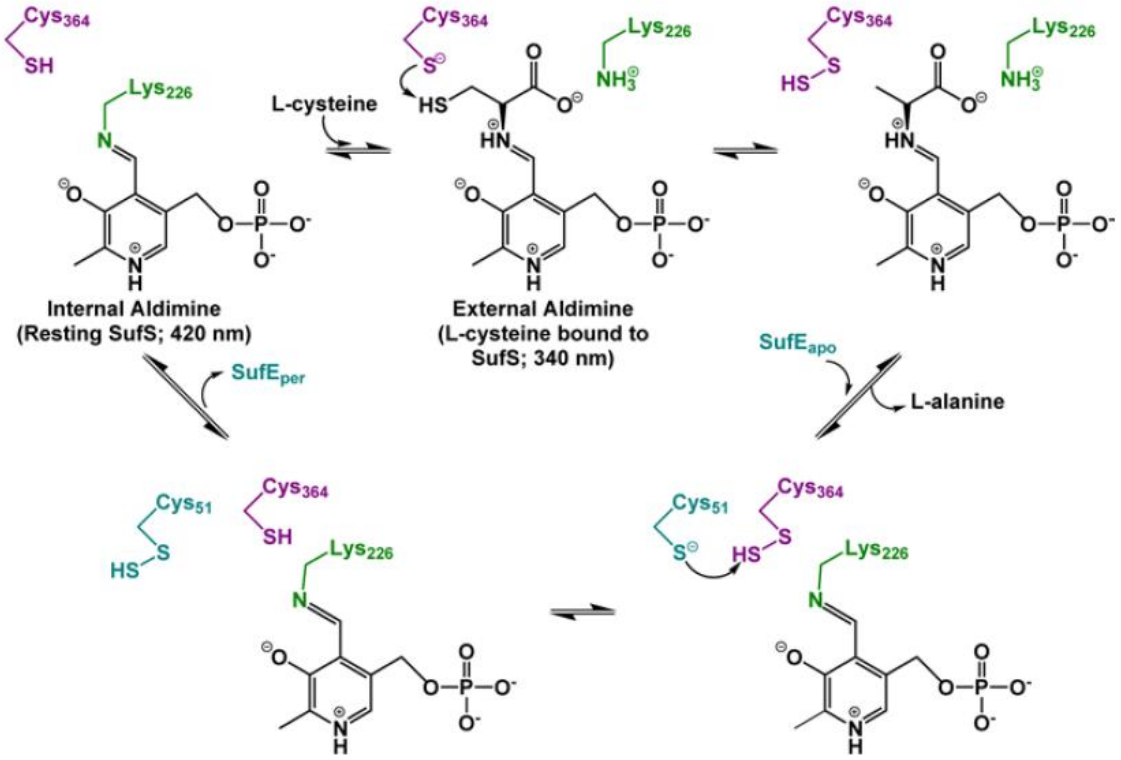

Figure 3.1: SufS cysteine desulfurase mechanism in *E. coli*. An abbreviated reaction mechanism for SufS is shown with SufS Lys226 in green and Cys364 in purple. SufE Cys51 is in teal. PLP cofactor and substrate cysteine are in black (Hidese et al., 2011).

In *Plasmodium*, the first report of an active cysteine desulfurase SufS was shown in *P. falciparum* where the *Pf*SufS complemented the loss of *E. coli* SufS. For the

same, an iron starvation phenotype Δ*sufS E. coli* was transformed with the mature form of *Pf*SufS (pGEXT-*Pf*SufS) and it was found that these transformed cells were able to grow in the presence of an iron chelator (2,29-dipyridyl) but, Δ*sufS E. coli* transformed with empty vector (pGEXT) were unable to grow. This study mainly depicted two important things: first that the loss of *Ec*SufS can be complemented by *Pf*SufS, representing that the parasite protein has cysteine desulfurase activity and second that despite the fact that *Pf*SufS shares only 30% identity with *Ec*SufS, it has an ablity to participate in an active *E. coli* SUF complex (Gisselberg et al., 2013). Following this, Charan et al., measured the ability of recombinant *Pf*SufS to function as a cysteine desulfurase in the presence of the L-cysteine substrate where *Pf*SufS showed very low cysteine desulphurase activity on its own, but it increased to ~17 folds in the presence of *Pf*SufE. In order to confirm the role of cysteine residue in desulfurase activity, a *Pf*SufS Cys497Ala mutant corresponding to the active Cys_{364} in *E. coli*, was generated. The mutant protein *Pf*SufS was unable to mobilize sulfur, and no desulfurase activity was detected even in the presence of *Pf*SufE, thus establishing that Cys497 is the critical residue involved in sulfur mobilization from the cysteine substrate (Charan et al., 2014). The systematic genetics studies in *P. berghei* also indicate that *Pb*SufS perform critical functions during blood stage infection of the malarial parasite (Haussig et al., 2014). However, as in all these studies, SufS was characterized only from *P. falciparum* and *P. berghei* and there is no experimental evidence for a functional cysteine desulphurase from *P. vivax*, thus this study was an attempt to characterize a functional cysteine desulphurase from this neglected parasite.

3.2 Results and Discussion

The data mining from PlasmoDB gave two proteins as cysteine desulphurases: cysteine desulphurase, mitochondrial precursor (PVX_081665) and cysteine desulphurase, putative (PVX_000600). We started the work taking both these cysteine desulphurases in consideration and predicted the targeting of this gene by checking the presence of N-terminal bipartite leader sequences using various available online servers as described in methodology section 2.1.

3.2.1 Targeting of *Pv*SufS

The amino acid sequences for above cysteine desulphurases, when submitted to the online targeting servers, showed strikingly unexpected results. The PlasmoAP results for PVX_000600 gave three out of total four tests positive while, PVX_081665 gave four out of four tests positive for the signal peptide. In PlasmoAP, the transit of protein through the apicoplast membranes is predicted on the basis of different parameters; like presence of basic amino acids and KN enriched regions at the N-terminal. Surprisingly for PVX_081665 all five tests were positive suggestive of it being "very likely" to be targeted to the apicoplast (**Figure 3.2a**); while for PVX_000600 only three out of five tests were positive, indicating its "unlikely" targeting to the apicoplast (**Figure 3.2b**).

a)

Criterion	Value	Decision
Signalpeptide	4 of 4 tests positive	++
apicoplast-targeting peptide	5 of 5 tests positive	++
Ruleset 1		
Ratio acidic/basic residues in first 22 amino acids <=0.7	0.143	yes
Does a KN-enriched region exist (40 AA with min. 9 K or N) with a ratio acidic/basic <=0.9	0.182	yes
Ruleset 2		
number of acidic residues in first 15 amino acids (<=2)	0	yes
Does a KN-enriched region exist (40 AA with min. 9 K or N) ? Ratio acidic/basic residues in this region <0.6	0.182	yes
Is the first charged amino acid basic ?		yes

b)

Criterion	Value	Decision
Signalpeptide	3 of 4 tests positive	+
apicoplast-targeting peptide	3 of 5 tests positive	-
Ruleset 1		
Ratio acidic/basic residues in first 22 amino acids <=0.7	0.167	yes
Does a KN-enriched region exist (40 AA with min. 9 K or N) with a ratio acidic/basic <=0.9	0.000	no
Ruleset 2		
number of acidic residues in first 15 amino acids (<=2)	1	yes
Does a KN-enriched region exist (40 AA with min. 9 K or N) ? Ratio acidic/basic residues in this region <0.6	0.000	no
Is the first charged amino acid basic ?		yes

Note: The **final decision** is indicated by "++, +, 0 or -", where apicoplast-localisation for a given sequence is considered as "++ very likely; + likely; 0 undecided; - unlikely

Figure 3.2: Prediction of bi-partite N-terminal leader sequence with PlasmoAP for a) PVX_081665 b) PVX_000600.

To confirm the PlasmoAP results, we used the PATS server, which again showed no probability for the presence of an apicoplast targeting peptide in PVX_000600 with a score of 0.135. However, for PVX_081665, it showed a high probability for the presence of an apicoplast targeting peptide with a score of 0.938 (where score near 1 indicates likely probability of the protein being targeted to the apicoplast). As the scores obtained for apicoplast targeting were not satisfactory, we went ahead to

check if mitochondrial signals are present in these sequences. We submitted the sequences to MitoProtII and PlasMit online servers. However, we again got contradictory results for both the proteins. MitoprotII showed a high probability of targeting of PVX_000600 to the mitochondria (0.9182/1) while a very low probability of mitochondrial targeting was observed for PVX_081665 (0.6136/1). In contrast, PlasMit predicted both the proteins as non-mitochondrial (99% non-mitochondrial). The doubt created by these mixed-up results thus demands a deeper investigation into targeting of this protein, possibly using localization studies.

During the study, the first report of *Plasmodium* cysteine desulphurases was published which clearly suggested that in *P. falciparum*, two different cysteine desulphurases namely: IscS and SufS are present and these are specifically targeted to the mitochondrion and the apicoplast respectively (Gisselberg et al., 2013). Taking into consideration this report, we aligned the respective *Pf*IscS and *Pf*SufS with PVX_081665 and PVX_000600. The results (**Table 3.1**) clearly indicate that *Pf*IscS shares more similarity with PVX_081665 and *Pf*SufS is more similar to PVX_000600 thus, contradicting the predictions by targeting softwares.

Table 3.1: Pairwise Sequence Alignment Scores of *P. falciparum* and *P. vivax* cysteine desulphurases.

	PVX_081665	**PVX_000600**
***Pf*IscS**	68.14	49.96
***Pf*SufS**	47.71	55.96

Since these results indicate that *Pf*SufS is more similar to PVX_000600, for our further studies we moved forward with PVX_000600 (Hereafter we will designate it as *Pv*SufS).

3.2.2 Amplification of *PvsufS* gene

3.2.2.1 Primer designing and amplification of *PvsufS*

The *sufS* gene (putative) of *P. vivax* Salvador I (Gene ID: PVX_000600) is 1656bp long and expands from 442,905 - 444,763 position on chromosome no. 3. It has a

5'UTR and an intron and the gene encodes for 1533 bases mRNA. To amplify the complete *sufS* gene from different *P. vivax* field isolates, two sets of primers excluding the 5'UTR were designed from genomic sequence of PVX_000600 (**Figure 3.3 & Table 3.2)**. Amplification of the full-length gene was achieved with genomic DNA and cDNA using primers VS66 and VS68 following conditions given in **Table 3.3**. The obtained amplicons (**Figure 3.4**) were purified using QIAquick Gel Extraction kit, commercially sequenced and analysed by different software as described in materials and methods.

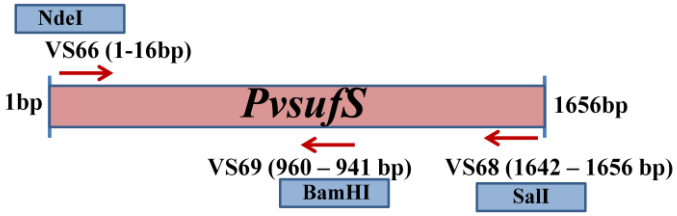

Figure 3.3: Position of primers designed for amplification of *sufS* gene from *P. vivax*.

Table 3.2: Primer sequences for the amplification of *sufS* gene from *P. vivax* genome

Lab Id	Primer sequence	Restriction enzyme site
VS66	5' CTA **CAT ATG** ATG CGG CCC TCG AGC G 3'	NdeI
VS68	5' GTA **GTC GAC** CTA GTT CAT CCC ACT CAG CAT 3'	SalI
VS69	5' CGG **GGA TCC** AGT TGT TAT CAT GTT GCT TCC 3'	BamHI

Table 3.3: Reaction conditions employed for the amplification of *PvsufS* gene from genomic and cDNA

Reaction Steps	Primers Used		
	VS66 & VS68 (1656bp) (Genomic DNA)	VS66 & VS69 (960bp) (Genomic DNA)	VS66 & VS68 (1533bp) (cDNA)
Pre-Denaturation	94°C for 3 min	94°C for 3 min	95°C for 3 min
Deanturation	94°C for 1.5 min	94°C for 1 min	95°C for 1.5 min
Annealing	59.5°C for 1.5 min x35	59.5°C for 1 min x35	59.5°C for 1 min x35
Extension	72°C for 2.5 min	72°C for 1.5 min	72°C for 2.5 min
Post Extension	72°C for 4min	72°C for 4min	72°C for 4min

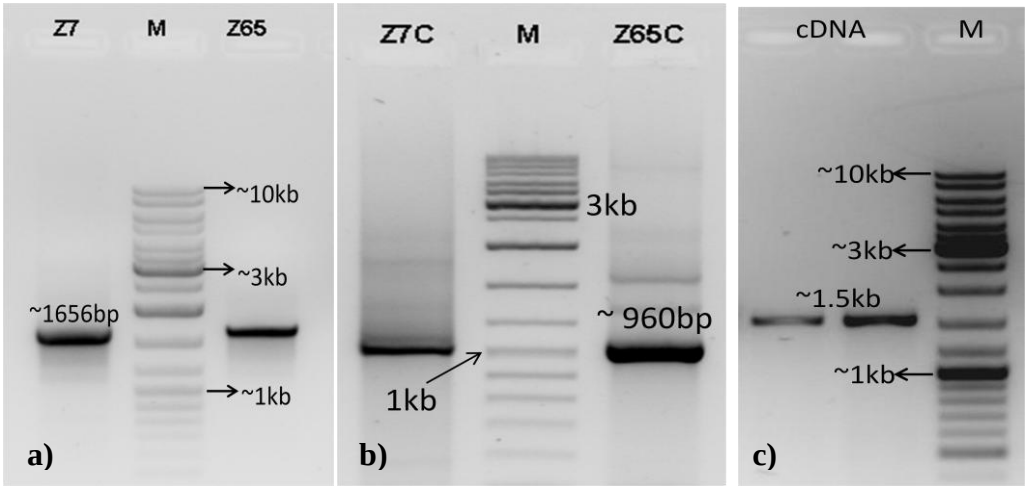

Figure 3.4: *PvsufS* gene amplification (Parasite DNA samples: Z7, and Z65; M: Gene Ruler DNA Ladder mix Fermentas SM0331). (a) Genomic DNA full gene amplification (1656bp) (b) Central region (960bp) (c) cDNA Complete *PvsufS* gene (1533bp).

3.2.3 Sequence Analysis and Multiple Sequence Alignment

The obtained sequences of Indian *PvsufS* (BankIt ID: KY662008) was analysed at the nucleotide and amino acid level, amongst different Indian isolates as well as with standard *P. vivax* Salvador I. The Indian *PvsufS* showed complete match to SufS sequence from Sal-1 strain, except an insertion of 41 amino acids. In the multiple sequence alignment with *Plasmodium*, different Apicomplexans, and prokaryotes the Indian *P. vivax* sequences showed percent identity ranging from 35.82 to 86.27 (**Table 3.4a)**. Within the *Plasmodium* genus, the *Pv*SufS showed percent identity of 86.27% with *P. cynomolgi*, 82.87% with *P. knowlesi* and 50.20% with *P. falciparum* (**Table 3.4b**). Alignment between SufS protein of prokaryotes and apicomplexans showed a long gap at the N-terminal region because of the absence of N-terminal targeting sequence. Other residues that interact with PLP in the internal aldimine and substrate-bound external aldimine forms (Mihara et al., 2002) were found conserved as T187, H216, D296, Q299, H303, S324, H326. *Pv*SufS also possesses the conserved Cys_{500} residue (corresponding to *E. coli* Cys_{364}) which falls in the RXGHHCA (position 495-501) consensus region (**Figure 3.5**), which is typically found in NifS-like proteins and classified as group II cysteine desulfurases (Zafrilla et al., 2010).

Table 3.4: Percent identity of *Pv*SufS protein sequence from Indian field isolates with SufS sequence from a.) Apicomplexans, prokaryotes, eukaryotes b.) other *Plasmodium* species

a.)

Nucleotide/ Amino acid	***P. vivax***	***Arabi***	***Pseudo***	***Babe***	***E. coli***	***Bacill***	***Toxo***	***Thermo***	***Mycob***	***Therm***
P. vivax		47.28	44.74	45.02	44.83	47.73	35.82	44.29	45.15	48.36
Arabidopsis	33.48		43.20	51.57	47.99	52.58	42.63	46.31	43.54	50.45
Pseudomonas	29.97	39.20		42.41	50.00	48.21	30.34	45.72	53.47	53.09
Babesia	31.41	37.03	34.86		45.74	46.74	33.56	44.37	42.39	46.81
E. coli	34.33	47.65	39.90	39.22		51.86	32.67	48.96	52.19	53.23
Bacillus	37.22	51.60	40.10	38.31	47.76		34.06	53.45	49.96	53.67
Toxoplasma	31.78	43.14	37.69	34.54	44.44	41.63		34.56	31.69	31.70
Thermotoga	31.09	39.85	34.18	31.07	39.25	45.89	35.31		49.21	50.46
Mycobacterium	30.64	45.15	39.45	30.94	45.52	43.14	41.40	42.04		56.63
Thermus	34.65	51.98	41.12	37.46	47.37	51.37	45.79	43.00	49.38	

b.)

Nucleotide/ Amino acid	***P. vivax***	***P. falciparum***	***P. berghei***	***P. chabaudi***	***P. cynomolgi***	***P. knowlesi***	***P. yoelii***
P. vivax		52.09	53.36	54.09	85.65	83.82	53.58
P. falciparum	50.20		67.58	67.20	57.87	58.95	67.46
P. berghei	50.89	55.03		91.62	58.18	57.09	94.44
P. chabaudii	52.07	53.51	87.86		59.37	58.51	90.78
P. cynomolgi	86.27	51.84	52.35	54.31		85.08	57.99
P. knowlesi	82.87	53.42	52.66	54.24	84.99		57.33
P. yoelii	52.19	54.98	92.60	87.86	54.06	54.18	

3.2.4 Conserved domain and Signature motif analysis

The CDD analysis of *Pv*SufS showed the presence of an aspartate aminotransferase (AAT) superfamily (fold type-I) of Pyridoxal Phosphate (PLP) dependent enzymes domain spanning the amino acid residues 77-533 (**Figure 3.6**).

This domain contains a PLP-binding motif (SGHK, position 324-327 amino acids) with a conserved Lys residue (327 position) that forms an internal aldimine with PLP. This specific pattern of signature motif is present throughout the SufS orthologues. The presence of these conserved domain and signature motifs confirms this protein as SufS protein that participates in the SUF pathway for Fe-S cluster biogenesis.

Figure 3.5: Multiple sequence alignment of *P. vivax* SufS sequence with other *Plasmodium* spp.

The red lines depict the conserved signature motifs SGHK and RXGHHCA in *Pv*SufS protein.

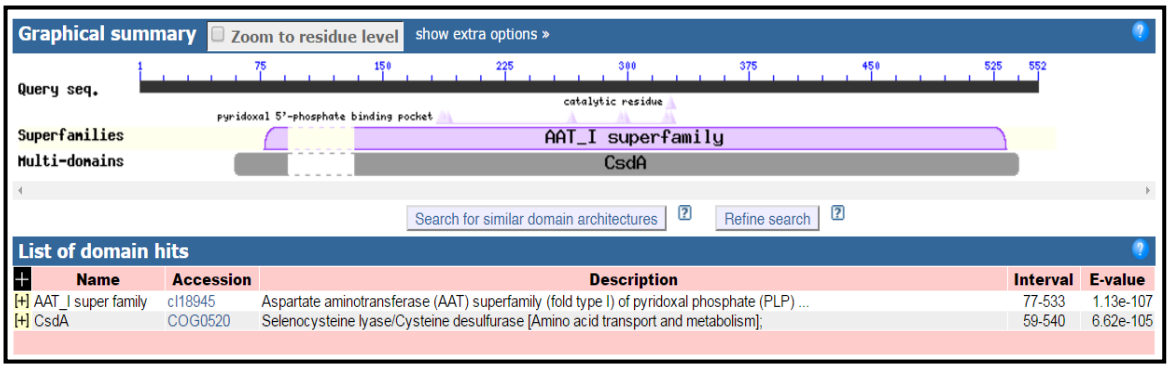

Figure 3.6: Conserved domain detection (CDD) of *Pv*SufS protein. The region spanning the amino acid position 77-533 of the query protein sequence showed a match with AAT superfamily.

3.2.4 Phylogenetic analysis

The evolutionary position of *Pv*SufS was predicted by constructing a phylogenetic tree using MEGA 6.0 (Tamura et al., 2013). The MSA generated for phylogenetic tree construction included 19 amino acid sequences including major apicomplexans (*Plasmodium, Toxoplasma, Hammondia, Babesia*), prokaryotes (*E. coli, Pseudomonas, Thermus thermophilus, Mycobacterium, Thermotoga maritima*), plant (*A. thaliana*) (Accession numbers mentioned in Materials & Methods). The evolutionary history was inferred by using the Maximum Likelihood method based on the JTT matrix-based model. The tree with the highest log likelihood (-8517.8702) is shown. The tree is drawn to scale, with branch lengths measured in the number of substitutions per site. The analysis involved 19 amino acid sequences. All positions containing gaps and missing data were eliminated. There were a total of 341 positions in the final dataset (**Figure 3.7**).

On analysis of different clades, *Pv*SufS protein grouped along with other primate parasites *P. knowlesi* and *P. cynomolgi* while rodent malaria parasite *P. berghei*, *P. chabaudii* and *P. yoelii* were present in different clade. These two clades diverge out of *P. falciparum* clade indicating a separate origin of *P. falciparum*. This evolutionary analysis of *Pv*SufS protein is in agreement to other *Plasmodium* genome members reported in various studies (Rathore et al., 2001; Escalante et al., 2005; Saxena et al., 2007 & 2012; Martinsen et al., 2008) detailing the origin of *P. vivax* as primate parasite and a major divergence of *P. vivax* from *P. falciparum*. All the apicomplexans apart from the *Plasmodium* species formed a separate clade in close proximity to *Plasmodium* clade. *A. thaliana* bearing a photosynthetic plastid was placed in close proximity with Apicomplexans which bear a non-photosynthetic plastid. All the prokaryotic species formed a separate clade showing its distinct divergence from the eukaryotic counter-part.

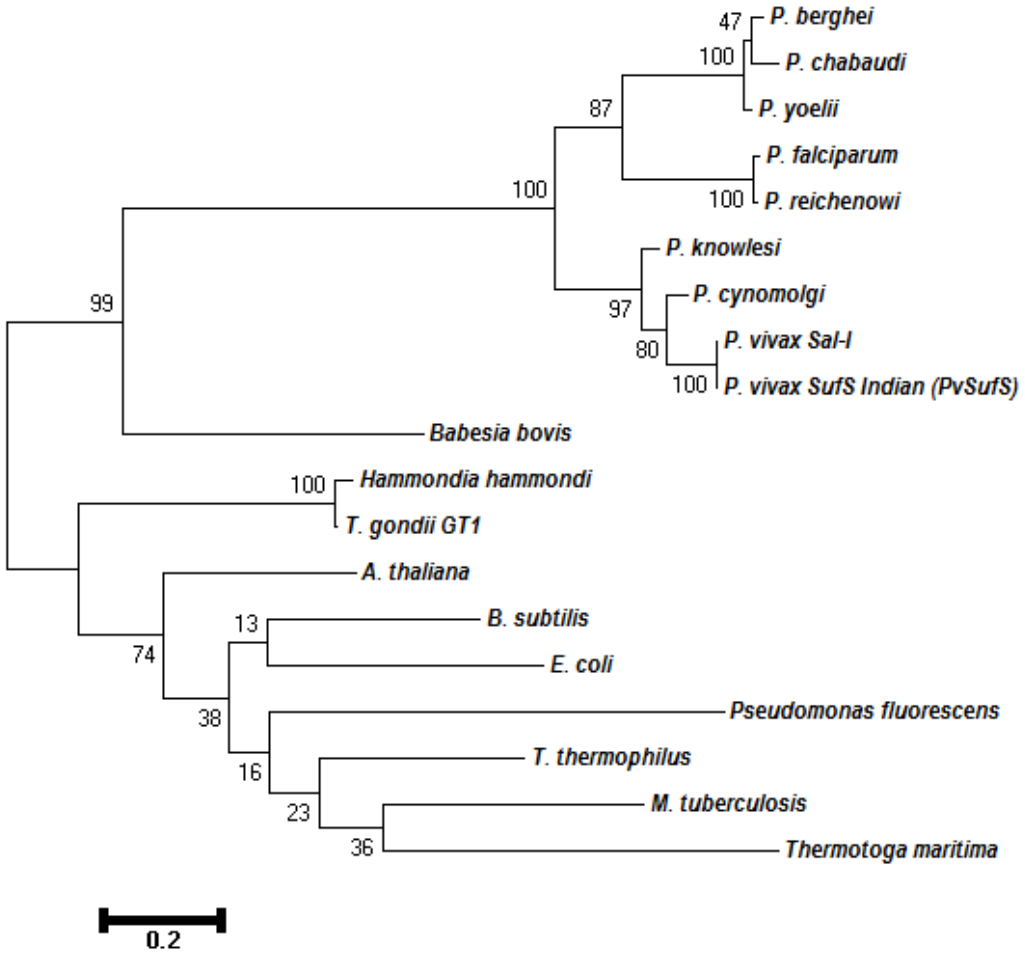

Figure 3.7: Phylogenetic analysis of SufS protein sequences. SufS protein sequence of Indian *P. vivax* with orthologues. Boot strapping done for 1000 iteration and percentage of trees in which the associated taxa clustered together shown next to the branches.

3.2.6 Cloning and expression of *PvsufS* gene

After the confirmation of the amplified product as *PvsufS* gene, we proceeded with the cloning of amplicons first in a TA cloning vector. The successful recombinant clones were confirmed by colony PCR (**Figure 3.8**) and utilized to sub-clone the gene in pRSET A expression vector at BglII and SacI restriction enzyme sites (**Figure 3.9**). Further to screen the recombinant colonies containing desired gene, colony PCR was performed (**Figure 3.10**). The correct orientation of *PvsufS* gene was confirmed using restriction digestion (**Figure 3.11**). Sequencing using T7 and gene specific primers confirmed the integrity of the gene in the recombinant clone and the presence of start codon in-frame.

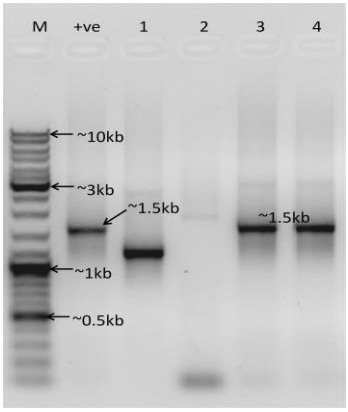

Figure 3.8: Colony PCR to check for the colonies showing recombinant construct in TA vector. (M: Gene Ruler DNA Ladder Mix; +ve: PCR positive control from cDNA; 1, 2, 3 4: colony number after vector insert ligation and transformation).

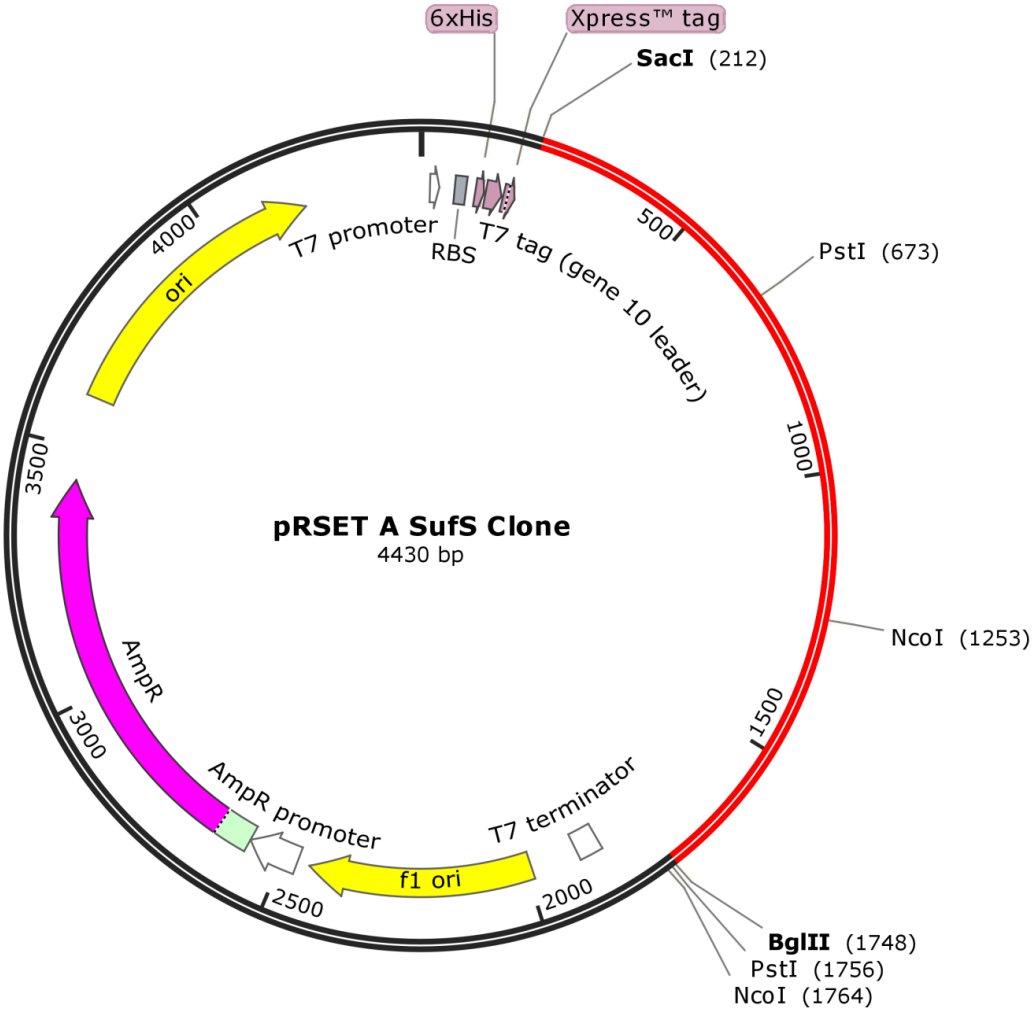

Figure 3.9: The pRSET A – *PvsufS* clone map: Red part depicts *PvsufS* gene and black part shows the regions of pRSETa vector. The restriction sites in bold depict the site of gene insertion. The remaining restriction sites depict the sites used to confirm the clone.

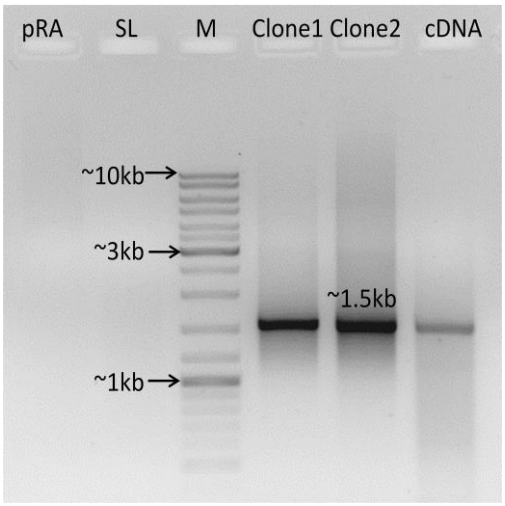

Figure 3.10: Colony PCR to check for the colonies showing recombinant construct (pRA: pRSETa Vector; SL: Self-ligation; M: Gene Ruler DNA Ladder Mix; Clone1 & Clone2: colony number after vector insert ligation and transformation; cDNA: PCR positive control from cDNA).

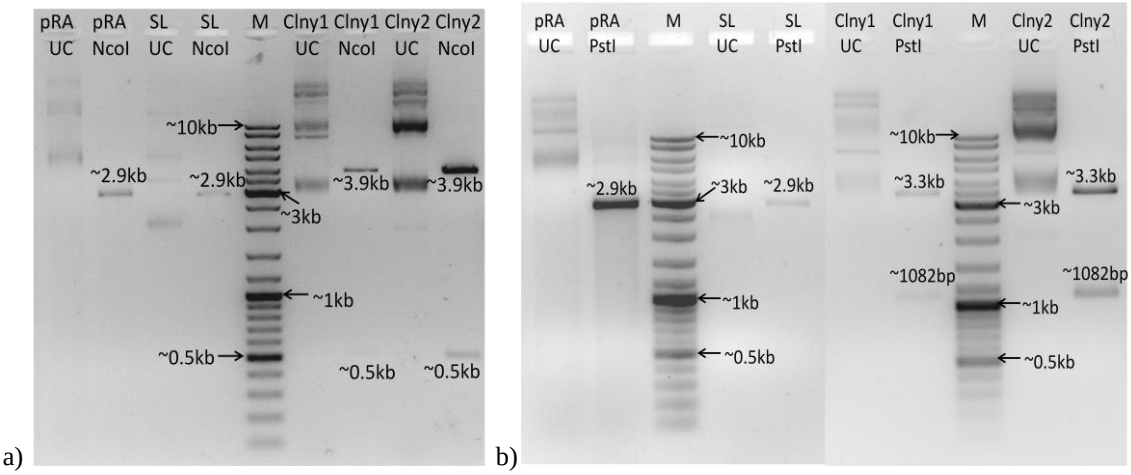

Figure 3.11: Restriction analysis of *PvsufS* recombinant constructs with a.) NcoI enzyme b.) PstI enzyme. M: Gene Ruler DNA Ladder Mix (Thermo Scientific, USA); pRA: pRSET A Vector; SL: Self-ligated vector; UC: Uncut Plasmid; Clny1 & Clny2 : Recombinant contructs 1 & 2 digested with restriction enzymes.

After successful validation, the obtained recombinant clone was transformed into *E. coli* BL21(DE3)pLysS host cells, induced with 0.5mM IPTG at 37˚C for 2hr, 4hr and 6hr to perform protein expression studies (Chapter 2, 2.8). The bacterial cells containing the recombinant construct were harvested by centrifugation, resuspended in lysis buffer and checked on SDS PAGE after staining with Coomassie brilliant blue R250 (**Figure 3.12**). The recombinant *Pv*SufS protein expressed as a fusion protein of ~61.2 kDa carrying a 6X-His tag. The expression for the recombinant protein was confirmed by western blotting (**Figure 3.13**) using anti-His antibody

(Qiagen, USA) as per the manufacturer's protocol, where a band at ~61.2 kDa in the recombinant clone induced sample shows the presence of the desired protein.

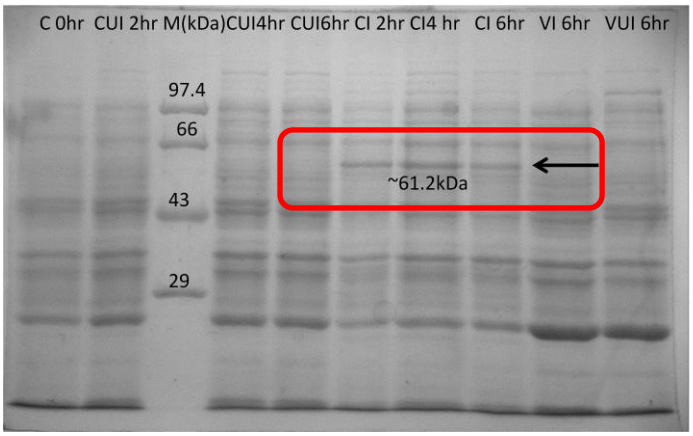

Figure 3.12: Over expression of full length *Pv*SufS protein in *E. coli*. M: Protein Molecular Heavy Weight Marker (Genei); CUI: pRSETa *Pv*SufS clone uninduced; CI: pRSETa *Pv*SufS clone induced samples;VUI: pRSETa vector uninduced sample VI: pRSETa vector induced sample).

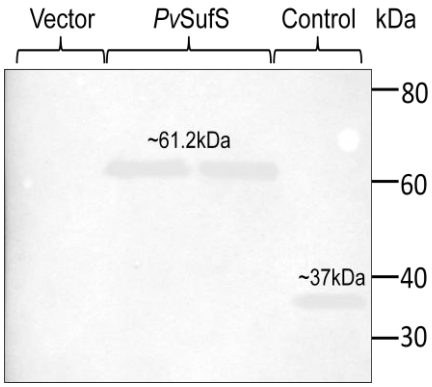

Figure 3.13: Expression of His tagged *Pv*SufS protein confirmation by western blotting. Control: Positive lab control of a His tagged protein.

3.2.7 Protein purification

To perform enzyme kinetics studies and sub-cellular localization, pure protein is required. Thus, the *Pv*SufS recombinant protein was purified following gel elution protocol discussed in materials and methods (Chapter 2, 2.10.2). For the same, the protein was over-expressed, subjected to the above protocol and analysed (**Figure 3.14**).

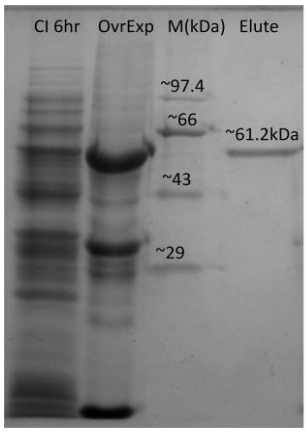

Figure 3.14: Purification of recombinant His-tagged *Pv*SufS protein. (CI & OvrExp: pRSET A *PvsufS* induced recombinant protein; M: Protein High Molecular Weight Marker (Merck Bio Science); Elute: Recombinant Pure protein *Pv*SufS).

3.2.8 Functional characterization of *Pv*SufS protein

3.2.8.1 PLP-Binding Assay and Cysteine Desulphurase Assay:

For the PLP-binding assay, UV-visible absorption spectra of purified *Pv*SufS in 50mM TrisHCl and 200mM NaCl buffer (pH 7.5) was recorded at wavelengths of 250 to 500 nm. The binding of pure *Pv*SufS to PLP was indicated by its light yellow colour, which is a characteristic feature of PLP-binding enzymes. The UV-visible absorption spectrum of purified recombinant *Pv*SufS displayed a hump at around 420 nm in addition to the major protein peak at 280 nm (**Figure 3.15**). The 420-nm shoulder is suggestive of bound pyridoxal in an aldimine linkage in the SufS enzyme.

For determining the desulphurase activity of *Pv*SufS briefly, the enzymatic assays were carried out anaerobically where the reaction mixtures contained 5µM *Pv*SufS in sodium carbonate buffer (pH 9.0), 25mM Tris-Cl, 100mM NaCl buffer, 100µM PLP, 2mM DTT. The reactions was initiated by the addition of L-cysteine to a final concentration of 1mM and allowed to proceed for 20 min. The excess of L-cysteine was removed using Amicon Ultra-4 filters (Merck, Germany). The filtrate was then subjected to Methylene blue assay (Siegel, 1965). For the same, sodium sulfide standards were prepared in sodium carbonate buffer (pH 9.0) with concentration varying from 0.01mM to 0.1mM. Standards and protein sample were further treated with 0.02M N, N-Dimethyl-p-phenylene-diamine sulfate (DPD) and 0.03M Ferric chloride ($FeCl_3$). After incubation at room temperature for 10 min, absorbance was taken at 650 nm. The calibration curve was prepared for sulfur standards and protein (**Figure 3.16)**. Quantity of sulfur released by *Pv*SufS protein was calculated by extrapolating the absorbance of these calibration curves.

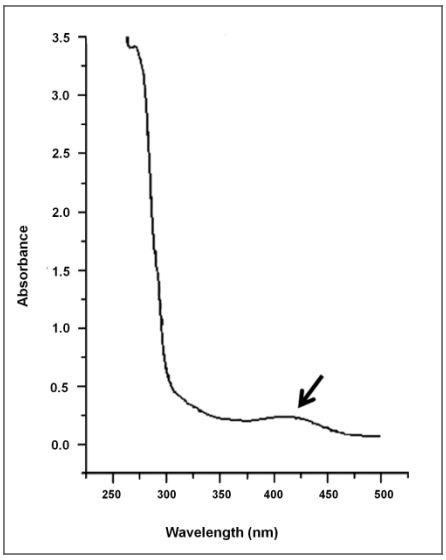

Figure 3.15: UV-VIS absorption spectrum of *Pv*SufS indicating *Pv*SufS is a PLP cofactor-dependent desulfurase.

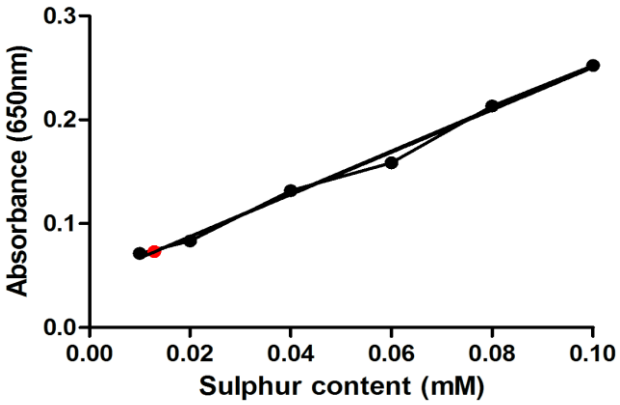

Figure 3.16: A regular standard curve to determine the sulfide content by methylene blue assay. The red dot indicates the extrapolated value for *Pv*SufS protein.

The capability of recombinant *Pv*SufS to function as a cysteine desulfurase in the presence of L-cysteine substrate was measured (2.575 µmole/ µmole protein) and it was seen that, *Pv*SufS alone exhibited very low cysteine desulfurase activity. Thus, it is possible that *Pv*SufE is required for increasing the activity of *Pv*SufS. The details for the same are discussed in Chapter 6.

3.2.9 Antibody raising and Immuno-localization

The SUF pathway is said to be localized to the apicoplast in *Plasmodium*. PlasmoAP showed less probability of targeting of *Pv*SufS to the apicoplast and this was supported by PATS data. MitoProt also showed this protein to be targeted to mitochondria, raising questions about its localization in the parasite. Thus to confirm the sub-cellular localization of *Pv*SufS, antibodies were raised against recombinant *Pv*SufS in mice by injecting ~28µg of pure *Pv*SufS protein with Freund's adjuvant followed by three booster doses at an interval of 21 days (Chapter 2.12.1). Antibody concentration was calculated for the sera collected after different booster doses of *Pv*SufS protein using standard ELISA where serum collected from mice injected with 1X PBS was used as a control. Pre-immune sera were collected to check presence of any cross-reactive antibodies. Best antibody concentration was observed at third booster dose (**Figure 3.17**). Specific band obtained at the desired position in western blotting using both recombinant protein and parasite lysate confirms specificity of antibodies towards *Pv*SufS protein (**Figure 3.18**).

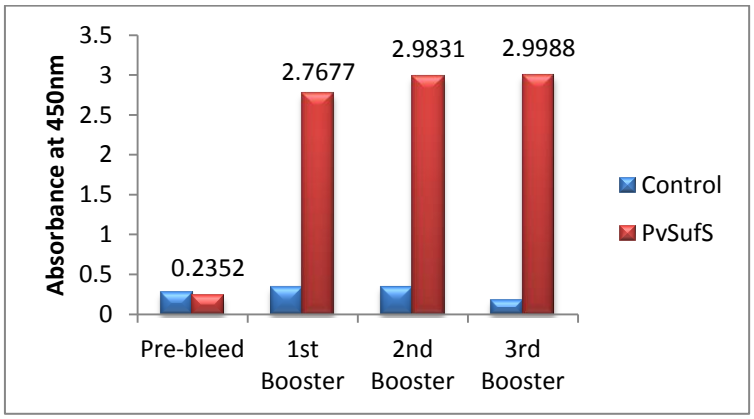

Figure 3.17: Antibody concentration determination for *Pv*SufS protein by ELISA.

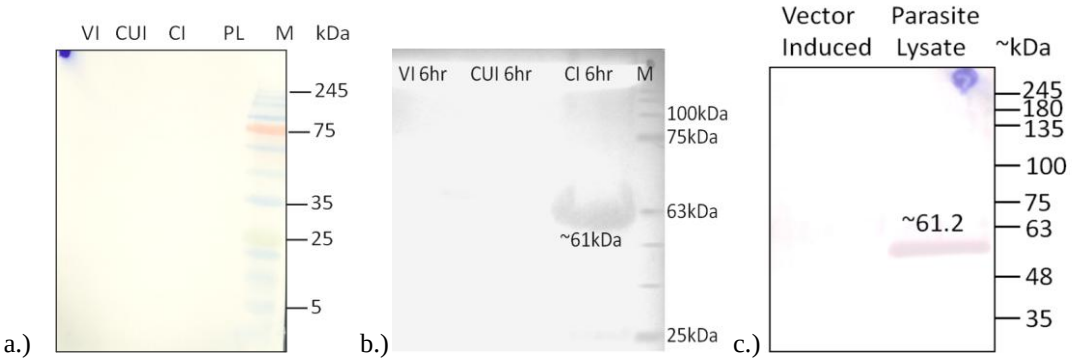

Figure 3.18: Western blot of anti- *Pv*SufS antibodies with a.) pre-immune sera b.) recombinant *Pv*SufS c.) parasite lysate (VI 6hr: pRSET A Induced 6 hours; CUI 6hr: pRSET A *PvsufS* uninduced 6 hours; CI 6hr: pRSET A *PvsufS* induced 6 hours; PL: parasite lysate; M: Prestained Protein Molecular Weight Marker (B. R. Biochem).

To perform sub-cellular localization on blood smears prepared from *P. vivax* infected patients, parasite cells were fixed with methanol, permeabilised with 0.05% saponin and 0.1% TritonX-100 and sequentially treated with mouse polyclonal anti-*Pv*SufS sera (1:100) followed by goat anti-mouse monoclonal IgG FITC antibodies (1:2000). DAPI (75ng/ml) and Qdot® 585 Streptavidin conjugate (10nM) counter staining was done to observe the parasite's nucleus and apicoplast respectively. Slides were observed using the respective filters, where a bright field was used to identify the RBCs infected with parasite, green fluorescence to localize the *Pv*SufS protein, blue and red fluorescence for nucleus and apicoplast respectively (**Figure 3.19**). The *Pv*SufS protein was localized as a green fluorescing spot with an overlapping red spot of apicoplast and a blue spot staining nucleus adjacent to this merged yellowish spot. This study confirms that *Pv*SufS protein is functionally active in the apicoplast.

3.2.10 *In-silico* studies for *Pv*SufS

The *in vitro* biochemical assays mentioned above confirm *Pv*SufS to be a cysteine desulphurase enzyme and suggest that it donates sulphur from the cysteine for the formation of a Fe-S cluster. We further wanted to investigate the interacting residues involved in the interaction of *Pv*SufS with PLP and its partner protein *Pv*SufE. For the same, a structure of *Pv*SufS was necessary, but, due to lack of availability of crystal structure for SufS from *Plasmodium*, a homology model was constructed.

3.2.10.1 Secondary structure prediction

To generate the model of *Pv*SufS protein, the first step performed was secondary structure prediction using PSI-PRED (McGuffin et al., 2000). In *Pv*SufS protein, presence of 15 α-helices and 13 β-strands were observed which were joined with the help of 30 coils (**Figure 3.20**). The intrinsic disordered profile was analysed to verify the stability of the structure and their interactions with environment. Information related to characteristic features and chemical properties of *Pv*SufS protein provided by PSIPRED are enlisted in **Table 3.5.**

Table 3.5: Characteristics features of *Pv*SufS protein analysis based on Secondary structure

Characteristic features	*Pv*SufS
Molar extinction coefficient	46510
Molecular weight	62460.30
Isoelectric point	9.98
Percent negative residues	0.08
Percent positive residues	0.14
Charge	42.45
Signal peptide	Not detected
Transmembrane topology	321-336
Aliphatic index (0-100)	85.64
Hydrophobicity (-4 to 3)	-0.23

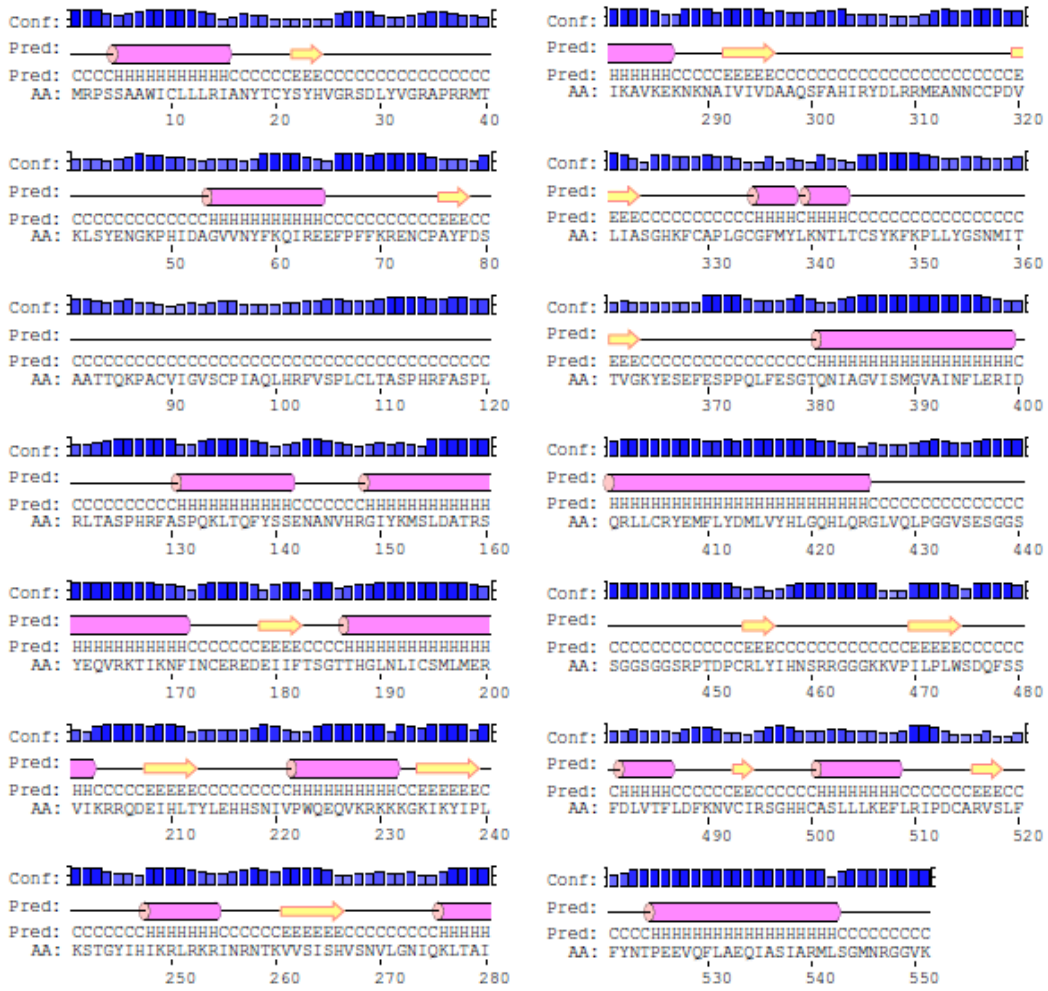

Figure 3.20: Secondary Structure predictions for *Pv*SufS protein using PSIPRED.

The secondary structure of *Pv*SufS protein was also compared with SufS of *Plasmodium*, other apicomplexans and prokaryotes using Geneious software (http://www.geneious. com, Kearse et al., 2012). It was found that the secondary structure of *Pv*SufS showed high conservation with the other *Plasmodium spp.* but strikingly it did not show conservation with other apicomplexans like *Toxoplasma gondii* and *Babesia bovis* (**Figure 3.21**).

3.2.10.2 Comparative modelling and Energy Minimization

Three-dimensional (3D) homology model of *Pv*SufS protein from an Indian isolate was built by homology modelling using the program MODELLER 9v11 (Sali and Blundell, 1993; Eswar et al., 2006). The *Pv*SufS amino acid sequence obtained from

Plasmodium Indian field isolate (Ind*Pv*SufS) was submitted to HHpred online server for template search. Crystal structure of *Bacillus subtilis* SufS (PDB; 5J8Q) protein with 1.7 Å resolution was selected as a template for *Pv*SufS protein. SufS sequence of *Plasmodium* parasite shares only 38.24% amino acid identity with *B. subtilis* SufS, mainly in the conserved domain region. The major difference in the template and target sequences was because of the presence of apicoplast targeting sequences on the N-terminal of the target. This sequence is cleaved as soon as these proteins reach their site of action and thus, this region might not be important for the catalytic activity of these enzymes. Taking care of these points, after the removal of targeting sequence, the sequences were submitted for protein modeling, which yielded 3D model of the target with all non-hydrogen atoms without any user intervention. Since the Indian *Pv*SufS had an insertion which is different from the Sal-I *Pv*SufS (Sal-I*Pv*SufS), a 3D model using the same template mentioned above was also generated for *P. vivax* Sal-I sequence.

The best models with minimum DOPE score were selected and quality of the structure was further improved by energy minimization using online server YASARA (Krieger et al., 2009). The structure were evaluated by using different servers where PROCHECK showed a G-score 'BETTER'. 96.84% & 95.28% of the residues of Ind*Pv*SufS and Sal-I*Pv*SufS had an average 3D-1D score less than 0.2 (passed) for VERIFY3D respectively. A negative Z-score of homology model is compulsory to hold the characteristic of being a good model and both Ind*Pv*SufS and Sal-I*Pv*SufS structures gave a Z-score of -5.42 and -6.12 suggesting that the generated models are good. These results exhibited high quality of homology modelled protein and its reasonable accuracy in terms of dihedral distribution and stereochemistry features. The main chain conformations for 98% of amino acid residues were within the favoured or allowed regions for both the protein structures in the Ramachandran plot analysis (**Figure 3.22a)**. The ERRAT scores for Ind*Pv*SufS and Sal-I*Pv*SufS protein structures were 96.364 and 93.756 respectively and these value indicated that the molecular geometry of the models is of good quality (**Figure 3.22b**) Root-mean-square deviation (RMSD) value of 0.105 Å and 0.116Å between the backbone atoms of the template and Ind*Pv*SufS and Sal-

I*Pv*SufS structures respectively indicated the significant homology between the structures.

a) **Ind*Pv*SufS** **Sal-I*Pv*SufS**

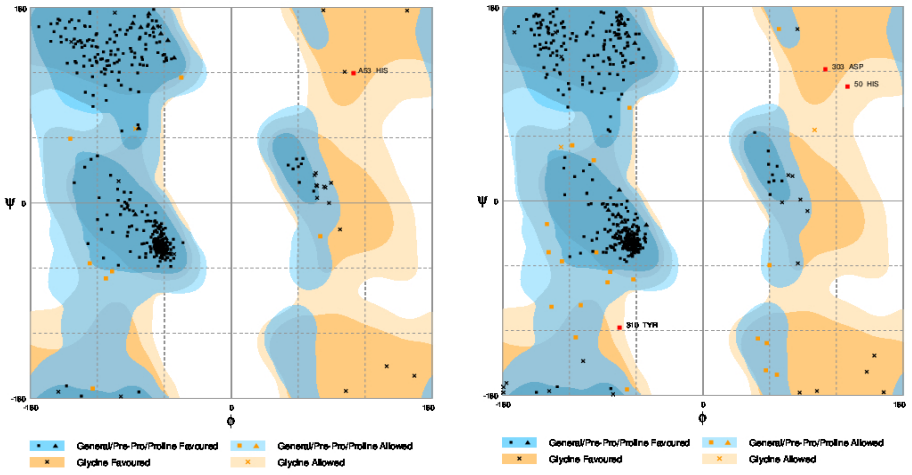

b) **Ind*Pv*SufS**

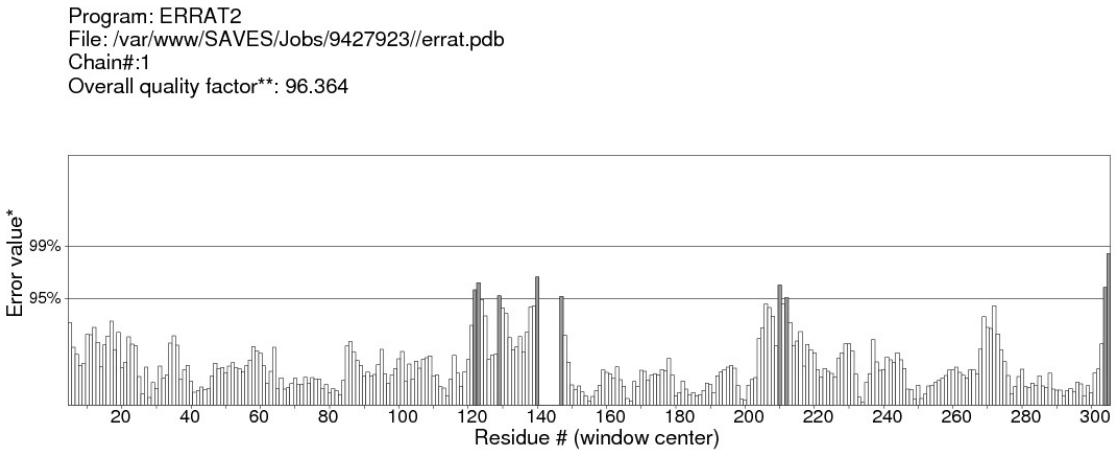

Sal-I*Pv*SufS

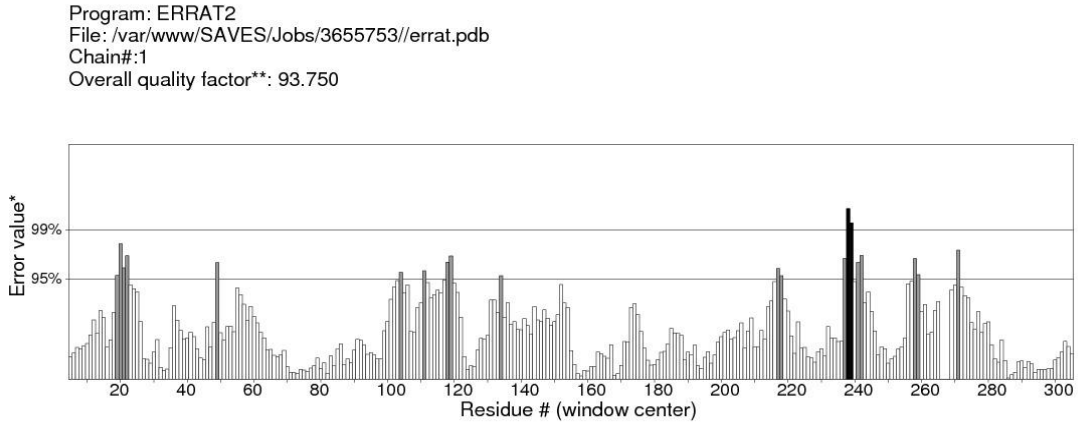

Figure 3.22: Validation of 3-dimensional structure of *Pv*SufS using a.) Ramachandran Plot and b.) ERRAT score.

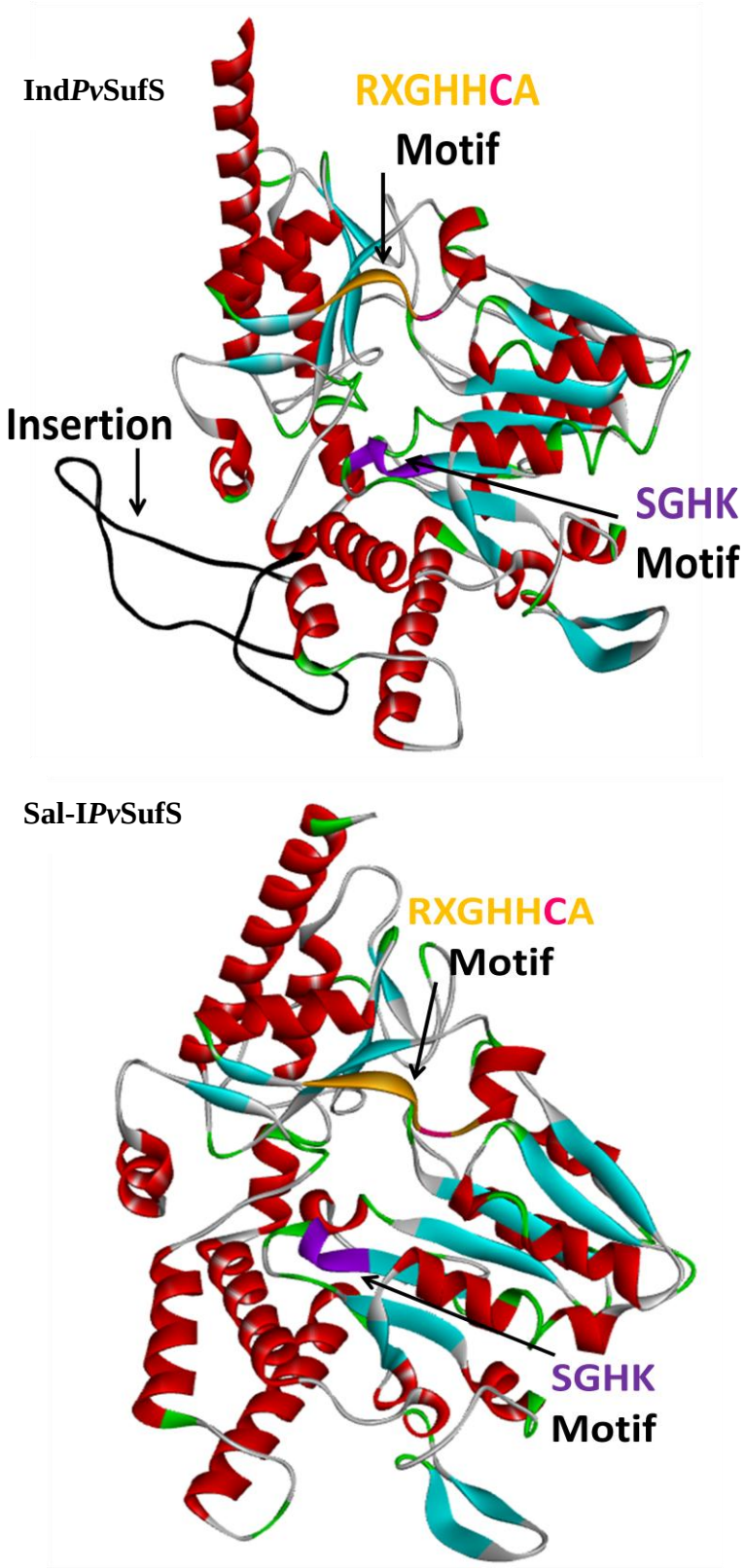

Figure 3.23: *Pv*SufS protein structure prediction: Three dimensional homology model of *Pv*SufS was predicted using *B. subtilis* SufS (5J8Q) as template. The conserved motifs (SGHK in violet color and RXGHHCA in orange color) are marked.

3.2.10.3 Active site architecture and docking with PLP Substrate

Our *in vitro* biochemical assays showed that a *Pv*SufS has a PLP binding domain. In order to get insights into the residues participating in the interaction of *Pv*SufS with PLP substrate we carried out docking studies. The binding pocket of *Pv*SufS was predicted and the PLP substrate was docked in the active site. The PLP cofactor showed interactions with the amino acids His_{216}, Glu_{299}, Asp_{296}, Lys_{327}, His_{303} in the binding pocket (**Figure 3.24a**) of Ind*Pv*SufS whereas it interacted with only three residues namely His_{176}, Glu_{258}, Lys_{286} in the binding pocket of Sal-I*Pv*SufS corresponding to His_{216}, Glu_{299}, Asp_{296}, Lys_{327} of Ind*Pv*SufS (**Figure 3.24b)**. The binding energies for PLP with Ind*Pv*SufS and Sal-I*Pv*SufS were -202.64kal/mol and -145.39kcal/mol respectively.

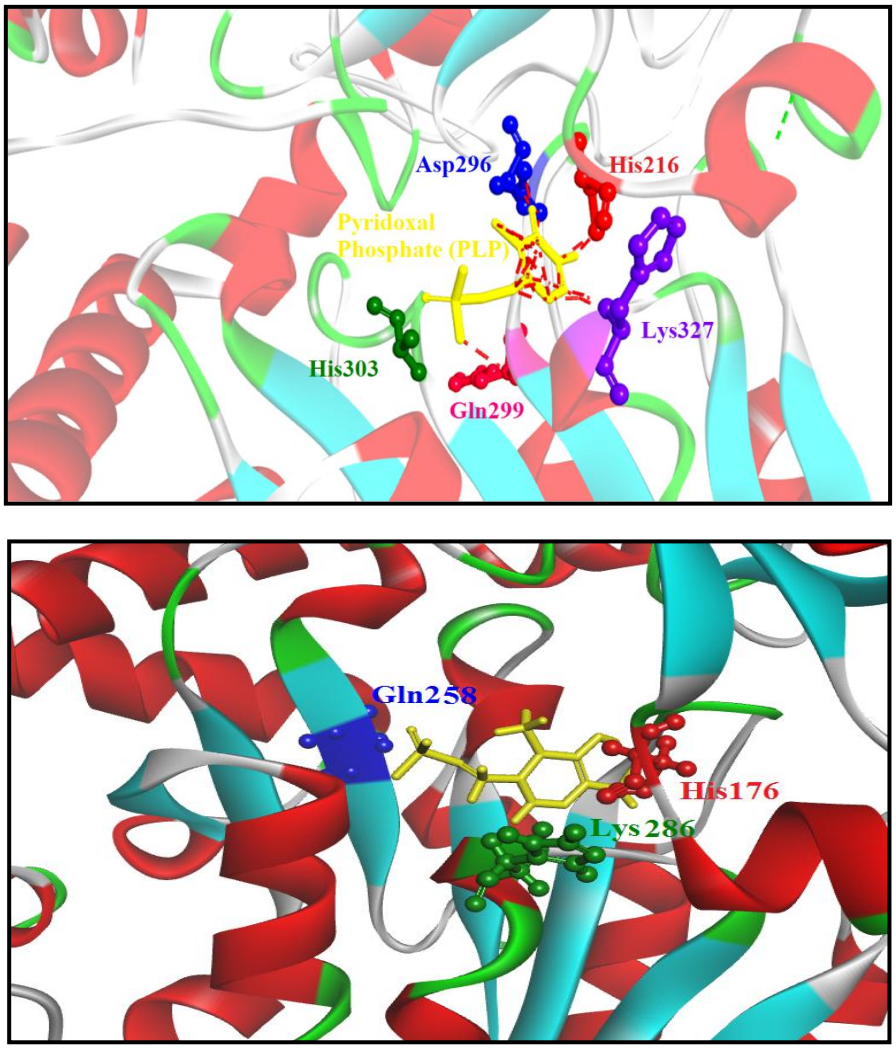

a)

b)

Figure 3.24: Active site prediction and docking analysis of PLP substrate to *Pv*SufS protein a.) Ind*Pv*SufS b.) Sal-ISufS **(**Interaction of PLP (yellow) with *Pv*SufS shown with ball and stick model).

3.2.10.4 Docking with a potential inhibitor D-cycloserine

The inhibitors of PLP-dependent enzymes that form adducts with the PLP-cofactor have been used as irreversible inhibitors of enzyme activity (Eliot and Kirsch, 2004). D-cycloserine is a second-line drug for the treatment of tuberculosis against *Mycobacterium tuberculosis* (Fenn et al., 2003). The potential for this inhibitor has been explored against *P. falciparum in vitro* (Charan et al., 2014). We further wanted to check whether D-cycloserine can be used against *P. vivax* or not. For the same, we docked D-cycloserine with Ind*Pv*SufS and Sal-I*Pv*SufS.

Ind*Pv*SufS and D-cycloserine

a)

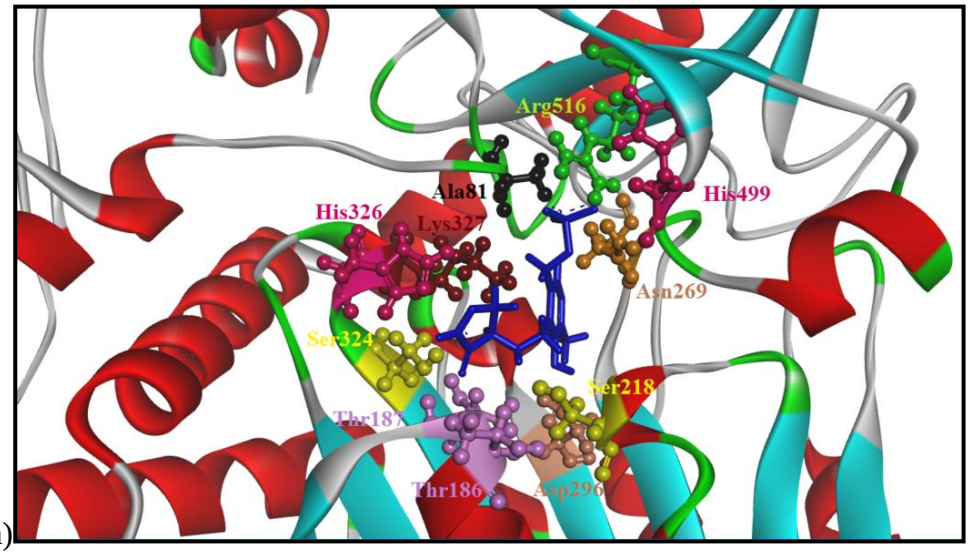

Sal-I*Pv*SufS and D-cycloserine

b)

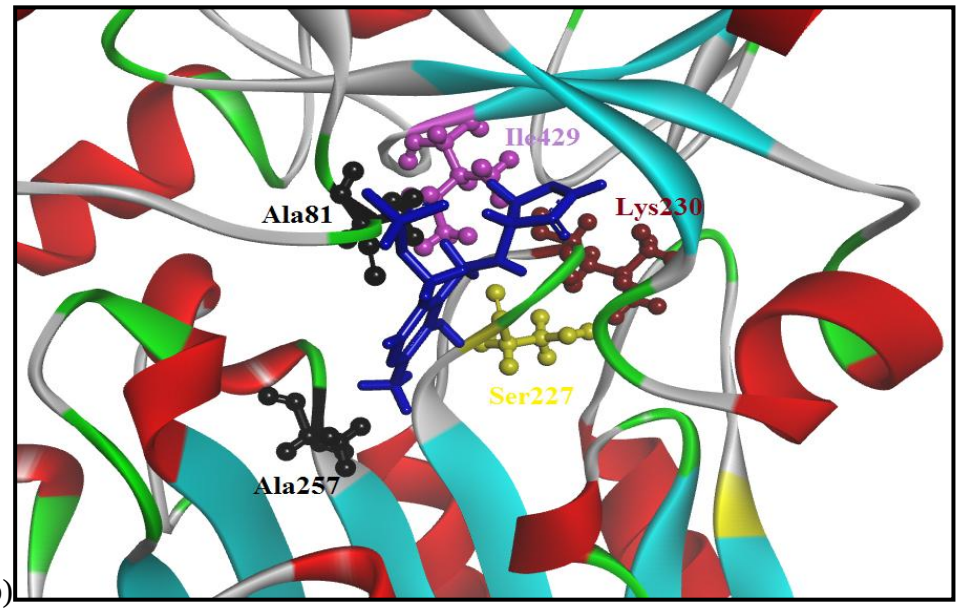

Figure 3.25: Interaction of SufS with a potential inhibitor D-cycloserine (Blue).

The Ind*Pv*SufS interacted with a total of 11 residues in the binding pocket used by PLP cofactor for binding to *Pv*SufS (**Figure 3.25a**). It also showed binding to *Pv*SufS with two residues namely Asp_{296} and Lys_{327} common to the binding residues of Ind*Pv*SufS and PLP. The other residues involved also showed some conservation with residues involved in binding of D-cycloserine with cysteine desulphurase in *Salmonella typhimurium* (Lys_{51}, Ser_{78}, Asn_{79}, His_{80}) (Bharath et al., 2012) and *Hordeum vulgare* (Asn_{230}, Asp_{258}, Ser_{296}, Lys_{299}, Arg_{452}) (Duff et al., 2012). In contrary to this, the Sal-I*Pv*SufS showed participation of only five residues when D-cycloserine was docked in the binding pocket of the enzyme (**Figure 3.25b)**. Neither did these residues showed any conservation with the residues involved in the binding of PLP with SufS nor did with any of the prokaryotic species mentioned above. The binding energies for Ind*Pv*SufS and Sal-I*Pv*SufS with D-cycloserine were -303.23kcal/mol and -289.93kcal/mol respectively. Thus, these results suggest that D-cycloserine may act as a inhibitor of PvSufS, however an experimental validation is needed for the same.

3.3 Conclusion

The *Pv*SufS protein participates in the initial steps of SUF pathway for Fe-S cluster biosynthesis and belongs to the aspartate aminotransferase (AAT) superfamily (fold type-I) of Pyridoxal Phosphate (PLP) dependent enzymes. It acts as a cysteine desulphurase that essentially donates the sulphur for the formation of Fe-S clusters. The comparative sequence analysis of the Indian *Pv*SufS (GenBank: KY662008) with PVX_000600 showed similarity of 93.39% with an insertion of 41 amino acids, while on comparison with bacterial orthologues, it showed similarity of approx. 50%, suggesting that the function may have retained during the course of evolution. Between two major human parasites; *P. falciparum* and *P. vivax*, an identity of approx. 54.81% was observed in the conserved region of SufS, while a high similarity was observed with the SufS protein of other primate malaria parasite like *P. knowlesi and P. cynomolgi*.

Recombinant *Pv*SufS protein expressed in the prokaryotic expression system exhibited the presence of the PLP-binding domain as depicted by the light yellow

colour of the protein and the hump obtained at 420nm in the UV-Vis absorption spectrum. The *in vitro* cysteine desulphurase assay followed by the quantitation of sulphur release by Methylene blue assay further confirmed the function of *Pv*SufS as a cysteine desulphurase enzyme. Further, the co-localization of the SufS protein on thin blood smears made from *P. vivax* parasite infected patient to the apicoplast of the parasite confirmed its functionality in the SUF pathway for Fe-S cluster biogenesis. The specificity of the antibodies was also confirmed using parasite lysate.

As this enzyme has not been crystallized from any of the *Plasmodium* species or apicomplexans and there is no structure available for the enzyme from these organisms, a homology model for *Pv*SufS from Indian isolate and the Sal-I sequence based on a prokaryotic organism *B. subtilis* was generated. The refined model showed five interactions between the Ind*Pv*SufS and PLP in contrast to three between Sal-I*Pv*SufS and PLP, suggesting that the insertion in the field isolate is facilitating the binding between the two molecules with the help of some conformational changes in the protein structure. The results clearly indicated the conservation between *Pv*SufS and *E. coli* in the residues involved in the interaction of the PLP substrate and SufS. Further, the potential of D-cycloserine to act as an anti-malarial when tested by *in silico* analysis showed better binding efficiency for clinical isolates than the Sal-I structure. These docking results also suggest that D-cycloserine may act as an inhibitor of *Pv*SufS as it involves the participation of a few residues similar to that used for binding of Ind*Pv*SufS and PLP cofactor. However, this has to be further validated by *in vivo* studies.

In conclusion, our results ascertain the cysteine desulfurase putative protein PVX_000600 identified from the PlasmoDB database to function as SufS protein in the apicoplast of *P. vivax*. In order to elucidate the partner enzyme of SufS i.e. SufE, we further moved to characterize the SufE protein from *P. vivax* as discussed in the next chapter.

Chapter IV

Characterization of SufE from P. vivax

Characterization of SufE from *P. vivax*

4.1 Introduction

As mentioned in the previous chapter the Fe-S cluster biogenesis pathway begins with the cysteine desulphurase reaction of SufS. The cysteine desulphurase SufS mobilizes sulfur from free cysteine *via* a pyridoxal phosphate-dependent mechanism. The liberated sulfur atom is then donated from SufS to an active site cysteine on the SufE protein. Consequently, the presence of SufE stimulates the basal activity of SufS and the two proteins together form a novel sulfur transfer system (Sendra et al., 2007).

The SUF pathway in *E. coli*, Gram-negative bacteria, is the best studied. The *sufABCDSE* operon of *E. coli* is induced by oxidative stress and iron deprivation. Mihara et al., (1999) first identified *sufS* as a gene encoding an *E. coli* counterpart of mammalian selenocysteine lyase due to its high specific activity for L-selenocysteine (5.5 units/mg) compared to that for L-cysteine (0.019 units/mg). Later the same group also reported that SufS protein from *E. coli* is not a Michaelis-Menten enzyme when using cysteine as a substrate in the presence of Pyruvate (Mihara et al., 2000). Further, Outten et al., in 2003 reported that SufE accepts sulfane sulfur from SufS and that it can enhance the cysteine desulphurase activity of the SufS enzyme up to 8-folds. Based on the analysis of the available crystal structures of the proteins and on the experimental evidence of its resistance to the added reductants it has been suggested that this process of sulfur transfer from SufS to SufE is protected from the environment. They also found the effect of SufB, SufC, and SufD proteins on the activity of SufS, where firstly they observed that SufB, SufC and SufD associate in a stable complex and secondly, in the presence of SufE, the $SufBC_2D$ complex enhances the SufS activity up to 32-fold. The mechanism proposed was that first the cysteine desulfurase SufS donates sulfur to the transfer protein SufE and then SufE in turn interacts with the SufB protein for sulfur transfer to SufB. More importantly, this interaction of SufE and SufB occurs only if SufC is present. The sulfur incorporated into SufB was proposed to be involved in iron-sulfur cluster assembly (Layer et al., 2007). Based on protein

interaction and sulfur trapping with mass spectrometry, the present proposed route in *E. coli* is; SufS liberates sulfur atom from cysteine with a persulfide intermediate on catalytic cysteine C_{364} of SufS. SufS then transfers persulfide to SufE, and finally SufE transfers persulfide to $SufBC_2D$ for cluster assembly. The exact cysteine receiving sulfur in SufB is unclear. SufBC is the minimal complex for further enhancement of SufSE activity. The mechanism for the enhancement likely involves release of persulfide from SufE which can then serve as a substrate for the next round of SufS activity. This sulfur transfer route from SufS to $SufBC_2D$ via SufE may be important for limiting sulfide release during oxidative stress conditions *in vivo*.

In *E. coli*, a conserved cysteine (Cys_{51}) of SufE is required for rapid transfer of sulfur from SufS to the SufBCD complex and a mutated SufE (C51S) binds to SufS and the SufBCD complex in a non-functional manner (Outten et al., 2003; Layer et al., 2007). In *Plasmodium*, an attempt was made to obstruct the Fe-S cluster synthesis and downstream metabolic pathways by generating an over-expression construct of *P. falciparum* SufE with the corresponding cysteine substituted with serine, *Pf*SufE(C154S)-HA. The parasites expressing SufE(C154S)-HA were selected in the presence of 200mM IPP, but this parasite line was independent of IPP for growth. This mutant SufE(C154S)-HA was expressed and trafficked to the apicoplast, but it did not interfere with apicoplast metabolism (Gisselberg et al., 2013). Since no experimental evidence is available till date on *P. vivax* SufE, this study was carried out to characterize SufE from *P. vivax*.

4.2 Results and Discussion

Based on various alignments and conserved domain analysis, as discussed in Chapter 2, we shortlisted a conserved hypothetical protein (Gene ID: PVX_003740) which is now designated as *P. vivax* SufE. Further, we predicted the targeting of this gene by checking the presence of N-terminal bipartite leader sequences using various available online servers as described in methodology section 2.1.

4.2.1 Targeting of *Pv*SufE

The amino acid sequence of putative *Pv*SufE (PVX_003740) when submitted to online server PlasmoAP, showed three out of total four tests positive for the signal peptide. Based on different parameters considered by PlasmoAP like the presence of basic amino acids and KN enriched regions at the N terminal, *Pv*SufE gave 5/5 tests positive, indicating high probability of targeting of this protein to the apicoplast (**Figure 4.1**). To confirm the PlasmoAP results, we used the PATS server, which showed a high probability for the presence of an apicoplast targeting peptide in *Pv*SufS with a score of 0.951 (where score near 1 indicates likely probability of the protein being targeted to the apicoplast). We further wanted to check if mitochondrial signals are present in the given sequence. We submitted the sequence to MitoProtII and PlasMit online servers. Here, we got satisfactory results where MitoprotII showed no probability of targeting of *Pv*SufE to mitochondria (0.2619) and PlasMit predicted the protein as non-mitochondrial (99% non-mitochondrial). However, the server dependent data still demands validation into targeting of this protein using localization studies as previously we saw contradictory results in case of *Pv*SufS protein.

Criterion	**Value**	**Decision**
Signalpeptide	3 of 4 tests positive	+
apicoplast-targeting peptide	5 of 5 tests positive	++
Ruleset 1		
Ratio acidic/basic residues in first 22 amino acids <=0.7	0.091	yes
Does a KN-enriched region exist (40 AA with min. 9 K or N) with a ratio acidic/basic <=0.9	0.059	yes
Ruleset 2		
number of acidic residues in first 15 amino acids (<=2)	1	yes
Does a KN-enriched region exist (40 AA with min. 9 K or N) ? Ratio acidic/basic residues in this region <0.6	0.059	yes
Is the first charged amino acid basic ?		yes

Note: The **final decision** is indicated by "++, +, 0 or -", where apicoplast-localisation for a given sequence is considered as "++ very likely; + likely; 0 undecided; - unlikely

Figure 4.1: Prediction of bi-partite N-terminal leader sequence with PlasmoAP for *Pv*SufE.

4.2.2 Amplification of *PvsufE* gene

4.2.2.1 Primer designing and amplification of *PvsufE*

The *Pv*SufE putative protein (Gene ID: PVX_003740) of *P. vivax* Salvador I is 1264bp long and expands from 654,284 – 655,547 position on chromosome no. 4. It has three introns and the gene encodes for 744 bases mRNA. To amplify the complete gene from different *P. vivax* field isolates, one set of primers were designed from genomic sequence of PVX_003740 (**Figure 4.2 & Table 4.1)**. Amplification of the full-length gene from genomic DNA and cDNA was achieved using primers VS64 and VS65 following conditions given in **Table 4.2** (**Figure 4.3**). The obtained amplicons were purified using QIAquick Gel Extraction kit, commercially sequenced and analysed by different software as described in materials and methods.

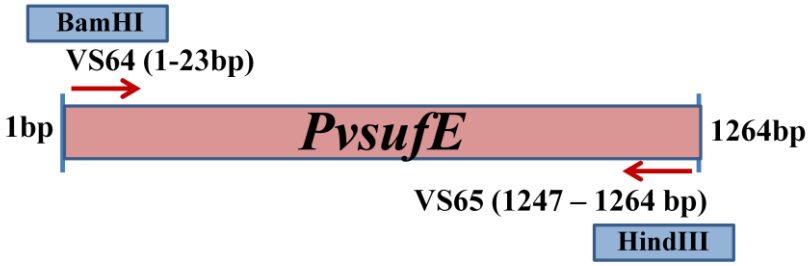

Figure 4.2: Position of primers designed for amplification of *sufE* gene from *P. vivax*.

Table 4.1: Primer sequences for the amplification of *sufE* gene from *P. vivax* genome

Lab Id	Primer sequence	Restriction enzyme site
VS64	5'GCG GGA TCC ATG AAG AAA AGG GAA ATA AAA AA 3'	BamHI
VS65	5' GCG AAG CTT TTA GCG TTC CCC GTT CT 3'	HindIII

Table 4.2: Reaction conditions employed for the amplification of *PvsufE* gene from genomic and cDNA.

Reaction Steps	Primers Used			
	VS64 & VS65 (1264bp) Genomic DNA		VS64 & VS 65 (744bp) cDNA	
Pre-Denaturation	94˚C for 3min		94˚C for 3min	
Denaturation	94˚C for 1.5min	x35	94˚C for 1min	x35
Annealing	57.1˚C for 1min		57.1˚C for 45sec	
Extension	72˚C for 2min		72˚C for 2min	
Post Extension	72˚C for 4min		72˚C for 4min	

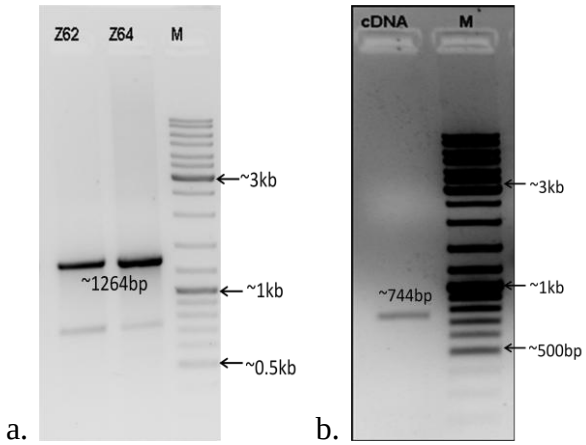

Figure 4.3: *PvsufE* gene amplification (Parasite DNA samples: Z62 and Z64; M: Gene Ruler DNA Ladder mix Fermentas SM0331). (a) Full gene amplification from Genomic DNA (1264bp) (b) Complete *PvsufE* gene amplification from cDNA(744bp).

4.2.3 Sequence Analysis and Multiple Sequence Alignment

The obtained sequences of Indian *PvsufE* (BankIt ID: KY662009) was analysed at the nucleotide and amino acid level, amongst different Indian isolates as well as with Salvador I, and were found to have 97.3% similarity with Salvador-I strain. In the multiple sequence alignment, the Indian *P. vivax* sequences showed percent identity ranging from 35.55 to 89.10 with *Plasmodium*, apicomplexans and prokaryotes (**Table 4.3a and Figure 4.5**). Within the *Plasmodium* genus, the *Pv*SufE showed percent identity of 89.10% with *P. cynomolgi*, 85.10 with *P. knowlesi* and 55.84% with *P. falciparum* (**Table 4.3b**). Alignment between SufE protein of prokaryotes and apicomplexans showed a long gap at the N-terminal region because of the absence of N-terminal targeting sequence. A deletion of 5 amino acids was observed from all the field isolates (**Figure 4.4**).

The motif GCQS was conserved throughout the *Plasmodium spp*. including *P. vivax* and was positioned just after the deletion observed. As it was just adjacent to the conserved region of the protein, we assumed that it may affect the functional activity of the protein. The cysteine residue known to receive sulfur from SufS i.e Cys_{148} (corresponding to Cys_{51} in *E. coli* SufE) (Ollagnier-de-Choudens et al., 2003) was also conserved in *Pv*SufE.

Table 4.3: Percent identity of *Pv*SufE protein and nucleotide sequences from Indian field isolate with SufE sequence from a) Prokaryotes, plant, Apicomplexans b) *Plasmodium* species

a.)

Nucleotide/ Amino acid	***P. vivax***	***Arabi***	***Pseudo***	***Droso***	***E. coli***	***Klebs***	***Toxo***	***Neosp***	***Mycob***	***Therm***
P. vivax		34.11	35.75	35.55	36.93	36.93	39.17	45.09	35.99	38.41
Arabidopsis	28.79		30.95	35.83	30.92	29.86	41.88	39.25	31.81	33.07
Pseudomonas	20.31	30.60		42.96	43.48	47.31	39.26	37.00	41.98	43.30
Drosophila	23.57	26.53	27.82		43.31	45.26	38.78	39.58	40.45	39.10
E. coli	23.66	25.55	29.85	34.56		72.66	40.82	39.53	38.60	38.66
Klebsiella	24.43	26.28	32.09	36.03	82.61		39.86	39.23	43.01	41.64
Toxoplasma	27.73	28.50	27.61	21.09	24.82	24.09		69.91	44.23	46.94
Neospora	27.72	27.36	26.87	21.09	24.82	24.82	68.57		41.53	43.79
Mycobacterium	20.30	27.74	24.24	22.22	17.04	20.00	28.06	28.06		53.43
Thermus	29.23	23.70	20.16	23.48	15.15	15.91	30.88	30.15	39.26	

b.)

Nucleotide/ Amino acid	***P. vivax***	***P. falciparum***	***P. berghei***	***P. chabaudi***	***P. cynomolgi***	***P. knowlesi***	***P. yoelii***
P. vivax		55.84	58.44	57.83	89.10	85.10	57.92
P. falciparum	49.57		69.46	70.11	60.56	61.68	69.37
P. berghei	52.34	60.43		90.30	61.00	61.14	95.56
P. chabaudi	54.11	60.61	87.65		60.48	61.76	90.85
P. cynomolgi	82.16	53.59	56.90	57.87		90.55	60.71
P. knowlesi	79.67	53.81	57.74	60.00	88.62		61.26
P. yoelii	53.16	59.58	94.33	88.48	56.85	59.34	

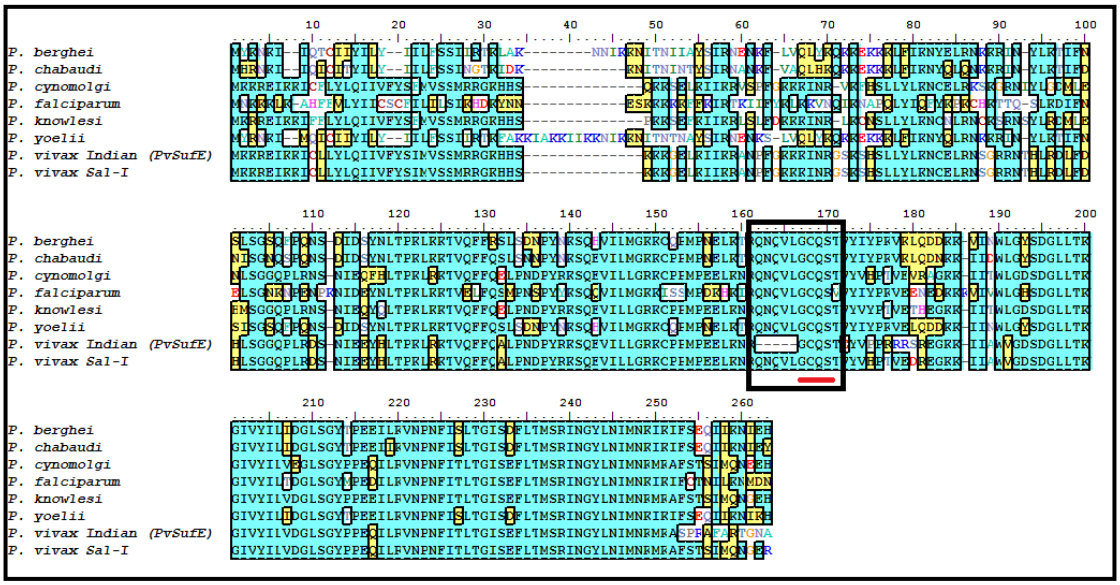

Figure 4.4: Multiple sequence alignment of *P. vivax* SufE sequence with other *Plasmodium* spp. The red lines depict the conserved signature motif GCQS and the black box contains the deletion of 5 amino acids.

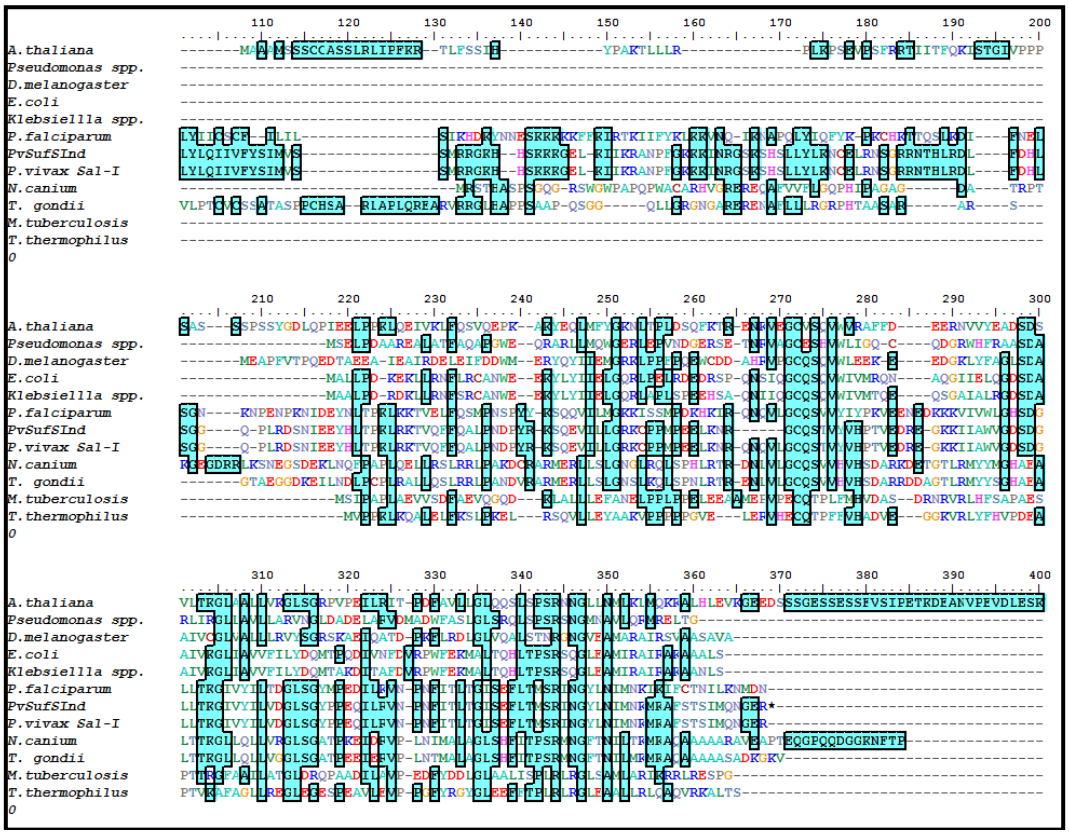

Figure 4.5: Multiple sequence alignment of *P. vivax* SufE sequence with other prokaryotes, apicomplexans and plant.

4.2.4 Conserved domain and Signature motif analysis

The CDD analysis of *Pv*SufE showed the presence of a SufE superfamily domain spanning the amino acid residues 129-231 (**Figure 4.6**). The conserved motif (GCQS, position 146-149 amino acids) and the specific pattern of signature motif was present throughout the SufE orthologues, which confirms this protein as SufE protein participating in the SUF pathway for Fe-S cluster biogenesis.

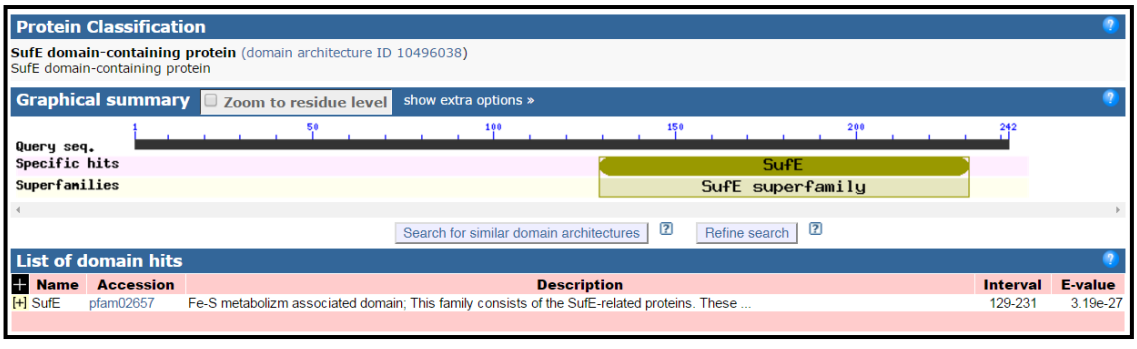

Figure 4.6: Conserved domain detection (CDD) of *Pv*SufE protein. The region spanning the amino acid position 129-231 of the query protein sequence showed a match with SufE superfamily.

4.2.5 Phylogenetic analysis

The evolutionary position of *Pv*SufE was predicted by constructing a phylogenetic tree using MEGA 6.0 (Tamura et al., 2013). The MSA generated for phylogeny included 16 amino acid sequences including major apicomplexans (*Plasmodium*, *Toxoplasma*, *Neospora canium*), plant (*A. thaliana*), prokaryotes (*E. coli*, *T. thermophilus*, *M. tuberculosis*, *Pseudomonas spp.*, *Klebsiella spp.*) (**Figure 4.7**). The evolutionary history was inferred by Maximum Likelihood method based on JTT matrix based methods using Neighbor-Join and BioNJ algorithms. The tree with the highest log likelihood (-2512.8618) is shown. The tree is drawn to scale, with branch lengths measured in the number of substitutions per site. All positions containing gaps and missing data were eliminated. There were a total of 122 positions in the final dataset.

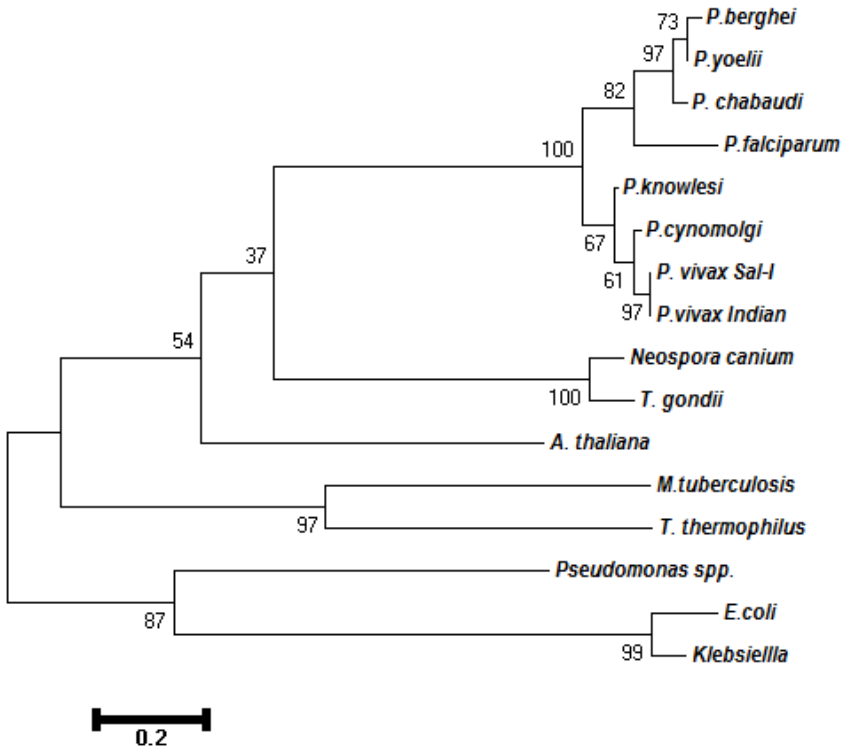

Figure 4.7: Phylogenetic analysis of SufE protein sequences. SufE protein sequence of Indian *P. vivax* with orthologues. Boot strapping done for 1000 iteration and percentage of trees in which the associated taxa clustered together shown next to the branches.

The results were similar to the *Pv*SufS protein, where *Pv*SufE protein grouped along with other primate parasites *P. knowlesi* and *P. cynomolgi* while rodent malaria

parasite *P. berghei*, *P. chabaudii* and *P. yoelii* were present in different clade. *P. falciparum* diverged out of these two clades suggesting its different origin. The apicomplexans formed a separate clade in close proximity to *Plasmodium* clade. *A. thaliana* bearing a photosynthetic plastid was placed in a closer proximity with Apicomplexans which bear a non-photosynthetic plastid than the clade containing prokaryotic species which diverged distinctly from the eukaryotic counter-part.

4.2.6 Cloning and expression of *PvsufE* gene

After the confirmation of the amplified product as *PvsufE* gene, we proceeded with the cloning of amplicons in a TA cloning vector. The colonies consisting of proper recombinant clones after confirming by colony PCR (**Figure 4.8**) were utilized to sub-clone the gene in pRSET A expression vector at BamHI and KpnI restriction enzyme sites (**Figure 4.9**). Further to screen the recombinant colonies containing desired gene, gel shift assay (**Figure 4.10a**) and colony PCR were performed (**Figure 4.10b**). The correct orientation of *PvsufE* gene was confirmed using restriction digestion (**Figure 4.11**). Sequencing using T7 and gene specific primers confirmed the integrity of the gene in the recombinant clone and the presence of start codon in-frame.

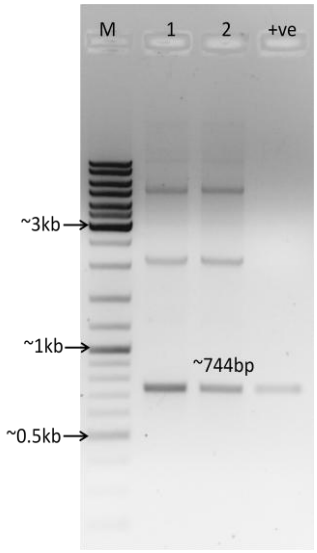

Figure 4.8: Colony PCR to check for the colonies showing recombinant construct in TA vector. (M: Gene Ruler DNA Ladder Mix; +ve: PCR positive control from cDNA; 1, 2: colony number after vector insert ligation and transformation).

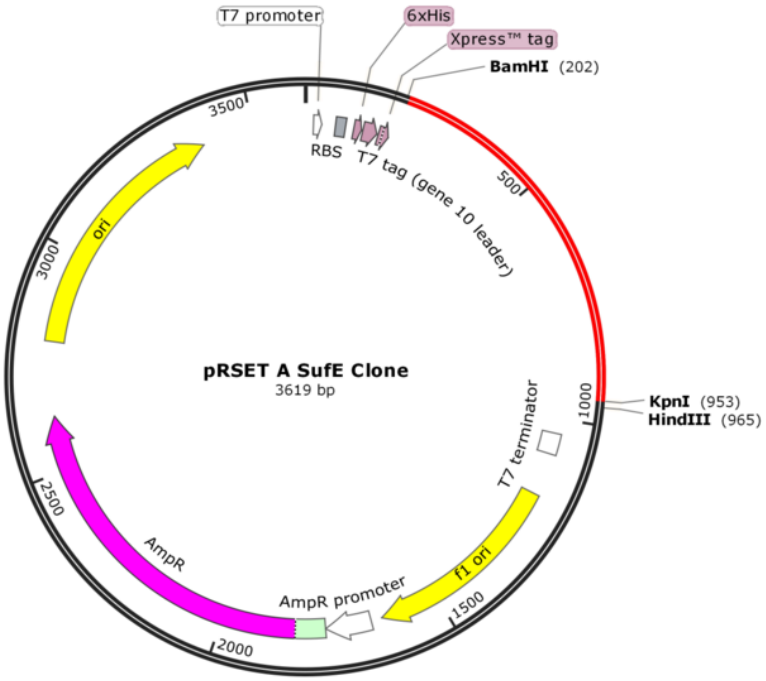

Figure 4.9: The pRSET A – *PvsufE* clone map: Red part depicts *PvsufE* gene and black part shows the regions of pRSETa vector. The restriction sites depicted were used for gene insertion and restriction analysis of the clone.

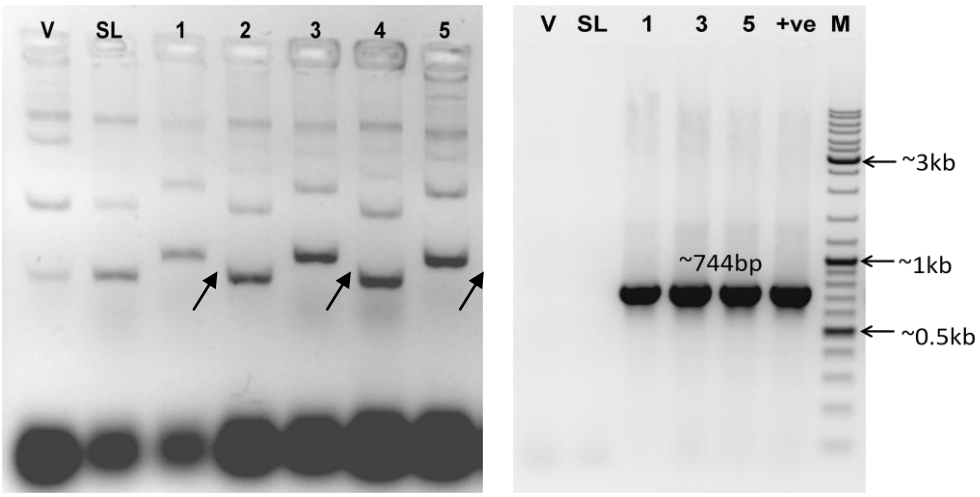

Figure 4.10: Screening of recombinant clones by a.) Gel shift assay b.) Colony PCR (V: pRSETa Vector; SL: Self-ligation; M: Gene Ruler DNA Ladder Mix; 1, 2, 3, 4 5: colony number after vector insert ligation and transformation; +ve: PCR positive control from cDNA).

After successful validation, the obtained recombinant clone was transformed into *E. coli* BL21(DE3)pLysS host cells, induced with 0.5mM IPTG at 37˚C for 2hr, 4hr and 6hr to perform protein expression studies (Chapter 2, 2.8). The bacterial cells containing the recombinant construct were cultured and harvested by centrifugation,

resuspended in lysis buffer and checked on SDS PAGE after staining with Coomassie brilliant blue R250 (**Figure 4.12**). The recombinant *Pv*SufE protein expressed as a fusion protein of ~23kDa carrying a 6X-His tag.

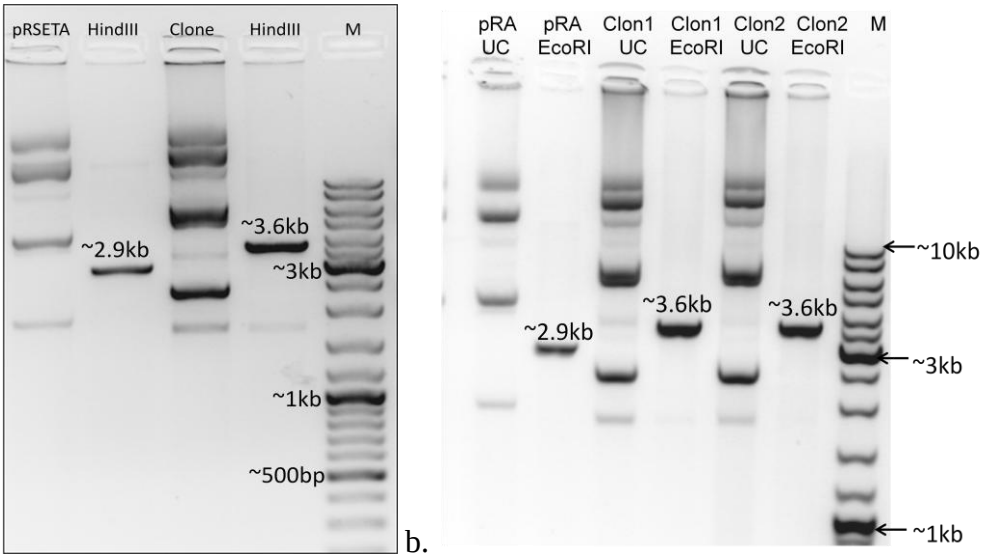

Figure 4.11: Restriction analysis of *PvsufE* recombinant constructs a.) HindIII enzyme b.) EcoRI enzyme. (M: Gene Ruler DNA Ladder Mix (Thermo Scientific, USA); pRA: pRSET A Vector; UC: Uncut plasmid).

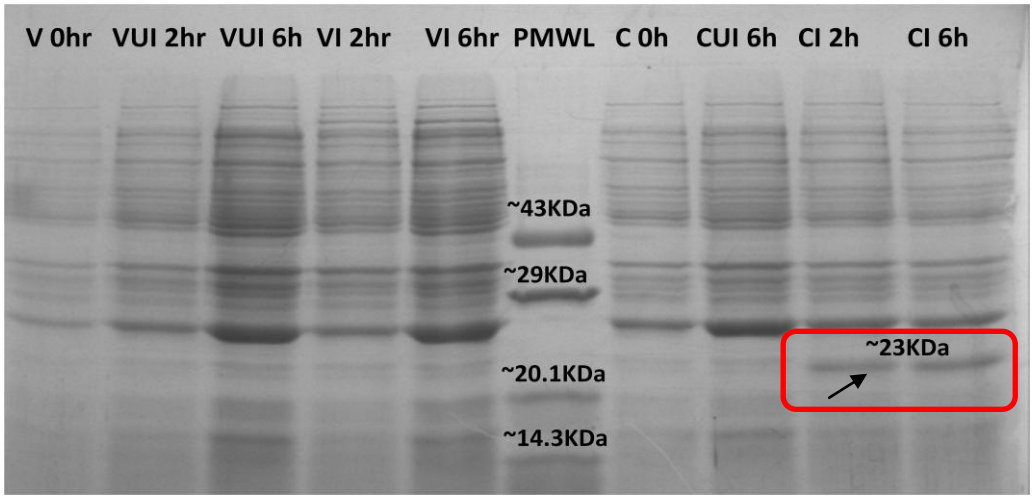

Figure 4.12: Over expression of full length *Pv*SufE protein in *E. coli*. M: Protein Molecular Low Weight Marker (Genei); CUI: pRSET A *Pv*SufE clone uninduced; CI: pRSET A *Pv*SufE clone induced samples; VUI: pRSET A vector uninduced sample VI: pRSET A vector induced sample).

The obtained expression for the recombinant protein was confirmed by western blotting (**Figure 4.13**) using anti-His antibody (Qiagen, USA) as per the manufacturer's protocol where a band at ~23 kDa in the recombinant clone induced sample shows the presence of the desired protein.

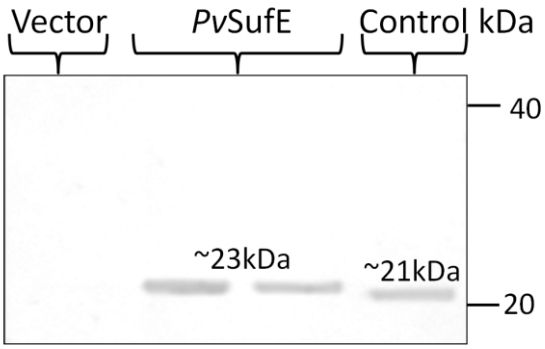

Figure 4.13: Expression of His tagged *Pv*SufE protein confirmation by western blotting.
Control: Positive lab control of a His-tagged protein.

4.2.7 Protein purification

Further, for performing enzyme kinetics studies and sub-cellular localization, *Pv*SufE recombinant protein was purified using Ni-NTA agarose resin following the protocol discussed in materials and methods (Chapter 2, 2.10.1). Multiple elute fractions (**Figure 4.14**) of purified protein were analysed. The fractions with maximum intensity for the desired band and minimum non-specific bands were used for further experiments.

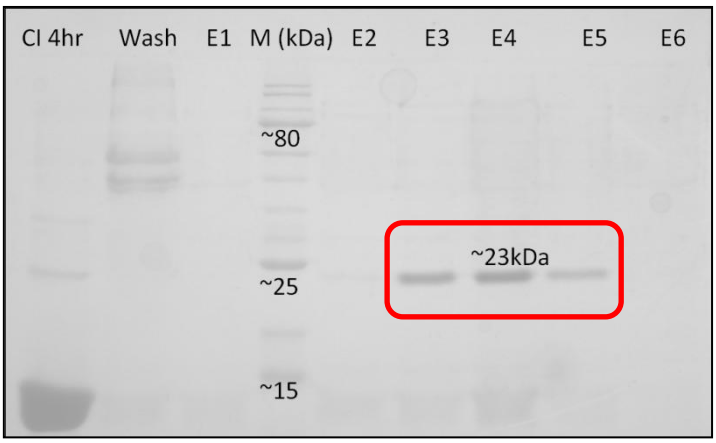

Figure 4.14: Purification of recombinant His-tagged *Pv*SufE protein. M: Protein Ladder (New England Biolabs). (CI: pRSET A *PvsufE* induced; Wash: *Pv*SufE protein wash fractions; E1-E6: *Pv*SufE protein eluted fractions).

4.2.8 Functional characterization of *Pv*SufE protein

As mentioned earlier, SufE is a partner protein of SufS and plays a major role in increasing the efficiency of release of sulphur from cysteine. To ascertain this fact the cysteine desulphurase assay mentioned in the previous chapter was performed

with *Pv*SufE as well maintaining the same parameters. *Pv*SufE showed almost negligible cysteine desulphurase activity suggesting that it may not be functional as a cysteine desulphurase all by itself. Thus, previous reports about SufE acting as an accessory protein to increase the activity of SufS may hold true in case of *P. vivax* also.

4.2.9 Antibody raising and Immuno-localization

All the bioinformatic tools gave a clear indication that SufE is targeted to the apicoplast of *P. vivax.* However, to validate the sub-cellular localization of *Pv*SufE, antibodies were raised against recombinant *Pv*SufE in mice by injecting ~30µg of pure *Pv*SufE protein with Freund's adjuvant, followed by three booster doses at an interval of 21 days (Chapter 2.12.1). Antibody titer was calculated for the sera collected after different booster doses of *Pv*SufE protein using standard ELISA where serum collected from mice injected with 1X PBS with Freund's Adjuvant was used as a control. Pre-immune sera were collected to check presence of any cross-reactive antibodies. Best antibody concentration was observed at third booster dose (**Figure 4.15**). Specific band obtained at the desired position in western blotting using recombinant protein as well as parasite lysate confirms specificity of antibodies towards *Pv*SufE protein (**Figure 4.16**).

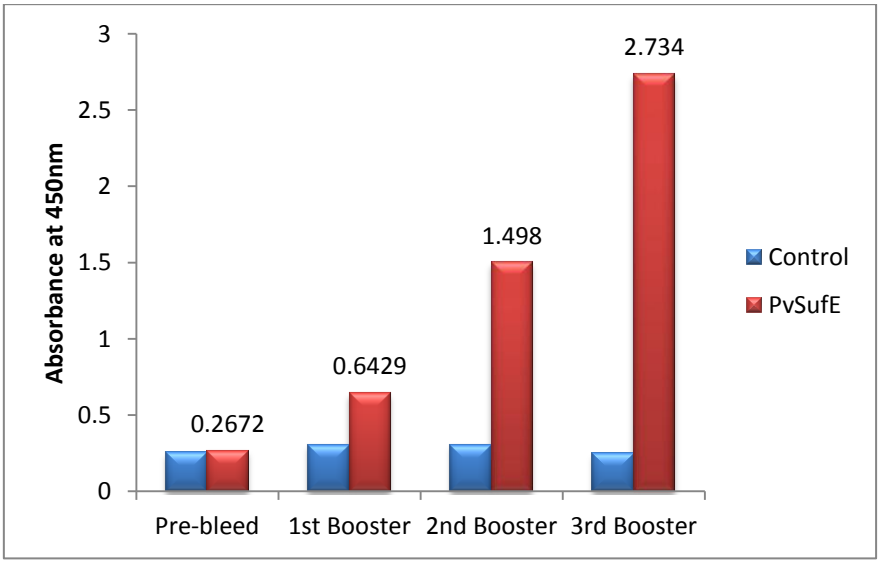

Figure 4.15: Antibody concentration determination for *Pv*SufE protein by ELISA.

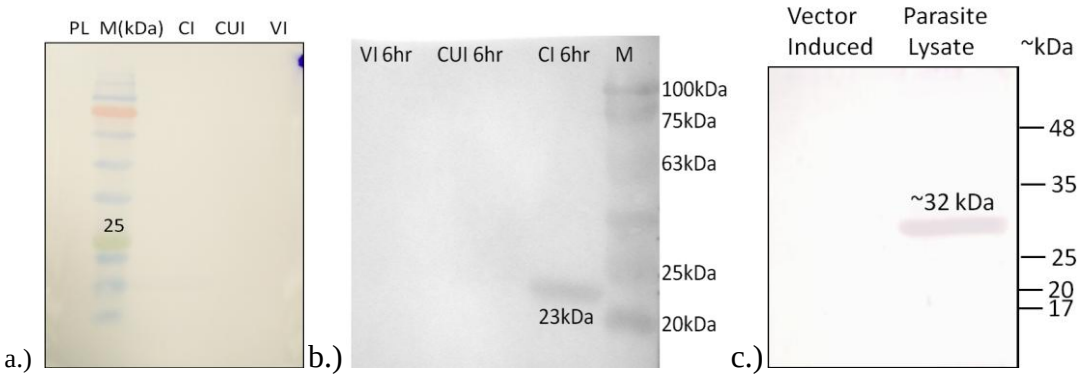

Figure 4.16: Western blot of anti- *Pv*SufE antibodies with a.) pre-immune sera b.) recombinant *Pv*SufE c.) parasite lysate. (VI 6hr: pRSET A Induced 6 hours; CUI 6hr: pRSET A *PvsufE* uninduced 6 hours; CI 6hr: pRSET A *PvsufE* induced 6 hours; PL: parasite lysate; M: Prestained Protein Molecular Weight Marker (B. R. Biochem).

To perform sub-cellular localization on blood smears prepared from *P. vivax* infected patients, parasite cells were fixed with chilled methanol, permeabilised with 0.05% saponin and 0.1% tritonX-100 and sequentially treated with mouse polyclonal anti-*Pv*SufE (1:50) sera followed by goat anti-mouse monoclonal IgG FITC antibodies (1:2000). DAPI (75ng/ml) and Qdot® 585 Streptavidin conjugate (10nM) counter staining was done to observe the parasite's nucleus and apicoplast respectively (Chapter 2.12.2). Slides were observed using the respective filters, where a bright field was used to identify the RBCs infected with parasite, green fluorescence to localize the *Pv*SufE protein, blue and red fluorescence for nucleus and apicoplast respectively (**Figure 4.17**). The *Pv*SufE protein was localized as a green fluorescing spot with an overlapping red spot of apicoplast and a blue spot staining nucleus adjacent to this merged yellowish spot. This study confirms that *Pv*SufE protein is functionally active in the apicoplast.

4.2.10 *In-silico* studies for *Pv*SufE

We further wanted to investigate the interacting residues involved in the interaction of *Pv*SufS with its partner protein *Pv*SufE. For the same, a structure of *Pv*SufE was constructed using homology modelling.

4.2.10.1 Secondary structure prediction

To start with, first the secondary structure of *Pv*SufE was predicted using PSIPRED (Buchan et al., 2013). In *Pv*SufE protein, presence of 7 α-helices and 5 β-strands were observed which were joined with the help of 12 coils (**Figure 4.18**). The structure was analysed to verify its stability and its interaction with environment. Information related to characteristic features and chemical properties of *Pv*SufE protein provided by PSIPRED are enlisted in **Table 4.4.**

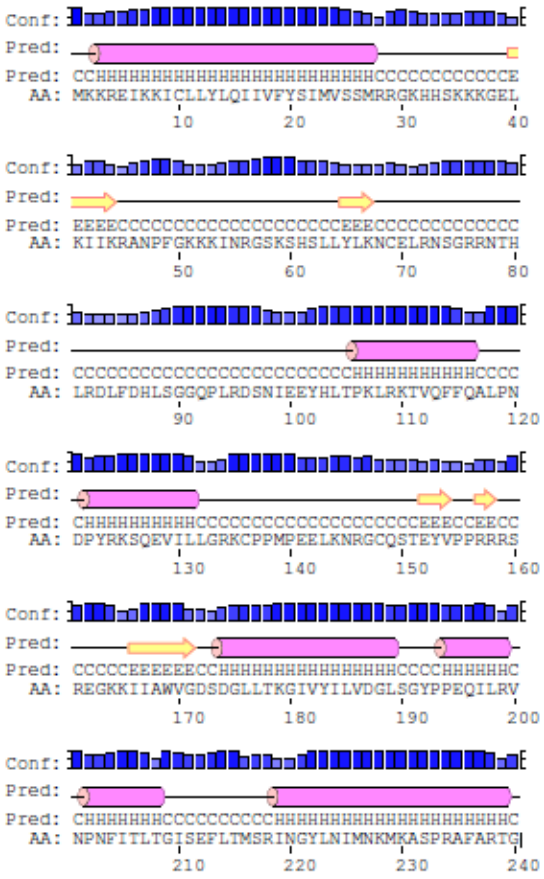

Figure 4.18: Secondary Structure predictions for *Pv*SufE protein using PSIPRED.

Table 4.4: Characteristics features of *Pv*SufE protein analysis based on Secondary structure

Characteristic features	*Pv*SufE
Molar extinction coefficient	17210.00
Molecular weight	27839.00
Isoelectric point	10.94
Percent negative residues	0.08

Percent positive residues	0.19
Charge	31.02
Signal peptide	1-16
Transmembrane topology	174-189
Aliphatic index (0-100)	86.2
Hydrophobicity (-4 to 3)	-0.57

Secondary structure of *Pv*SufE protein was also compared with SufE protein from other *Plasmodium spp*., apicomplexans, prokaryotes and plants using Geneious software (http://www.geneious.com, Kearse et al., 2012). In sync with the data obtained for *Pv*SufS, the *Pv*SufE secondary structure also showed high conservation among the *Plasmodium spp*. but did not match significantly with *T. gondii*, *Neospora canium* and *A. thaliana* (**Figure 4.19**). It can also be seen that the prokaryotic sequences are much smaller than the eukaryotic counterparts, thus making the comparison little difficult between them.

4.2.10.2 Comparative Modelling and Energy Minimization

Three-dimensional (3D) model of *Pv*SufE protein was built by homology modelling using the program MODELLER 9v11 (Sali and Blundell, 1993; Eswar et al., 2006). The *Pv*SufE amino acid sequence obtained from *Plasmodium* Indian field isolates was submitted to HHpred online server for template search. Crystal structure of *E. coli* SufE (PDB; 1MZG) protein with 2Å resolution was selected as a template for Ind*Pv*SufE protein. SufE sequence of *Plasmodium* parasite shares only 23.53% amino acid identity with *E. coli* SufE, mainly in the conserved domain region. The major difference in the template and target sequences was because of the presence of apicoplast targeting sequences on the N-terminal of the target. Taking care of these points, the targeting sequence was removed and the protein sequence was submitted for protein modeling, which yielded 3D model of the target with all non-hydrogen atoms without any user intervention. Since there was a deletion in the field sample, to compare it with the Sal-I structure, a structure for the Sal-I*Pv*SufE was also generated using the above mentioned template.

The best model with minimum DOPE score was selected and quality of the structure was further improved by energy minimization using online server YASARA (Krieger et al., 2009). The structure was evaluated by using different servers where PROCHECK showed a G-score 'BETTER' and 88.73% & 89.26% of the residues of Ind*Pv*SufE and Sal-I*Pv*SufE respectively showed an average 3D-1D score less than 0.2 (passed) using VERIFY3D. The Z-score from WHATIF server gave a score of -6.31 for Ind*Pv*SufE and -6.19 for Sal-I*Pv*SufE indicating that the generated structure was good. The main chain conformations for 94.2% and 94.5% of amino acid residues of Ind*Pv*SufE and Sal-I*Pv*SufE respectively were within the favoured or allowed regions for the protein in the Ramachandran plot analysis (**Figure 4.20a)**. The ERRAT scores for Ind*Pv*SufE protein was 94.741 and Sal-I*Pv*SufE was 97.101 and these value indicated that the molecular geometry of the models is of good quality (**Figure 4.20b**) Root-mean-square deviation (RMSD) value of 0.102 Å and 111 Å between the backbone atoms of the template with Ind*Pv*SufE and Sal-I*Pv*SufE structures respectively indicated the significant homology between the structures.

Ind*Pv*SufE **Sal-I*Pv*SufE**

a)

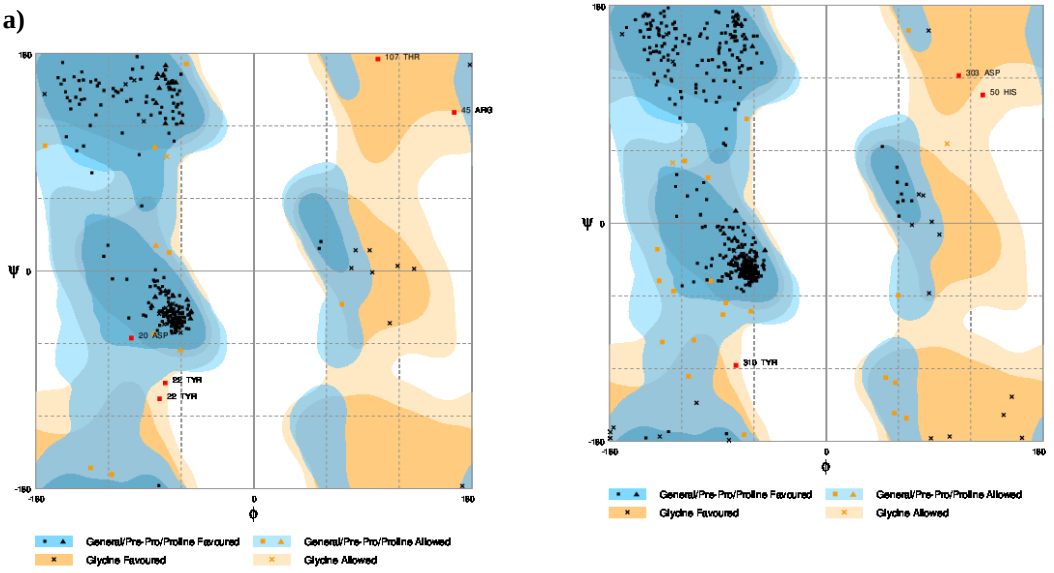

b)

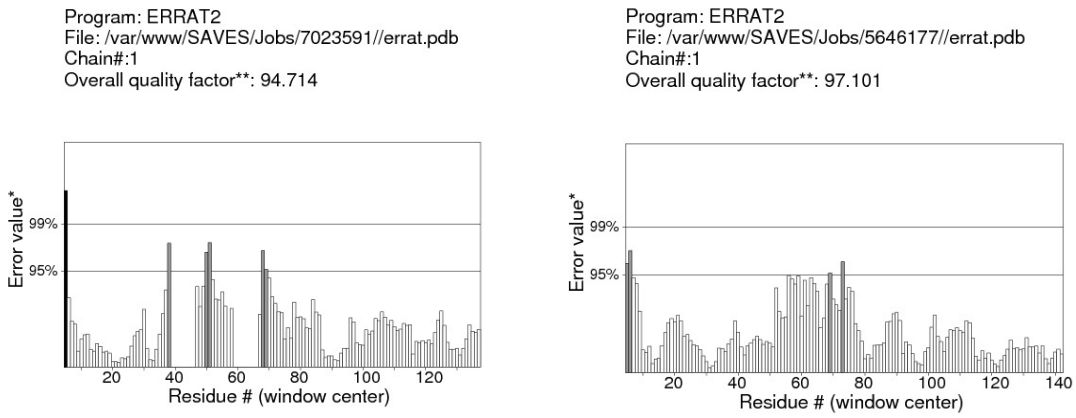

Figure 4.20: Validation of 3-D structure of *Pv*SufE using a) Ramachnadran plot b) ERRAT score.

*Pv*SufE shows an α/β fold with helices α1, α2, α5, and α6 packed around a central core formed by helix α3. The two β-strands form a single antiparallel β-sheet that packs onto one face of the resulting helical bundle, making extensive interactions with core helix α3 and peripheral helix α6. The invariant persulfide-forming residue Cys_{148} occurs at the tip of the turn between strands β1 and β2, where its side-chain is buried from solvent exposure in a hydrophobic cavity. Apart from this, an extended loop connecting helix α2 to strand β1 passes around the β-sheet on the face opposite the helical bundle. (**Figure 4.21**)

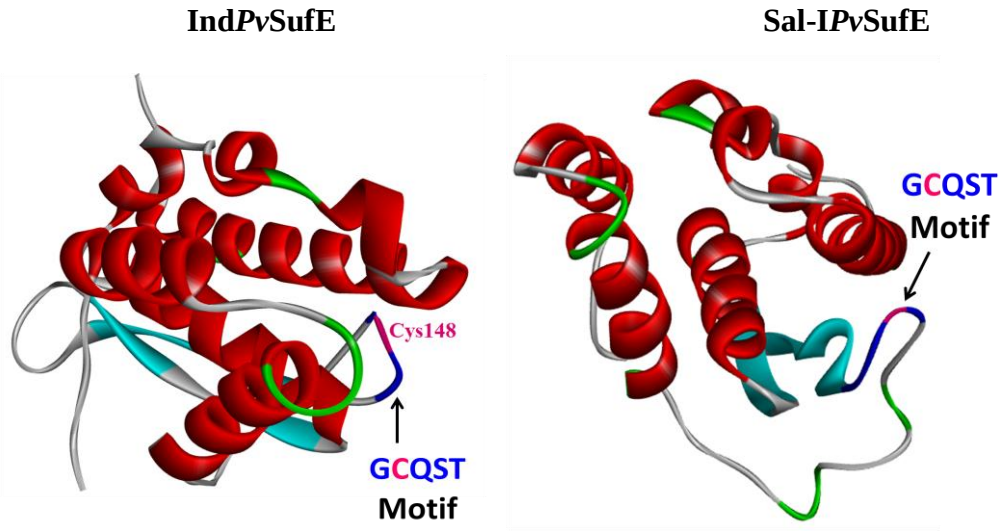

Figure 4.21: *Pv*SufE protein structure prediction: The structure prediction was done by homology modelling. *E. coli* SufE (1MZG) crystal structure was used as a template. The conserved GCQS motif (blue) with the cysteine residue (pink) required for sulfur acquisition are highlighted.

The major difference between the two structures was in the deleted region, which formed a loop in the Sal-I structure. These validated structures of *Pv*SufE were further used for studying its interaction with *Pv*SufS. The results for the same would be discussed in the next chapter.

4.3 Conclusion

The *Pv*SufE protein characterized by the SufE superfamily domain participates as partner protein for SufS to enhance its efficiency as a cysteine desulphurase. The comparative sequence analysis of the Indian *Pv*SufE (GenBank: KY662009), *P. vivax* Sal-I and sequences from other *Plasmodium*, apicomplexans and bacterial orthologues showed similarity of 55-97%, suggesting that the function has been retained during the course of evolution. Similar to PvSufS, the SufE showed a high similarity with other primate malaria parasite like *P. knowlesi and P. cynomolgi*, but exhibited an identity of only 68.26% with *P. falciparum*. A deletion of 5 amino acids just before the conserved GCQST motif in the Indian isolate substantiated the need for confirmation of the functional activity of the protein.

To characterize the *Pv*SufE protein functionally, *Pv*SufE protein was purified after expressing the gene in a prokaryotic system. Cysteine desulphurase assay when performed with pure *Pv*SufE protein exhibited negligible cysteine desulphurase activity, due to lack of its ability to bind to PLP and absence of aspartate aminotransferase domain. Localization of the protein to *P. vivax* apicoplast using anti-*Pv*SufE antibodies raised against recombinant *Pv*SufE protein on thin blood smears made from *P. vivax* parasite infected patient proved its functionality in the SUF pathway for Fe-S cluster biogenesis.

Further to analyse the correct positioning of the conserved cysteine residue and the interacting partners of *Pv*SufE protein, we generated a homology model for *Pv*SufE of Indian isolates and the Sal-I*Pv*SufE based on a prokaryotic organism *E. coli*. The presence of the invariant persulfide-forming residue Cys148 at the tip of the turn between β1 and β2 strands, makes it available to interact with SufS. In conclusion,

our results ascertain the hypothetical protein identified from the PlasmoDB database to function as SufE protein in the apicoplast of *P. vivax*.

Chapter V

Characterization of SufA from P. vivax

Characterization of scaffold protein SufA from *P. vivax*

5.1 Introduction:

The final step of the pathway involves the assembly and the transfer of the Fe-S clusters, which is facilitated by scaffold proteins. The literal meaning of the word "scaffold" suggests it to be a temporary structure used to support a work crew and materials to aid in the construction of something. In sync with the literal meaning, scaffold proteins in this pathway provide the temporary structure to assemble and transfer the Fe-S clusters. The broad classification of scaffold proteins includes two categories A-type and U-type. The A-type proteins of Fe-S cluster biosynthesis pathways contain three highly conserved Cys residues (C-X_{42-44}-D-X_{20}-C-G-C) in their C-terminal regions. The exact function of these broadly classified A-type scaffold proteins in Fe-S cluster assembly is yet not clear. But, two hypotheses pertaining to their biochemical function have been postulated. The first states that the A-type proteins are substitute Fe-S scaffolds and that they may be utilized for cluster donation to Fe-S apoproteins or may act as intermediates in cluster transfer from U-type scaffolds to apoproteins. The latter probability of the A-type protein being an intermediate, has some evidence in the ISC system where *in vitro* studies have showed that IscA can accept a cluster from IscU but cannot transfer a cluster to IscU (Ollagnier-de-Choudens et al., 2004). The second hypothesis suggests that the A-type scaffolds are actually iron chaperones that donate iron for Fe-S cluster assembly on U-type scaffolds. However, there is no significant experimental evidence in support of this hypothesis (Ayala-Castro et al., 2008).

During *in vitro* reconstitution using sulfide generated by cysteine desulfurase from cysteine and ferrous iron, $[2Fe\text{-}2S]^{2+}$ and $[4Fe\text{-}4S]^{2+}$ clusters can form on A-type proteins (Krebs et al., 2001; Ollagnier-de-Choudens et al., 2001; Ollagnier-de-Choudens et al., 2003; Ollagnier-de-Choudens et al., 2004). Mutagenesis and spectroscopic studies of the A-type proteins reveal that all three conserved Cys residues are involved in Fe-S cluster ligation (Krebs et al., 2002; Zeng et al., 2007). The holoforms of A-type proteins can transfer Fe-S clusters to target apoproteins *in vitro*, leading to the hypothesis that they act as scaffolds (Krebs et al., 2001,

Ollagnier-de-Choudens et al., 2001; Ollagnier-de-Choudens et al., 2003). Additionally, protein-protein interactions between A-type scaffolds and apoproteins have also been reported for IscA and IscFdx in the ISC system and for SufA and BioB for the SUF system (Ollagnier-de-Choudens et al., 2001; Ollagnier-de-Choudens et al., 2004).

The *E. coli* SUF machinery employs several proteins that exhibit sequence, structural, and/or functional similarities with the ISC proteins. For example, SufA and IscA are 40% identical in amino acid sequence and both can assemble [2Fe-2S] and [4Fe-4S] clusters *in vitro*, a characteristic that earned them the proposed role of "alternative scaffolds". Neither the presence of SufA nor IscA by itself is vital for the cell, but a double IscA-/SufA- mutant results in a null-growth phenotype during aerobic growth conditions, indicating functional redundancy between the two proteins (Lu et al., 2008).

Extensive studies of SufA have also been conducted in *Erwinia chrysanthemi* and a lot of common features have been identified between IscA and SufA, the major one being both of them have in common three fully conserved cysteines. The others include, both the purified proteins (IscA and SufA) are found in the homodimeric form with some propensity to aggregate into larger polymers. The clusters in SufA from *E. chrysanthemi* are air sensitive and are rapidly decomposed when exposed to air. A similar observation of this oxidative and reductive lability of SufA clusters was also noted for IscA from *E. coli* or *Azotobacter vinelandii* and ISA1p from *S. pombe* (Ollagnier-De-Choudens *et al.*, 2001, Kreb's et al., 2001; Wu et al., 2002). It should be noted that, in both SufA and IscA, iron is tightly bound to the protein only in the presence of sulfide. These proteins are not able to, although in some cases only very weakly, chelate ferrous iron alone. Like IscA, SufA was demonstrated to assemble [2Fe-2S] and [4Fe-4S] clusters and transfer them to apo-ferredoxin and apo-BioB (biotin synthase) respectively (Ollagnier-De Choudens et al., 2003). This occurs in a biphasic reaction that involves a fast scaffold-target complex formation followed by a slower (~60 min) transfer of the cluster (Ollagnier-De-Choudens *et al.*, 2004). SufA could activate apo-BioB from different organisms suggesting little species specificity (Ollagnier-De-Choudens et al., 2004).

The crystal structure of SufA, obtained in its apo, homodimeric form (Wada et al., 2005), revealed a globular protein largely covered in acidic residues, a feature that is also conserved in the IscA crystal structure. The two conserved cysteines (CXC) in the C- terminal region of the protein are positioned such that they could ligate an [Fe-S] cluster positioned at the interface of two subunits. The conserved Cys_{50} is located too far away from the active site to be involved in cluster binding. Therefore, it could be involved in reactions that would facilitate *de novo* cluster assembly, release, or acceptance from other proteins if not assembled on SufA (Wada et al., 2005).

SufA has also been characterized at the biochemical level. SufA from cyanobacteria, *Synechocystis sp.* strain PCC 6803, encoded by *slr1417*, can be reconstituted with a [2Fe-2S] cluster and can transfer that cluster to both [2Fe-2S] and [4Fe-4S] proteins (Wollenberg et al., 2003). These extensive studies in different species suggest that SufA is a Fe-S assembly scaffold. Since the *suf* operon is not always found with a SufU type scaffold protein, it is hypothesized that SufA may function as the main scaffold for the SUF pathway in some organisms, such as *E. coli.* However, genetic analysis of *suf* mutant phenotypes of *E. coli* does not support this model, as deletion of *sufA* results in a much less severe phenotype than does deletion of the other *suf* genes (Takahashi and Tokumoto, 2002; Outten et al., 2004). Alternatively, IscA may compensate for the loss of SufA in a *sufA* deletion strain. This hypothesis has not been tested directly (Ayala-Castro et al., 2008).

Recently in *P. berghei*, repeated successful deletion of *sufA* was achieved by transfection experiments which indicated non-vital roles of the target gene for erythrocytic parasite propagation. Their analysis further demonstrated that absence of *sufA* is compatible with effective host switch, parasite stage conversion, and population expansion throughout the entire *Plasmodium* life cycle (Haussig et al., 2014). But, this study did not shed any light on the functional importance of this particular protein in the parasite. Thus, this indicated a lacuna in our knowledge of the above study under stress conditions and the functional importance of this protein in *Plasmodium*. Apart from this, none of the SUF pathway components involved in the assembly and transfer of the Fe-S clusters have been characterized from any of

the *Plasmodium spp*., which makes it a need of the hour to study this part of the assembly system. Therefore, in the present work an attempt has been made to completely characterize the SufA protein from field isolates of *P. vivax.*

5.2 Results and Discussion

As the sequence of *Pv*SufA was not available in the database, we looked for different genes associated with Fe-S cluster biogenesis. Based on conserved domain analysis (**Figure 5.1**), we shortlisted a putative protein: iron sulfur cluster assembly accessory protein (Gene ID: PVX_080115) as *P. vivax* SufA. Further, we performed various multiple sequence alignments, where this putative protein showed matches with IscA and SufA of various species.

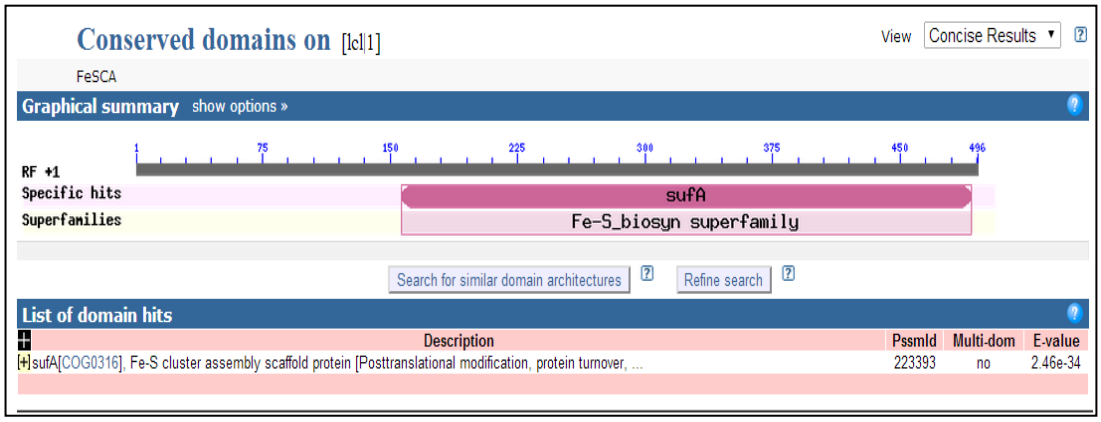

Figure 5.1: Conserved domain detection (CDD) of PVX_080115 putative protein.

5.2.1 Dual Targeting of *Pv*SufA

As the SUF pathway is suggested to be functional in the apicoplast, we predicted the targeting of this gene by checking the presence of N-terminal bipartite leader sequences using various available online servers as described in methodology section 2.1. The amino acid sequence of putative *Pv*SufA (PVX_080115) when submitted to online server PlasmoAP, showed four out of total four tests positive for the signal peptide. However, it showed only 3/5 tests positive for apicoplast targeting peptide, indicating "unlikely" probability of targeting of this protein to the apicoplast (**Figure 5.2**). Thus, to further check for the presence of apicoplast transit peptide we submitted our sequence to the PATS server, which showed a probability for the presence of an apicoplast targeting peptide in *Pv*SufA with a score of 0.741 (where values close to one indicate the protein to be "likely targeted to the

apicoplast"). As the scores obtained for apicoplast targeting were not that high for *Pv*SufA by the above online servers, we went ahead to check if mitochondrial signals are present in this sequence. We submitted the sequence to MitoProtII and PlasMit online servers. Here to add on to our confusion, we got contradictory results where MitoprotII showed a high probability of targeting of *Pv*SufA to mitochondria (0.8424/1), while PlasMit predicted the proteins as non-mitochondrial (99% non-mitochondrial). The doubt created by these mixed-up results thus necessitates a deeper investigation into targeting of this protein, using localization studies.

Criterion	Value	Decision
Signalpeptide	4 of 4 tests positive	++
apicoplast-targeting peptide	3 of 5 tests positive	-
Ruleset 1		
Ratio acidic/basic residues in first 22 amino acids <=0.7	0.000	yes
Does a KN-enriched region exist (40 AA with min. 9 K or N) with a ratio acidic/basic <=0.9	1.000	no
Ruleset 2		
number of acidic residues in first 15 amino acids (<=2)	0	yes
Does a KN-enriched region exist (40 AA with min. 9 K or N) ? Ratio acidic/basic residues in this region <0.6	1.000	no
Is the first charged amino acid basic ?		yes

Note: The **final decision** is indicated by "++, +, 0 or -", where apicoplast-localisation for a given sequence is considered as "++ very likely; + likely; 0 undecided; - unlikely

Figure 5.2: Prediction of bi-partite N-terminal leader sequence with PlasmoAP for *Pv*SufA.

5.2.2 Amplification of *PvsufA* gene

5.2.2.1 Primer designing and amplification of *PvsufA*

The iron sulfur cluster assembly accessory protein, putative of *P. vivax* Salvador-I (Gene ID: PVX_080115) is 1178bp long and expands from 38,1748 – 38,2925 position on chromosome no. 10. It has four introns and the gene encodes for 546 bases of mRNA. To amplify the complete *sufA* gene from different *P. vivax* field

isolates, one set of primers were designed from genomic sequence of PVX_080115 (**Figure 5.3 & Table 5.1)**. Amplification of the gene was achieved using primers VS62 and VS63 from both genomic DNA and cDNA following conditions given in **Table 5.2 (Figure 5.4**). The obtained amplicons were purified using QIAquick Gel Extraction kit as per manufacturer's instructions and commercially sequenced. The sequences obtained were subjected to NCBI BLAST against the genome database and submitted to NCBI (BankIt ID: KU556730).

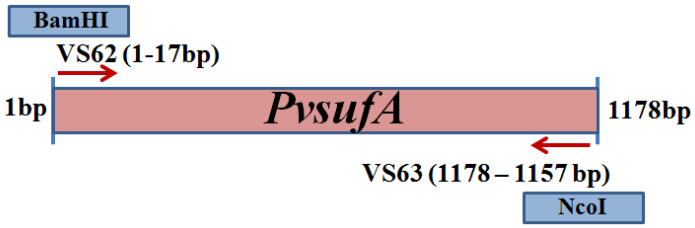

Figure 5.3: Position of primers designed for amplification of *sufA* gene from *P. vivax*.

Table 5.1: Primer sequences for the amplification of *sufA* gene from *P. vivax* genome

Lab Id	Primer sequence	Restriction enzyme site
VS62	5' GCG **GGA TCC** ATG GCA ACG ACA AAG GC 3'	BamHI
VS63	5' GCG **CCA TGG** CTA AAC ATT GAA TGA CTT CCC 3'	NcoI

Table 5.2: Reaction conditions employed for the amplification of *PvsufA* gene from genomic and cDNA.

Reaction Steps	Primers Used	
	VS62 & VS63 (1178bp) Genomic DNA	VS62 & VS63 (546bp) cDNA
Pre-Denaturation	94˚C for 3min	94˚C for 3min
Denaturation	94˚C for 1min	94˚C for 1min
Annealing	60.5˚C for 45sec x35	60.5˚C for 45sec x35
Extension	72˚C for 2min	72˚C for 1.5min
Post Extension	72˚C for 4min	72˚C for 4min

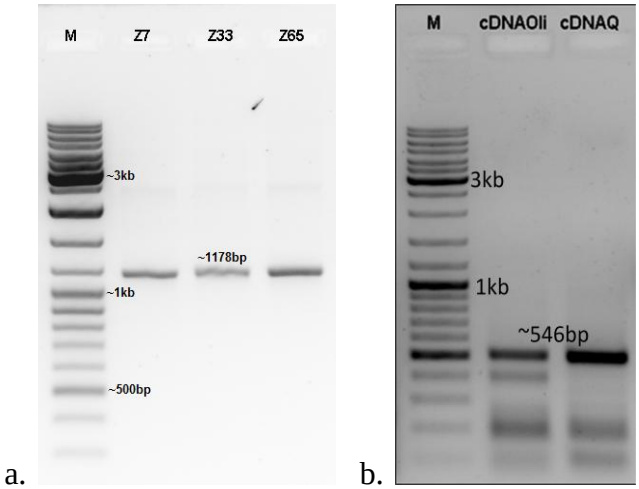

a. b.

Figure 5.4: *PvsufA* full gene amplification a.) Genomic DNA b.) cDNA (Parasite DNA samples: Z7, Z33, Z65; M: Gene Ruler DNA Ladder mix Fermentas SM0331).

5.2.3 Sequence Analysis and Multiple Sequence Alignment

The obtained sequences of Indian *PvsufA* (BankIt ID: KU556730) was analysed at the nucleotide and amino acid level, amongst different Indian isolates as well as with Salvador I, and were found to have 99.9% similarity at nucleotide level with Salvador-I. These sequences when analysed with homologues/orthologues from other organisms including prokaryotes and apicomplexans, showed percent identity ranging from 44.26 to 91.50% at nucleotide level. The similarity score of Indian *Pv*SufA and *Pf*SufA with other *Plasmodium* species, apicomplexans and prokaryotes at the nucleotide and amino acid level is as shown in **Table 5.3.** Within the *Plasmodium* genus, the *Pv*SufA showed percent identity of 91.5% with *P. cynomolgi*, 92.12% with *P. knowlesi* and 44.63% with *P. falciparum* at nucleotide level. Alignment between SufA protein of prokaryotes and apicomplexans showed a long gap at the N-terminal region because of the absence of N-terminal targeting sequence (**Figure 5.5**). The cysteine residues at positions 88, 156 and 158 known as signature residues of the A-type scaffold protein (corresponding to cysteine residues at 50, 114, 116 in *E. coli* and 324, 392, 392 in *P. falciparum*) were found to be conserved. Apart from these, other residues including I55, L57, T58, A61, I65, L79, K80, L81, G87, G90, Y93, I98, K100, L119, I121, I129, L134, D135, Y136, I141, F145 and N149 were also found to be conserved in all the *Plasmodium* spp.

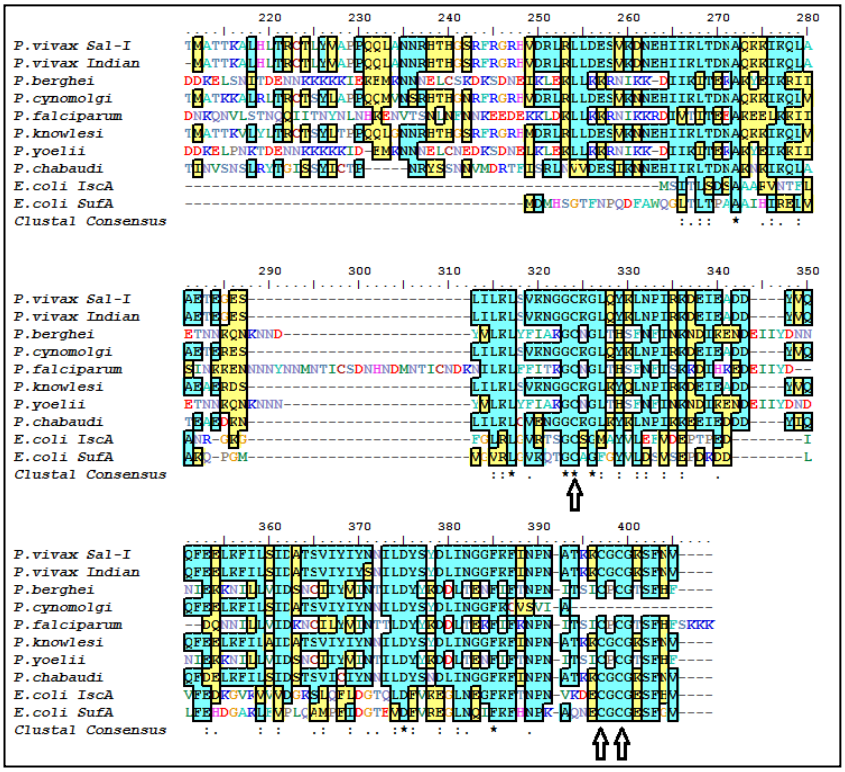

Figure 5.5: MSA (Clustal Omega) of Indian *P. vivax* SufA sequence with SufA orthologues from different organisms. The marked arrows depict the conserved residues in the signature motifs.

Table 5.3: Percent identity of *Pv*SufA protein sequence from Indian field isolates with SufA sequence from other a) *Plasmodium* species (b) prokaryotes, apicomplexans and others

(a)

Nucleotide/ Amino acid	***P. vivax***	***P. falciparum***	***P. berghei***	***P. chabaudi***	***P. cynomolgi***	***P. knowlesi***	***P. yoelii***	***P. reichenowi***
P. vivax		44.63	45.51	66.46	91.50	92.12	46.26	44.63
P. falciparum	28.12		63.37	50.96	42.04	45.63	64.71	91.96
P. berghei	27.67	46.31		52.66	42.89	48.32	95.00	63.69
P. chabaudii	66.67	26.86	28.74		62.99	66.10	53.77	50.77
P. cynomolgi	88.82	24.24	22.70	61.87		89.61	44.23	42.45
P. knowlesi	90.24	29.38	26.29	66.86	56.39		48.61	46.20
P. yoelii	27.67	46.94	91.97	28.74	22.09	26.29		65.12
P. reichenowi	27.50	94.19	51.60	25.71	24.24	28.81	51.00	

(b)

Nucleotide/ Amino acid	***P. vivax***	***P. falciparum***	***O. acuminata***	***E. praecoxi***	***E. coli***
P. vivax		44.63	49.72	46.22	43.72
P. falciparum	28.12		35.43	38.73	31.97
O. acuminate	42.50	25.00		43.5	52.90
E. praecox	25.64	38.73	25.42		46.93
E. coli	27.50	18.85	25.49	34.19	

5.2.4 Conserved domain and Signature motif analysis

The Conserved Domain Detection tool (NCBI) confirmed the presence of Fe-S cluster biosynthesis superfamily domain in Indian *Pv*SufA protein spanning the amino acid residues at position 53-165 as depicted in **Figure 5.6**. The Fe-S cluster biosynthesis superfamily mainly includes IscA, HesB, YadR and YfhF proteins. Other members of this family include various hypothetical proteins that contain the NifU-like domain suggesting that they too are able to bind iron and are involved in Fe-S cluster biogenesis. IscA, a member of the *hesB* family of proteins, binds iron and [2Fe-2S] clusters, and participates in the biosynthesis of iron-sulfur proteins (Cupp-Vickery et al., 2004). The A-type proteins of Fe-S cluster biosynthesis pathways are known to possess three highly conserved Cys residues ($X_{34}CX_{63}CGCX_{67}$) in their C-terminal regions. The *Pv*SufA protein showed the presence of the above mentioned signature motif, viz., ($X_{87}CX_{155}CGCX_{159}$) motif where the cysteine residues were located at positions 88, 156 and 158 respectively (**Figure 5.5**). This specific pattern of signature motif confirms this protein as SufA protein that participates in the SUF pathway for Fe-S cluster biogenesis.

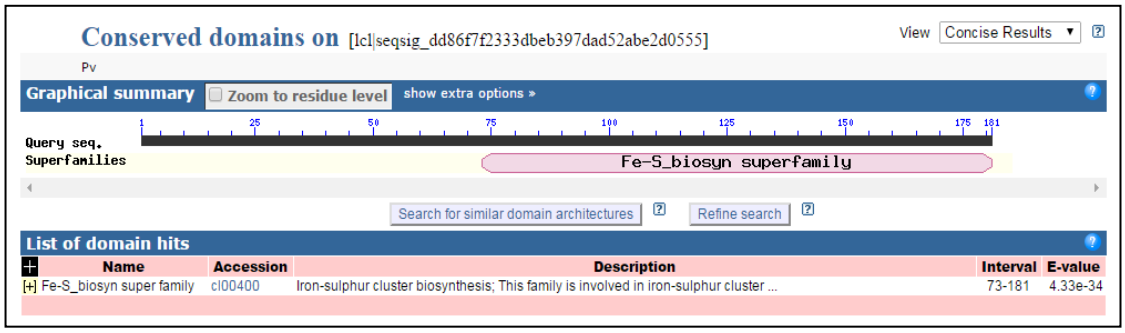

Figure 5.6: Conserved domain detection (CDD) of *Pv*SufA protein. The region spanning the amino acid position 75-181 of the query protein sequence showed a match with Fe-S biosynthesis superfamily.

5.2.4 Phylogenetic analysis

The evolutionary position of *Pv*SufA was predicted by constructing a phylogenetic tree using MEGA 6.0 (Tamura et al., 2013). For the analysis, 18 amino acid sequences were used including major apicomplexans (*Plasmodium*, *Toxoplasma*, *Emeria*), prokaryotes (*E. coli*), chlorophyta (*Chlamydomonas)* and algae (*Synechococcus*, *Oscillatoria*, *Anabena*) (**Figure 5.7**). The evolutionary history was

inferred using Maximum Likelihood method based on JTT matrix after removing the gaps and missing data. Initially the trees for the heuristic search were obtained automatically by applying NJ and BioNJ algorithm to a matrix of pairwise distance established using JTT model and finally the tree with the highest log likelihood value (-1689.7342) was chosen. The branch lengths were measured as the number of substitutions per site.

On analysis of different clades, *Pv*SufA protein grouped along with other primate parasites *P. knowlesi* and *P. cynomolgi* while rodent malaria parasite *P. berghei*, *P. chabaudi*, *P. yoelii* and *P. vinckei* were present in different clade along with *P. falciparum*. As seen earlier, these two clades seem to diverge out of *P. falciparum* clade indicating a separate origin of *P. falciparum*. The apicomplexans *Eimerria* and *Toxoplasma* formed a separate clade close to the prokaryotic clade. All the species bearing a photosynthetic plastid formed a separate clade.

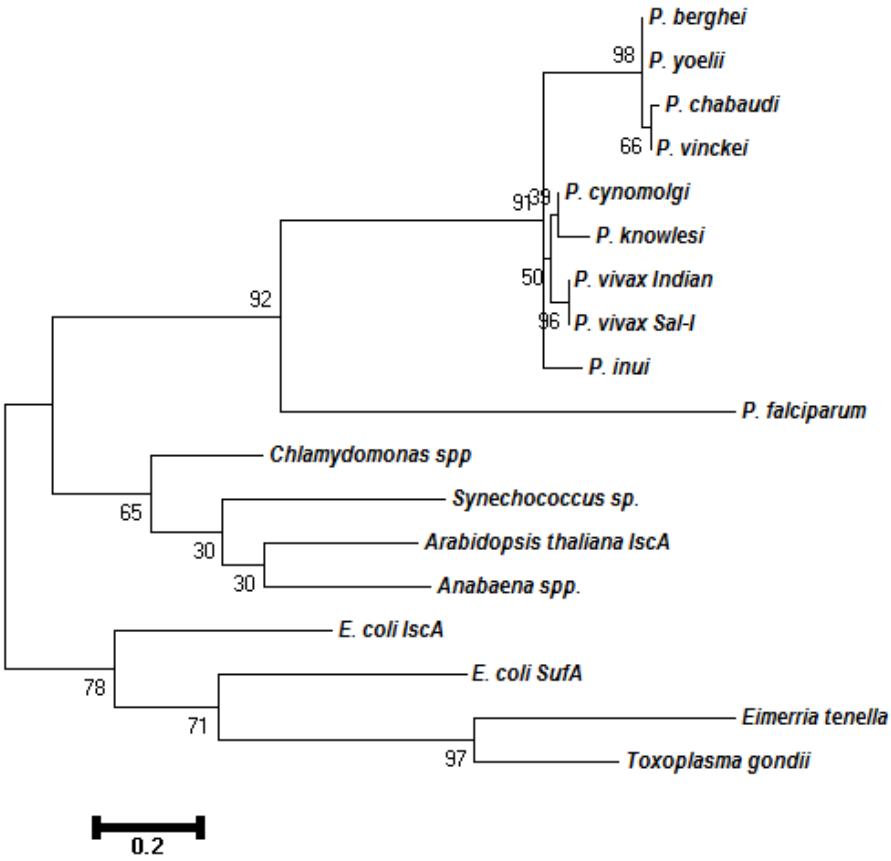

Figure 5.7: Phylogenetic analysis of SufA protein sequences. [SufA protein sequence of Indian *P. vivax* with orthologues]. Boot strapping done for 1000 iteration and percentage of trees in which the associated taxa clustered together shown next to the branches.

5.2.6 Cloning and expression of *PvsufA* gene

After the confirmation of the amplified product as *PvsufA* gene by sequencing and conserved domain analysis, we proceeded with the cloning of amplicons in pRSET A expression vector at BamHI and NcoI restriction enzyme sites (**Figure 5.8**). The recombinant molecules containing desired gene, were screened by Gel Shift assays and colony PCR (**Figure 5.9**). Once the presence of *PvsufA* gene was confirmed, to check the orientation of *PvsufA* in our clone, we performed restriction digestion. For this, we selected BamHI (which was used for cloning) and HincII (which was present in the gene at 377 position) enzymes. The obtained bands at 3.1 kb and ~0.34 kb confirmed the presence of *PvsufA* in the correct orientation (**Figure 5.10**). Sequencing using T7 and gene specific primers confirmed the integrity of the gene in the recombinant clone and the presence of start codon in-frame.

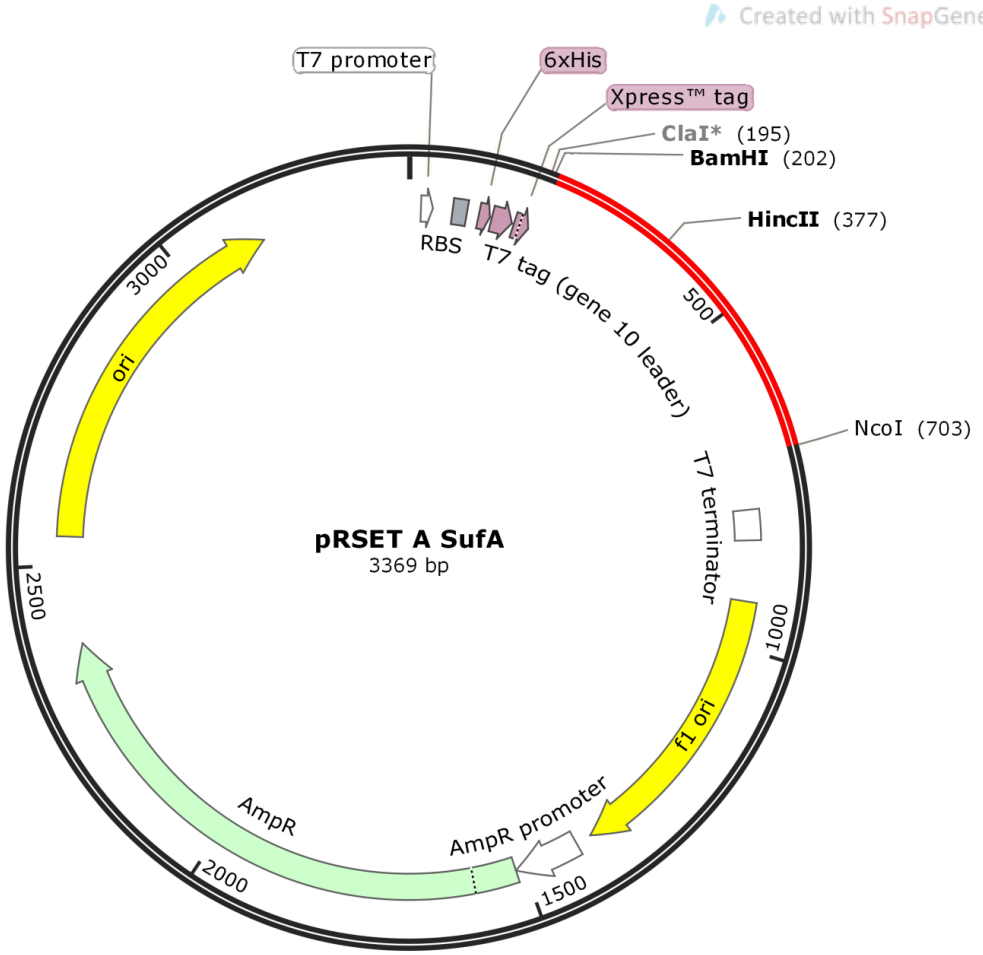

Figure 5.8: The pRSET A – *PvsufA* clone map: Red part depicts *PvsufA* gene and black part shows the regions of pRSET A vector. Restriction sites marked in the gene were used for restriction analysis of the clone.

a)

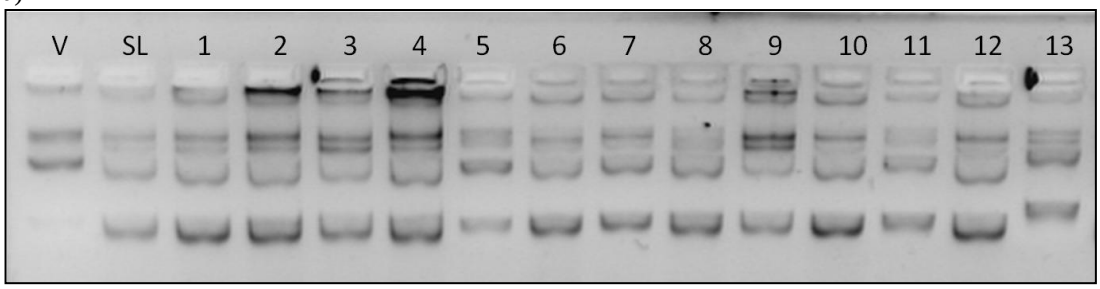

b)

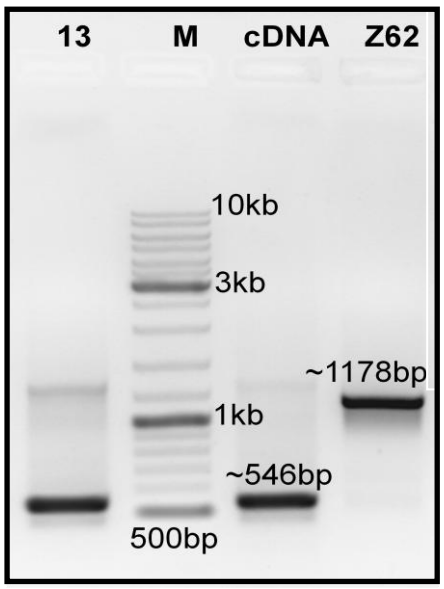

Figure 5.9: Confirmation of Clone by a.) Gel Shift Assay and b.) Colony PCR to check for the colonies showing recombinant construct (V: Vector pRSET A, SL: Self ligation; 1 to 13 indicate the no. of colonies; 13, 45: colony number after vector insert ligation and transformation; M: Gene Ruler DNA Ladder Mix; Z62: PCR positive control from genomic DNA Z62 sample).

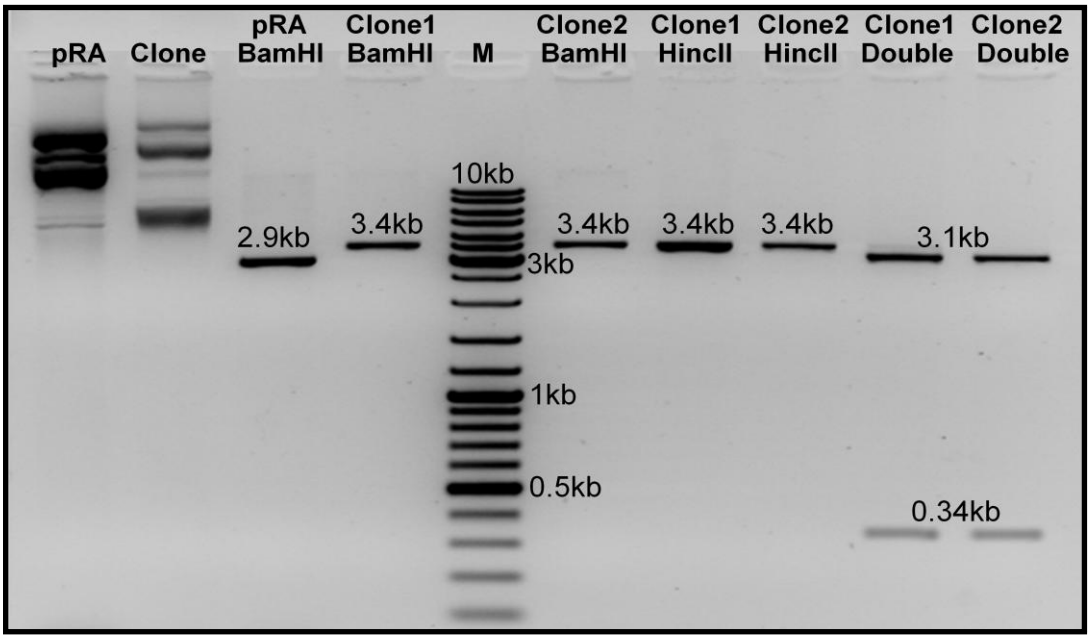

Figure 5.10: Restriction analysis of *PvsufA* recombinant constructs. M: Gene Ruler DNA Ladder Mix (Thermo Scientific, USA); pRA: pRSETa Vector; Recombinant contructs 1 & 2 digested with BamHI and HincII restriction enzymes alone and in combination.

After successful validation, the obtained recombinant clone was transformed into *E. coli* BL21(DE3) pLysS host cells to express the *Pv*SufA protein (Chapter 2, 2.8). For this, the clone culture was induced with 0.5mM IPTG and samples were collected at different time points of 2hr, 4hr, 6hr, 8hr. The bacterial cells were harvested by centrifugation, resuspended in lysis buffer and checked on SDS PAGE. The presence of protein was checked after staining with Coomassie brilliant blue R250 (**Figure 5.11**). The recombinant *Pv*SufA protein expressed as a fusion protein of ~21 kDa carrying a 6X-His tag.

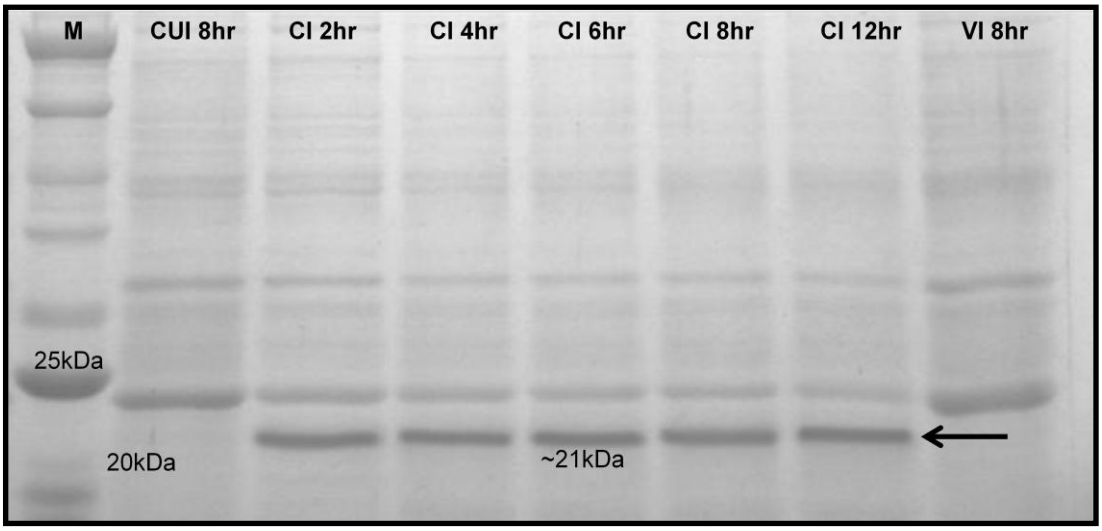

Figure 5.11: Over expression of full length *Pv*SufA protein in *E. coli*. M: NEB Protein Ladder (NEB). (CUI: pRSET A *Pv*SufA clone uninduced 8hr sample; CI: pRSET A *Pv*SufA clone induced samples 2-12 hrs; VI: pRSET A vector induced sample 8hr).

The obtained expression for the recombinant protein was further confirmed by western blotting (**Figure 5.12**) using anti-His antibody (Qiagen, USA) as per the manufacturer's protocol. A band at ~21 kDa in the recombinant clone induced sample shows the presence of the desired protein.

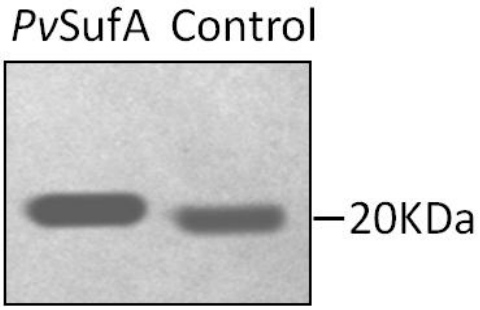

Figure 5.12: Expression of His-tagged *Pv*SufA protein confirmation by western blotting. Control: Positive lab control of a His tagged protein.

5.2.7 Protein purification

To perform enzyme kinetics studies and sub-cellular localization, pure protein is required. As the *Pv*SufA was expressed as a His-tagged protein, the *Pv*SufA recombinant protein was purified using Ni-NTA agarose resin following the protocol discussed in materials and methods (Chapter 2, 2.10.1). Multiple fractions (**Figure 5.13**) of purified protein were collected as eluted product. The fraction with maximum intensity for the desired band and minimum/absence of non-specific bands were included for further experiments.

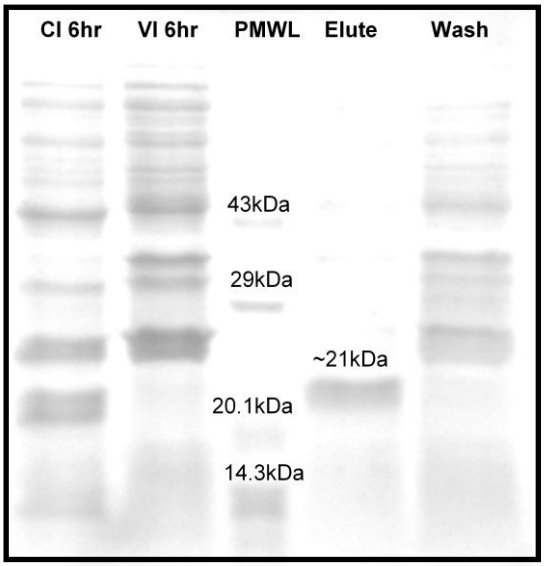

Figure 5.13: Purification of Recombinant His-tagged *Pv*SufA protein. PMWL: Protein Low Molecular Weight Marker (Merck Bio Science). (VI: pRSET A induced; CI: pRSETa *PvsufA* induced; Elute: *Pv*SufA protein eluted fractions; Wash: *Pv*SufA protein wash fractions).

5.2.8 Functional characterization of *Pv*SufA protein

5.2.8.1 Reconstitution of Fe-S clusters on *Pv*SufA protein

In order to determine the functional role of *Pv*SufA protein as a scaffold protein required in the assembly of Fe-S clusters, several biochemical assays were performed. However, as the Fe-S clusters are sensitive to oxygen and the purification of *Pv*SufA protein was done in aerobic conditions, it resulted in the oxidation of this protein which ultimately led to the removal or no formation of the Fe-S cluster on the protein. To reconstitute these clusters on the protein, the whole reaction setup was done under anaerobic environmental conditions. For the same, 4µM of purified *Pv*SufA protein was incubated with 5 folds molar excess of

ammonium iron (II) sulphate (as iron source) and 5 folds molar excess Na_2S (as sulphur source) in the presence of 5mM dithiothreitol (DTT) (as reducing agent) prepared in 0.1 M Tris–HCl (pH 8.0), at 25˚C for 3 hours. This resulted in a brown coloured precipitate after 3 hours of incubation indicating the presence of Fe-S clusters on the pure protein. In order to remove the unbound iron and sulphur the reaction mix was subjected to desalting with Amicon® Ultra-4 filters 10K (Merck Millipore, UK) which were already equilibrated with 50mM HEPES-NaOH buffer (pH 7.5). To further confirm the presence of Fe-S clusters on *Pv*SufA, the UV-visible absorption spectrum of purified protein without reconstitution and after reconstitution was taken. For the same, a fraction of the reconstituted protein was directly transferred into a cuvette, which was closed with a septum before being removed from the anaerobic chamber. The protein UV- visible spectra of originally purified protein and reconstituted protein were analysed at 350-450 nm (**Figure 5.14**). Maximum absorption was obtained at ~415 nm for the reconstituted protein which is typical for protein containing Fe-S clusters, thus confirming the reconstitution of these clusters.

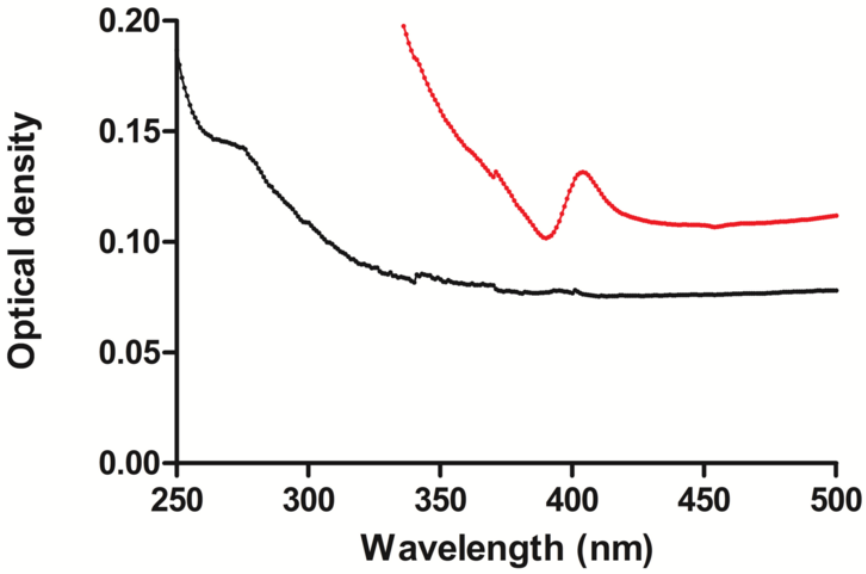

Figure 5.14: Absorption spectra of the purified *Pv*SufA protein before (black) and after reconstitution (red) of Fe-S clusters. The characteristic peak at ~415nm represents the Fe-S cluster bound protein under anaerobic condition.

5.2.8.2 Rapid Colorimetric Assay: Iron and Sulphur determination

After reconstitution, to check the amount of Fe and S bound to SufA, the Ferrozine and methylene blue assay was performed according to Fish, 1988 and Siegel, 1965 respectively. For the Ferrozine assay, the iron standard solutions of varying concentration (1µg to 6µg/mL) were prepared by dissolving required concentration of ferrous ethylene diammonium sulfate tetra hydrate salt (SIGMA, USA) in 0.01M HCl. To these standard solutions and the protein sample, 0.5mL of freshly prepared iron releasing reagent containing 0.6M HCl and 0.142M potassium permanganate ($KMnO_4$) was added. The digested mixture was incubated in dark for 2 hr at 60°C followed by the addition of 0.1mL of reducing, iron chelating reagent containing 6.5mM ferrozine (disodium 3-(2-pyridyl)-5,6-bis(4-phenylsulfonate)-1,2,4-triazine), 13.1mM neocuprine (2,9-dimethyl-1,10-phenanthroline), 2M ascorbic acid and 5M ammonium acetate. The solution was left to stand at room temperature for at least 30 min, after which, the absorbance of standards and protein samples were measured at 562 nm (Fish, 1988).

For methylene blue assay, sodium sulfide standards with concentration varying from 0.01mM to 0.1mM and the protein sample were prepared in sodium carbonate buffer (pH 9.0), were treated with 0.02M N, N-Dimethyl-p-phenylene-diamine sulfate (DPD) and 0.03M Ferric chloride ($FeCl_3$). After incubation at room temperature for 10 min, absorbance was taken at 650 nm (Siegel, 1965).

The absorbance for iron and sulphur standards was plotted and quantity of iron and sulfur released by *Pv*SufA protein was calculated by extrapolating the absorbance of these calibration curves (**Figure 5.15 (a) & (b)).** The total iron content of reconstituted *Pv*SufA was calculated as 2.20384µM (µmole protein)$^{-1}$ by the Ferrozine assay while the sulphur content was found to be 2.464µM (µmole protein)$^{-1}$ in methylene blue assay, indicating binding of Fe-S clusters.

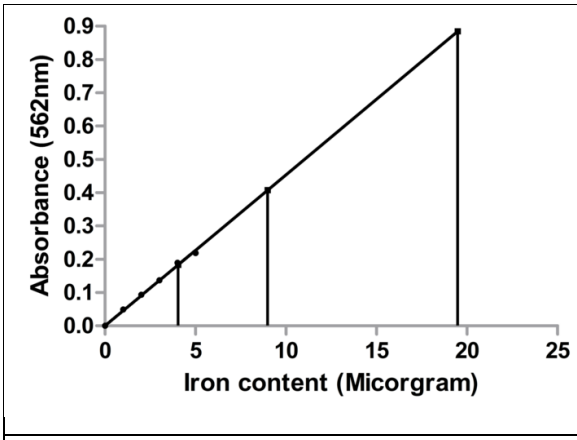

Figure 5.15a: A regular standard curve to determine the iron content by Ferrozine assay

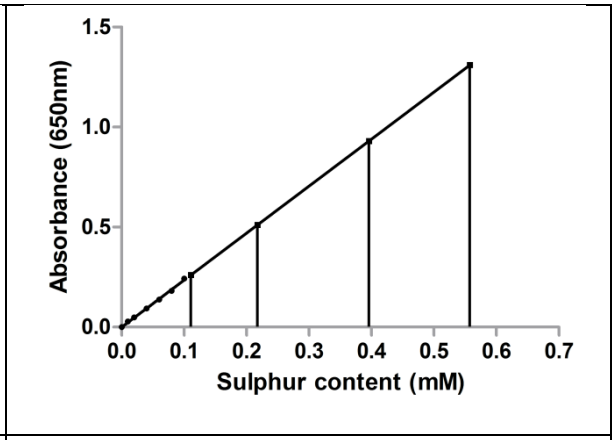

Figure 5.15b: A regular standard curve to determine the sulfide content by methylene blue assay

5.2.8.3 Electron Paramagnetic Resonance (EPR) Study

Further the above reconstituted protein complexed with Fe-S clusters was analyzed by EPR Spectroscopy to check for the oxidation state of bound Fe-S cluster (Wang et al., 2011). Briefly, the samples were diluted to a concentration of 5µM in 20mM phosphate buffer containing 0.5M NaCl (pH 7.4) followed by incubation with 5mM ammonium persulfate for 30 min to oxidize *Pv*SufA for spectra analysis. X-band EPR spectra were recorded at 100K on a JES-FA200 spectrometer. Parameters for recording the EPR spectra were typically 15–30mT/ min sweep rate, 0.63mT modulation amplitude, 9.44GHz frequency, and 4mW incident microwave power with a sweep time of 2 min. The spectra of purified *Pv*SufA protein in the reduced state does not exhibited any EPR activity, however, the oxidized *Pv*SufA gave an S=5/2 signal which shows the presence of Fe^{3+} oxidation state of iron (**Figure 5.16**).

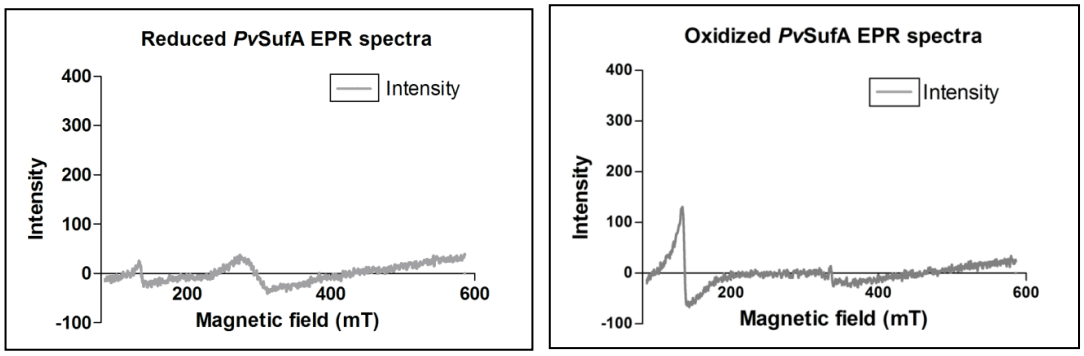

Figure 5.16: Electron paramagnetic resonance spectra of reduced and oxidized recombinant *Pv*SufA.

The g value was estimated as 2.13. The results are in agreement with previous reports for proteins acting as scaffold proteins for Fe-S cluster assembly and indicate that the [4Fe-4S] clusters were successfully assembled on *Pv*SufA protein upon reconstitution.

5.2.9 Antibody raising and Immuno-localization

After successful constitution of Fe-S clusters on PvSufA, we proceeded to solve the discrepancy of its localization. As our targeting predictions suggested dual targeting, thus, to confirm the sub-cellular localization of *Pv*SufA, antibodies were raised against recombinant *Pv*SufA in mice following the procedure detailed in Chapter 2. Antibody titer was calculated for the sera collected after different booster doses of protein, using standard ELISA taking serum collected from mice injected with 1X PBS along with Freund's adjuvant as a control. Pre-immune sera were also collected to check presence of any cross-reactive antibodies. We could observe the best antibody titre at third booster dose (**Figure 5.17**). The pre-immune sera were also tested for cross-reactivity of the antibodies and no non-specific signals were obtained for the same (**Figure 5.18a**). The specificity of antibodies towards *Pv*SufA protein was confirmed by western blot with pure protein, where a specific band at the desired position was obtained (**Figure 5.18b**). Further, the specificity of antibodies for *P. vivax* was confirmed was also done using *P. vivax* infected patient blood parasite lysate. The western blot again gave a specific band at the desired position with the anti-*Pv*SufA antibodies, confirmed the specificity of the antibodies (**Figure 5.18b**).

The raised antibodies after confirmation were used to perform sub-cellular localization on blood smears prepared from *P. vivax* infected patients. For this, the parasite cells were fixed, permeabilised and sequentially treated with mouse polyclonal anti-*Pv*SufA sera (1:1000) followed by goat anti-mouse monoclonal IgG FITC antibodies. The cells were counter stained with DAPI and Qdot® 585 Streptavidin conjugate viewing the parasite's nucleus and apicoplast respectively. First the RBC infected with the parasite was confirmed using bright field. After the confirmation of the infected RBC, green fluorescence was used to localize the

*Pv*SufA protein, blue and red fluorescence for nucleus and apicoplast respectively (**Figure 5.19**). The *Pv*SufA protein was localized as a green fluorescing spot with an overlapping red spot depicting the apicoplast and a blue spot staining nucleus adjacent to this merged yellowish spot. This study confirms that *Pv*SufA protein is functionally active in the apicoplast.

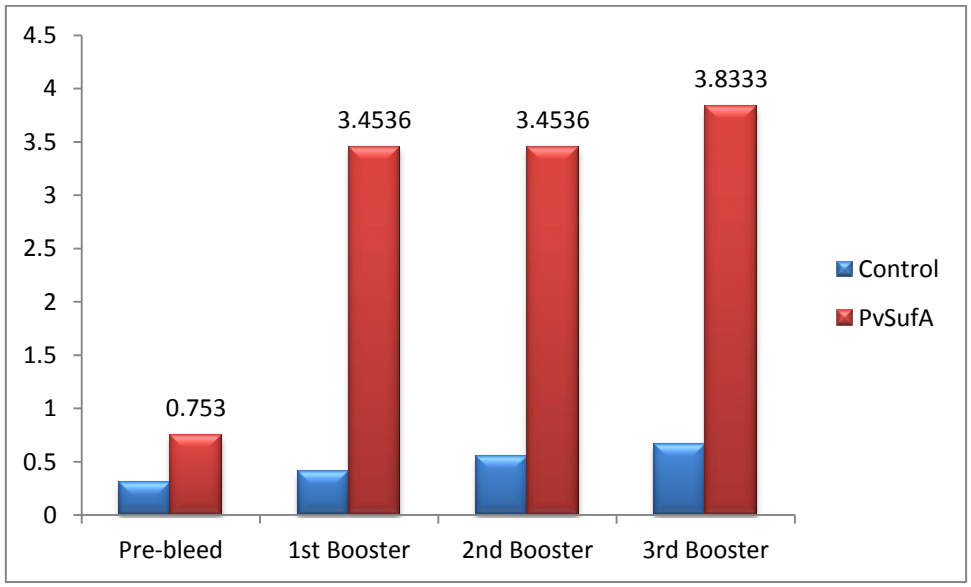

Figure 5.17: Antibody concentration determination titre for *Pv*SufA protein by ELISA.

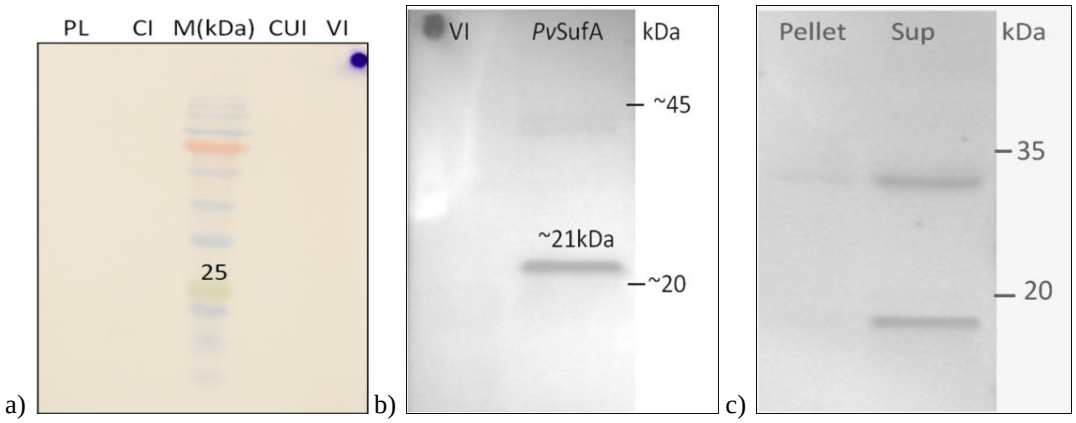

a) b) c)

Figure 5.18: Western blot of anti- *Pv*SufA antibodies with a.) Pre-immune sera b.) *Pv*SufA pure protein c.) *P. vivax* infected patient blood parasite lysate. c.) (VI: pRSET A Induced sample; *Pv*SufA: Pure protein *Pv*SufA; Pellet and Sup: Pellet and Supernatant obtained after parasite lysate preparation; PL: Parasite lysate; CI: pRSETA + *Pv*SufA Induced sample; CUI: pRSETA + *Pv*SufA uninduced sample.

5.2.10 *In-silico* studies for *Pv*SufA

The *in vitro* biochemical assays mentioned above confirm *Pv*SufA to be a scaffold protein and suggest that a [4Fe-4S] cluster is formed onto it. We further wanted to investigate the interacting residues involved in the interaction of this cluster and *Pv*SufA protein. Apart from this we also wanted to look into the interacting partners of the *Pv*SufA protein which further help in transfer of these clusters in *Plasmodium*. For the same, a structure of all the proteins involved in the SUF pathway was necessary and thus we went ahead for construction of homology model.

5.2.10.1 Secondary structure prediction

In order to generate a *Pv*SufA structure, we performed a secondary structure prediction using PSIPRED (Buchan et al., 2013). In *Pv*SufA protein, presence of 3 α-helices and 7 β-strands were observed which were joined with the help of 12 coils (**Figure 5.20**). The characteristic features and chemical properties of *Pv*SufA protein provided by PSIPRED are enlisted in **Table 5.4.**

Secondary structure of *Pv*SufA protein was also compared with orthologues of SufA available from different organisms including apicomplexans and prokaryotes where high level of variation was observed (http://www.geneious.com, Kearse et al., 2012). This deviation was mainly because of the high variation in sequence length of the SufA protein obtained from different organisms. However, a conserved signature motif was observed at the C-terminal of all the sequences (**Figure 5.21**).

5.2.10.2 Comparative modelling and Energy Minimization

Three-dimensional (3D) model of *Pv*SufA protein was built by homology modelling using the program MODELLER 9v11 (Sali and Blundell, 1993; Eswar et al., 2006). The *Pv*SufA amino acid sequence obtained from *Plasmodium* Indian field isolates was submitted to HHpred online server for template search. Crystal structure of *E. coli* SufA (PDB; A chain of 2D2A) protein with 2.7 Å resolution was selected as a template for *Pv*SufA protein. SufA sequence of *Plasmodium* parasite shares only 27.5% amino acid identity with *E. coli* SufA, mainly in the conserved domain region. After the removal of non-similar targeting sequences, the remaining

sequence was submitted for protein modeling, which yielded 3D models of the targets with all non-hydrogen atoms without any user intervention.

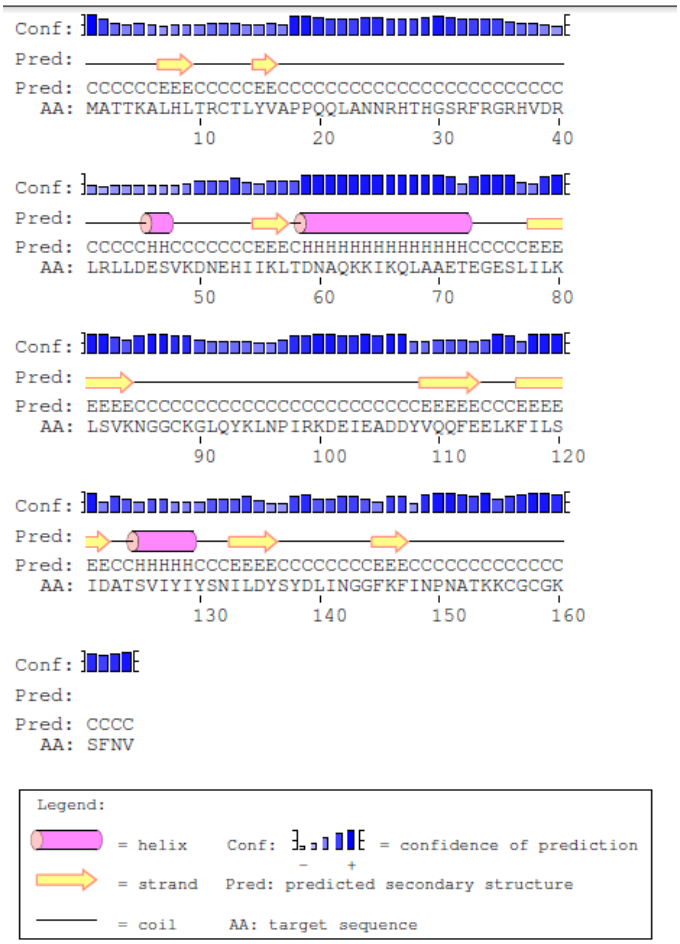

Figure 5.20: Secondary Structure predictions for *Pv*SufA protein using PSIPRED.

Table 5.4: Characteristics features of *Pv*SufA protein analysis based on Secondary structure

Characteristic features	***Pv*SufA**
Molar extinction coefficient	8960
Molecular weight	18603
Isoelectric point	9.13
Percent negative residues	0.12
Percent positive residues	0.15
Charge	7.51
Signal peptide	1-35
Transmembrane topology	130-145
Aliphatic index (0-100)	92.20
Hydrophobicity (-4 to 3)	-0.45

The best model with minimum DOPE score was selected and quality of the structure was further improved by energy minimization using online server YASARA (Krieger et al., 2009). The structure was evaluated by using different servers where PROCHECK showed a G-score 'BETTER' while 95.88% of the residues obtained an average 3D-1D score less than 0.2 (passed) using VERIFY3D. The Z-score from WHATIF server gave a score of -5.34 indicating that the generated structure was good. The main chain conformations for 99% of amino acid residues were within the favoured or allowed regions for *Pv*SufA structures in the Ramachandran plot analysis (**Figure 5.22a)**. The ERRAT score for *Pv*SufA is 98.810, indicating that the molecular geometry of the model is of good quality (**Figure 5.22b**). Root-mean-square deviation (RMSD) value between the backbone atoms of the template and *Pv*SufA models is 0.102Å.

The obtained monomeric *Pv*SufA structure consisted of two helices and seven beta-strands. The seven beta-strands were divided amongst the two helices in which A1, A2, A3 belong to Helix A and B1, B2, B3, B4 belong to Helix B. The generated *Pv*SufA structure showed a high level of conservation amongst the important residues involved in the interaction of the scaffold protein with the iron sulphur clusters, including the three invariant cysteine residues at positions Cys88, Cys156, and Cys158. The residues involved in forming hydrophobic interactions or salt bridges to stabilize the structure were also found to be conserved.

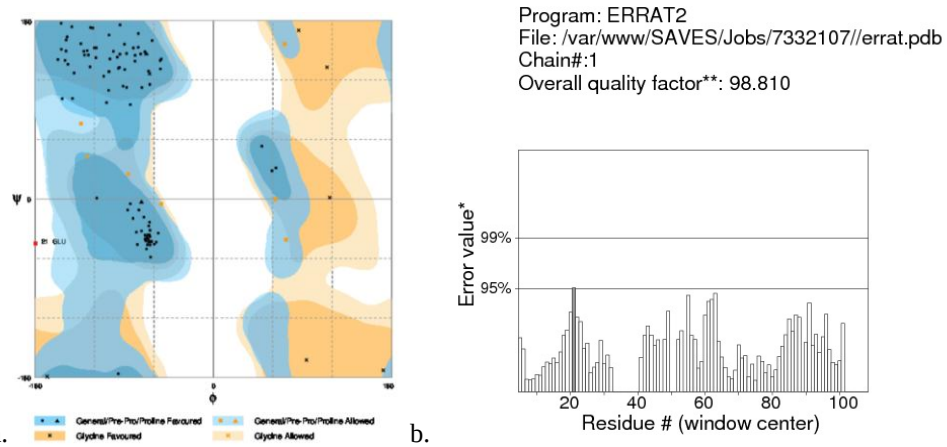

Figure 5.22: Validation of 3-dimensional structures of *Pv*SufABCD using a.) Ramachandran Plot b.) ERRAT score.

Two characteristic loop structures were found namely, A2-L_{A23}-A3 and B1-L_{B12}-B2, which were stabilized by hydrophobic interactions involving conserved residues Leu_{57}, Val_{83}, Tyr_{93}, Leu_{95}, Phe_{145} and Phe_{147} (**Figure 5.23**). A type IV turn structure, specific to A-type scaffold protein, from Asn_{107} to Ala_{110} linked to the B2 beta strand by a hydrogen bond between Tyr_{55} & Asn_{107} was also present.

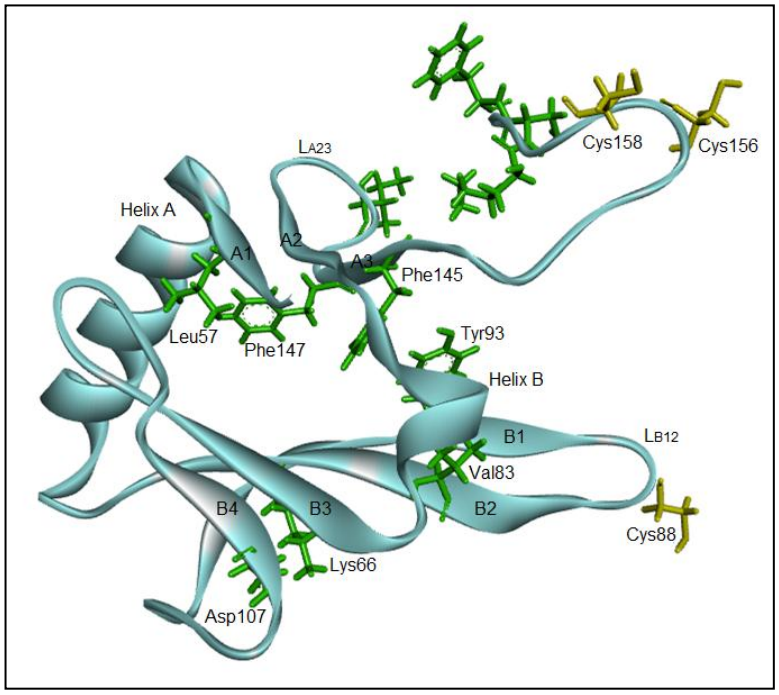

Figure 5.23: *Pv*SufA protein structure prediction: The structure prediction was done by homology modelling. *E. coli* SufA (2D2A) crystal structure was used as a template. The conserved cysteine residues are marked in yellow and the conserved residues involved in the hydrophobic interactions are marked in green.

However, the B1 strand was linked to B3 strand by a salt bridge between residues Lys_{69} and Asp_{107} unlike the *E. coli* salt bridge which is between Arg_{42} and Asp_{67}. The negatively charged residues contributing to the acidic nature of the protein were found to be conserved and distributed throughout the structure, typical of A-type scaffold proteins.

5.2.10.3 Active site architecture and docking with Fe-S cluster

Our *in vitro* biochemical assays showed that a [4Fe-4S] cluster binds to *Pv*SufA protein. In order to further validate this result and also get an insight into the residues participating in the interaction of *Pv*SufA and the [4Fe-4S] cluster we carried out docking studies. As the monomeric SufA lacked the Fe-S cluster binding pocket, and SufA has been reported to exist as a dimer, the dimeric model of *Pv*SufA was generated (**Figure 5.24**) and the [4Fe-4S] cluster was docked to gain an insight into the interaction of the cluster with the protein. To predict the binding pocket with conserved amino acid residues, COFACTOR server (Roy et

al., 2012) was used. Once the binding cavity was identified (**Table 8)**, the [4Fe-4S] cluster was docked in the active site. The cysteine residues at positions 88, 156 and 158 were shown to be ligating with the 4Fe-4S cluster and the distances between the cysteine residues and the corresponding iron atoms of the 4Fe-4S cluster were all found to be within 3.2Å (**Figure 5.25**). The molecular modelling results were in agreement with that of the experimental results in *A. ferrooxidans* (Zeng et al., 2007), where the sulfhydryl groups of the conserved cysteine residues at the corresponding positions 35, 99 and 101 were essential for the 4Fe-4S cluster binding. Sequence alignment of *Pv*SufA with *E. coli* SufA indicated a change in the conserved residue Glu103 which is proposed to be involved in the interaction with the Fe-S cluster. The corresponding residue in *Pv*SufA was found to be Lys160 with a distance of 0.86Å and this change was found not to pose any difficulty in ligating with the Fe-S cluster.

Table 5.5: *Pv*SufA active site prediction

Rank	**C-score**	**Cluster size**	**PDB Hit**	**Ligand Name**	***Ligand Binding Site Residues***
1	0.04	8	2D2A	[4Fe-4S]	42-45, 50, 114, 116, 118

*(The C - score is the confidence score of the prediction ranging from [0-1], where a higher score indicates more reliable prediction; **Cluster size** is the total number of templates in a cluster)

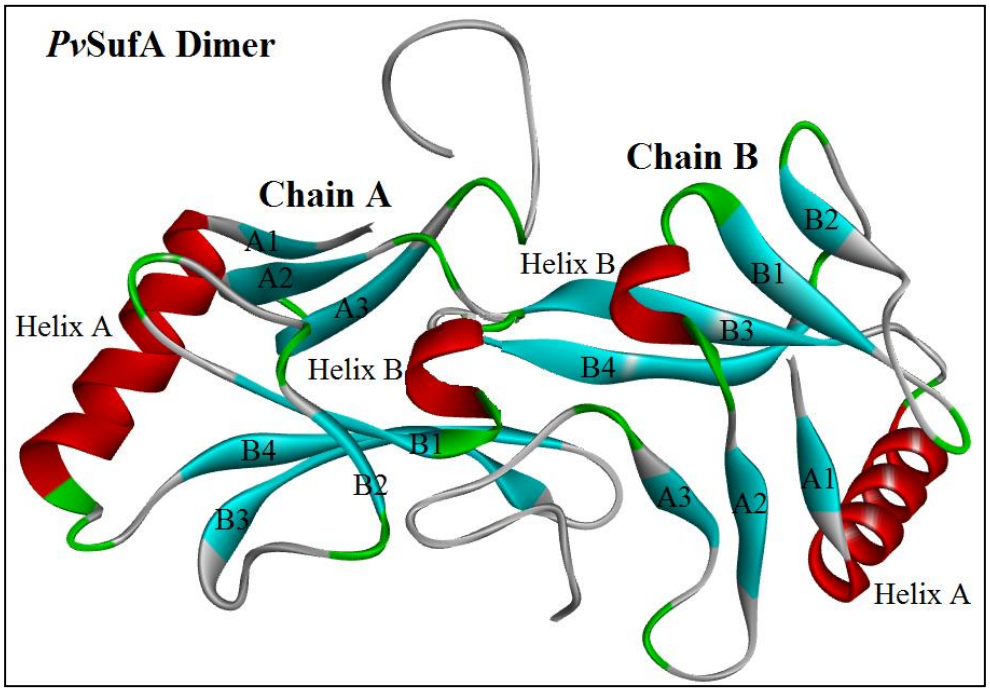

Figure 5.24: *Pv*SufA dimeric protein structure prediction.

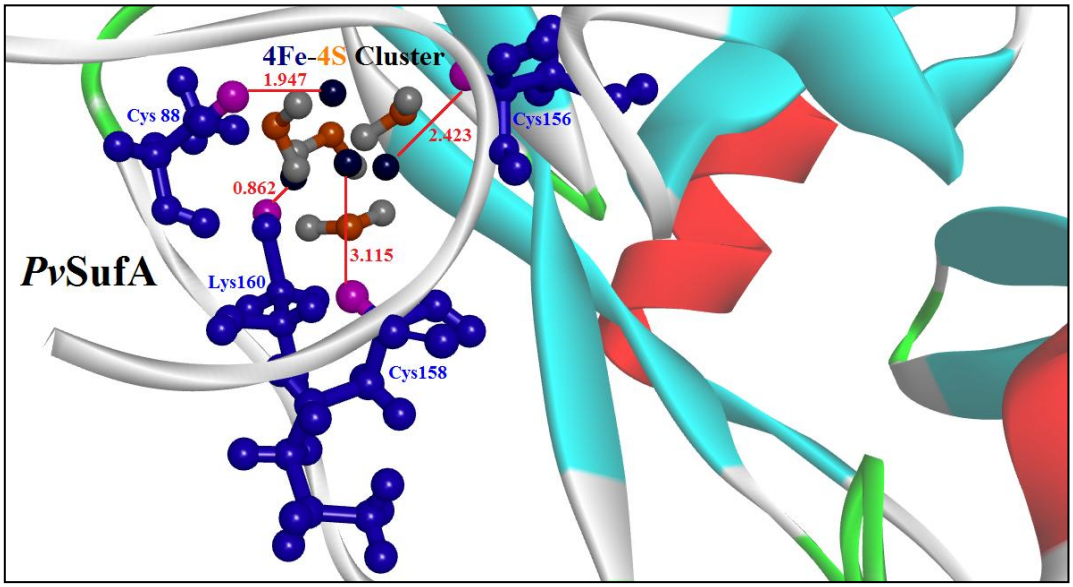

Figure 5.25: Active site prediction and docking analysis of [4Fe-4S] cluster to *Pv*SufA protein
(Interaction of iron (in blue) and sulfur (in yellow) atoms with *Pv*SufA shown with red lines)

5.3 Conclusion

The *Pv*SufA protein is characterized by the Fe-S cluster biosynthesis superfamily domain and participates in the concluding steps of SUF pathway for Fe-S cluster biosynthesis. The Fe-S clusters are ancient cofactors known to play an important role in several enzymatic and metabolic processes. The sequence similarity between different SufA orthologs varied from 22-90% with a high number of conserved residues in the Fe-S biosynthesis superfamily domain. The protein was found to be evolutionary conserved, showing high level of similarity among different apicomplexans and bacterial species. A close association was observed with the primate parasites as reported for other genes from nuclear as well as apicoplast genome of the parasite (Escalante et al., 2005; Saxena et al., 2007; Saxena et al., 2012). The protein co-localised to the apical end of the parasite along with the apicoplast, suggesting it's targeting to the apicoplast, the suggested site of action for this pathway (Kumar et al., 2011; Gisselberg et al., 2013; Charan et al., 2014).

In *E. coli*, the sulphur mobilized by SufSE is received by SufB which acts as a scaffold in complex with SufD (to channel iron from unknown sources) and SufC (an ATPase), while SufA acts as a Fe-S cluster shuttle protein receiving clusters from the SufBCD complex prior to their insertion onto the target apo-enzymes

(Chahal et al., 2009). In *Plasmodium*, the SufBCD interaction has been shown, but as the SufB lacks CXXCXXXC motif present in *E. coli* SufB, its role as a scaffold protein is unclear (Kumar et al., 2011; Saxena et al., 2012). Along with it, there are no reports detailing the transfer of these clusters to the apo-proteins in *Plasmodium.*

Thus, we analysed the *Pv*SufA protein for its potential to form and transfer Fe-S clusters. The predicted *Pv*SufA protein structure showed all the characteristic features of an A-type scaffold protein. In all A-type scaffold proteins, the position of three cysteine residues is conserved as $X_{34}CX_{63}CGCX_{67}$, and these invariant cysteine residues are important for interaction with Fe-S clusters (Vinella et al., 2009). In Indian *Pv*SufA protein, these three cysteine residues were conserved as $X_{87}CX_{155}CGCX_{159}$, and showed interactions with the Fe-S clusters, suggesting the formation of Fe-S clusters on this protein. However, instead of Glu103 as reported in *E. coli* (Wadaa et al., 2005), Lys160 was found to interact with the Fe-S clusters in *P. vivax.* The results of colorimetric assays and EPR spectra further confirmed the successful incorporation of [4Fe-4S] cluster in *Pv*SufA, illustrating its role as a scaffold protein for the Fe-S cluster assembly in *P. vivax*.

Chapter VI

Interaction of different components of SUF Pathway from P. vivax

Interaction of different components of SUF pathway from *P. vivax*

6.1 Introduction

As mentioned earlier, all the Fe-S cluster assembly pathways (NIF, ISC, SUF and CIA) share a common paradigm: the assembly of a Fe-S cluster, which occurs on a scaffold protein which is followed by the transfer and integration of the cluster into the polypeptide chain of the target apo-protein. Each of these steps involves the participation of several proteins and cofactors that perform biosynthetic reactions. The basic requirements for the formation of a Fe-S cluster include an inorganic iron and sulphide, yet cells have to prevent an unregulated release of these potentially toxic components.

To guarantee accurate iron delivery to scaffold proteins, specific iron donors are needed. The iron source for building Fe-S clusters has not been clearly identified so far. In order to prevent the leakage of harmful free iron in the cellular environment, Fe ions must also be provided by a shielded pathway. Thus, it is expected that there should be a close interaction between the iron donor and components of the Fe-S assembly system. In bacteria, CyaY protein which interacts with IscS and the scaffold protein IscU have been identified as a potential Fe donor (Py and Barras 2010). In eukaryotes, the CyaY homologue frataxin, has been investigated as a potential iron donor. Frataxin is highly conserved in prokaryotes and eukaryotes, and loss of its function in humans leads to the neurodegenerative disorder Friedreich's ataxia (Busi and Gomez-Casati, 2012). Another possible source of iron which has been speculated to act as an iron donor on the basis of *in vitro* studies is IscA (Py and Barras 2010). It is hypothesized that in the malaria parasite, a possible source of iron could be the iron-rich haemoglobin protein, which is digested in the parasite food vacuole (van Dooren et al., 2006). It is postulated that, since all the heme released from hemoglobin is not polymerized to hemozoin (Egan et al. 2002), a small fraction of this heme might be degraded to supply iron for integration into Fe-S clusters (Charan et al., 2013).

The SUF pathway specifically possesses a class of two-component cysteine desulfurases – SufS and SufE, where, SufS releases the required sulfur from cysteine

and converts this cysteine to alanine. The desulphurase activity of the SufS protein is enhanced by a helper protein SufE up to 50-fold (Loiseau et al. 2003; Outten et al. 2003). The sulfur (S^0) is transiently bound to the cysteine desulfurase *via* a persulfide group at a conserved cysteine residue and is subsequently transferred to a scaffold protein *via* SufE. Mutagenesis experiments coupled with ^{35}S-radiolabeling and mass spectrometry studies have given the experimental evidence of the sulfurtransferase function of SufE (Ollagnier-de-Choudens et al. 2003; Outten et al. 2003). Therefore, the superficial transfer of cysteine persulfides formed on SufS to a cysteine residue within SufE has been considered to be responsible for the SufE dependent enhancement of cysteine desulfurase activity.

Hydrogen Deuterium Exchange – Mass Spectrometry (HDX-MS) analysis reveals that SufE binds near the SufS active site to accept persulfide and initiates allosteric changes in other parts of the SufS structure. SufE enhances the efficiency at two important steps: first the initial L-cysteine substrate binding to SufS and second the formation of an external aldimine required for early steps in SufS catalysis. HDX-MS analysis also suggests a more active role for SufE in promoting SufS reaction for Fe-S cluster assembly and provides a new picture of the SufS-SufE sulfur transferase pathway, which is different from IscS-IscU sulfur system in ISC pathway working under normal conditions (Outten et al., 2003).

In *P. falciparum*, a pulldown assay with beads crosslinked to anti-*Pf*SufS antibodies confirmed the interaction of recombinant *Pf*SufS and *Pf*SufE proving the *in vitro* complex of the two proteins. Co-immunoprecipitation studies of *Pf*SufS and *Pf*SufE from parasite lysates, as well as the size of the dithiobis(succinimidyl propionate) (DSP)-cross-linked complex (74 kDa), further proved that monomers of *Pf*SufS (56 kDa) and *Pf*SufE (18 kDa) interact within the parasite to mobilize sulfur released from L-cysteine (Charan et al., 2014). The first part of this chapter focuses on the *in vitro* and *in silico* interaction of these two components SufS and SufE in *P. vivax*.

The next step of the SUF pathway is the assembly of the Fe-S clusters on the scaffold protein. The scaffold proteins further serves as a platform for the *de novo*

synthesis of a Fe-S clusters, a process that is still not understood completely in the malaria parasite. The prokaryotic system possesses the SufBCD complex for this function where, SufBD function as a scaffold for the assembly of the Fe-S cluster and SufC imparts the energy and acts as an ATPase. As mentioned in the previous chapter, the *Plasmodium* SufB however lacks this CXXCXXXC motif for it to function as a scaffold protein. So in later part of this chapter, we have analysed the potential to of *Pv*SufA to function as a scaffold protein in conjunction with the SufBCD complex to assemble Fe-S clusters.

The final step in the biogenesis is the transfer of the transient Fe-S cluster from the scaffold to the protein, which is converted from the apo form to the holo form. The new cluster is transiently bound to the conserved cysteine residues of the scaffold and hence, it can be transferred to the target apo-protein. The SUF pathway is said to provide Fe-S clusters to the last two enzymes of the nonmevalonate DOXP pathway of isoprenoid biosynthesis (IspG) and (IspH) (Zepeck et al., 2005; Rekittke et al., 2008; Lee et al., 2010) functional in the apicoplast. Activity of both of these enzymes is highly dependent on the redox environment and Fe-S clusters (Rohrich et al., 2005; Partow et al., 2012). IspG catalyses the reduction of MECP through a multistep reaction and converts it into 4-hydroxy-3-methyl-2-(E)-butenyl-4-phosphate (HMBDP) and then IspH converts it to IPP and DMAPP (Rohdich et al., 2001). The Isoprenoid pathway has been shown to be indispensable for the parasite and IspG has been reported to be one of the key enzymes.

In the last part of this chapter, an attempt has been made to reconstitute the entire Fe-S cluster biogenesis *in vitro*. For this, the Fe-S clusters assembled on the scaffold protein *Pv*SufA were checked for their possibility to be transferred to the apo-protein *Pv*IspG.

6.2 Results and Discussion

The earlier chapters focused on the individual characterization of *Pv*SufS, *Pv*SufE and *Pv*SufA that included; the cloning, protein expression analysis, localization, *in vitro* functional assays and *in silico* structure prediction for all the proteins. The

following table gives comparative analysis of the three important proteins of the SUF pathway undertaken in this study (**Table 6.1**). All the three proteins show conservation in their function across all the species. Further in the chapter we have discussed the interaction of all these components with other components of the pathway to elucidate the complete SUF pathway from *P. vivax*. The results discussed below would further help us understand the interaction of all these components with each other and finally elucidating the complete SUF pathway from *P. vivax*.

Table 6.1: Comparative analysis of SufS, SufE, SufA genes from *Plasmodium spp*. with *E. coli*.

Sr. No.	Gene	Species	Molecular Weight (kDa)	Similarity with *E. coli* (%)	Function	Experimental Evidence
1.	SufS	*P. falciparum*	64.5	30.27	Cysteine Desulfurase	Gisselberg et al., 2013
		P. vivax	57.9	35.57	Cysteine Desulfurase	Manuscript under Review (Pala et al.,)
		P. berghei	62.3	31.09	Cysteine Desulfurase	Haussig et al., 2014
		E. coli	44	-	Cysteine Desulfurase	Loiseau et al., 2003
2.	SufE	*P. falciparum*	29.1	25	Cysteine Desulfurase Partner Protein	Gisselberg et al., 2013
		P. vivax	28.4	26.67	Cysteine Desulfurase Partner Protein	Manuscript under Review (Pala et al.,)
		P. berghei	28.8	24.44	Cysteine Desulfurase Partner Protein	Haussig et al., 2014
		E. coli	15.8	-	Cysteine Desulfurase Partner Protein	Loiseau et al., 2003
3.	SufA	*P. falciparum*	49.2	20.17	Fe-S cluster assembly accessory protein	No evidence
		P. vivax	20.4	18.03	Fe-S cluster assembly accessory protein	Pala et al., 2016
		P. berghei	36.1	28.69	Fe-S cluster assembly accessory protein	Haussig et al., 2014
		E. coli	13.3	-	Scaffold/Carrier Protein	Wada et al., 2004

6.2.1 Mobilization of Sulfur for Fe-S cluster biogenesis

6.2.1.1 *In silico* interaction of *Pv*SufS and *Pv*SufE

To confirm whether the conserved cysteine residues in *Pv*SufS and *Pv*SufE interact with each other, *in silico* docking analysis was performed. In *E. coli*, L-cysteine binds to PLP to form PLP cysteine adduct as a Schiff base between PLP and the α-amino group of Cys_{364} of SufS. This cysteine adduct *via* a nucleophilic attack results in the formation of an enzyme bound persulfide, which is further transferred to Cys_{51} of SufE (Hidese et al., 2011). To facilitate this procedure, the two cysteine of the interacting partners SufS and SufE must be in close proximity. However, the crystal structure of the *E. coli* SufS-SufE complex and the potential conformational changes that result from their interaction are not yet defined. Since the structure of a SufS-SufE complex is not available, we predicted the binding interaction between *Pv*SufS and *Pv*SufE of both the Indian isolate and the Sal-I by protein-protein docking using GRAMM-X docking server. Forty possible interactions for the *Pv*SufS-*Pv*SufE were generated. The docked complex revealed the proximity of the critical cysteine residues of *Pv*SufS and *Pv*SufE, where Cys_{500} of *Pv*SufS and Cys_{148} of *Pv*SufE are present in the protein-protein interface and the distance between the sulfur atoms of the two cysteines for Ind*Pv*SufS and Ind*Pv*SufE is ~2 Å (**Figure 6.1a**). However, for Sal-I*Pv*SufS and Sal-I*Pv*SufE, this distance was ~8.2 Å (**Figure 6.1b**). The difference in the distance between the two molecules clearly indicates that the insertion and deletion in the Indian isolates of *Pv*SufS and *Pv*SufE is causing some major conformational changes leading to much more proximity between the two proteins in comparison to the Sal-I structures. This distance may further reduce by the additional sulfur atom of the persulfide on the *Pv*SufS cysteine, thus facilitating direct transfer of sulphur to *Pv*SufE.

This interaction has been checked between *P. falciparum* SufS and SufE structures as well and it has been reported that the distance between the two proteins in ~8.7 Å (Charan et al., 2014). Thus, our analysis clearly indicate that the Indian field isolates of *Pv*SufS and *Pv*SufE interact in a much more closer proximity than the *P. vivax*

Sal-I and *P. falciparum* 3D7 structures suggesting the difference between the field samples and the *in vitro* culture data.

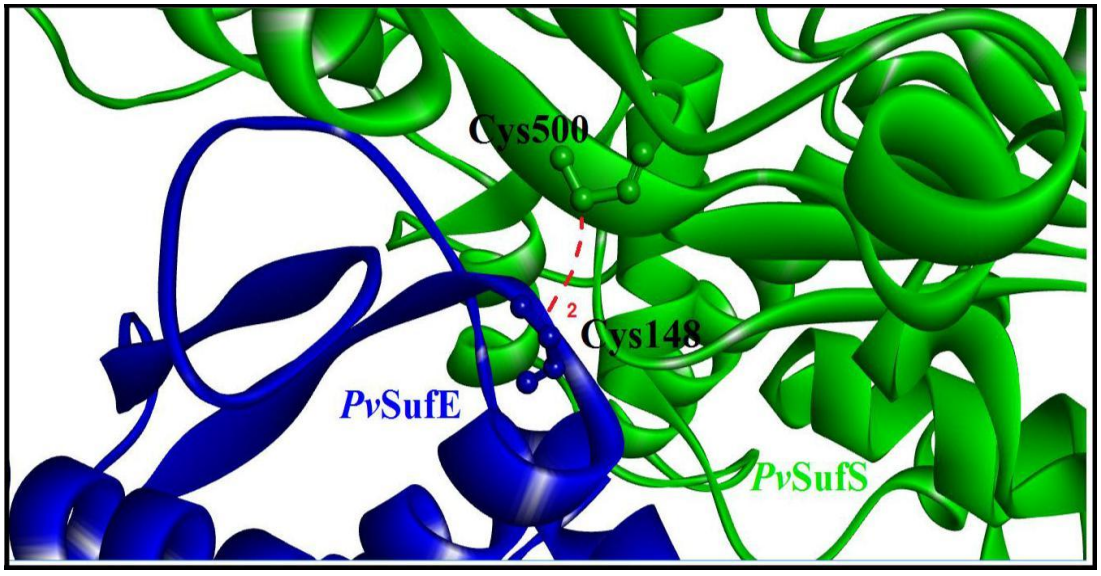

Figure 6.1a: Interaction between *IndPvSufS and IndPvSufE*

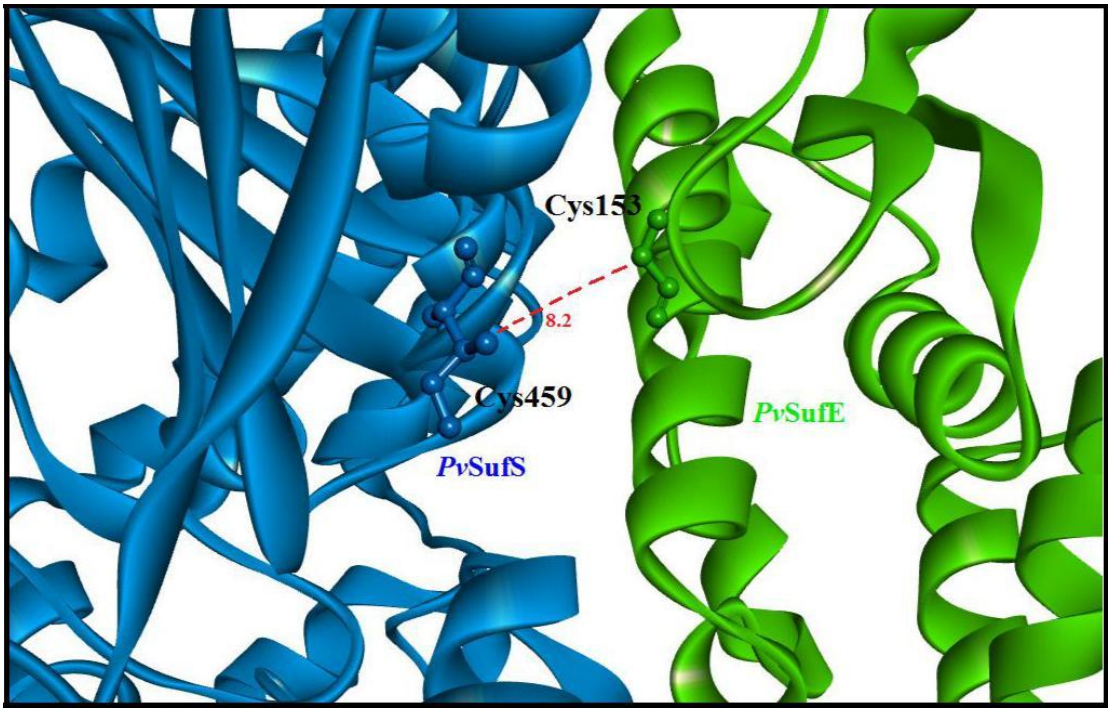

6.1b: Interaction between *Sal-IPvSufS and Sal-IPvSufE*

6.2.1.2 Cysteine Desulphurase Assay

For determining the effect of *Pv*SufE on the desulphurase activity of *Pv*SufS, similar reaction was performed as described earlier in Chapter 3 and 4. Briefly, the enzymatic assays consisted of reaction mixtures containing 5µM of *Pv*SufS

alone/*Pv*SufE alone/both *Pv*SufS and *Pv*SufE in sodium carbonate buffer (pH 9.0), 25mM Tris-Cl, 100mM NaCl, 100µM PLP, 2mM DTT under anaerobic conditions. The reaction was initiated by the addition of L-cysteine to a final concentration of 1mM and allowed to proceed for 20 min. The excess of L-cysteine was removed using Amicon Ultra-4 filters (Merck, Germany). The filtrate was then subjected to Methylene blue assay (Siegel, 1965). Sulfide production was quantified colorimetrically by measuring absorbance at 650nm. As discussed previously, the recombinant *Pv*SufS alone exhibited low cysteine desulfurase activity (2.575 µmole/ µmole protein), *Pv*SufE alone had minimal cysteine desulfurase activity (0.8 µmole/ µmole protein), but the activity of *Pv*SufS was enhanced to almost 5-folds by *Pv*SufE (12.205 µmole/ µmole protein) (**Figure 6.2**), suggesting that the desulphurase activity of *Pv*SufS increases to many folds in the presence of *Pv*SufE.

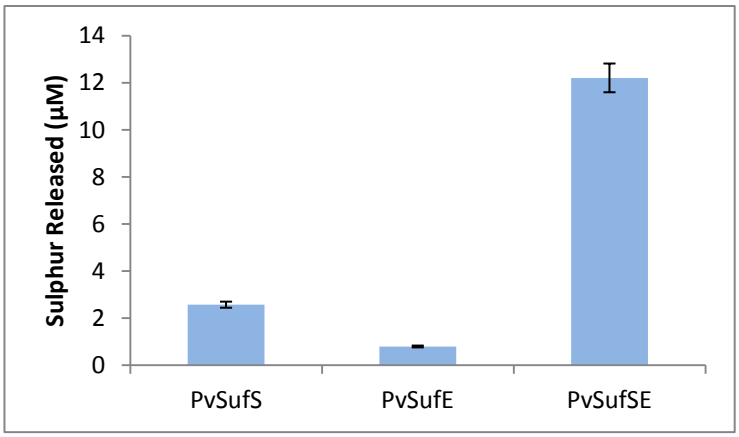

Figure 6.2: Enhancement of cysteine desulfurase activity of *Pv*SufS by *Pv*SufE.

6.2.2 *Pv*SufA functions as a scaffold protein in conjunction with *Pv*SufBCD complex

To look into the interacting partners of the *Pv*SufA protein with other components of the pathway, 3-D structures of *Pv*SufB, *Pv*SufC and *Pv*SufD proteins were built by homology modelling using the program MODELLER 9v11 (Sali and Blundell, 1993; Eswar et al., 2006). The sequences for *Pv*SufB, *Pv*SufC, *Pv*SufD obtained from PlasmoDB database were submitted to HHpred online server for template search. Based on the results obtained, structures for *P. vivax* SufBD and SufC were generated using crystal structure of *E. coli* stabilizer iron transporter (PDB ID: 1VH4) with resolution of 1.75Å and crystal structure of *E. coli* SufC (PDB ID:

2D3W) with a resolution of 2.5Å respectively. The *Pv*SufBD and *Pv*SufC showed a similarity of 34.56% and 49.38% identity with the respective template structures.

The best models with minimum DOPE score were selected and quality of the structure was further improved by energy minimization using online server YASARA (Krieger et al., 2009). The PROCHECK results for all the three structures showed a G-score 'BETTER' and VERIFY3D showed that 97.83%, 95.91% and 94.65% of the residues for *Pv*SufB, *Pv*SufD and *Pv*SufC respectively having an average 3D-1D score less than 0.2 (passed). As mentioned earlier, a negative Z-score of homology model is compulsory to hold the characteristic of being a good model and *Pv*SufB, *Pv*SufD and *Pv*SufC structures gave a Z-score of -6.12, -6.32 and -4.73 respectively suggesting that the generated models were of good quality. The Ramachandran plot analysis for main chain conformations suggested 99% of amino acid residues were within the favoured or allowed regions for all the protein structures (*Pv*SufBCD) (**Figure 6.3)**.

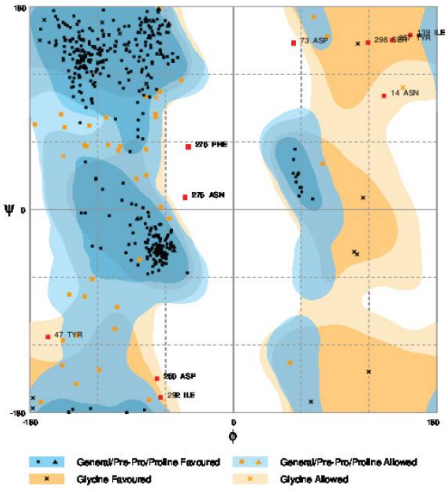

a.) *Pv*SufB

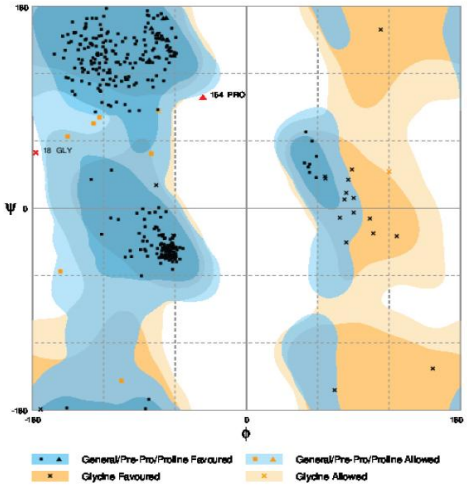

b.) *Pv*SufC

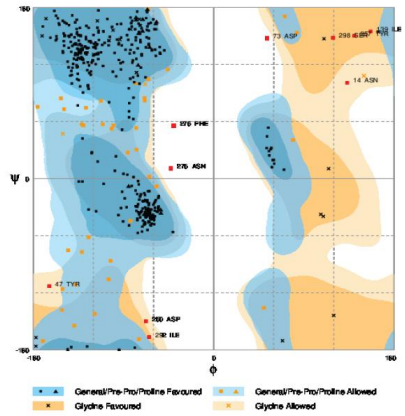

c.) *Pv*SufD

Figure 6.3: Validation of 3-dimensional structures of *Pv*SufBCD using Ramachandran Plot. a.) *Pv*SufB b.) *Pv*SufC, d.) *Pv*SufD.

The ERRAT scores for *Pv*SufBCD obtained are depicted in **Table 6.2**, and the values indicated that the molecular geometry of the models is of good quality (**Figure 6.4**). The root-mean-square deviation (RMSD) values between the backbone atoms of the template and *Pv*SufBCD models are as in **Table 6.2** and it indicated the significant homology between the structures.

Table 6.2: Structure validation results of *Pv*SufB, *Pv*SufC, *Pv*SufD

Sr. No.	Protein	ERRAT score	RMSD
2.	*Pv*SufB	95.381	0.199Å
3.	*Pv*SufC	94.421	0.215Å
4.	*Pv*SufD	93.998	0.183Å

As SufD is said to be evolved via gene duplication of SufB and they shares very good identity with each other, the 3D structures of *Pv*SufB and *Pv*SufD were found to be similar, sharing a common domain organization comprising of: an N-terminal helical domain, a core domain consisting of a right-handed parallel β-helix, and a C-terminal helical domain that contains the SufC binding site (**Figure 6.5**). The only minor difference in the structure of the two proteins is that the β-helix in the core domain of *Pv*SufB is partly composed of shorter strands than the corresponding domain of SufD. As mentioned above, the C-terminal helical domains are remarkably similar between both the proteins. The C-terminal domain shows the presence of certain conserved residues like R_{1200}, G_{1201}, A_{1207}, F_{1215} (Corresponding to R_{378}, G_{379}, A_{385}, F_{393} respectively in *E. coli*) in both *Pv*SufB and *Pv*SufD. The functional importance of these residues is yet unknown. These strictly conserved residues in both the structures further indicate a conserved function of both the proteins and that they may form a functional heterodimer *in vivo*.

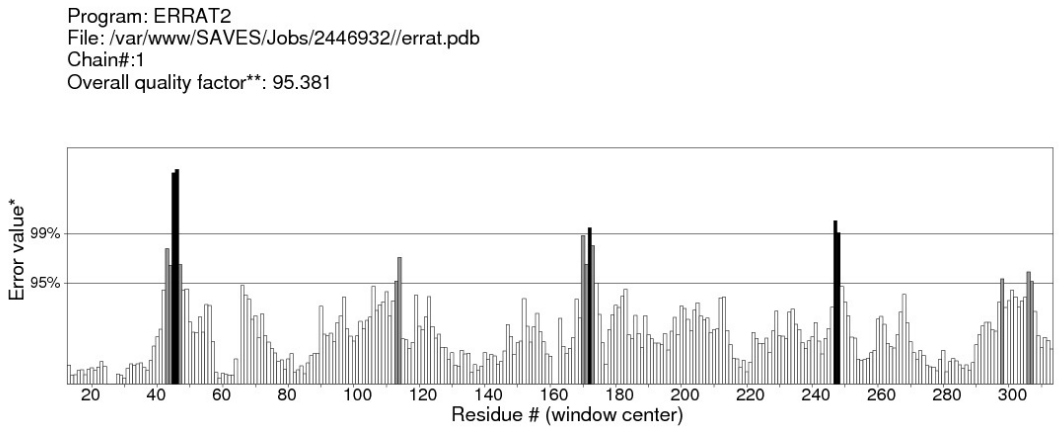

a.) *Pv*SufB

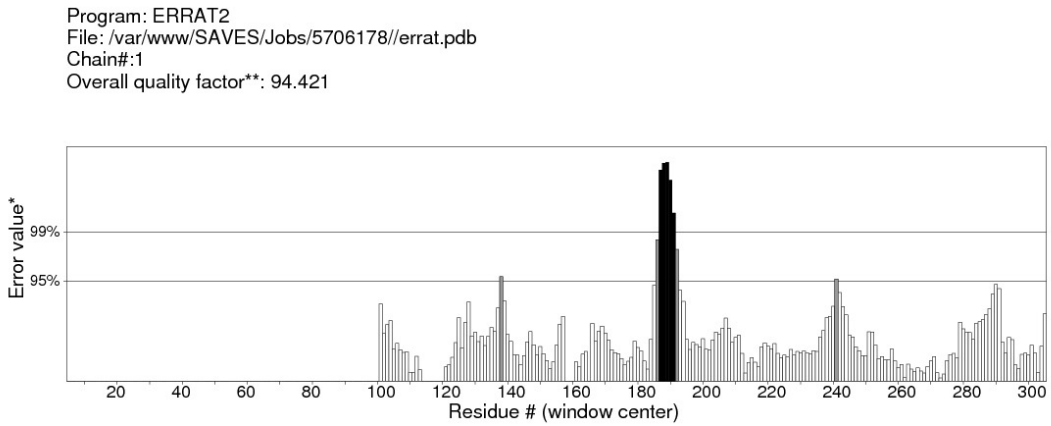

b.) *Pv*SufC

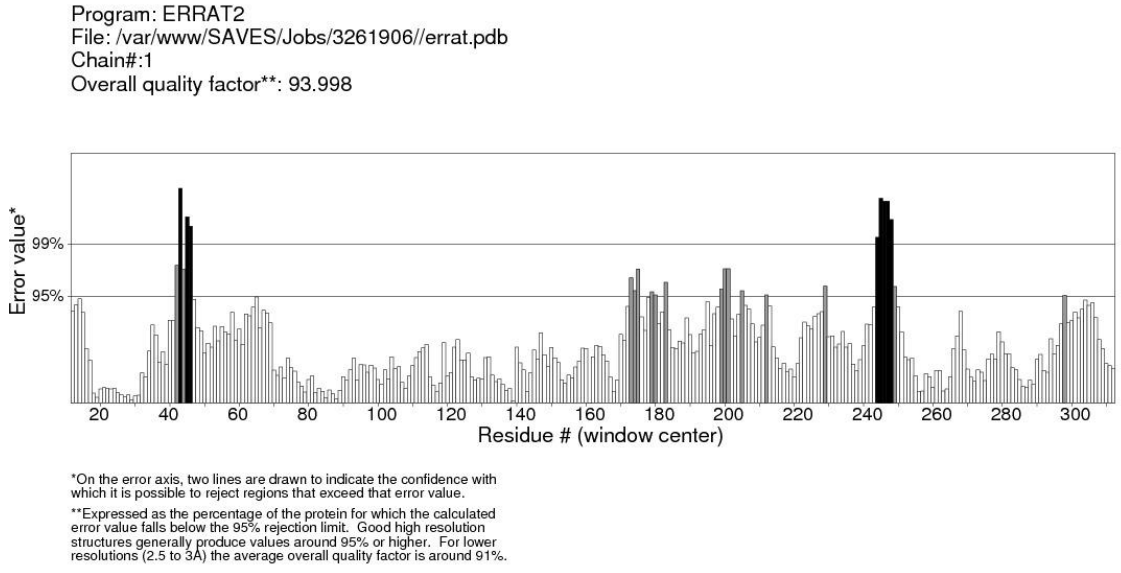

d.) *Pv*SufD

Figure 6.4: Validation of three dimensional structures of *Pv*SufBCD proteins using ERRAT score.

a.) *Pv*SufB b.) *Pv*SufC, d.) *Pv*SufD.

SufC is known as a member of an ABC ATPase superfamily. The *Pv*SufC like the other members of ABC ATPase superfamily also consists of two domains: a catalytic α/β domain that contains the nucleotide-binding Walker A and Walker B motifs, and a helical domain specific to ABC ATPases containing an ABC signature motif. The two domains are connected by a Q-loop that contains a strictly conserved glutamine residue. In addition to the Q loop, Walker A and Walker B motifs, SufC also possesses highly conserved sets of amino acid residues including an ABC signature motif, D-loop, and H-motif, all of which are characteristic features of proteins belonging to ABC ATPases superfamily (**Figure 6.6**). *Pv*SufC showed conservation with the three strictly conserved amino acid residues namely: K143 of the Walker A motif (corresponding to the K40 in *E. coli*), E274 of the Walker B motif (corresponding to E171 in E. coli), and H306 of the H-motif (corresponding to H203 in *E. coli*) which are considered to be essential for ATP hydrolysis in the ABC ATPases (Hung et al., 1998; Smith et al., 2002; Zaitseva et al., 2005; Hirabayashi et al., 2015).

a.

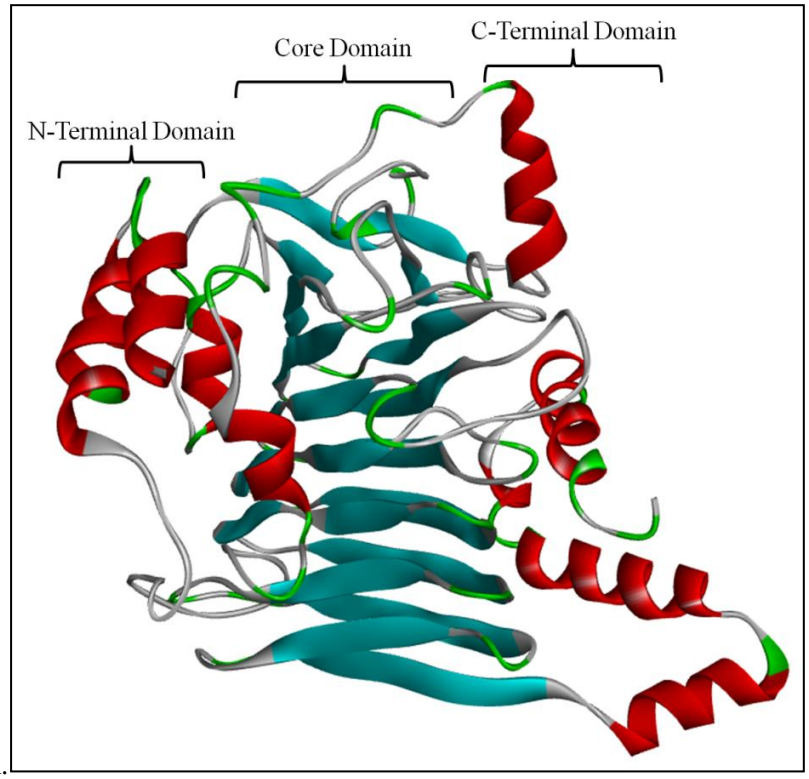

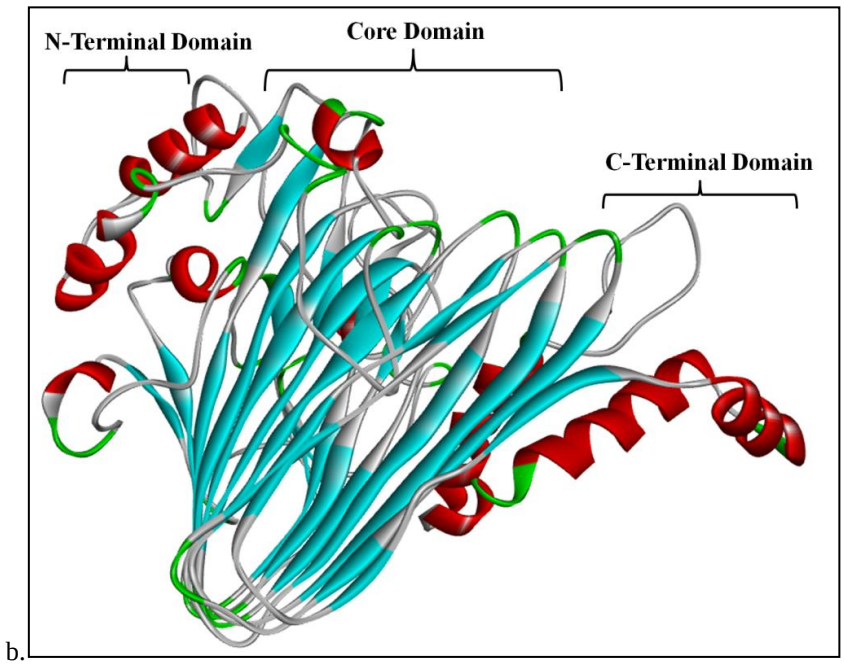

Figure 6.5: a.) *Pv*SufB and b) PvSufD protein structure prediction: The helical regions in red depict the N-terminal and the C-terminal of the protein whereas the blue coloured β-sheets depict the core domain.

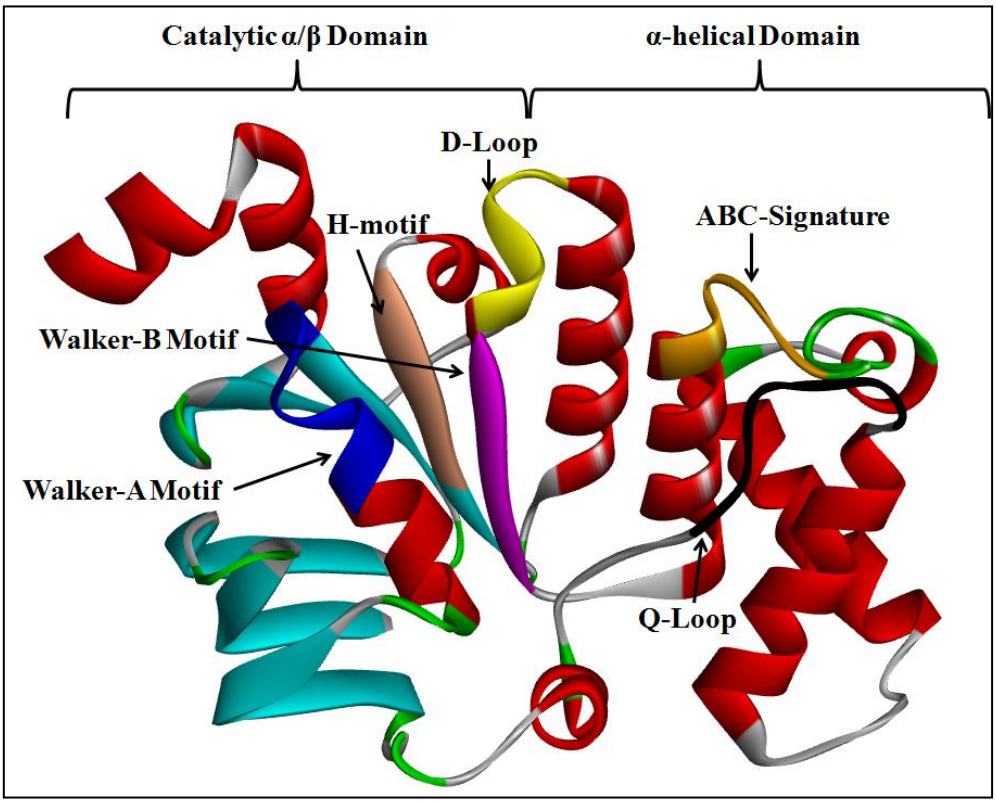

Figure 6.6: *Pv*SufC protein structure prediction: The conserved motifs are depicted in different colours: Walker-A motif (blue), Walker-B motif (Lavender), Q-Loop (Black), ABC-Signature motif (Yellow).

The above generated structures were utilized further for protein-protein docking in order to study the interacting partners of the SUF pathway in *P. vivax*.

To investigate the interactions between *Pv*SufA and *Pv*SufBCD, individual components of the SufBCD complex were docked to the *Pv*SufA structure (**Figure 6.7**). Since the template structure used for *Pv*SufB and *Pv*SufD was same, similar residues were found interacting between *Pv*SufA and *Pv*SufBD. Twelve possible interactions involving both chain A and chain B of dimeric *Pv*SufA were found to be involved in the hydrogen bonds present at the interface (**Table 6.3**). The interaction studies between *Pv*SufA and *Pv*SufC did not result in any significant binding residues. This may suggest that *Pv*SufC is not directly involved in the binding with *Pv*SufA.

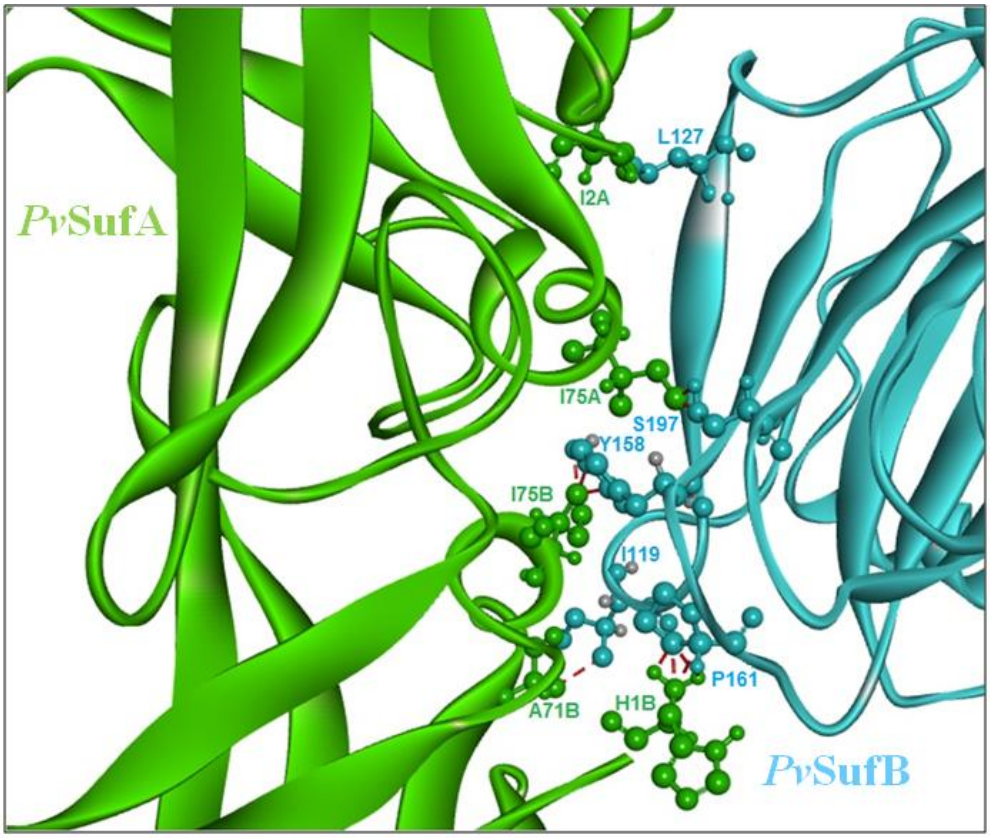

Figure 6.7: Interaction of *Pv*SufA (green) and *Pv*SufB (blue). The hydrogen bonds involved in the interaction are depicted by red lines.

Table 6.3: List of interface residues found to be involved in hydrogen bonding in *P. vivax Pv*SufA and *Pv*SufB.

	*Pv*SufA domain	Distance(Å)	*Pv*SufB domain
Chain A			
1	ILE 2 [CG1]	2.15	LE 127[CD1]
2	ILE 75 [CG2]	1.91	TYR 158 [OH]
3	ILE 75 [CG2]	1.64	TYR 158 [CZ]
4	ILE 75 [CG2]	1.55	TYR 158 [CE1]
Chain B			
5	HIS 1 [HT2]	1.40	PRO 161 [CB]
6	HIS 1 [N]	1.83	PRO 161 [CB]
7	HIS 1 [HT1]	1.75	PRO 161 [CB]
8	HIS 1 [N]	2.25	PRO 161 [CA]
9	HIS 1 [HT1]	1.49	PRO 161 [CA]
10	ALA 71 [CB]	2.52	ILE 119 [CG2]
11	ILE 75 [CD1]	1.26	SER 197 [HG]
12	ILE 75 [CD1]	1.29	SER 197 [OG]

6.2.3 Reconstitution and Transfer of the Fe-S clusters *in vitro*

To confirm the incorporation of liberated sulfur (from SufSE complex) to form Fe-S clusters on *Pv*SufA protein, purified *Pv*SufS and *Pv*SufE along with *Pv*SufA (5µM each) were incubated anaerobically *in vitro* at 25˚C for 3hrs following the protocol as detailed previously (Chapter 5). The reconstituted *P. vivax* SufA with the Fe-S clusters was then concentrated with Amicon Ultra-4 filters of M. W. 10K (Merck, Germany) and the presence of clusters was confirmed by UV-Vis Spectra analysis. The amount of iron and sulfur bound was determined using Ferrozine and Methylene blue colorimetric assays respectively under anaerobic conditions as described earlier.

Anaerobic incubation of purified *Pv*SufA, *Pv*SufS and *Pv*SufE protein with 5-fold molar excess of $Fe(NH_4)_2(SO_4)_2$ and L- cysteine at a final concentration of 1mM along with 100µM PLP for 3hrs in the presence of 5mM dithiothreitol resulted in a brownish coloured solution indicating the presence of Fe-S clusters. The UV–Vis

spectra of the purified mixture of *Pv*SufA, *Pv*SufS and *Pv*SufE showed no significant absorption between 350–450nm while the iron-sulphur cluster loaded mixture of *Pv*SufA, *Pv*SufS and *Pv*SufE showed significant absorption, with maximum visible absorption at 415nm, which is typical for proteins containing Fe-S clusters (**Figure 6.8**). The total iron content of the purified reconstituted *Pv*SufASE was found to be 3.804 µmol (µmol protein)$^{-1}$, and the sulphide content was detected to be 11 µmol (µmol protein)$^{-1}$.

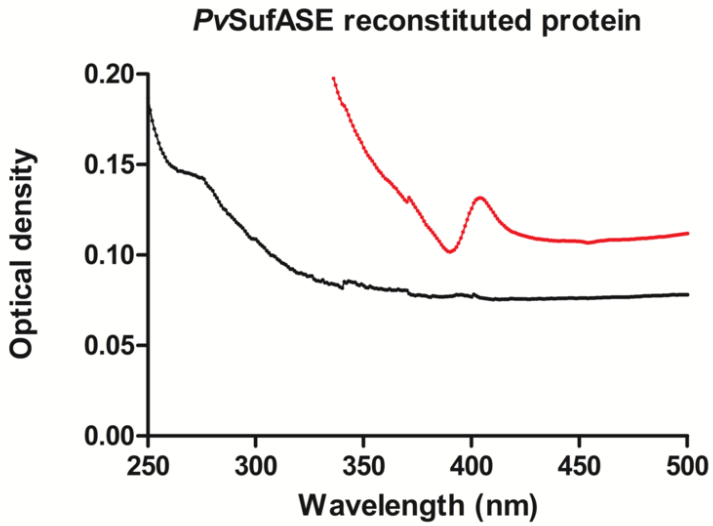

Figure 6.8: Absorption spectra of the purified *Pv*SufASE protein before (black) and after reconstitution (red) of Fe-S clusters. The characteristic peak at ~415nm represents the Fe-S cluster bound protein under anaerobic condition.

To check whether the Fe-S clusters formed on the *Pv*SufA protein can be transferred to any other protein, the Fe-S clusters were reconstituted on *Pv*SufA protein as described above. Once the reconstitution of Fe-S clusters on *Pv*SufA was confirmed, this reconstituted *Pv*SufA was incubated with *Pv*IspG under anaerobic conditions in the presence of 5mM dithiothreitol at 25˚C for 4 hours. This mixture was now purified with Amicon Ultra-4 filters with M.W. 50K (for retaining the *Pv*IspG protein) and the flow through obtained from this was further passed through Amicon Ultra-4 filters with M.W. 10K (to retain the *Pv*SufA protein). Both these fractions were tested for presence of Fe-S clusters and the iron and sulfur bound were again determined as mentioned above.

The reconstituted *Pv*SufA when incubated with apo-*Pv*IspG under anaerobic conditions showed transfer of Fe-S clusters as evident by the UV-Vis spectra analysis. The fraction consisting of *Pv*IspG showed significant absorption between 350 and 450 nm, with maximum visible absorption at 395 nm, typical for IspG proteins containing iron–sulfur clusters. The total iron (**Figure 6.9a**) and sulfur (**Figure 6.9b**) content of the purified reconstituted *Pv*IspG was found to be 5.178 µmol (µmol protein)$^{-1}$ and 8.2 µmol (µmol protein)$^{-1}$ respectively. Also, the remaining holo-*Pv*SufA from this reaction was tested for the presence of Fe-S clusters, where the total iron and sulfide content of the remaining reconstituted *Pv*SufA was reduced to 2.210 µmol (µmol protein)$^{-1}$ & 1.2 µmol (µmol protein)$^{-1}$ respectively as compared to 2.986 µmol(µmol protein)$^{-1}$ & 3 µmol(µmol protein)$^{-1}$ respectively.

a.

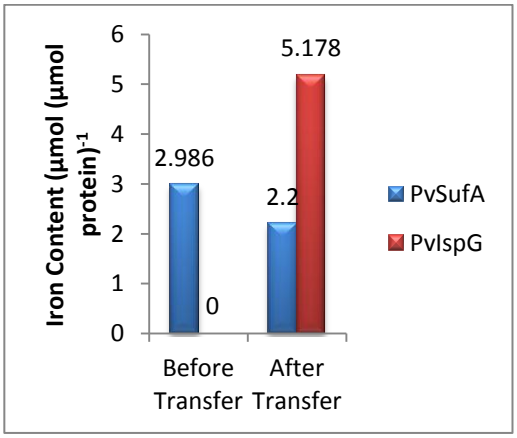

b.

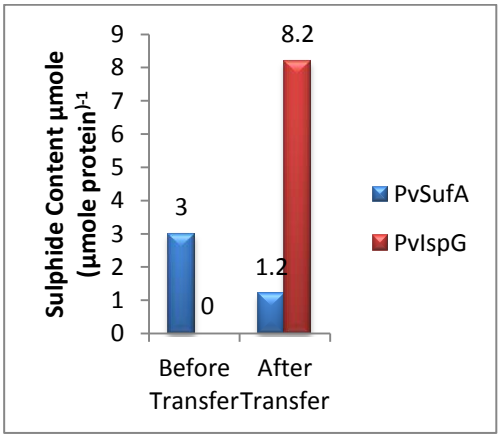

Figure 6.9: Determination of a) iron and b) sulphide content before and after the transfer of Fe-S clusters by *Pv*SufA on *Pv*IspG protein.

The drop in the iron and sulfide content clearly indicates that some amount of Fe-S clusters have been transferred from the scaffold protein *Pv*SufA to the apo-*Pv*IspG protein. Thus, *Pv*SufA seems to act not only as a scaffold protein, but also aids in the transfer of these clusters to the downstream apo-proteins.

6.3 Conclusion

In *P. vivax*, as seen in other apicomplexans and prokaryotes, different components of SUF pathway interact with each other for assembly and transfer of Fe-S clusters. The *Pv*SufS and *Pv*SufE function as a complex where the *in vitro*

cysteine desulphurase activity of *Pv*SufS is enhanced significantly in the presence of *Pv*SufE. This ascertains that the obtained addition and deletion in the field isolates of *Pv*SufS and *Pv*SufE respectively, does not affect the functionality of the proteins. In addition, the *in silico* interaction suggest the closer proximity of Ind*Pv*SufS and Ind*Pv*SufE than compared to Sal-I*Pv*SufS and Sal-I*Pv*SufE which is required for the transpersulfuration reaction between the two proteins, suggesting that the insertion and deletion in the field samples are enhancing the efficiency of interaction between the two proteins. However, the *in vivo* complex formation and functional characterization for *P. vivax* could not be performed due to the difficulty in obtaining a culture for the same.

The *in silico* interaction of *Pv*SufA and *Pv*SufBCD complex indicate that *Pv*SufA might be acting in combination with *Pv*SufBD for the assembly and transfer of [4Fe-4S] clusters to the apo-proteins. As no interaction was seen between *Pv*SufA and *Pv*SufC, thus it is assumed that SufC might be interacting with SufBD only to function as an ATPase in *Plasmodium*.

To elucidate the complete SUF pathway from *P. vivax*, we mobilized the sulfur from *Pv*SufSE complex and along with external iron, successfully constituted the Fe-S clusters on *Pv*SufA, which were transferred to an apo-protein IspG under anaerobic conditions. This affirms the hypothesis that *Pv*SufA may act as a scaffold protein in addition to an A-type carrier protein. Earlier reports in *P. falciparum* have highlighted the accessory role of SufBCD complex in assembly and transfer of Fe-S clusters, however, the exact role of this complex and its interaction with other components of the pathway is yet to be tested experimentally in *Plasmodium*. In *E. coli*, it has been suggested that SufB enhances the activity of SufSE complex many folds *in vivo*, which indicates that SufB might be involved *in vivo* to increase the efficiency of sulphur mobilization for Fe-S cluster formation. This study thus, lays a foundation for such future experimental validation *in vivo* from other *Plasmodium spp*.

Chapter VII

Conclusions and Future Prospects

CONCLUSIONS AND FUTURE PROSPECTS

7.1 Specific Conclusions

1. The genes encoding for the SUF pathway in *Plasmodium vivax* were shortlisted from the PlasmoDB database based on their conserved domains and signature motifs. Based on different sequence alignments and functional domain analysis, iron sulphur cluster assembly accessory protein (PVX_080115) was designated as *Pv*SufA, hypothetical protein (PVX_003740) as *Pv*SufE, and cysteine desulphurase, putative (PVX_000600) as *Pv*SufS.

2. Targeting prediction using online servers like PlasmoAP, PlasMit, PATS, MitoProt suggested dual targeting for *Pv*SufA to mitochondria and apicoplast, apicoplast targeting for *Pv*SufE and ambiguous targeting for *Pv*SufS. Immunolocalization studies performed on *P. vivax* infected blood smears from patients for all these proteins using antibodies raised against recombinant protein suggested their apicoplast localization. This suggests that the online targeting prediction servers need to be standardized more with the *P. vivax* database, as currently they are based on the sequences of *P. falciparum* only.

3. The cysteine desulphurase *Pv*SufS and its partner protein *Pv*SufE were expressed as His-tagged recombinant proteins. The activity of *Pv*SufS increased to ~5 folds in the presence of *Pv*SufE, even after the presence of a deletion in *Pv*SufE near the active site of the protein. When the structure of Ind*Pv*SufS and Sal-I *Pv*SufS were analysed for PLP binding, only three residues were involved in the interaction of PLP cofactor in Sal-I *Pv*SufS compared to five in Ind*Pv*SufS. The protein-protein docking studies between Sal-I *Pv*SufS and *Pv*SufE also revealed a distance of 8.2Å, which is far when compared with the Ind*Pv*SufS and Ind*Pv*SufE. Thus the close association of the two cysteines (~2Å) in *Pv*SufS and *Pv*SufE in *in silico* studies suggests their close interaction for sulphur transfer.

4. The *Plasmodium* SufB lacks the CXXCXXXC motif required for it to function as a scaffold protein, thus suggesting the presence of an alternative scaffold protein for

the assembly of Fe-S clusters. *Pv*SufA showed the presence of three conserved cysteine residues as $X_{55}CX_{185}CGCX_{189}$ comparable to the *E. coli* counterpart of the same protein. *In silico* docking studies of *Pv*SufA and [4Fe-4S] cluster revealed the involvement of these three conserved cysteine residues and $Lys_{160,}$ further validating the formation of Fe-S clusters on this protein.

5. Recombinant *Pv*SufA was observed to form Fe-S clusters *in vitro* under anaerobic conditions proving the function of *Pv*SufA protein as a scaffold protein to assemble the Fe-S clusters in *P. vivax*. These clusters were shown to have iron in +3 oxidation state thus showing the formation of [4Fe-4S] clusters.

6. *In silico* docking studies of *Pv*SufA with the *Pv*SufBCD complex showed 12 possible interactions between *Pv*SufA and *Pv*SufBD, but no interaction with *Pv*SufC. Thus, *Pv*SufA is acting in combination with *Pv*SufBD for the assembly and transfer of [4Fe-4S] clusters to the apo-proteins. As no interaction was evident between *Pv*SufA and *Pv*SufC, thus SufC might be interacting with SufBD only to function as an ATPase in *Plasmodium*.

7. *In vitro* biochemical assays further indicated the incorporation of sulphur mobilized by *Pv*SufSE complex in the Fe-S clusters assembled on *Pv*SufA and their transfer from *Pv*SufA onto an apo-protein *Pv*IspG. This further validates our hypothesis that *Pv*SufA acts as both a scaffold and an A-type carrier protein.

8. With the elucidation of the complete pathway, the concern is to find an inhibitor for its components to inhibit the parasite growth. Thus the potential of D-cycloserine, an inhibitor for the enzymes of the aminotransferase family, was explored by *in silico* docking studies. Eleven residues in the binding pocket of Ind*Pv*SufS interacted with D-cycloserine, of which two of the residues are also involved in the interaction of PLP cofactor. This suggests that D-cycloserine may act as a competitive inhibitor for cysteine desulphurase SufS in *P. vivax* similar to as observed in *P. falciparum*.

Hypothesized SUF pathway (Figure 7.1) for Fe-S cluster assembly in *Plasmodium vivax*

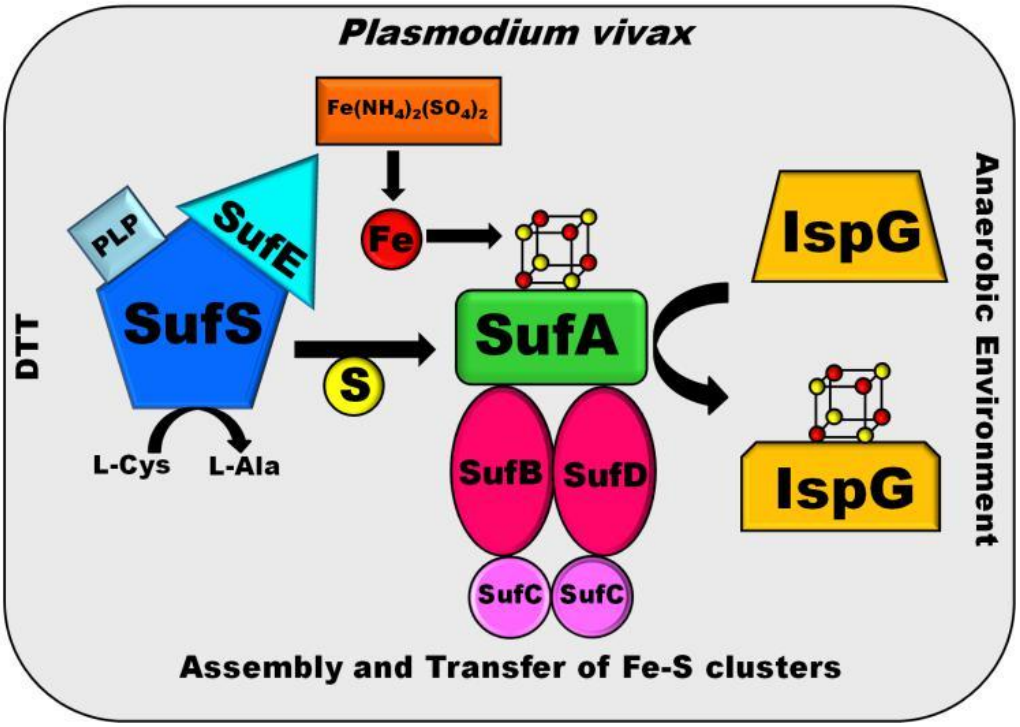

7.2 Direction for future research (future perspectives)

- The present study details the structural and functional characterization of three major enzymes SufS, SufE and SufA involved in the SUF pathway for Fe-S cluster biogenesis in *Plasmodium*. This study is the first report of characterization of any component involved in this pathway and hence, can open new doors for designing new inhibitors for this pathway to target *P. vivax* malaria parasite.

- In prokaryotes, the SUF system is said to be functional under oxidative stress or iron starvation conditions. Since there is no study available till date for any of the *Plasmodium* species under any of these stress conditions, a future study under the influence of different stress conditions can be conducted.

- The source of iron in the formation of the Fe-S clusters is yet unknown in *Plasmodium* and is yet to be explored.

- The other components of the *P. vivax* SUF pathway majorly, SufBCD complex, has to be characterized experimentally.

- An *in silico* analysis of the interaction of SufBCD complex with SufA has been shown in this study, however further experimental validation will be required.

REFERENCES

1. "Life cycle of the malaria parasite" from Epidemiology of Infectious Diseases. Available at: http://ocw.jhsph.edu. Copyright © Johns Hopkins Bloomberg School of Public Health. Creative Commons BY-NC-SA.
2. Adinolfi, S., Iannuzzi, C., Prischi, F., Pastore, C., Iametti, S., Martin, S. R., ... & Pastore, A. (2009). Bacterial frataxin CyaY is the gatekeeper of iron-sulfur cluster formation catalyzed by IscS. *Nature Structural & Molecular Biology*, *16*(4), 390-396.
3. Agar, J. N., Krebs, C., Frazzon, J., Huynh, B. H., Dean, D. R., & Johnson, M. K. (2000). IscU as a scaffold for iron− sulfur cluster biosynthesis: sequential assembly of [2Fe-2S] and [4Fe-4S] clusters in IscU. *Biochemistry*, *39*(27), 7856-7862.
4. Albrecht, A. G., Netz, D. J., Miethke, M., Pierik, A. J., Burghaus, O., Peuckert, F., ... & Marahiel, M. A. (2010). SufU is an essential iron-sulfur cluster scaffold protein in *Bacillus subtilis*. *Journal of Bacteriology*, *192*(6), 1643-1651.
5. Angelini, S., Gerez, C., Ollagnier-de Choudens, S., Sanakis, Y., Fontecave, M., Barras, F., & Py, B. (2008). NfuA, a new factor required for maturing Fe/S proteins in *Escherichia coli* under oxidative stress and iron starvation conditions. *Journal of Biological Chemistry*, *283*(20), 14084-14091.
6. Arisue, N., Hashimoto, T., Mitsui, H., Palacpac, N. M., Kaneko, A., Kawai, S., ... & Horii, T. (2012). The *Plasmodium* apicoplast genome: conserved structure and close relationship of *P. ovale* to rodent malaria parasites. *Molecular Biology and Evolution*, *29*(9), 2095-2099.
7. Aurrecoechea, C., Brestelli, J., Brunk, B. P., Dommer, J., Fischer, S., Gajria, B., ... & Heiges, M. (2009). PlasmoDB: a functional genomic database for malaria parasites. *Nucleic Acids Research*, *37*(suppl 1), D539-D543.
8. Ayala-Castro, C., Saini, A., & Outten, F. W. (2008). Fe-S cluster assembly pathways in bacteria. *Microbiology and Molecular Biology Reviews*, *72*(1), 110-125.

9. Babcock, M., De Silva, D., Oaks, R., Davis-Kaplan, S., Jiralerspong, S., Montermini, L., ... & Kaplan, J. (1997). Regulation of mitochondrial iron accumulation by Yfh1p, a putative homolog of frataxin. *Science*, *276*(5319), 1709-1712.
10. Badger, J., Sauder, J. M., Adams, J. M., Antonysamy, S., Bain, K., Bergseid, M. G., ... & Emtage, S. (2005). Structural analysis of a set of proteins resulting from a bacterial genomics project. *Proteins: Structure, Function, and Bioinformatics*, *60*(4), 787-796.
11. Balk, J., Netz, D. J. A., Tepper, K., Pierik, A. J., & Lill, R. (2005). The essential WD40 protein Cia1 is involved in a late step of cytosolic and nuclear iron-sulfur protein assembly. *Molecular and Cellular Biology*, *25*(24), 10833-10841.
12. Balk, J., Pierik, A. J., Netz, D. J. A., Mühlenhoff, U., & Lill, R. (2004). The hydrogenase-like Nar1p is essential for maturation of cytosolic and nuclear iron–sulphur proteins. *The EMBO Journal*, *23*(10), 2105-2115.
13. Bannister, L. H., Hopkins, J. M., Fowler, R. E., Krishna, S., & Mitchell, G. H. (2000). A brief illustrated guide to the ultrastructure of *Plasmodium falciparum* asexual blood stages. *Parasitology Today*, *16*(10), 427-433.
14. Barras, F., Loiseau, L., & Py, B. (2005). How *Escherichia coli* and *Saccharomyces cerevisiae* build Fe/S proteins. *Advances in Microbial Physiology*, *50*, 41-101.
15. Begley, T. P., Xi, J., Kinsland, C., Taylor, S., & McLafferty, F. (1999). The enzymology of sulfur activation during thiamin and biotin biosynthesis. *Current opinion in chemical biology*, *3*(5), 623-629.
16. Behshad, E., & Bollinger Jr, J. M. (2009). Kinetic analysis of cysteine desulfurase CD0387 from *Synechocystis sp.* PCC 6803: formation of the persulfide intermediate. *Biochemistry*, *48*(50), 12014-12023.
17. Behshad, E., Parkin, S. E., & Bollinger, J. M. (2004). Mechanism of cysteine desulfurase Slr0387 from *Synechocystis sp.* PCC 6803: kinetic analysis of cleavage of the persulfide intermediate by chemical reductants. *Biochemistry*, *43*(38), 12220-12226.
18. Beinert, H., & Kiley, P. J. (1999). Fe-S proteins in sensing and regulatory functions. *Current Opinion in Chemical Biology*, *3*(2), 152-157.

19. Beinert, H., Holm, R. H., & Münck, E. (1997). Iron-sulfur clusters: nature's modular, multipurpose structures. *Science*, *277*(5326), 653-659.
20. Bender, A., van Dooren, G. G., Ralph, S. A., McFadden, G. I., & Schneider, G. (2003). Properties and prediction of mitochondrial transit peptides from *Plasmodium falciparum*. *Molecular and Biochemical Parasitology*, *132*(2), 59-66.
21. Berkner, L. V., & Marshall, L. C. (1965). On the origin and rise of oxygen concentration in the Earth's atmosphere. *Journal of the Atmospheric Sciences*, *22*(3), 225-261.
22. Biederbick, A., Stehling, O., Rösser, R., Niggemeyer, B., Nakai, Y., Elsässer, H. P., & Lill, R. (2006). Role of human mitochondrial Nfs1 in cytosolic iron-sulfur protein biogenesis and iron regulation. *Molecular and Cellular Biology*, *26*(15), 5675-5687.
23. Bimboim, H. C., & Doly, J. (1979). A rapid alkaline extraction procedure for screening recombinant plasmid DNA. *Nucleic Acids Research*, *7*(6), 1513-1523.
24. Blauenburg, B., Mielcarek, A., Altegoer, F., Fage, C. D., Linne, U., Bange, G., & Marahiel, M. A. (2016). Crystal structure of *Bacillus subtilis* cysteine desulfurase SufS and its dynamic interaction with frataxin and scaffold protein SufU. *PLoS One*, *11*(7), e0158749.
25. Botté, C. Y., Dubar, F., McFadden, G. I., Maréchal, E., & Biot, C. (2011). *Plasmodium falciparum* apicoplast drugs: targets or off-targets?. *Chemical Reviews*, *112*(3), 1269-1283.
26. Boyd, E. S., Thomas, K. M., Dai, Y., Boyd, J. M., & Outten, F. W. (2014). The interplay between oxygen and Fe-S cluster biogenesis: Insights from the Suf pathway. *Biochemistry*, *53*(37), 5834-5847.
27. Bradford, M. M. (1976). A rapid and sensitive method for the quantitation of microgram quantities of protein utilizing the principle of protein-dye binding. *Analytical Biochemistry*, 72(1-2), 248-254.
28. Buchan, D. W., Minneci, F., Nugent, T. C., Bryson, K., & Jones, D. T. (2013). Scalable web services for the PSIPRED Protein Analysis Workbench. *Nucleic acids research*, *41*(W1), W349-W357.

29. Burgess, B. K., & Lowe, D. J. (1996). Mechanism of molybdenum nitrogenase. *Chemical Reviews*, *96*(7), 2983-3012.
30. Busi, M. V., & Gomez-Casati, D. F. (2012). Exploring frataxin function. *IUBMB life*, *64*(1), 56-63.
31. Carlton, J. M., Adams, J. H., Silva, J. C., Bidwell, S. L., Lorenzi, H., Caler, E., ... & Cheng, Q. (2008). Comparative genomics of the neglected human malaria parasite *Plasmodium vivax*. *Nature*, *455*(7214), 757-763.
32. Carter R, Graves PM (1988). Gametocytes. In Malaria Principles and Practice of Malariology. (ed . W. H. Wernsdorfer & I. McGregor), pp. 253-305. Edinburgh. Churchill Livingstone.
33. CDC 'Malria', http://www.cdc.gov/malaria/about/disease/html.
34. Chahal, H. K., & Outten, F. W. (2012). Separate Fe S scaffold and carrier functions for $SufB_2C_2$ and SufA during in vitro maturation of [2Fe 2S] Fdx. *Journal of Inorganic Biochemistry*, *116*, 126-134.
35. Chahal, H. K., Dai, Y., Saini, A., Ayala-Castro, C., & Outten, F. W. (2009). The SufBCD Fe−S scaffold complex interacts with SufA for Fe−S cluster transfer. *Biochemistry*, *48*(44), 10644-10653.
36. Chan, M. K., Kim, J., & Rees, D. C. (1993). The nitogenase FeMo-cofactor and P-cluster pair 2.2 A Resolution Structures. *Science*, *260*, 7.
37. Chandramouli, K., Unciuleac, M. C., Naik, S., Dean, D. R., Huynh, B. H., & Johnson, M. K. (2007). Formation and properties of [4Fe-4S] clusters on the IscU scaffold protein. *Biochemistry*, *46*(23), 6804-6811.
38. Charan, M., & Habib, S. (2013). Biosynthesis of Fe-S proteins and their roles. *Encyclopedia of malaria. SpringerReference, New York, NY*.
39. Charan, M., Singh, N., Kumar, B., Srivastava, K., Siddiqi, M. I., & Habib, S. (2014). Sulfur mobilization for Fe-S cluster assembly by the essential SUF pathway in the *Plasmodium falciparum* apicoplast and its inhibition. *Antimicrobial Agents and Chemotherapy*, *58*(6), 3389-3398.
40. Chen, O. S., Hemenway, S., & Kaplan, J. (2002). Inhibition of Fe-S cluster biosynthesis decreases mitochondrial iron export: evidence that Yfh1p affects Fe-S cluster synthesis. *Proceedings of the National Academy of Sciences*, *99*(19), 12321-12326.

41. Claros, M. G., & Vincens, P. (1996). Computational method to predict mitochondrially imported proteins and their targeting sequences. *European Journal of Biochemistry*, *241*(3), 779-786.
42. Clausen, T., Kaiser, J. T., Steegborn, C., Huber, R., & Kessler, D. (2000). Crystal structure of the cystine CS lyase from *Synechocystis*: stabilization of cysteine persulfide for FeS cluster biosynthesis. *Proceedings of the National Academy of Sciences*, *97*(8), 3856-3861.
43. Colovos, C., & Yeates, T. O. (1993). Verification of protein structures: patterns of nonbonded atomic interactions. *Protein Science*, *2*(9), 1511-1519.
44. COMBRINCK, J. M., Joanne, E. G. A. N., HEARNE, G. R., MARQUES, H. M., NTENTENI, S., SEWELL, B. T., ... & WALDEN, J. C. (2002). Fate of haem iron in the malaria parasite *Plasmodium falciparum*. *Biochemical Journal*, *365*(2), 343-347.
45. Corliss, J. O. (1994). An interim utilitarian ("user-friendly") hierarchical classification and characterization of the protists. *Acta Protozoologica*, *33*, 1-1.
46. Cupp-Vickery, J. R., Peterson, J. C., Ta, D. T., & Vickery, L. E. (2004). Crystal structure of the molecular chaperone HscA substrate binding domain complexed with the IscU recognition peptide ELPPVKIHC. *Journal of Molecular Biology*, *342*(4), 1265-1278.
47. Cupp-Vickery, J. R., Urbina, H., & Vickery, L. E. (2003). Crystal structure of IscS, a cysteine desulfurase from *Escherichia coli*. *Journal of molecular biology*, *330*(5), 1049-1059.
48. Das, A., Holloway, B., Collins, W. E., Shama, V., Ghosh, S. K., Sinha, S., Hasnain, S. E., Talwar, G. P., and Lal, A. A. (1995). Species-specific 18S rRNA gene amplification for the detection of *P. falciparum* and *P. vivax* malaria parasites. *Mol Cell Probe* 9, 161-165.
49. Dean, D. R., Bolin, J. T., & Zheng, L. I. M. I. N. (1993). Nitrogenase metalloclusters: structures, organization, and synthesis. *Journal of Bacteriology*, *175*(21), 6737.
50. Desnoyers, G., Morissette, A., Prévost, K., & Massé, E. (2009). Small RNA-induced differential degradation of the polycistronic mRNA iscRSUA. *The EMBO Journal*, *28*(11), 1551-1561.

51. Djaman, O., Outten, F. W., & Imlay, J. A. (2004). Repair of oxidized iron-sulfur clusters in *Escherichia coli*. *Journal of Biological Chemistry*, *279*(43), 44590-44599.
52. Doolan, D. L., Dobaño, C., & Baird, J. K. (2009). Acquired immunity to malaria. *Clinical Microbiology Reviews*, *22*(1), 13-36.
53. Duby, G., Foury, F., Ramazzotti, A., Herrmann, J., & Lutz, T. (2002). A non-essential function for yeast frataxin in iron–sulfur cluster assembly. *Human Molecular Genetics*, *11*(21), 2635-2643.
54. Eccleston, J. F., Petrovic, A., Davis, C. T., Rangachari, K., & Wilson, R. I. (2006). The kinetic mechanism of the SufC ATPase the cleavage step is accelerated by SufB. *Journal of Biological Chemistry*, *281*(13), 8371-8378.
55. Eichner, M., Diebner, H. H., Molineaux, L., Collins, W. E., Jeffery, G. M., & Dietz, K. (2001). Genesis, sequestration and survival of *Plasmodium falciparum* gametocytes: parameter estimates from fitting a model to malariatherapy data. *Transactions of the Royal Society of Tropical Medicine and Hygiene*, *95*(5), 497-501.
56. Eisenberg, D., Lüthy, R., & Bowie, J. U. (1997). VERIFY3D: Assessment of protein models with three-dimensional profiles. *Methods in Enzymology*, *277*, 396-404.
57. Ellis, K. E. S., Clough, B., Saldanha, J. W., & Wilson, R. J. M. (2001). Nifs and Sufs in malaria. *Molecular Microbiology*, *41*(5), 973-981.
58. Escalante, A. A., Cornejo, O. E., Freeland, D. E., Poe, A. C., Durrego, E., Collins, W. E., and Lal, A. A. (2005). A monkey's tale: the origin of *Plasmodium vivax* as a human malaria parasite. *PNAS* 102, 1980-1985.
59. Eswar N., Webb B., Marti-Renom, M.A., Madhusudhan, M., Eramian, D., Shen, M.Y., Pieper, U., Sali, A. Comparative protein structure modeling using Modeller. *Current Protocols in Bioinformatics.* 2006;5(6) 1-30.
60. Felsenstein, J. (1985). Confidence limits on phylogenies: an approach using the bootstrap. *Evolution*, 783-791.
61. Fish, W. (1988). Rapid colorimetric micromethod for the quantitation of complexed iron in biological samples. *Methods in Enzymology*, 158, 357-364.

62. Foth, B. J., Ralph, S. A., Tonkin, C. J., Struck, N. S., Fraunholz, M., Roos, D. S., ... & McFadden, G. I. (2003). Dissecting apicoplast targeting in the malaria parasite *Plasmodium falciparum*. *Science*, *299*(5607), 705-708.
63. Foury, F., & Cazzalini, O. (1997). Deletion of the yeast homologue of the human gene associated with Friedreich's ataxia elicits iron accumulation in mitochondria. *FEBS Letters*, *411*(2-3), 373-377.
64. Frazzon, J., & Dean, D. R. (2003). Formation of iron–sulfur clusters in bacteria: an emerging field in bioinorganic chemistry. *Current Opinion in Chemical Biology*, *7*(2), 166-173.
65. Frazzon, J., Fick, J. R., & Dean, D. R. (2002). Biosynthesis of iron-sulphur clusters is a complex and highly conserved process. *Biochemical Society Transactions*, 30(4), 680-685.
66. Fu, W., Jack, R. F., Morgan, T. V., Dean, D. R., & Johnson, M. K. (1994). nifU gene product from *Azotobacter vinelandii* is a homodimer that contains two identical [2Fe-2S] clusters. *Biochemistry*, *33*(45), 13455-13463.
67. Fujii, T., Maeda, M., Mihara, H., Kurihara, T., Esaki, N., & Hata, Y. (2000). Structure of a NifS Homologue: X-ray Structure Analysis of CsdB, an *Escherichia coli* Counterpart of Mammalian Selenocysteine Lyase†. *Biochemistry*, *39*(6), 1263-1273.
68. Gardner, M. J., Hall, N., Fung, E., White, O., Berriman, M., Hyman, R. W., ... & Paulsen, I. T. (2002). Genome sequence of the human malaria parasite *Plasmodium falciparum*. *Nature*, *419*(6906).
69. Gardner, M. J., Williamson, D. H., & Wilson, R. J. (1991). A circular DNA in malaria parasites encodes an RNA polymerase like that of prokaryotes and chloroplasts. *Molecular and Biochemical Parasitology*, *44*(1), 115-123.
70. Giel, J. L., Rodionov, D., Liu, M., Blattner, F. R., & Kiley, P. J. (2006). IscR-dependent gene expression links iron-sulphur cluster assembly to the control of O2-regulated genes in *Escherichia coli*. *Molecular Microbiology*, *60*(4), 1058-1075.
71. Gisselberg, J. E., Dellibovi-Ragheb, T. A., Matthews, K. A., Bosch, G., & Prigge, S. T. (2013). The suf iron-sulfur cluster synthesis pathway is required for apicoplast maintenance in malaria parasites. *PLoS Pathog*, *9*(9), e1003655.

72. Greenwood, B. M., Fidock, D. A., Kyle, D. E., Kappe, S. H., Alonso, P. L., Collins, F. H., & Duffy, P. E. (2008). Malaria: progress, perils, and prospects for eradication. *The Journal of Clinical Investigation*, *118*(4), 1266-1276.
73. Grishin, N. V., Phillips, M. A., & Goldsmith, E. J. (1995). Modeling of the spatial structure of eukaryotic ornithine decarboxylases. *Protein Science*, *4*(7), 1291-1304.
74. Hall, T. A. (1999). BioEdit: a user-friendly biological sequence alignment editor and analysis program for Windows 95/98/NT. *Nucleic Acids Symposium Series* 41, 95-98.
75. Harlow, E., and Lane, D. (1988). Antibodies - A Laboratry Manual, Cold Spring Harbor Laboratory Press, NY, USA.
76. Hausmann, A., Netz, D. J. A., Balk, J., Pierik, A. J., Mühlenhoff, U., & Lill, R. (2005). The eukaryotic P loop NTPase Nbp35: an essential component of the cytosolic and nuclear iron–sulfur protein assembly machinery. *Proceedings of the National Academy of Sciences of the United States of America*, *102*(9), 3266-3271.
77. Haussig, J. M., Matuschewski, K., & Kooij, T. W. (2013). Experimental genetics of Plasmodium berghei NFU in the apicoplast iron-sulfur cluster biogenesis pathway. *PloS one*, *8*(6), e67269.
78. Haussig, J. M., Matuschewski, K., & Kooij, T. W. (2014). Identification of vital and dispensable sulfur utilization factors in the *Plasmodium* apicoplast. *PloS One*, *9*(2), e89718.
79. Hidese, R., Mihara, H., & Esaki, N. (2011). Bacterial cysteine desulfurases: versatile key players in biosynthetic pathways of sulfur-containing biofactors. *Applied microbiology and biotechnology*, *91*(1), 47-61.
80. Hoff, K. G., Silberg, J. J., & Vickery, L. E. (2000). Interaction of the iron–sulfur cluster assembly protein IscU with the Hsc66/Hsc20 molecular chaperone system of *Escherichia coli*. *Proceedings of the National Academy of Sciences*, *97*(14), 7790-7795.
81. Hopkins, J., Fowler, R., Krishna, S., Wilson, I., Mitchell, G., & Bannister, L. (1999). The plastid in *Plasmodium falciparum* asexual blood stages: a three-dimensional ultrastructural analysis. *Protist*, *150*(3), 283-295.

82. Howe, R., Kelly, M., Jimah, J., Hodge, D., & Odom, A. R. (2013). Isoprenoid biosynthesis inhibition disrupts Rab5 localization and food vacuolar integrity in *Plasmodium falciparum*. *Eukaryotic Cell*, *12*(2), 215-223.
83. Howes, R. E., Battle, K. E., Mendis, K. N., Smith, D. L., Cibulskis, R. E., Baird, J. K., & Hay, S. I. (2016). Global epidemiology of *Plasmodium vivax*. *The American Journal of Tropical Medicine and Hygiene*, *95*(6 Suppl), 15-34.
84. Hu, Y., & Ribbe, M. W. (2014). A journey into the active centre of nitrogenase. *JBIC Journal of Biological Inorganic Chemistry*, *19*(6), 731-736.
85. Huangen, D. I. N. G., & Clark, R. J. (2004). Characterization of iron binding in IscA, an ancient iron-sulphur cluster assembly protein. *Biochemical Journal*, *379*(2), 433-440.
86. Huynen, M. A., Snel, B., Bork, P., & Gibson, T. J. (2001). The phylogenetic distribution of frataxin indicates a role in iron-sulfur cluster protein assembly. *Human Molecular Genetics*, *10*(21), 2463-2468.
87. Hwang, D. M., Dempsey, A., Tan, K. T., & Liew, C. C. (1996). A modular domain of NifU, a nitrogen fixation cluster protein, is highly conserved in evolution. *Journal of Molecular Evolution*, *43*(5), 536-540.
88. Imlay, J. A. (2006). Iron-sulphur clusters and the problem with oxygen. *Molecular Microbiology*, *59*(4), 1073-1082.
89. Jacobson, M. R., Cash, V. L., Weiss, M. C., Laird, N. F., Newton, W. E., & Dean, D. R. (1989). Biochemical and genetic analysis of the nifUSVWZM cluster from *Azotobacter vinelandii*. *Molecular and General Genetics MGG*, *219*(1-2), 49-57.
90. Jelenska, J., Crawford, M. J., Harb, O. S., Zuther, E., Haselkorn, R., Roos, D. S., & Gornicki, P. (2001). Subcellular localization of acetyl-CoA carboxylase in the apicomplexan parasite *Toxoplasma gondii*. *Proceedings of the National Academy of Sciences*, *98*(5),2723-2728.
91. Johnson, D. C., Dean, D. R., Smith, A. D., & Johnson, M. K. (2005). Structure, function, and formation of biological iron-sulfur clusters. *Annual Reviews of Biochemistry*, *74*, 247-281.

92. Jomaa, H., Wiesner, J., Sanderbrand, S., Altincicek, B., Weidemeyer, C., Hintz, M., ... & Soldati, D. (1999). Inhibitors of the nonmevalonate pathway of isoprenoid biosynthesis as antimalarial drugs. *Science*, *285*(5433), 1573-1576.
93. Jones, D. T., Taylor, W. R., & Thornton, J. M. (1992). The rapid generation of mutation data matrices from protein sequences. *Computer Applications in the Biosciences: CABIOS*, *8*(3), 275-282.
94. Jones, M. K., & Good, M. F. (2006). Malaria parasites up close. *Nature Medicine*, *12*(2), 170-172.
95. Kalanon, M., & McFadden, G. I. (2010). Malaria, *Plasmodium falciparum* and its apicoplast. *Biochemical Society Transactions*, *38*(part 3), 775-782.
96. Kambampati, R., & Lauhon, C. T. (2003). MnmA and IscS are required for in vitro 2-thiouridine biosynthesis in *Escherichia coli*. *Biochemistry*, *42*(4), 1109-1117.
97. Kearse, M., Moir, R., Wilson, A., Stones-Havas, S., Cheung, M., Sturrock, S., ... & Thierer, T. (2012). Geneious Basic: an integrated and extendable desktop software platform for the organization and analysis of sequence data. *Bioinformatics*, *28*(12), 1647-1649.
98. Kiley, P. J., & Beinert, H. (2003). The role of Fe–S proteins in sensing and regulation in bacteria. *Current Opinion in Microbiology*, *6*(2), 181-185.
99. Kispal, G., Sipos, K., Lange, H., Fekete, Z., Bedekovics, T., Janáky, T., ... & Lill, R. (2005). Biogenesis of cytosolic ribosomes requires the essential iron–sulphur protein Rli1p and mitochondria. *The EMBO Journal*, *24*(3), 589-598.
100. Kitaoka, S., Wada, K., Hasegawa, Y., Minami, Y., Fukuyama, K., & Takahashi, Y. (2006). Crystal structure of *Escherichia coli* SufC, an ABC-type ATPase component of the SUF iron–sulfur cluster assembly machinery. *FEBS Letters*, *580*(1), 137-143.
101. Kochar, D. K., Saxena, V., Singh, N., Kochar, S. K., Kumar, S. V., & Das, A. (2005). *Plasmodium vivax* malaria. *Emerg Infect Dis*, *11*(1), 132-4.
102. Koenderink, J. B., Kavishe, R. A., Rijpma, S. R., & Russel, F. G. (2010). The ABCs of multidrug resistance in malaria. *Trends in Parasitology*, *26*(9), 440-446.

103. Köhler, S., Delwiche, C. F., Denny, P. W., Tilney, L. G., Webster, P., Wilson, R. J. M., ... & Roos, D. S. (1997). A plastid of probable green algal origin in Apicomplexan parasites. *Science*, *275*(5305), 1485-1489.

104. Kořený, L., Oborník, M., & Lukeš, J. (2013). Make it, take it, or leave it: heme metabolism of parasites. *PLoS Pathogens*, *9*(1), e1003088.

105. Kornhaber, G. J., Snyder, D., Moseley, H. N., & Montelione, G. T. (2006). Identification of zinc-ligated cysteine residues based on 13Cα and 13Cβ chemical shift data. *Journal of Biomolecular NMR*, *34*(4), 259-269.

106. Krebs, C., Agar, J. N., Smith, A. D., Frazzon, J., Dean, D. R., Huynh, B. H., & Johnson, M. K. (2001). IscA, an alternate scaffold for Fe− S cluster biosynthesis. *Biochemistry*, *40*(46), 14069-14080.

107. Krieger, E., Joo, K., Lee, J., Lee, J., Raman, S., Thompson, J., ... & Karplus, K. (2009). Improving physical realism, stereochemistry, and side-chain accuracy in homology modeling: four approaches that performed well in CASP8. *Proteins: Structure, Function, and Bioinformatics*, *77*(S9), 114-122.

108. Kumar, B., Chaubey, S., Shah, P., Tanveer, A., Charan, M., Siddiqi, M. I., & Habib, S. (2011). Interaction between sulphur mobilisation proteins SufB and SufC: Evidence for an iron–sulphur cluster biogenesis pathway in the apicoplast of *Plasmodium falciparum*. *International Journal for Parasitology*, *41*(9), 991-999.

109. Kurien, B. T., & Scofield, R. H. (2012). Extraction of proteins from gels: a brief review. *Protein Electrophoresis: Methods and Protocols*, 403-405.

110. Lambeth, J. D., Kawahara, T., & Diebold, B. (2007). Regulation of Nox and Duox enzymatic activity and expression. *Free Radical Biology and Medicine*, *43*(3), 319-331.

111. Larkin, M. A., Blackshields, G., Brown, N., Chenna, R., McGettigan, P. A., McWilliam, H., Valentin, F., Wallace, I. M., Wilm, A., and Lopez, R. (2007). Clustal W and Clustal X version 2.0. *Bioinformatics* 23, 2947-2948.

112. Laskowski, R. A., MacArthur, M. W., Moss, D. S., & Thornton, J. M. (1993). PROCHECK: a program to check the stereochemical quality of protein structures. *Journal of Applied Crystallography*, *26*(2), 283-291.

113. Lauhon, C. T., & Kambampati, R. (2000). The iscS gene in *Escherichia coli* is required for the biosynthesis of 4-thiouridine, thiamin, and NAD. *Journal of Biological Chemistry*, *275*(26), 20096-20103.

114. Lauhon, C. T., Erwin, W. M., & Ton, G. N. (2004). Substrate specificity for 4-thiouridine modification in *Escherichia coli*. *Journal of Biological Chemistry*, *279*(22), 23022-23029.

115. Layer, G., Gaddam, S. A., Ayala-Castro, C. N., Ollagnier-de Choudens, S., Lascoux, D., Fontecave, M., & Outten, F. W. (2007). SufE transfers sulfur from SufS to SufB for iron-sulfur cluster assembly. *Journal of Biological Chemistry*, *282*(18), 13342-13350.

116. Layer, G., Ollagnier-de Choudens, S., Sanakis, Y., & Fontecave, M. (2006). Iron-Sulfur Cluster Biosynthesis: Characterization of *Escherichia coli cyaY* as an iron donor for the assembly of [2Fe-2S] clusters in the scaffold IscU. *Journal of Biological Chemistry*, *281*(24), 16256-16263.

117. Lee, J. H., Yeo, W. S., & Roe, J. H. (2004). Induction of the sufA operon encoding Fe-S assembly proteins by superoxide generators and hydrogen peroxide: involvement of OxyR, IHF and an unidentified oxidant-responsive factor. *Molecular Microbiology*, *51*(6), 1745-1755.

118. Lee, J. J., Leedale, G. F., & Bradbury, P. (2000). The illustrated guide to the protozoa. Organisms traditionally referred to as protozoa, or newly discovered groups. Society of Protozoologists. *Lawrence, Kansas*.

119. Lee, K. C., Yeo, W. S., & Roe, J. H. (2008). Oxidant-responsive induction of the suf operon, encoding a Fe-S assembly system, through Fur and IscR in *Escherichia coli*. *Journal of Bacteriology*, *190*(24), 8244-8247.

120. Lee, M., Gräwert, T., Quitterer, F., Rohdich, F., Eppinger, J., Eisenreich, W., ... & Groll, M. (2010). Biosynthesis of isoprenoids: crystal structure of the [4Fe–4S] cluster protein IspG. *Journal of molecular biology*, *404*(4), 600-610.

121. Lemgruber, L., Kudryashev, M., Dekiwadia, C., Riglar, D. T., Baum, J., Stahlberg, H., ... & Frischknecht, F. (2013). Cryo-electron tomography reveals four-membrane architecture of the *Plasmodium* apicoplast. *Malaria journal*, *12*(1), 25.

122. Levin N. D. (1973). The Apicomplexa and the coccidian proper in Protozoan parasites of domestic animals and man. Minneapoils: Burgress Publishing Company.

123. Lill, R., & Mühlenhoff, U. (2008). Maturation of iron-sulfur proteins in eukaryotes: mechanisms, connected processes, and diseases. *Annual Reviews of Biochemistry*, *77*, 669-700.

124. Lima, C. D. (2002). Analysis of the E. coli NifS CsdB protein at 2.0 Å reveals the structural basis for perselenide and persulfide intermediate formation. *Journal of molecular biology*, *315*(5), 1199-1208.

125. Liu, J., Oganesyan, N., Shin, D. H., Jancarik, J., Yokota, H., Kim, R., & Kim, S. H. (2005). Structural characterization of an iron–sulfur cluster assembly protein IscU in a zinc-bound form. *Proteins: Structure, Function, and Bioinformatics*, *59*(4), 875-881.

126. Loiseau, L., Gerez, C., Bekker, M., Ollagnier-de Choudens, S., Py, B., Sanakis, Y., ... & Barras, F. (2007). ErpA, an iron–sulfur (Fe–S) protein of the A-type essential for respiratory metabolism in *Escherichia coli*. *Proceedings of the National Academy of Sciences*, *104*(34), 13626-13631.

127. Loiseau, L., Ollagnier-de-Choudens, S., Nachin, L., Fontecave, M., & Barras, F. (2003). Biogenesis of Fe-S Cluster by the Bacterial Suf System: SufS and SufE form a new type of cysteine desulphurase. *Journal of Biological Chemistry*, *278*(40), 38352-38359.

128. Lovell, S. C., Davis, I. W., Arendall, W. B., de Bakker, P. I., Word, J. M., Prisant, M. G., ... & Richardson, D. C. (2003). Structure validation by Cα geometry: ϕ, ψ and Cβ deviation. *Proteins: Structure, Function, and Bioinformatics*, *50*(3), 437-450.

129. Malkin, R., & Rabinowitz, J. C. (1966). The reconstitution of clostridial ferredoxin. *Biochemical and Biophysical Research Communications*, *23*(6), 822-827.

130. Mansy, S. S., & Cowan, J. A. (2004). Iron− sulfur cluster biosynthesis: Toward an understanding of cellular machinery and molecular mechanism. *Accounts of Chemical Research*, *37*(9), 719-725.

131. Marchler-Bauer, A., Derbyshire, M. K., Gonzales, N. R., Lu, S., Chitsaz, F., Geer, L. Y., Geer, R. C., He, J., Gwadz, M., et al. (2015). CDD: NCBI's conserved domain database. *Nucleic Acids Research*, 28, 43.

132. Marquet, A. (2001). Enzymology of carbon–sulfur bond formation. *Current opinion in chemical biology*, *5*(5), 541-549.

133. Martinsen, E. S., Perkins, S. L., and Schall, J. J. (2008). A three-genome phylogeny of malaria parasites (*Plasmodium* and closely related genera): evolution of life-history traits and host switches. *Mol Phylogenet Evol* 47(1), 261-273.

134. Massé, E., & Gottesman, S. (2002). A small RNA regulates the expression of genes involved in iron metabolism in *Escherichia coli*. *Proceedings of the National Academy of Sciences*, *99*(7), 4620-4625.

135. Massé, E., Escorcia, F. E., & Gottesman, S. (2003). Coupled degradation of a small regulatory RNA and its mRNA targets in *Escherichia coli*. *Genes & Development*, *17*(19), 2374-2383.

136. Massé, E., Vanderpool, C. K., & Gottesman, S. (2005). Effect of RyhB small RNA on global iron use in *Escherichia coli*. *Journal of Bacteriology*, *187*(20), 6962-6971.

137. McFadden, G. I., Reith, M. E., Munhalland, J., & Lan-Unnasch, N. (1996). Plastid in human parasites. *Nature*, *381*(6582), 482.

138. McGuffin, L. J., Bryson, K., & Jones, D. T. (2000). The PSIPRED protein structure prediction server. *Bioinformatics*, *16*(4), 404-405.

139. Mihara, H., & Esaki, N. (2002). Bacterial cysteine desulfurases: their function and mechanisms. *Applied Microbiology and Biotechnology*, *60*(1), 12-23.

140. Mihara, H., Fujii, T., Kato, S., Kurihara, T., Hata, Y., and Esaki, N. (2002). Structure of external aldimine of *Escherichia coli* CsdB, an IscS/NifS homolog: implications for its specificity toward selenocysteine, *Journal of biochemistry131*, 679-685.

141. Mihara, H., Kurihara, T., Yoshimura, T., & Esaki, N. (2000). Kinetic and Mutational Studies of Three NifS Homologs from *Escherichia coli*: Mechanistic Difference between L-Cysteine Desulfurase and L-Selenocysteine Lyase Reactions1. *Journal of Biochemistry*, *127*(4).

142. Mihara, H., Kurihara, T., Yoshimura, T., & Esaki, N. (2000). Kinetic and mutational studies of three NifS homologs from *Escherichia coli*: mechanistic difference between L-cysteine desulfurase and L-selenocysteine lyase reactions. *The Journal of Biochemistry*, *127*(4), 559-567.

143. Mihara, H., Kurihara, T., Yoshimura, T., Soda, K., & Esaki, N. (1997). Cysteine Sulfinate Desulfinase, a NIFS-like Protein of *Escherichia coli* with Selenocysteine Lyase and Cysteine Desulfurase Activities: Gene cloning, purification and characterization of a novel pyridoxal enzyme. *Journal of Biological Chemistry*, *272*(36), 22417-22424.

144. Mihara, H., Maeda, M., Fujii, T., Kurihara, T., Hata, Y., & Esaki, N. (1999). A nifS-like Gene, csdB, Encodes an *Escherichia coli* Counterpart of Mammalian Selenocysteine Lyase GENE CLONING, PURIFICATION, CHARACTERIZATION AND PRELIMINARY X-RAY CRYSTALLOGRAPHIC STUDIES. *Journal of Biological Chemistry*, *274*(21), 14768-14772.

145. Molik, S., Lill, R., & Mühlenhoff, U. (2007). Methods for studying iron metabolism in yeast mitochondria. *Methods in Cell Biology*, *80*, 261-280.

146. Møller, S. G., Kunkel, T., & Chua, N. H. (2001). A plastidic ABC protein involved in intercompartmental communication of light signaling. *Genes & Development*, *15*(1), 90-103.

147. Morimoto, K., Yamashita, E., Kondou, Y., Lee, S. J., Arisaka, F., Tsukihara, T., & Nakai, M. (2006). The asymmetric IscA homodimer with an exposed [2Fe-2S] cluster suggests the structural basis of the Fe-S cluster biosynthetic scaffold. *Journal of Molecular Biology*, *360*(1), 117-132.

148. Moulis, J. M., Sieker, L. C., Wilson, K. S., & Dauter, Z. (1996). Crystal structure of the 2 [4Fe-4S] ferredoxin from *Chromatium vinosum*: Evolutionary and mechanistic inferences for [3/4Fe-4S] ferredoxins. *Protein Science*, *5*(9), 1765-1775.

149. Mühlenhoff, U., Balk, J., Richhardt, N., Kaiser, J. T., Sipos, K., Kispal, G., & Lill, R. (2004). Functional characterization of the eukaryotic cysteine desulfurase Nfs1p from *Saccharomyces cerevisiae*. *Journal of Biological Chemistry*, *279*(35), 36906-36915.

150. Mühlenhoff, U., Gerber, J., Richhardt, N., & Lill, R. (2003). Components involved in assembly and dislocation of iron–sulfur clusters on the scaffold protein Isu1p. *The EMBO Journal*, *22*(18), 4815-4825.

151. Mühlenhoff, U., Richhardt, N., Ristow, M., Kispal, G., & Lill, R. (2002). The yeast frataxin homolog Yfh1p plays a specific role in the maturation of cellular Fe/S proteins. *Human Molecular Genetics*, *11*(17), 2025-2036.

152. Nachin, L., Loiseau, L., Expert, D., & Barras, F. (2003). SufC: an unorthodox cytoplasmic ABC/ATPase required for [Fe—S] biogenesis under oxidative stress. *The EMBO Journal*, *22*(3), 427-437.

153. Nagaraj, V. A., Arumugam, R., Chandra, N. R., Prasad, D., Rangarajan, P. N., & Padmanaban, G. (2009). Localisation of *Plasmodium falciparum* uroporphyrinogen III decarboxylase of the heme-biosynthetic pathway in the apicoplast and characterisation of its catalytic properties. *International Journal for Parasitology*, *39*(5), 559-568.

154. Nagaraj, V. A., Arumugam, R., Prasad, D., Rangarajan, P. N., & Padmanaban, G. (2010). Protoporphyrinogen IX oxidase from *Plasmodium falciparum* is anaerobic and is localized to the mitochondrion. *Molecular and Biochemical Parasitology*, *174*(1), 44-52.

155. Nagaraj, V. A., Prasad, D., Arumugam, R., Rangarajan, P. N., & Padmanaban, G. (2010). Characterization of coproporphyrinogen III oxidase in *Plasmodium falciparum* cytosol. *Parasitology International*, *59*(2), 121-127.

156. Nagaraj, V. A., Sundaram, B., Varadarajan, N. M., Subramani, P. A., Kalappa, D. M., Ghosh, S. K., & Padmanaban, G. (2013). Malaria parasite-synthesized heme is essential in the mosquito and liver stages and complements host heme in the blood stages of infection. *PLoS Pathogens*, *9*(8), e1003522.

157. Netz, D. J. A., Stümpfig, M., Doré, C., Mühlenhoff, U., Pierik, A. J., and Lill, R. (2010). Tah18 transfers electrons to Dre2 in cytosolic iron-sulfur protein biogenesis. *Nature Chemical Biology*, 6, 758–765.

158. Nkhoma, S. C., Nair, S., Cheeseman, I. H., Rohr-Allegrini, C., Singlam, S., Nosten, F., & Anderson, T. J. (2012, July). Close kinship within multiple-

genotype malaria parasite infections. In *Proc. R. Soc. B* (Vol. 279, No. 1738, pp. 2589-2598). The Royal Society.

159. Ollagnier-de-Choudens, S., Lascoux, D., Loiseau, L., Barras, F., Forest, E., & Fontecave, M. (2003). Mechanistic studies of the SufS–SufE cysteine desulfurase: evidence for sulfur transfer from SufS to SufE. *FEBS Letters*, *555*(2), 263-267.

160. Ollagnier-de-Choudens, S., Mattioli, T., Takahashi, Y., & Fontecave, M. (2001). Iron-Sulfur Cluster Assembly CHARACTERIZATION OF IscA AND EVIDENCE FOR A SPECIFIC AND FUNCTIONAL COMPLEX WITH FERREDOXIN. *Journal of Biological Chemistry*, *276*(25), 22604-22607.

161. Ollagnier-de-Choudens, S., Sanakis, Y., & Fontecave, M. (2004). SufA/IscA: reactivity studies of a class of scaffold proteins involved in [Fe-S] cluster assembly. *JBIC Journal of Biological Inorganic Chemistry*, *9*(7), 828-838.

162. Outten, F. W., Djaman, O., & Storz, G. (2004). A suf operon requirement for Fe–S cluster assembly during iron starvation in *Escherichia coli*. *Molecular Microbiology*, *52*(3), 861-872.

163. Outten, F. W., Wood, M. J., Muñoz, F. M., & Storz, G. (2003). The SufE protein and the SufBCD complex enhance SufS cysteine desulfurase activity as part of a sulfur transfer pathway for Fe-S cluster assembly in *Escherichia coli*. *Journal of Biological Chemistry*, *278*(46), 45713-45719.

164. Pakalapati, D., Garg, S., Middha, S., Acharya, J., Subudhi, A. K., Boopathi, A. P., Saxena, V., Kochar, S. K., Kochar, D. K., and Das, A. (2013). Development and evaluation of a 28S rRNA gene-based nested PCR assay for *P. falciparum* and *P. vivax. Pathog Glob Health* 107, 180-188.

165. Pala, Z. R., Saxena, V., Saggu, G. S., Yadav, S. K., Pareek, R. P., Kochar, S. K., ... & Garg, S. (2016). Structural and functional characterization of an iron–sulfur cluster assembly scaffold protein-SufA from *Plasmodium vivax*. *Gene*, *585*(1), 159-165.

166. Parsons, M., Karnataki, A., Feagin, J. E., and DeRocher, A. (2007). Protein trafficking to the apicoplast: deciphering the apicomplexan solution to secondary endosymbiosis. *Eukaryotic Cell* 6, 1081–1088.

167. Partow, S., Siewers, V., Daviet, L., Schalk, M., and Nielsen, J. (2012). Reconstruction and Evaluation of the Synthetic Bacterial MEP Pathway in *Saccharomyces cerevisiae*. *PLoS ONE* 7(12), e52498.

168. Patzer, S. I., & Hantke, K. (1999). SufS is a NifS-like protein, and SufD is necessary for stability of the [2Fe-2S] FhuF protein in *Escherichia coli*. *Journal of Bacteriology*, *181*(10), 3307-3309.

169. Peters, J. W., & Broderick, J. B. (2012). Emerging paradigms for complex iron-sulfur cofactor assembly and insertion. *Annual Review of Biochemistry*, *81*, 429-450.

170. Pettersen, E. F., Goddard, T. D., Huang, C. C., Couch, G. S., Greenblatt, D. M., Meng, E. C., & Ferrin, T. E. (2004). UCSF Chimera—a visualization system for exploratory research and analysis. *Journal of computational chemistry*, *25*(13), 1605-1612.

171. Ponpuak, M., Klemba, M., Park, M., Gluzman, I. Y., Lamppa, G. K., & Goldberg, D. E. (2007). A role for falcilysin in transit peptide degradation in the *Plasmodium falciparum* apicoplast. *Molecular Microbiology*, *63*(2), 314-334.

172. Puccio, H., & Kœnig, M. (2000). Recent advances in the molecular pathogenesis of Friedreich ataxia. *Human Molecular Genetics*, *9*(6), 887-892.

173. Py, B., & Barras, F. (2010). Building Fe–S proteins: bacterial strategies. *Nature Reviews Microbiology*, *8*(6), 436-446.

174. Ralph, S. A., van Dooren, G. G., Waller, R. F., Crawford, M. J., Fraunholz, M. J., Foth, B. J., ... & McFadden, G. I. (2004). Tropical infectious diseases: metabolic maps and functions of the *Plasmodium falciparum* apicoplast. *Nature Reviews Microbiology*, *2*(3), 203-216.

175. Ram, E. R., Naik, R., Ganguli, M., & Habib, S. (2008). DNA organization by the apicoplast-targeted bacterial histone-like protein of *Plasmodium falciparum*. *Nucleic Acids Research*, *36*(15), 5061-5073.

176. Rangachari, K., Davis, C. T., Eccleston, J. F., Hirst, E. M. A., Saldanha, J. W., Strath, M., & Wilson, R. J. M. (2002). SufC hydrolyzes ATP and interacts with SufB from *Thermotoga maritima*. *FEBS Letters*, *514*(2-3), 225-228.

177. Rathore, D., Wahl, A. M., Sullivan, M., and McCutchan, T. F. (2001). A phylogenetic comparison of gene trees constructed from plastid, mitochondrial and genomic DNA of *Plasmodium* species. *Mol Biochem Parasitol* 114(1), 89-94.

178. Ratledge, C., & Dover, L. G. (2000). Iron metabolism in pathogenic bacteria. *Annual Reviews in Microbiology*, *54*(1), 881-941.

179. Rees, D. C., & Howard, J. B. (2003). The interface between the biological and inorganic worlds: iron-sulfur metalloclusters. *Science*, *300*(5621), 929-931.

180. Rekittke, I., Wiesner, J., Röhrich, R., Demmer, U., Warkentin, E., Xu, W., ... & Oldfield, E. (2008). Structure of (E)-4-hydroxy-3-methyl-but-2-enyl diphosphate reductase, the terminal enzyme of the non-mevalonate pathway. *Journal of the American Chemical Society*, *130*(51), 17206-17207.

181. Rohdich, F., Eisenreich, W., Wungsintaweekul, J., Hecht, S., Schuhr, C. A., and Bacher, A. (2001). Biosynthesis of terpenoids. 2C-methyl-D-erythritol 2,4-cyclodiphosphate synthase (IspF) from *Plasmodium falciparum*. *Eur J Biochem* 268, 3190-3197.

182. Röhrich, R. C., Englert, N., Troschke, K., Reichenberg, A., Hintz, M., Seeber, F., ... & Pfeiffer, M. (2005). Reconstitution of an apicoplast-localised electron transfer pathway involved in the isoprenoid biosynthesis of *Plasmodium falciparum*. *FEBS letters*, *579*(28), 6433-6438.

183. Rouault, T. A. (2015). Mammalian iron-sulphur proteins: novel insights into biogenesis and function. *Nature reviews Molecular cell biology*, *16*(1), 45-55.

184. Roy, A., Solodovnikova, N., Nicholson, T., Antholine, W., & Walden, W. E. (2003). A novel eukaryotic factor for cytosolic Fe–S cluster assembly. *The EMBO Journal*, *22*(18), 4826-4835.

185. Ruzicka, F. J., & Beinert, H. E. L. M. U. T. (1978). The soluble" high potential" type iron-sulfur protein from mitochondria is aconitase. *Journal of Biological Chemistry*, *253*(8), 2514-2517.

186. Saggu, G. S., Garg, S., Pala, Z. R., Yadav, S. K., Kochar, S. K., Kochar, D. K., & Saxena, V. (2017). Characterization of 4-hydroxy-3-methylbut-2-en-1-yl diphosphate synthase (IspG) from *Plasmodium vivax* and it's potential as

an antimalarial drug target. *International Journal of Biological Macromolecules*, *96*, 466-473.

187. Sali, A., Blundell, T.L. (1993). Comparative protein modelling by satisfaction of spatial restraints. *Journal of Molecular Biology* ;*234*:779-815.

188. Sambrook, J., and Russell, D. W. (2001). Molecular Cloning A Laboratory manual 3rd ed., Cold Spring Harbor Laboratory Press, NY, USA.

189. Sasaki, N., Hirai, M., Maeda, K., Yui, R., Itoh, K., Namiki, S., ... & Kita, K. (2009). The *Plasmodium* HU homolog, which binds the plastid DNA sequence-independent manner, is essential for the parasite's survival. *FEBS Letters*, *583*(9), 1446-1450.

190. Sato, S. (2002). The genome of *Plasmodium falciparum* encodes an active δ-aminolevulinic acid dehydratase. *Current Genetics*, *40*(6), 391-398.

191. Sato, S., Clough, B., Coates, L., & Wilson, R. J. M. (2004). Enzymes for heme biosynthesis are found in both the mitochondrion and plastid of the malaria parasite *Plasmodium falciparum*. *Protist*, *155*(1), 117-125.

192. Sato, S., Rangachari, K., & Wilson, R. I. (2003). Targeting GFP to the malarial mitochondrion. *Molecular and Biochemical Parasitology*, *130*(2), 155-158.

193. Sato, S., Tews, I., & Wilson, R. J. M. (2000). Impact of a plastid-bearing endocytobiont on apicomplexan genomes. *International journal for parasitology*, *30*(4), 427-439.

194. Saxena, V., Garg, S., Ranjan, S., Kochar, D., Ranjan, A., and Das, A. (2007). Analysis of elongation factor Tu (tuf A) of apicoplast from Indian *Plasmodium vivax* isolates. *Infect Genet Evol* 7, 618-626. doi:10.1016/j.meegid.2007.05.012

195. Saxena, V., Garg, S., Tripathi, J., Sharma, S., Pakalapati, D., Subudhi, A. K., ... & Das, A. (2012). *Plasmodium vivax* apicoplast genome: a comparative analysis of major genes from Indian field isolates. *Acta Tropica*, *122*(1), 138-149.

196. Schwartz, C. J., Djaman, O., Imlay, J. A., & Kiley, P. J. (2000). The cysteine desulfurase, IscS, has a major role in in vivo Fe-S cluster formation in *Escherichia coli*. *Proceedings of the National Academy of Sciences*, *97*(16), 9009-9014.

197. Schwartz, C. J., Giel, J. L., Patschkowski, T., Luther, C., Ruzicka, F. J., Beinert, H., & Kiley, P. J. (2001). IscR, an Fe-S cluster-containing transcription factor, represses expression of *Escherichia coli* genes encoding Fe-S cluster assembly proteins. *Proceedings of the National Academy of Sciences*, *98*(26), 14895-14900.

198. Seeber, F., & Soldati-Favre, D. (2010). Metabolic pathways in the apicoplast of Apicomplexa. *International Review of Cell and Molecular Biology*, *281*, 161-228.

199. Sekar, V., (1987). A Rapid Screening Procedure for the Identification of Recombinant Bacterial Clone. *BioTech* 5(1), 11-13.

200. Selbach, B. P., Chung, A. H., Scott, A. D., George, S. J., Cramer, S. P., & Dos Santos, P. C. (2013). Fe-S cluster biogenesis in Gram-positive bacteria: SufU is a zinc-dependent sulfur transfer protein. *Biochemistry*, *53*(1), 152-160.

201. Selbach, B., Earles, E., & Dos Santos, P. C. (2010). Kinetic analysis of the bisubstrate cysteine desulfurase SufS from *Bacillus subtilis*. *Biochemistry*, *49*(40), 8794-8802.

202. Sendra, M., Ollagnier de Choudens, S., Lascoux, D., Sanakis, Y., & Fontecave, M. (2007). The SUF iron–sulfur cluster biosynthetic machinery: Sulfur transfer from the SUFS–SUFE complex to SUFA. *FEBS letters*, *581*(7), 1362-1368.

203. Sheiner, L., Vaidya, A. B., & McFadden, G. I. (2013). The metabolic roles of the endosymbiotic organelles of *Toxoplasma* and *Plasmodium spp. Current Opinion in Microbiology*, *16*(4), 452-458.

204. Shimomura, Y., Wada, K., Fukuyama, K., & Takahashi, Y. (2008). The asymmetric trimeric architecture of [2Fe–2S] IscU: implications for its scaffolding during iron–sulfur cluster biosynthesis. *Journal of Molecular Biology*, *383*(1), 133-143.

205. Siegel, S. M. (1965). A Direct Microdetermination for Sulfide. *Anal Biochem* 11, 126-132.

206. Sievers, F., Wilm, A., Dineen, D., Gibson, T. J., Karplus, K., Li, W., ... & Thompson, J. D. (2011). Fast, scalable generation of high-quality protein

multiple sequence alignments using Clustal Omega. *Molecular Systems Biology*, *7*(1), 539.

207. Sigrist, C. J., De Castro, E., Cerutti, L., Cuche, B. A., Hulo, N., Bridge, A., ... & Xenarios, I. (2012). New and continuing developments at PROSITE. *Nucleic Acids Research*, gks1067.

208. Silberg, J. J., Hoff, K. G., & Vickery, L. E. (1998). The Hsc66-Hsc20 Chaperone System in *Escherichia coli*: Chaperone Activity and Interactions with the DnaK-DnaJ-GrpE System. *Journal of Bacteriology*, *180*(24), 6617-6624.

209. Silberg, J. J., Hoff, K. G., & Vickery, L. E. (1998). The Hsc66-Hsc20 Chaperone System in *Escherichia coli*: Chaperone Activity and Interactions with the DnaK-DnaJ-GrpE System. *Journal of Bacteriology*, *180*(24), 6617-6624.

210. Silberg, J. J., Hoff, K. G., Tapley, T. L., & Vickery, L. E. (2001). The Fe/S assembly protein IscU behaves as a substrate for the molecular chaperone Hsc66 from *Escherichia coli*. *Journal of Biological Chemistry*, *276*(3), 1696-1700.

211. Singh, B., Sung, L. K., Matusop, A., Radhakrishnan, A., Shamsul, S. S., Cox-Singh, J., ... & Conway, D. J. (2004). A large focus of naturally acquired *Plasmodium knowlesi* infections in human beings. *The Lancet*, *363*(9414), 1017-1024.

212. Smith, B. E., & Eady, R. R. (1993). Metalloclusters of the nitrogenases. In *EJB Reviews* (pp. 79-93). Springer Berlin Heidelberg.

213. Söding, J., Biegert, A., & Lupas, A. N. (2005). The HHpred interactive server for protein homology detection and structure prediction. *Nucleic Acids Research*, *33*(suppl 2), W244-W248.

214. Sommer, M. S., Gould, S. B., Lehmann, P., Gruber, A., Przyborski, J. M., & Maier, U. G. (2007). Der1-mediated preprotein import into the periplastid compartment of chromalveolates?. *Molecular Biology and Evolution*, *24*(4), 918-928.

215. Spork, S., Hiss, J. A., Mandel, K., Sommer, M., Kooij, T. W., Chu, T., ... & Przyborski, J. M. (2009). An unusual ERAD-like complex is targeted to the apicoplast of *Plasmodium falciparum*. *Eukaryotic Cell*, *8*(8), 1134-1145.

216. Stanway, R. R., Witt, T., Zobiak, B., Aepfelbacher, M., & Heussler, V. T. (2009). GFP-targeting allows visualization of the apicoplast throughout the life cycle of live malaria parasites. *Biology of the Cell*, *101*(7), 415-435.

217. Stehling, O., Smith, P. M., Biederbick, A., Balk, J., Lill, R., & Mühlenhoff, U. (2007). Investigation of iron-sulfur protein maturation in eukaryotes. *Mitochondria: Practical Protocols*, 325-342.

218. Sullivan, A. D., & Meshnick, S. R. (1996). Haemozoin: identification and quantification. *Parasitology Today*, *12*(4), 161-163.

219. Surolia, N., & Padmanaban, G. (1992). De novo biosynthesis of heme offers a new chemotherapeutic target in the human malarial parasite. *Biochemical and Biophysical Research Communications*, *187*(2), 744-750.

220. Surolia, N., & Surolia, A. (2001). Triclosan offers protection against blood stages of malaria by inhibiting enoyl-ACP reductase of *Plasmodium falciparum*. *Nature Medicine*, *7*(2), 167-173.

221. Ta, T. H., Hisam, S., Lanza, M., Jiram, A. I., Ismail, N., & Rubio, J. M. (2014). First case of a naturally acquired human infection with *Plasmodium cynomolgi*. *Malaria journal*, *13*(1), 68.

222. Takahashi, Y., & Tokumoto, U. (2002). A third bacterial system for the assembly of iron-sulfur clusters with homologs in archaea and plastids. *Journal of Biological Chemistry*, *277*(32), 28380-28383.

223. Tamura, K., Stecher, G., Peterson, D., Filipski, A., & Kumar, S. (2013). MEGA6: molecular evolutionary genetics analysis version 6.0. *Molecular Biology and Evolution*, *30*(12), 2725-2729.

224. Tarun, A. S., Vaughan, A. M., & Kappe, S. H. (2009). Redefining the role of de novo fatty acid synthesis in *Plasmodium* parasites. *Trends in Parasitology*, *25*(12), 545-550.

225. Thomsen, R., and Christensen, M. H. (2006). MolDock: a new technique for high-accuracy molecular docking. *J Med Chem* 49, 3315-3321.

226. Tirupati, B., Vey, J. L., Drennan, C. L., & Bollinger, J. M. (2004). Kinetic and Structural Characterization of Slr0077/SufS, the Essential Cysteine Desulfurase from *Synechocystis sp*. PCC 6803†. *Biochemistry*, *43*(38), 12210-12219.

227. Tokumoto, U., Kitamura, S., Fukuyama, K., & Takahashi, Y. (2004). Interchangeability and distinct properties of bacterial Fe-S cluster assembly systems: functional replacement of the isc and suf operons in *Escherichia coli* with the nifSU-like operon from Helicobacter pylori. *Journal of biochemistry*, *136*(2), 199-209.

228. Tovchigrechko, A., & Vakser, I. A. (2006). GRAMM-X public web server for protein–protein docking. *Nucleic Acids Research*, *34*(suppl 2), W310-W314.

229. Trotter, V., Vinella, D., Loiseau, L., Choudens, D., Ollagnier, S., Fontecave, M., & Barras, F. (2009). The CsdA cysteine desulphurase promotes Fe/S biogenesis by recruiting Suf components and participates to a new sulphur transfer pathway by recruiting CsdL (ex-YgdL), a ubiquitin-modifying-like protein. *Molecular Microbiology*, *74*(6), 1527-1542.

230. Untergasser, A., Cutcutache, I., Koressaar, T., Ye, J., Faircloth, B. C., Remm, M., & Rozen, S. G. (2012). Primer3—new capabilities and interfaces. *Nucleic Acids Research*, *40*(15), e115-e115.

231. van Dooren, G. G., Marti, M., Tonkin, C. J., Stimmler, L. M., Cowman, A. F., & McFadden, G. I. (2005). Development of the endoplasmic reticulum, mitochondrion and apicoplast during the asexual life cycle of *Plasmodium falciparum*. *Molecular Microbiology*, *57*(2), 405-419.

232. van Dooren, G. G., Stimmler, L. M., & McFadden, G. I. (2006). Metabolic maps and functions of the *Plasmodium* mitochondrion. *FEMS Microbiology Reviews*, *30*(4), 596-630.

233. van Dooren, G. G., Su, V., D'Ombrain, M. C., & McFadden, G. I. (2002). Processing of an Apicoplast Leader Sequence in *Plasmodium falciparum* and the Identification of a Putative Leader Cleavage Enzyme. *Journal of Biological Chemistry*, *277*(26), 23612-23619.

234. van Dooren, G. G., Su, V., D'Ombrain, M. C., & McFadden, G. I. (2002). Processing of an Apicoplast Leader Sequence in *Plasmodium falciparum* and the Identification of a Putative Leader Cleavage Enzyme. *Journal of Biological Chemistry*, *277*(26), 23612-23619.

235. van Schaijk, B. C., Kumar, T. S., Vos, M. W., Richman, A., van Gemert, G. J., Li, T., ... & Kennedy, M. (2014). Type II fatty acid biosynthesis is

essential for *Plasmodium falciparum* sporozoite development in the midgut of *Anopheles* mosquitoes. *Eukaryotic Cell*, *13*(5), 550-559.

236. Varadharajan, S., Dhanasekaran, S., Bonday, Z. Q., Rangarajan, P. N., & Padmanaban, G. (2002). Involvement of δ-aminolaevulinate synthase encoded by the parasite gene in de novo haem synthesis by *Plasmodium falciparum*. *Biochemical Journal*, *367*(2), 321-327.
237. Vaughan, A. M., O'Neill, M. T., Tarun, A. S., Camargo, N., Phuong, T. M., Aly, A. S., ... & Kappe, S. H. (2009). Type II fatty acid synthesis is essential only for malaria parasite late liver stage development. *Cellular Microbiology*, *11*(3), 506-520.
238. Vickery, L. E., Silberg, J. J., & Ta, D. T. (1997). Hsc66 and Hsc20, a new heat shock cognate molecular chaperone system from *Escherichia coli*. *Protein Science*, *6*(5), 1047-1056.
239. Vinella, D., Brochier-Armanet, C., Loiseau, L., Talla, E., & Barras, F. (2009). Iron-sulfur (Fe/S) protein biogenesis: phylogenomic and genetic studies of A-type carriers. *PLoS Genet*, *5*(5), e1000497.
240. Volbeda, A., Charon, M. H., Piras, C., & Hatchikian, E. C. (1995). Crystal structure of the nickel-iron hydrogenase from *Desulfovibrio gigas*. *Nature*, *373*(6515), 580.
241. Vriend, G. (1990). WHAT IF: a molecular modeling and drug design program. *Journal of Molecular Graphics*, *8*(1), 52-56.
242. Wächtershäuser, G. (1992). Groundworks for an evolutionary biochemistry: the iron-sulphur world. *Progress in Biophysics and Molecular Biology*, *58*(2), 85-201.
243. Wada, K., Hasegawa, Y., Gong, Z., Minami, Y., Fukuyama, K., & Takahashi, Y. (2005). Crystal structure of Escherichia coli SufA involved in biosynthesis of iron–sulfur clusters: implications for a functional dimer. *FEBS letters*, *579*(29), 6543-6548.
244. Waller, R. F., Keeling, P. J., Donald, R. G., Striepen, B., Handman, E., Lang-Unnasch, N., ... & McFadden, G. I. (1998). Nuclear-encoded proteins target to the plastid in *Toxoplasma gondii* and *Plasmodium falciparum*. *Proceedings of the National Academy of Sciences*, *95*(21), 12352-12357.

245. Waller, R. F., Ralph, S. A., Reed, M. B., Su, V., Douglas, J. D., Minnikin, D. E., ... & McFadden, G. I. (2003). A type II pathway for fatty acid biosynthesis presents drug targets in *Plasmodium falciparum*. *Antimicrobial Agents and Chemotherapy*, *47*(1), 297-301.

246. Waller, R. F., Reed, M. B., Cowman, A. F., & McFadden, G. I. (2000). Protein trafficking to the plastid of *Plasmodium falciparum* is via the secretory pathway. *The EMBO Journal*, *19*(8), 1794-1802.

247. White, M. F., & Dillingham, M. S. (2012). Iron–sulphur clusters in nucleic acid processing enzymes. *Current Opinion in Structural Biology*, *22*(1), 94-100.

248. Wilson, R. B., & Roof, D. M. (1997). Respiratory deficiency due to loss of mitochondrial DNA in yeast lacking the frataxin homologue. *Nature Genetics*, *16*(4), 352-357.

249. Wilson, R. J. M. (2005). Parasite plastids: approaching the endgame. *Biological Reviews*, *80*(1), 129-153.

250. Wilson, R. J., & Williamson, D. H. (1997). Extrachromosomal DNA in the Apicomplexa. *Microbiology and Molecular Biology Reviews*, *61*(1), 1-16.

251. Wilson, R. J., Denny, P. W., Preiser, P. R., Rangachari, K., Roberts, K., Roy, A., ... & Williamson, D. H. (1996). Complete gene map of the plastid-like DNA of the malaria parasite *Plasmodium falciparum*. *Journal of Molecular Biology*, *261*(2), 155-172.

252. Wollenberg, M., Berndt, C., Bill, E., Schwenn, J. D., & Seidler, A. (2003). A dimer of the FeS cluster biosynthesis protein IscA from cyanobacteria binds a [2Fe2S] cluster between two protomers and transfers it to [2Fe2S] and [4Fe4S] apo proteins. *European journal of biochemistry*, *270*(8), 1662-1671.

253. Wollers, S., Layer, G., Garcia-Serres, R., Signor, L., Clemancey, M., Latour, J. M., ... & de Choudens, S. O. (2010). Iron-Sulfur (Fe-S) Cluster Assembly: the SufBCD complex is a new type of Fe-S scaffold with a flavin redox cofactor. *Journal of Biological Chemistry*, *285*(30), 23331-23341.

254. World Malaria Report, World Health Organization 2016.

255. World Malaria Report, World Health Organization, 2015.

256. Wu, G., Mansy, S. S., Wu, S. P., Surerus, K. K., Foster, M. W., & Cowan, J. A. (2002). Characterization of an iron− sulfur cluster assembly protein (ISU1) from *Schizosaccharomyces pombe*. *Biochemistry*, *41*(15), 5024-5032.

257. Wu, S. P., Wu, G., Surerus, K. K., & Cowan, J. A. (2002). Iron− Sulfur Cluster Biosynthesis. Kinetic Analysis of [2Fe-2S] Cluster Transfer from Holo ISU to Apo Fd: Role of Redox Chemistry and a Conserved Aspartate. *Biochemistry*, *41*(28), 8876-8885.

258. Wu, Y., & Brosh, R. M. (2012). DNA helicase and helicase–nuclease enzymes with a conserved iron–sulfur cluster. *Nucleic Acids Research*, *40*(10), 4247-4260.

259. www.malariasite.com/malaria-parasites/

260. Xu, X. M., & Møller, S. G. (2008). Iron–sulfur cluster biogenesis systems and their crosstalk. *Chembiochem*, *9*(15), 2355-2362.

261. Xu, X. M., Adams, S., Chua, N. H., & Møller, S. G. (2005). AtNAP1 represents an atypical SufB protein in *Arabidopsis* plastids. *Journal of Biological Chemistry*, *280*(8), 6648-6654.

262. Ye, J., Coulouris, G., Zaretskaya, I., Cutcutache, I., Rozen, S., & Madden, T. L. (2012). Primer-BLAST: a tool to design target-specific primers for polymerase chain reaction. *BMC Bioinformatics*, *13*(1), 134.

263. Yeh, E., & DeRisi, J. L. (2011). Chemical rescue of malaria parasites lacking an apicoplast defines organelle function in blood-stage *Plasmodium falciparum*. *PLoS Biology*, *9*(8), e1001138.

264. Yeo, W. S., Lee, J. H., Lee, K. C., & Roe, J. H. (2006). IscR acts as an activator in response to oxidative stress for the suf operon encoding Fe-S assembly proteins. *Molecular Microbiology*, *61*(1), 206-218.

265. Yu, M., Kumar, T. S., Nkrumah, L. J., Coppi, A., Retzlaff, S., Li, C. D., ... & Valderramos, J. C. (2008). The fatty acid biosynthesis enzyme FabI plays a key role in the development of liver-stage malarial parasites. *Cell Host & Microbe*, *4*(6), 567-578.

266. Zafrilla, B., Martínez-Espinosa, R. M., Esclapez, J., Pérez-Pomares, F., & Bonete, M. J. (2010). SufS protein from Haloferax volcanii involved in Fe-S cluster assembly in haloarchaea. *Biochimica et Biophysica Acta (BBA)-Proteins and Proteomics*, *1804*(7), 1476-1482.

267. Zeng, J., Geng, M., Jiang, H., Liu, Y., Liu, J., & Qiu, G. (2007). The IscA from *Acidithiobacillus ferrooxidans* is an iron–sulfur protein which assemble the [Fe 4 S 4] cluster with intracellular iron and sulfur. *Archives of Biochemistry and Biophysics*, *463*(2), 237-244.

268. Zepeck, F., Gräwert, T., Kaiser, J., Schramek, N., Eisenreich, W., Bacher, A., & Rohdich, F. (2005). Biosynthesis of isoprenoids. Purification and properties of IspG protein from Escherichia coli. *The Journal of organic chemistry*, *70*(23), 9168-9174.

269. Zhang, B., Watts, K. M., Hodge, D., Kemp, L. M., Hunstad, D. A., Hicks, L. M., & Odom, A. R. (2011). A second target of the antimalarial and antibacterial agent fosmidomycin revealed by cellular metabolic profiling. *Biochemistry*, *50*(17), 3570-3577.

270. Zheng, L., Cash, V. L., Flint, D. H., & Dean, D. R. (1998). Assembly of Iron-Sulfur Clusters: Identification of an *iscSUA-hscBA-fdx* gene cluster from *Azotobacter vinelandii*. *Journal of Biological Chemistry*, *273*(21), 13264-13272.

271. Zheng, L., White, R. H., Cash, V. L., & Dean, D. R. (1994). Mechanism for the desulfurization of L-cysteine catalyzed by the nifS gene product. *Biochemistry*, *33*(15), 4714-4720.

272. Zheng, L., White, R. H., Cash, V. L., Jack, R. F., & Dean, D. R. (1993). Cysteine desulfurase activity indicates a role for NIFS in metallocluster biosynthesis. *Proceedings of the National Academy of Sciences*, *90*(7), 2754-2758.

273. Zheng, M., Wang, X., Templeton, L. J., Smulski, D. R., LaRossa, R. A., & Storz, G. (2001). DNA microarray-mediated transcriptional profiling of the *Escherichia coli* response to hydrogen peroxide. *Journal of Bacteriology*, *183*(15), 4562-4570.

274. Zuegge, J., Ralph, S., Schmuker, M., McFadden, G. I., & Schneider, G. (2001). Deciphering apicoplast targeting signals–feature extraction from nuclear-encoded precursors of *Plasmodium falciparum* apicoplast proteins. *Gene*, *280*(1), 19-26.

APPENDIX

A.1 List of Publications

1. Saggu, G. S., Garg, S., **Pala, Z. R.,** Yadav, S. K., Kochar, S. K., Kochar, D. K., & Saxena, V. (2017). Characterization of 4-hydroxy-3-methylbut-2-en-1-yl diphosphate synthase (IspG) from *Plasmodium vivax* and it's potential as an antimalarial drug target. *International Journal of Biological Macromolecules*, *96*, 466-473.

2. **Pala, Z. R.,** Saxena, V., Saggu, G. S., Yadav, S. K., Pareek, R. P., Kochar, S. K., ... & Garg, S. (2016). Structural and functional characterization of an iron–sulfur cluster assembly scaffold protein-SufA from *Plasmodium vivax*. *Gene*, *585*(1), 159-165.

3. Saggu G. S., **Pala Z. R.**, Garg S., Saxena V. (2016). New Insight into Isoprenoids Biosynthesis Process and Future Prospects for Drug Designing in *Plasmodium*. *Frontiers in Microbiology*, 7:1421.

4. **Pala, Z. R.,** Saxena, V., Saggu, G. S., Mani S. K., Pareek, R. P., Kochar, S. K., Garg, S. SUF machinery in *Plasmodium vivax*: Mobilization of sulfur via SufSE complex for Fe-S cluster assembly on SufA and its transfer to apo-protein. (Manuscript Under Review)

5. **Pala, Z. R.,** Saxena, V., Saggu, G. S., Garg, S. Recent advances in the [Fe-S] Cluster Biogenesis (SUF) pathway functional in the apicoplast of *Plasmodium*. (Manuscript Submitted)

6. **Pala Z. R.**, Shukla V., Alok A., Kudale S., Desai N. S. Enhanced production of an anti-malarial compound artesunate by hairy root cultures and phytochemical analysis of *Artemisia pallens* Wall. *3Biotech*. 2016 December 6:182.

7. Shukla V., **Pala Z.,** Alok A., Desai N. Screening of Different *Artemisia spp*. from Western Ghats of Maharashtra for an Anti-Malarial Compound—Artemisinin. *American Journal of Plant Sciences* 6(6):1619-1632. June 2015.

8. Alok A., Shukla V., **Pala Z.,** Kumar J., Kudale S., Desai N. *In vitro* regeneration and optimization of factors affecting *Agrobacterium* mediated transformation in *Artemisia pallens*, an important medicinal plant. *Physiology and Molecular Biology of Plants*. 2016 April. 22(2):261-9.

A.2 Details of Conferences Attended

1. **Zarna R. Pala**, Shilpi Garg, Gagandeep Singh Saggu, Vishal Saxena. "Iron-sulphur cluster assembly in *Plasmodium vivax*: An insight into the SUF machinery." 27th Annual Molecular Parasitology Meeting 2016, at Woods Hole, Massachusetts, U.S.A., from 18th – 22nd September, 2016.

2. **Zarna Pala Rajeshkumar**, Vishal Saxena, Gagandeep Singh Saggu, Sushil Kumar Yadav, R. P. Pareek, Sanjay Kumar Kochar, Dhanpat Kumar Kochar, Shilpi Garg. "Structural and Functional Characterization of an Iron-Sulfur Cluster Assembly Scaffold Protein-SufA from *Plasmodium vivax*." BITS Conference on Gene and Genome Regulation", at BITS Pilani, India, from 18th – 20th February, 2016. **(Best Poster Award)**

3. **Zarna Pala**, Shilpi Garg, Sanjay K. Kochar, Dhanpat K. Kochar, Vishal Saxena. 2014."Characterization of a nuclear encoded hypothetical protein involved in Fe-S cluster biogenesis in *Plasmodium vivax*" in 25th National Conference of Parasitology on "Global Challenges in the Management of Parasitic Diseases" organised jointly by CSIR-CDRI and Indian Society of Parasitologists at CDRI, Lucknow from October 16 – 18. **(Best Poster Award)**

4. **Zarna R. Pala**, Shilpi Garg, Gagandeep S. Saggu, Vishal Saxena. 2014. "Characterization of nuclear encoded hypothetical proteins involved in *Plasmodium vivax* apicoplast metabolic pathways" in Recent Trends and Future Prospects of Microbiology and Biotechnology organized by Shri Jagdishprasad Jhabarmal Tiberwala University, Jhunjhunu, Rajasthan, from March 03 – 04. **(Best Poster Award)**

5. **Zarna Pala**, Ritika Lakhotia, Shilpi Garg, Gagandeep S. Saggu, Vishal Saxena. 2013. "Characterization and analysis of the RimM protein encoding gene in *Plasmodium vivax*" in National Conference on Fight Against Malaria: Prospects and Perspectives held at Centre for Biotechnology & Centre for Medical Biotechnology, Maharishi Dayanand University, Rohtak, Haryana on March 9th.

6. **Zarna R. Pala**, Vishnu Kumar Shukla, Neetin Desai. "Hairy root induction in *Artemisia pallens* Wall. Ex. DC. & Quantification of Artesunate using HPLC." Presented at "National Seminar on Frontiers in Biotechnology and Bioinformatics", March 5th – 6th 2010, organized by Department of Biotechnology and Bioinformatics, Padmashree Dr. D. Y. Patil University, Navi Mumbai. **(Best Poster Award)**

7. Gagandeep S. Saggu, Shilpi Garg, **Zarna Pala**, Sushil K. Yadav, Sanjay K. Kochar, Dhanpat K. Kochar, Vishal Saxena. 2016 "Characterization of 4-Hydroxy-3-Methylbut-2-en-1-yl diphosphate Synthase (GcpE) enzyme from *Plasmodium vivax*" in BITS conference on Gene and Genome Regulation (BCGGR 2016) at Department of Biological Sciences, Birla Institute of Technology and Sciences, Pilani, India from Feb 18-20.

8. Gagandeep S. Saggu, **Zarna Pala**, Shilpi Garg, Sanjay K. Kochar, Vishal Saxena. 2013. "Characterization of IspD enzyme from Indian *Plasmodium vivax* field isolates" in 24th National Congress of Parasitology held at Regional Medical Research Centre for Tribal's, Jabalpur from April 27 – 29.

Conference & Workshop Attended

1. Search for Antimalarial: Mechanism Based Approach (2012), National conference conducted by Jawaharlal Nehru University Delhi, India from April 27-29, 2012.

2. National Workshop on Computational Systems Biology and Dose Response Modeling. Organized by Mahatma Gandhi Doerenkamp Centre for Alternatives to Use of Animals in Life Science Education, Tiruchirapalli, India from March, 2013.

A.3 Brief biography of Prof. Vishal Saxena, Ph. D.

Prof. Vishal Saxena is working as an Associate Professor in Molecular Parasitology & Systems Biology Lab, Department of Biological Sciences, Birla Institute of Technology and Science, Pilani, Rajasthan, India since 2015. Previous to this he joined as Assistant Professor in the current department in 2006. Prof. Saxena did B. Pharmacy (University of Rajasthan, Jaipur, August 1999) followed by M. E. Biotechnology (BITS, Pilani, June 2001) and Ph. D. (Biological Sciences Group, BITS, Pilani, October 2006). During his Ph.D., he had worked as CSIR-Senior Research Fellow (2003-2006). He has over 17 years (7 year's Pre-doctoral experiences, about 10 year's job tenure) of teaching and research experience. His major thrust area of research is Molecular Biology and Immunology with special emphasis to Genomics and Proteomics of Malaria parasites, *Plasmodium vivax* and *P. falciparum*. His group is focusing on various aspects related to *P. vivax* infections in humans, apicoplast and its genome, metabolic pathways functional in the apicoplast, hypothetical proteins encoded by *P. vivax* nuclear genome. He was a Visiting Scholar at Department of Global Health, College of Public Health, University of South Florida, Tampa, Florida, USA from June- July 2015. He has been awarded the INSA Bilateral Exchange 2017 Fellowship to visit Institute of Parasitology, Ceske Budejovice, Czech Republic during June 2017 and also "2017 ASM-IUSSTF Indo-US Research Professorship" to pursue research in US. He was recipient of DST Fast Track Project (2010 – 2013). He is actively involved in teaching and research, has handled projects from various funding agencies, has supervised 2 Ph.D. thesis, many graduate and post-graduate student thesis and is currently supervising 4 PhD students. He was a recipient of **Young Scientist Award** for Best Poster Presentation at International Conference on Molecular Epidemiology & Immunology of Malaria and other vector Borne Diseases at RMRCT, Jabalpur, M. P., INDIA, 2007. He has published research papers in Scopus indexed journals of high repute and good impact. He has authored a book on Genetic Engineering. He has participated in many national and international conferences in India and abroad.

A.4 Biography of Ms. Zarna Rajeshkumar Pala

Zarna Rajeshkumar Pala has completed her B. Tech. (Biotechnology) and M. Tech (Biotechnology) from Padmashree Dr. D. Y. Patil Institute of Biotechnology and Bioinformatics, Navi Mumbai, Maharashtra. During her Masters, she had successfully completed a project entitled as "Screening of *Artemisia spp.* from Western Ghats of Maharashtra for antimalarial compound – Artemisinin" under the supervision of Prof. Neetin Desai, Dean, Department of Biotechnology, AMITY University, Mumbai. She was the Gold Medalist of the batch during her Masters. She also qualified Graduate Aptitude Test in Engineering (GATE) in 2010 (94.4 percentile). Following her masters she joined the Department of Biological Sciences, BITS, Pilani, Pilani Campus as a Project Assistant in a DST funded project of Prof. Vishal Saxena and was also enrolled as a Ph. D. student (2011). She was awarded with DST-INSPIRE Fellowship (January 2013) from Department of Science and Technology, Govt. of India and CSIR-Senior Research Fellowship from Centre for Scientific and Industrial Research, Govt. of India. During her Ph. D. she has published research articles in journals of international repute and has presented her research work in national and international conferences and workshops. She is a recipient of **four Best Poster Presentation Awards** in total. Her current research interest includes functional characterization of SUF pathway and other biosynthesis pathways functional in the apicoplast of human malaria parasites.

Characterization of Major Components of SUF Pathway (Iron-Sulphur Cluster Biogenesis) Functional in the Apicoplast of *Plasmodium vivax*

THESIS

Submitted in partial fulfilment
of the requirements for the degree of
DOCTOR OF PHILOSOPHY

by

ZARNA RAJESHKUMAR PALA

Under the Supervision of

Prof. Vishal Saxena

BITS Pilani
Pilani I Dubai I Goa I Hyderabad

BIRLA INSTITUTE OF TECHNOLOGY AND SCIENCE

PILANI (RAJASTHAN)

2017

Chapter VII

Conclusions and Future Prospects

CONCLUSIONS AND FUTURE PROSPECTS

7.1 Specific Conclusions

1. The genes encoding for the SUF pathway in *Plasmodium vivax* were shortlisted from the PlasmoDB database based on their conserved domains and signature motifs. Based on different sequence alignments and functional domain analysis, iron sulphur cluster assembly accessory protein (PVX_080115) was designated as *Pv*SufA, hypothetical protein (PVX_003740) as *Pv*SufE, and cysteine desulphurase, putative (PVX_000600) as *Pv*SufS.

2. Targeting prediction using online servers like PlasmoAP, PlasMit, PATS, MitoProt suggested dual targeting for *Pv*SufA to mitochondria and apicoplast, apicoplast targeting for *Pv*SufE and ambiguous targeting for *Pv*SufS. Immunolocalization studies performed on *P. vivax* infected blood smears from patients for all these proteins using antibodies raised against recombinant protein suggested their apicoplast localization. This suggests that the online targeting prediction servers need to be standardized more with the *P. vivax* database, as currently they are based on the sequences of *P. falciparum* only.

3. The cysteine desulphurase *Pv*SufS and its partner protein *Pv*SufE were expressed as His-tagged recombinant proteins. The activity of *Pv*SufS increased to ~5 folds in the presence of *Pv*SufE, even after the presence of a deletion in *Pv*SufE near the active site of the protein. When the structure of Ind*Pv*SufS and Sal-I *Pv*SufS were analysed for PLP binding, only three residues were involved in the interaction of PLP cofactor in Sal-I *Pv*SufS compared to five in Ind*Pv*SufS. The protein-protein docking studies between Sal-I *Pv*SufS and *Pv*SufE also revealed a distance of 8.2Å, which is far when compared with the Ind*Pv*SufS and Ind*Pv*SufE. Thus the close association of the two cysteines (~2Å) in *Pv*SufS and *Pv*SufE in *in silico* studies suggests their close interaction for sulphur transfer.

4. The *Plasmodium* SufB lacks the CXXCXXXC motif required for it to function as a scaffold protein, thus suggesting the presence of an alternative scaffold protein for

the assembly of Fe-S clusters. *Pv*SufA showed the presence of three conserved cysteine residues as $X_{55}CX_{185}CGCX_{189}$ comparable to the *E. coli* counterpart of the same protein. *In silico* docking studies of *Pv*SufA and [4Fe-4S] cluster revealed the involvement of these three conserved cysteine residues and $Lys_{160,}$ further validating the formation of Fe-S clusters on this protein.

5. Recombinant *Pv*SufA was observed to form Fe-S clusters *in vitro* under anaerobic conditions proving the function of *Pv*SufA protein as a scaffold protein to assemble the Fe-S clusters in *P. vivax*. These clusters were shown to have iron in +3 oxidation state thus showing the formation of [4Fe-4S] clusters.

6. *In silico* docking studies of *Pv*SufA with the *Pv*SufBCD complex showed 12 possible interactions between *Pv*SufA and *Pv*SufBD, but no interaction with *Pv*SufC. Thus, *Pv*SufA is acting in combination with *Pv*SufBD for the assembly and transfer of [4Fe-4S] clusters to the apo-proteins. As no interaction was evident between *Pv*SufA and *Pv*SufC, thus SufC might be interacting with SufBD only to function as an ATPase in *Plasmodium*.

7. *In vitro* biochemical assays further indicated the incorporation of sulphur mobilized by *Pv*SufSE complex in the Fe-S clusters assembled on *Pv*SufA and their transfer from *Pv*SufA onto an apo-protein *Pv*IspG. This further validates our hypothesis that *Pv*SufA acts as both a scaffold and an A-type carrier protein.

8. With the elucidation of the complete pathway, the concern is to find an inhibitor for its components to inhibit the parasite growth. Thus the potential of D-cycloserine, an inhibitor for the enzymes of the aminotransferase family, was explored by *in silico* docking studies. Eleven residues in the binding pocket of Ind*Pv*SufS interacted with D-cycloserine, of which two of the residues are also involved in the interaction of PLP cofactor. This suggests that D-cycloserine may act as a competitive inhibitor for cysteine desulphurase SufS in *P. vivax* similar to as observed in *P. falciparum*.

Hypothesized SUF pathway (Figure 7.1) for Fe-S cluster assembly in *Plasmodium vivax*

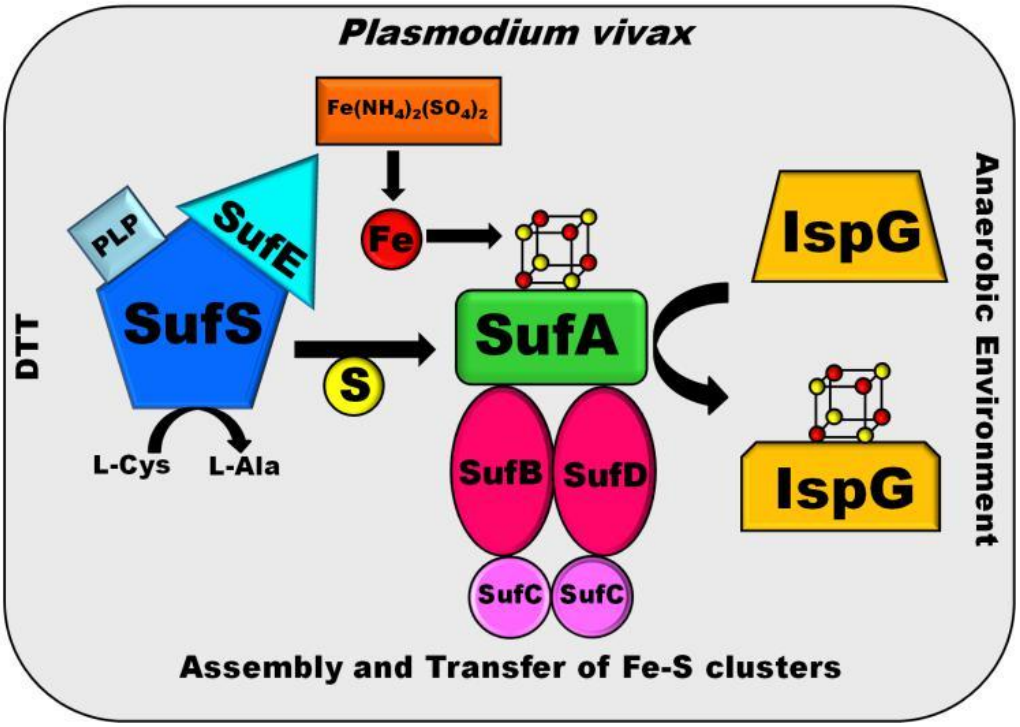

7.2 Direction for future research (future perspectives)

- The present study details the structural and functional characterization of three major enzymes SufS, SufE and SufA involved in the SUF pathway for Fe-S cluster biogenesis in *Plasmodium*. This study is the first report of characterization of any component involved in this pathway and hence, can open new doors for designing new inhibitors for this pathway to target *P. vivax* malaria parasite.

- In prokaryotes, the SUF system is said to be functional under oxidative stress or iron starvation conditions. Since there is no study available till date for any of the *Plasmodium* species under any of these stress conditions, a future study under the influence of different stress conditions can be conducted.

- The source of iron in the formation of the Fe-S clusters is yet unknown in *Plasmodium* and is yet to be explored.

- The other components of the *P. vivax* SUF pathway majorly, SufBCD complex, has to be characterized experimentally.

- An *in silico* analysis of the interaction of SufBCD complex with SufA has been shown in this study, however further experimental validation will be required.